

2013-01-01

Evaluation of Emission Control Strategies to Reduce Ozone Pollution in the Paso del Norte Region Using a Photochemical Air Quality Modeling System

Victor Hugo Valenzuela

University of Texas at El Paso, vvalenz@swbell.net

Follow this and additional works at: https://digitalcommons.utep.edu/open_etd



Part of the [Atmospheric Sciences Commons](#)

Recommended Citation

Valenzuela, Victor Hugo, "Evaluation of Emission Control Strategies to Reduce Ozone Pollution in the Paso del Norte Region Using a Photochemical Air Quality Modeling System" (2013). *Open Access Theses & Dissertations*. 1947.
https://digitalcommons.utep.edu/open_etd/1947

This is brought to you for free and open access by DigitalCommons@UTEP. It has been accepted for inclusion in Open Access Theses & Dissertations by an authorized administrator of DigitalCommons@UTEP. For more information, please contact lweber@utep.edu.

EVALUATION OF EMISSION CONTROL STRATEGIES TO REDUCE OZONE
POLLUTION IN THE PASO DEL NORTE REGION USING A
PHOTOCHEMICAL AIR QUALITY MODELING SYSTEM

Victor Hugo Valenzuela

Environmental Science and Engineering

APPROVED:

Wen-Whai Li, P.E., Ph.D., Co-Chair

Alberto M. Correa, Ph.D., Co-Chair

Ruey Long (Kelvin) Cheu, Ph.D.

Rosa Fitzgerald, Ph.D.

Huiyan Yang, Ph.D.

Benjamin C. Flores, Ph.D.
Dean of the Graduate School

Copyright ©

By

Victor Hugo Valenzuela

2013

DEDICATION

To my parents

Hilda and Ernesto Valenzuela

Thank you

EVALUATION OF EMISSION CONTROL STRATEGIES TO REDUCE OZONE
POLLUTION IN THE PASO DEL NORTE REGION USING A
PHOTOCHEMICAL AIR QUALITY MODELING SYSTEM

by

Victor Hugo Valenzuela, M.P.A.

DISSERTATION

Presented to the Faculty of the Graduate School of
The University of Texas at El Paso
in Partial Fulfillment
of the Requirements
for the Degree of

Doctor of Philosophy

Department of Engineering
THE UNIVERSITY OF TEXAS AT EL PASO

May 2013

ACKNOWLEDGEMENTS

The author expresses his appreciation to the faculty of the UTEP Environmental Science and Engineering Program. Your guidance, patience, and enthusiasm influence students to strive and achieve our best potential. Much appreciation is extended to Dr. Wen-Whai Li for his guidance which allowed me to complete the ESE program. I also extend my gratitude to the doctoral committee, Drs. Rosa Fitzgerald, Huiyan Yang, Kelvin Cheu, and Alberto Correa, for your participation, your technical support, and sharing your knowledge which helped improve my skills.

The author extends his appreciation to Mr. Sergio Rocha for committing many hours in explaining the FORTRAN scripts which comprise the CAMx photochemical model.

The author also extends an appreciation to his brother Ernesto and sisters Patricia Valenzuela-Barth and Hilda Jeanette Valenzuela for being my best influence to become a better person. To my parents, Hilda and Ernesto, for patience and guidance that keeps me on a better path in life.

Most importantly, the author extends his love and appreciation to Amabilia, his wife, and daughter Angelica for your words of encouragement to pursue and accomplish this academic achievement and making each day better than the day before.

ABSTRACT

Air pollution emissions control strategies to reduce ozone precursor pollutants are analyzed by applying a photochemical modeling system. Simulations of air quality conditions during an ozone episode which occurred in June, 2006 are undertaken by increasing or reducing area source emissions in Ciudad Juárez, Chihuahua, Mexico.

Two air pollutants are primary drivers in the formation of tropospheric ozone. Oxides of nitrogen (NO_x) and volatile organic compounds (VOC) undergo multiple chemical reactions under favorable meteorological conditions to form ozone, which is a secondary pollutant that irritates respiratory systems in sensitive individuals especially the elderly and young children. The U.S. Environmental Protection Agency established National Ambient Air Quality Standards (NAAQS) to limit ambient air pollutants such as ozone by establishing an 8-hour average concentration of 0.075 ppm as the threshold at which a violation of the standard occurs.

Ozone forms primarily due reactions in the troposphere of NO_x and VOC emissions generated primarily by anthropogenic sources in urban regions. Data from emissions inventories indicate area sources account for ~15 of NO_x and ~45% of regional VOC emissions. Area sources include gasoline stations, automotive paint bodyshops and nonroad mobile sources. Multiplicity of air pollution emissions sources provides an opportunity to investigate and potentially implement air quality improvement strategies to reduce emissions which contribute to elevated ozone concentrations.

A baseline modeling scenario was established using the CAMx photochemical air quality model from which a series of sensitivity analyses for evaluating air quality control strategies were conducted. Modifications to area source emissions were made by

varying NO_x and / or VOC emissions in the areas of particular interest. Model performance was assessed for each sensitivity analysis. Normalized bias (NB) and normalized error (NE) were used to identify variability of the PREDICTED to OBSERVED ozone concentrations of both BASELINE model and simulations with modified emissions assessed by the sensitivity analysis. All simulations were found to vary within acceptable ranges of these two criteria variables.

Simulation results indicate ozone formation in the PdN region is VOC-limited. Under VOC-limited conditions, modifications to NO_x emissions do not produce a marked increase or decrease in ozone concentrations. Modifications to VOC emissions generated the highest variability in ozone concentrations. Increasing VOC emissions by 75% produced results which minimized model bias and error when comparing PREDICTED and OBSERVED ozone concentrations. Increasing VOC emissions by 75% either alone or in combination with a 75% increase in NO_x emissions generated PREDICTED ozone concentrations very near to OBSERVED ozone.

By evaluating the changes in ambient ozone concentrations through photochemical modeling, air quality planners may identify the most efficient or effective VOC emissions control strategies for area sources. Among the strategies to achieve emissions reductions are installation of gasoline vapor recovery systems, replacing high-pressure low-volume surface coating paint spray guns with high-volume low-pressure spray paint guns, requiring emissions control booths for surface coating operations as well as undertaking solvent management practices, requiring the sale of low-VOC paint solvents in the surface-coating industry, and requiring low-VOC solvents in the dry cleaning industry. Other strategies to reduce VOC emissions include

initiating Eco-Driving strategies to reduce fuel consumption from mobile sources and minimize vehicle idling at the international ports of entry by reducing bridge wait times.

This dissertation depicts a tool for evaluating impacts of emissions on regional air quality by addressing the highly unresolved fugitive emissions in the Paso del Norte region. It provides a protocol for decision makers to assess the effects of various emission control strategies in the region. Impacts of specific source categories such as the international ports of entry, gasoline stations, paint body shops, truck stops, and military installations on the regional air quality can be easily and systematically addressed in a timely manner in the future.

TABLE OF CONTENTS

SIGNATURE PAGE	i
ACKNOWLEDGEMENTS	v
ABSTRACT	vi
TABLE OF CONTENTS	ix
LIST OF TABLES	xviii
LIST OF FIGURES.....	xx
1 Introduction	1
1.1 Purpose of the Dissertation	3
1.2 Background	4
1.3 Dissertation Objective	6
1.4 Organization of this Report.....	7
1.5 El Paso, Juárez, and the PdN Region	9
2 Air Quality in the Paso del Norte Region.....	11
2.1 Air Quality Standards	11
2.2 National Ambient Air Quality Standards	11
2.3 Ozone pollution in the Paso del Norte	13
2.3.1 Development of the 8-hour Ozone NAAQS	13
2.3.2 Ozone Design Value (DV) for El Paso	14
3 Air Quality Data for the PdN Region.....	16
3.1 Air Quality Parameters	16
3.2 Air Quality Monitoring Network.....	17
3.3 Ozone Conditions in El Paso, Texas	18

3.4	Air Quality Trends in the PdN Region.....	20
3.4.1	Ambient Air Quality Trends in El Paso, Texas	20
3.4.2	Air Quality Trends in Cd. Juárez, Chihuahua.....	22
3.5	Other Air Pollutants in the PdN	24
3.5.1	Carbon Monoxide	24
3.5.2	Particulate Matter.....	25
4	Reactive Hydrocarbons and Oxides of Nitrogen	27
4.1	Speciation of Volatile Organic Compounds	27
4.2	VOC Reactivity	28
4.3	Maximum Incremental Reactivity.....	29
4.4	Maximum Allowable Emissions Rate Tables.....	30
4.5	Highly Reactive VOCs.....	31
4.5.1	Big 12 HRVOCs.....	32
4.5.2	VOC Group Names and Constituents.....	33
4.6	TNMHC / NO _x Ratios	36
4.6.1	Empirical Kinetic Modeling Approach	39
4.6.2	NO _x -Limited Conditions.....	40
4.6.3	VOC-Limited Conditions	41
4.6.4	Transitional Conditions	41
4.6.5	CAMx Determination of VOC- or NO _x - Limited Conditions.....	47
4.7	Summary.....	48
5	State Implementation Plan for Control of Ozone Pollution in El Paso	50
5.1	1-hour Ozone State Implementation Plan	50

5.1.1	Empirical Kinetic Modeling Approach	51
5.1.2	Inspection and Maintenance SIP Revision	53
5.2	Development of the 8-hour Ozone SIP.....	54
5.3	8-Hour Ozone Maintenance SIP Revision.....	55
5.4	Summary.....	56
6	Basic Principles of Ozone Chemistry	59
6.1	Ozone Formation Processes	59
6.1.1	The Chapman Mechanism.....	60
6.2	Kinetics of Ozone Formation	62
6.3	Sensitivity of Ozone Formation to VOCs and NO _x	65
6.4	Summary.....	66
7	Previous Photochemical Ozone Studies in the PdN Region	68
7.1	The 1991 and 1994 Ozone Studies.....	68
7.2	The 1996 PdN Ozone Study	69
7.2.1	Photochemical Modeling.....	69
7.2.2	Meteorological Modeling.....	70
7.2.3	Emissions Inventory Development.....	71
7.2.4	Canister Sampling	72
7.3	Studies after 1996	75
7.3.1	Addressing Uncertainties of the 1996 Ozone Study	75
7.3.2	Community Multiscale Air Quality Modeling.....	76
7.3.3	Western U.S. Border-Region Ozone Study	77
7.3.4	MM5 Mesoscale Meteorological Modeling.....	78

7.4	Summary.....	79
8	Conceptual Model	80
8.1	The Conceptual Model for the Paso del Norte Region	80
8.2	Mesoscale Meteorological Conditions	82
8.3	HYSPLIT Model	83
8.4	Surface Wind Characteristics	86
8.4.1	Wind Statistics During Ozone Seasons	87
8.4.2	Wind Statistics During Ozone Episodes	95
8.4.3	Wind Statistics During Ozone Events	96
8.5	Selection of Photochemical Modeling Episode.....	99
8.6	Summary.....	100
9	The CAMx Photochemical Modeling System	102
9.1	The Continuity Equation.....	103
9.2	Domain Grid Cells	106
9.2.1	Grid Nesting.....	108
9.2.2	4-Kilometer Gridding Surrogates	112
9.3	CAMx Photochemical Modeling System Components	116
9.3.1	Meteorological Inputs.....	116
9.4	Model-Ready Emissions.....	117
9.4.1	Gridded Emissions.....	118
9.4.2	Elevated Point Emissions	119
9.4.3	Initial and Boundary Conditions	120
9.4.4	Photolysis Rates and Related Inputs	120

9.4.5	Total Ultraviolet Visible Radiative Transfer Model	121
9.5	Carbon Bond Mechanism Version 6.....	122
9.6	CAMx Input Files and Run Configuration	126
9.7	CAMx Post-Processing Tools.....	126
9.7.1	CAMxTRCT	127
9.7.2	AVGCAT	127
9.7.3	OBSCAT	128
9.7.4	CAMxPOST	128
9.7.5	CAMxSTAT.....	129
9.7.6	EXSTAT.....	130
9.8	Limitations of Photochemical Modeling	133
9.9	Summary.....	135
10	Emissions Inventories	136
10.1	Baseline Emissions Inventories.....	136
10.1.1	Ozone Season Emissions Inventory	136
10.2	Area Source Emissions	137
10.2.1	Review of El Paso Area Source Emissions	138
10.2.2	Review of Emission Development Methodology	145
10.2.3	Review of Activity Data	146
10.2.4	Review of Cd. Juárez Area Source Emissions Inventories	147
10.3	Point Sources.....	148
10.3.1	Regional Point Source Contributions and Trends.....	148
10.3.2	Point Source VOC Emissions in El Paso County, Texas	150

10.3.3	Point Source NO _x Emissions in El Paso County, Texas.....	152
10.3.4	Nonroad Mobile Source Emissions.....	153
10.3.5	Aviation Emissions.....	154
10.3.6	Review of Emissions.....	155
10.4	Summary.....	155
11	CAMx Modeling.....	157
11.1	CAMx Modeling Domain.....	157
11.1.1	Nested Grids.....	158
11.2	CAMx Modeling Inputs	161
11.2.1	Landuse.....	161
11.2.2	Biogenic Emissions.....	162
11.2.3	Landuse Data Processing Procedures	164
11.2.4	Albedo-Haze-Ozone	164
11.2.5	Total Ultraviolet Visible	165
11.2.6	Initial and Boundary Conditions	165
11.3	Emissions Processing	165
11.3.1	Emissions Processing System - Version 3	166
11.3.2	Emission Inputs	168
11.4	CAMx Processes	170
12	The CAMx Simulation	173
12.1	The Modeled Emissions Inventory	173
12.1.1	EPS3 and Biogenic Emissions	173
12.1.2	Daily Modeled Emissions.....	174

12.1.3	Regional Modeled Emissions	178
12.1.4	Sensitivity Analysis Emissions Assignments	184
12.2	Procedure for Preparing the Emissions Data Files.....	185
12.2.1	CAMx Simulation Emissions.....	185
13	CAMx Simulation Results and Model Performance.....	188
13.1	Model Performance Goals.....	189
13.2	Model Performance Definitions	189
13.3	Model Performance Summary for 1-Hour Ozone	191
13.4	Results and Statistics for 8-Hour Ozone	195
14	Model Performance Evaluations for Each Simulation.	199
14.1	BASELINE Model Performance	200
14.2	RUN 1 Model Performance Evaluation.....	204
14.3	RUN 2 Model Performance Evaluation.....	208
14.4	RUN 3 Model Performance Evaluation.....	212
14.5	RUN 4 Model Performance Evaluation.....	215
14.6	RUN 5 Model Performance Evaluation.....	219
14.7	RUN 6 Model Performance Evaluation.....	223
14.8	RUN 7 Model Performance Evaluation.....	227
14.9	RUN 8 Model Performance Evaluation.....	231
14.10	RUN 9 Model Performance Evaluation.....	235
14.11	RUN 10 Model Performance Evaluation.....	239
14.12	RUN 11 Model Performance Evaluation.....	243
14.13	RUN 12 Model Performance Evaluation.....	247

14.14	Summary	251
15	Time-Series Plots.....	252
15.1	Time-Series and Pairwise Scatterplots - BASELINE	253
15.2	Time-Series and Pairwise Scatterplots - RUN 9.....	255
15.3	Time-Series and Pairwise Scatterplots – RUN 10.....	257
15.4	Time-Series and Pairwise Scatterplots – RUN 11	259
15.5	Time-Series and Pairwise Scatterplots – RUN 12.....	262
16	Discussion.....	264
16.1	Purpose of the Dissertation	264
16.2	Meteorological Inputs	265
16.3	Emissions Inventories and Recommended Improvements.....	266
16.3.1	VOC Emissions.....	269
16.3.2	NOx Emissions	270
16.3.3	Emissions Inventory Summary	271
16.4	Model Performance Evaluation	272
16.4.1	Predicted Peak to Baseline Predicted Peak Comparison	275
16.4.2	Paired Predicted Peak Comparison.....	278
16.4.3	Predicted Peak to Observed Peak Comparison	282
16.5	Individual Simulation Results	288
16.6	Limiting Factors in Regional Ozone Formation	289
16.7	Attainment Demonstrations	290
17	Conclusions	292
18	References.....	294

19	Appendices	301
	Appendix 1: Acronyms and Abbreviations	302
	Appendix 2: Chemical Species Assessed by CAMx	309
	Appendix 3: List of Auto GC Volatile Organic Compounds	312
	Appendix 4: 7-Digit Source Classification Code Table	314
	Appendix 5: WRF Meteorology Applied to CAMx Modeling.....	315
	WRF 4 KM Meteorology	315
	WRFCAMx Preprocessing	326
20	Vita	330

LIST OF TABLES

Table 2.1	National Ambient Air Quality Standards	12
Table 2.2	Classification Ranges for the 8-hour Ozone Standard and Time Allowance for Compliance	14
Table 3.1	Paso del Norte CAMS and Monitored Parameters	18
Table 3.2	Ozone 8-Hour Average 4th Highest Value by Year	20
Table 4.1	Maximum Incremental Reactivity (IR) Table Excerpt	30
Table 4.2	Original "Big 12" HRVOC	32
Table 4.3	VOC Group Names and Constituents	34
Table 6.1	Major Steps of the Chapman Mechanism	61
Table 6.2	NO _x participation in Ozone Formation	62
Table 6.3	Kinetic Reactions in Ozone Formation	63
Table 8.1	Top 4 Ozone Exceedance Days During 2006	100
Table 9.1	NLCD Land Cover Classification Codes	113
Table 9.2	Mapping of NCLD codes to the EPS3 Surrogate Codes	115
Table 9.3	CAMx Meteorological Input Parameters	117
Table 9.4	Comparison of CB6 and CB05 chemical mechanisms	124
Table 10.1	Two-digit source classification categories	138
Table 10.2	2002 El Paso Area Source Emissions Inventory Summary (in TPY)	139
Table 10.3	2005 El Paso Area Source Emissions Inventory Summary (in TPY)	141
Table 10.4	2008 Area Source Emissions Inventory Summary (in TPY)	143
Table 10.5	Point Source Emissions in El Paso (TPY)	149
Table 10.6	Top 4 NO _x Sources in El Paso, TX by Industrial Classification	152

Table 10.7	Non Road Mobile Source Emissions (TPY) El Paso, TX	
	(2002, 2005, 2008)	154
Table 11.1	Source Categories processed by EPS3.....	169
Table 12.1	Daily Modeled VOC and NOx Emissions for Regional	
	Source Categories	176
Table 12.2	Modeled VOC and NOx Emissions by	
	Source Category and Jurisdiction (TPD).....	179
Table 12.3	BASELINE Daily Modeled Emissions in the PdN (TPD)	183
Table 12.4	Matrix of Area Source Emissions Modifications for CAMx Simulations..	184
Table 13.1	Results and Statistics for 1-Hour Ozone Simulations for 18 June, 2006	190
Table 13.2	Results and Statistics for 8-Hour Ozone Simulations for 18 June, 2006	195
Table 16.1	Simulation Results for 1-Hour Ozone.....	274
Table 16.2	Simulation Results for 8-Hour Ozone.....	274

LIST OF FIGURES

Figure 3.1	Maximum Ozone Design Values for El Paso Between 2002 and 2012 ...	19
Figure 3.2	10-Year Trend - Sum of Ozone Exceedance-Days at El Paso CAMS	21
Figure 3.3	10-Year Trend - Annual TNMHC Averages from Canister Samplers	22
Figure 3.4	8-Year Trend - Sum of Ozone Exceedance-Days, Juárez	23
Figure 3.5	Carbon Monoxide Trends at 2 El Paso CAMS	24
Figure 4.1	Examples of EKMA Diagrams	39
Figure 4.2	2006 TNMHC:NOx Ratios Based on 6-day canister sampling at C37	43
Figure 4.3	June 2006 TNMOC:NOx Ratios at C37	44
Figure 4.4	June 18, 2006 TNMHC:NOx Ratios	45
Figure 4.5	July 2006 VOC:NOx Ratios	46
Figure 4.6	Diurnal VOC:NOx ratios during ozone event	47
Figure 6.1	Generalized Ozone Formation Pathways	
	(From Smog Photochemistry in the Troposphere - undated)	60
Figure 8.1	Domain Coverage by the WRF Model	83
Figure 8.2	Backward Trajectories by Predominant Direction - Summer 2006	84
Figure 8.3	24-hour backward trajectory arriving at C37 on 00 UTC	
	on 12 July, 2006	85
Figure 8.4	Backward trajectory arriving at C37 on 19 June, 2006	86
Figure 8.5	Wind Speed Key	88
Figure 8.6	Wind Roses for the 2006 & 2008 Ozone Seasons at C12	88
Figure 8.7	Wind Roses for the 2006 & 2008 Ozone Seasons at 6ZN	89
Figure 8.8	Wind \Roses for the 2006 & 2008 Ozone Seasons at C663	90

Figure 8.9	Wind Roses for the 2006 & 2008 Ozone Seasons at C72	91
Figure 8.10	Wind roses for the 2006 & 2008 Ozone Seasons at C37	92
Figure 8.11	Wind roses for the 2006 & 2008 Ozone Seasons at C41	93
Figure 8.12	Wind roses for the 2006 & 2008 Ozone Seasons at C49	93
Figure 8.13	Wind Roses for the 2006 & 2008 Ozone Seasons at C414	94
Figure 8.14	Wind Roses for ozone Modeling Episodes	95
Figure 8.15	C12 and C37 Wind Rose for June 18, 2006 Ozone Event.....	97
Figure 8.16	C41 and C414 Wind Rose for June 18, 2006 Ozone Event.....	98
Figure 8.17	Wind Roses for Ozone Events at C12 on 7/11 and 8/26, 2006.....	99
Figure 9.1	Horizontal Grid Cell Indexing Convention	107
Figure 9.2	Horizontal Grid Nesting Arrangement	109
Figure 9.3	Vertical Layer Configuration and Nesting.....	110
Figure 10.1	2002 El Paso Area Source EI Criteria Pollutants	140
Figure 10.2	2005 Area Source EI Criteria Pollutants (TPY) – El Paso.....	142
Figure 10.3	2008 Area Source Emission Inventory (TPY) – El Paso	144
Figure 10.4	El Paso Source Emissions by Criteria Pollutant (TPY) -	
	2002, 2005, 2008.....	145
Figure 10.5	2008 Cd. Juárez Annual Area Source Emissions Inventory (TPY)	147
Figure 10.6	El Paso Point Source VOC and NO _x Emissions (TPY)	149
Figure 10.7	VOC Point Source Emissions by SIC (TPY)	151
Figure 10.8	El Paso VOC and NO _x Emissions 1999-2009 (TPY)	152
Figure 11.1	36-12-4 kilometer Modeling Grid.....	158
Figure 11.2	Paso del Norte 4-Kilometer Modeling Domain	159

Figure 11.3	Grid Cells of the 4 km Modeling Domain.....	160
Figure 11.4	EPS3 Flow Diagram.....	167
Figure 11.5	CAMx Data Processing Flow Chart	171
Figure 12.1	Total Emissions Processed by CAMx (TPD).....	175
Figure 12.2	Modeled VOC Emissions in TPD Processed by CAMx.....	177
Figure 12.3	Modeled NOx Emissions in TPD Processed by CAMx	178
Figure 12.4	Modeled VOC Emissions by Source Category - Juárez.....	180
Figure 12.5	Modeled NOx Emissions by Source Category - Cd. Juárez.....	180
Figure 12.6	Modeled VOC Emissions by Source Category – EP and DAC	181
Figure 12.7	Modeled NOx Emissions by Source Category - EP & DAC	182
Figure 12.8	VOC and NOx Emissions for BASELINE and Sensitivity Analysis.....	186
Figure 12.9	Modifications to the Juárez Area Source Daily Emissions	
	Simulation for both NOx and VOC	187
Figure 13.1	Paired Predicted Peak for CAMx Simulations and	
	1-Hour Ozone for 18 June, 2006	193
Figure 13.2	PREDICTED PEAK for CAMx Simulations and	
	1-Hour Ozone for 18 June, 2006	194
Figure 13.3	Paired Predicted Peak for CAMx Simulations and	
	8-Hour Ozone on 18 June, 2006.....	197
Figure 13.4	PREDICTED PEAK for CAMx Simulations and	
	1-Hour Ozone on 18 June, 2006.....	198
Figure 14.1	Model Performance Statistics – BASELINE	200

Figure 14.2	Diurnal Predicted and Observed 1-Hour Ozone (ppb) /	
	H ₂ O ₂ :HNO ₃ Ratios – BASELINE	201
Figure 14.3	Diurnal Predicted and Observed 8-Hour Ozone (ppb) /	
	H ₂ O ₂ :HNO ₃ Ratios – BASELINE	203
Figure 14.4	Model Performance Statistics – RUN 1	204
Figure 14.5	Diurnal Predicted and Observed 1-Hour Ozone (ppb) /	
	H ₂ O ₂ :HNO ₃ Ratios–6/18/2006 – RUN 1	205
Figure 14.6	Diurnal Predicted and Observed 8-Hour Ozone (ppb) /	
	H ₂ O ₂ :HNO ₃ Ratios – RUN 1	206
Figure 14.7	Model Performance Statistics – Run 2	208
Figure 14.8	Diurnal Predicted and Observed 1-Hour Ozone (ppb) /	
	H ₂ O ₂ :HNO ₃ Ratios – RUN 2	210
Figure 14.9	Diurnal Predicted and Observed 8-Hour Ozone (ppb) /	
	H ₂ O ₂ :HNO ₃ Ratios – RUN 2	211
Figure 14.10	Model Performance Statistics – Run3	212
Figure 14.11	Diurnal Predicted and Observed 1-Hour Ozone (ppb) /	
	H ₂ O ₂ :HNO ₃ Ratios – RUN 3	213
Figure 14.12	Diurnal Predicted and Observed 8-Hour Ozone (ppb) /	
	H ₂ O ₂ :HNO ₃ Ratios – RUN 3	214
Figure 14.13	Model Performance and Statistics - RUN 4	215
Figure 14.14	Diurnal Predicted and Observed 1-Hour Ozone (ppb) /	
	H ₂ O ₂ :HNO ₃ Ratios – RUN 4	216

Figure 14.15 Diurnal Predicted and Observed 8-Hour Ozone (ppb)	
H ₂ O ₂ :HNO ₃ Ratios – RUN 4.....	217
Figure 14.16 Model Performance Statistics – RUN 5.....	219
Figure 14.17 Diurnal Predicted and Observed 1-Hour Ozone (ppb) /	
H ₂ O ₂ :HNO ₃ Ratios – RUN 5.....	220
Figure 14.18 Diurnal Predicted and Observed 8-Hour Ozone (ppb) /	
H ₂ O ₂ :HNO ₃ Ratios – RUN 5.....	221
Figure 14.19 Model Performance Statistics - RUN 6	223
Figure 14.20 Diurnal Predicted and Observed 1-Hour Ozone (ppb) /	
H ₂ O ₂ :HNO ₃ Ratios – RUN 6.....	224
Figure 14.21 Diurnal Predicted and Observed 8-Hour Ozone (ppb) /	
H ₂ O ₂ :HNO ₃ Ratios – RUN 6.....	225
Figure 14.22 Model Performance and Statistics – RUN 7.....	227
Figure 14.23 Diurnal Predicted and Observed 1-Hour Ozone (ppb) /	
H ₂ O ₂ :HNO ₃ Ratios – RUN 7.....	228
Figure 14.24 Diurnal Predicted and Observed 8-Hour Ozone (ppb) /	
H ₂ O ₂ :HNO ₃ Ratios – RUN 7.....	229
Figure 14.25 Model Performance Statistics – Run 8.....	231
Figure 14.26 Diurnal Predicted and Observed 1-Hour Ozone (ppb) /	
H ₂ O ₂ :HNO ₃ Ratios – RUN 8.....	232
Figure 14.27 Diurnal Predicted and Observed 8-Hour Ozone (ppb) /	
H ₂ O ₂ :HNO ₃ Ratios – RUN 8.....	233
Figure 14.28 Model Performance Statistics – RUN 9.....	235

Figure 14.29 Diurnal Predicted and Observed 1-Hour Ozone (ppb) /	
H ₂ O ₂ :HNO ₃ Ratios – RUN 9.....	236
Figure 14.30 Diurnal Predicted and Observed 8-Hour Ozone (ppb) /	
H ₂ O ₂ :HNO ₃ Ratios – RUN 9.....	237
Figure 14.31 Model Performance Statistics - RUN 10	239
Figure 14.32 Diurnal Predicted and Observed 1-Hour Ozone (ppb) /	
H ₂ O ₂ :HNO ₃ Ratios – RUN 10.....	240
Figure 14.33 Diurnal Predicted and Observed 8-Hour Ozone (ppb) /	
H ₂ O ₂ :HNO ₃ Ratios – RUN 10.....	241
Figure 14.34 Model Performance Statistics - RUN 11	243
Figure 14.35 Diurnal Predicted and Observed 1-Hour Ozone (ppb) /	
H ₂ O ₂ :HNO ₃ Ratios – Run 11.....	244
Figure 14.36 Diurnal Predicted and Observed 8-Hour Ozone (ppb) /	
H ₂ O ₂ :HNO ₃ Ratios – Run 11.....	245
Figure 14.37 Model Performance Statistics – RUN 12.....	247
Figure 14.38 Diurnal Predicted and Observed 1-Hour Ozone (ppb) /	
H ₂ O ₂ :HNO ₃ Ratios – Run 12.....	248
Figure 14.39 Diurnal Predicted and Observed 8-Hour Ozone (ppb) /	
H ₂ O ₂ :HNO ₃ Ratios – Run 12.....	249
Figure 15.1 Time-Series Plots for BASELINE Simulation	253
Figure 15.2 Pairwise Scatterplots - BASELINE Simulation	254
Figure 15.3 Time-Series Plots - RUN 9.....	255
Figure 15.4 Pairwise Scatterplots - RUN 9	256

Figure 15.5	Time-Series Plot - RUN 10	257
Figure 15.6	Pairwise Scatterplots - RUN 10	258
Figure 15.7	Time-Series Plots - RUN 11.....	259
Figure 15.8	Pairwise Scatterplots - RUN 11	261
Figure 15.9	Time-Series Plots - RUN 12.....	262
Figure 15.10	Pairwise Scatterplots - RUN 12	263

Evaluation of Emission Control Strategies to Reduce Ozone Pollution in the Paso del Norte Region Using a Photochemical Air Quality Modeling System

1 Introduction

The role of modeling is to determine if a numerical simulation with multiple input parameters can be run to provide results which resemble observed data within acceptable parameters. Photochemical modeling integrates meteorology, ambient air quality data, initial and boundary conditions, and emissions inventories to obtain results which fall within acceptable parameters to air quality conditions observed during specific episodes.

Photochemical modeling is used to develop effective ozone control strategies initially by calibrating the modeling system with accurate information on emissions and meteorology to minimize the difference between observed and predicted ozone concentrations. The calibrated model can then be applied to evaluate future reductions in ambient ozone concentrations levels in accordance with precursor control strategies.

Photochemical modeling is best conducted for a temporal span encompassing multiple days during which the 8-hour average National Ambient Air Quality Standard (NAAQS) for ozone is observed to have been exceeded. The temporal span is considered an ozone “episode”. An ozone “event” occurs the day the 8-hour ozone NAAQS is exceeded during the episode.

This dissertation applies a photochemical modeling system consisting of a photochemical model, mesoscale meteorological models, atmospheric emissions by

various sources, and initial boundary conditions to evaluate emission control strategies for reduction of ozone pollution in the Paso del Norte (PdN) region.

The Comprehensive Air Quality Model with Extensions (CAMx) is the photochemical modeling application applied for research reported in this dissertation. CAMx is an Eulerian photochemical dispersion model that allows for an integrated 'one-atmosphere' assessment of gaseous and particulate air pollution over scales ranging from sub-urban to continental (ENVIRON, 2009). The Texas Commission on Environmental Quality (TCEQ) and United States Environmental Protection Agency (EPA) rely on CAMx as the air quality model of choice for State Implementation Plan (SIP) demonstrations.

CAMx is applied for the purpose of testing potential air quality control strategies (PAQCS) which may be implemented in the event that a metropolitan area such as El Paso, Texas is designated nonattainment of the 8-hour ozone NAAQS. Testing PAQCS allows modelers to ascertain the effect of actions a jurisdiction may undertake to improve regional air quality and attain the NAAQS. PAQCS, if or when undertaken, tend to be expensive endeavors. CAMx modeling tests the potential reduction in ozone concentrations prior to undertaking PAQCS. Photochemical modeling allows the jurisdiction responsible for air quality planning to test whether the PAQS is viable and acceptable in order to estimate the potential costs associated with various PAQCS.

The Weather Research and Forecasting (WRF) mesoscale meteorological model provides continent-scale meteorological conditions encompassing spatial scales of over 1,000 km for photochemical modeling. Meteorology plays an important role in ozone formation. A photochemical modeler must apply the large-scale atmospheric conditions

which occur during a period of elevated ozone into the photochemical model to establish accurate meteorological conditions for all modeling which follows.

1.1 Purpose of the Dissertation

Photochemical modeling is conducted in order to assess whether potential air quality control strategies (PAQCS) are effective at reducing ozone to a specified target prior to implementing a State Implementation Plan (SIP) which is a set of guidelines developed to help a metropolitan area attain the NAAQS for a particular pollutant. This dissertation evaluates the sensitivity of CAMx by focusing on area source VOC and NOx emissions generated in Cd. Juárez. The CAMx photochemical model was applied to conduct sensitivity analysis on 12 distinct simulations where VOC and or NOx emissions were increased or decreased by either 50% or 75% for each modeling simulation. It is possible that the sensitivity analysis may be applied for development of PAQCS based on results generated during the simulation.

Meteorology and emissions are potentially the most important parameters which establish the foundation of photochemical modeling simulations. An accurate meteorological platform is the initial step in building better photochemical modeling scenarios. Accurate emissions inventories (EIs) are also an overarching goal given this data is fundamental to recommending effective PAQCS. ENVIRON (2011) reports that the model may generate output which is within acceptable limits for bias and error, yet such output may be erroneous. Therefore quality assurance procedures should be developed to build confidence in both the meteorology and emissions integrated into the simulation. This dissertation builds upon a photochemical modeling platform developed

by ENVIRON in 2012 with the purpose of evaluating the impact of modifications to Juarez area source emissions.

1.2 Background

The County of El Paso is impacted by local generation of atmospheric emissions, additional air emissions from Cd. Juárez, Chihuahua Mexico plus emissions generated from the geographically larger Doña Ana County, New Mexico region. The international metropolitan community consisting of four U.S. counties and one Mexican municipality are discussed in this report. A portion of this report is included in a Conceptual Model (CM) which was previously prepared for the PdN region (consisting of El Paso, Juárez, and Sunland Park) by the air quality research group at the University of Texas at El Paso (UTEP). The CM is not discussed in this report.

The CM (Li, et.al., 2012) described multiple variables involved in the formation of tropospheric ozone as well as trends in ozone air pollution for the period 2001-2010. Multivariate analysis of the data indicates ambient temperature above 85°F, clear skies, high barometric pressure, low mixing height, low wind speed, and low wind gusts are meteorological conditions favorable for ozone formation.

The PdN region faces many challenges for a dynamic and rapidly growing region. Attainment of the 8-hour ozone NAAQS is of primary importance from an air quality planning perspective. Failure to attain the ozone NAAQS requires air quality control strategies costing millions of dollars to citizens within nonattainment communities. To meet this challenge, control strategies designed to reduce ozone precursor pollutants should be analyzed in a photochemical model prior to deployment

or application. An effective photochemical model should contain ozone and meteorological characteristics typically observed during high ozone events.

Ozone is a colorless gas. It has a very pungent odor which irritates nasal and bronchial passages, causes burning of the eyes, and may be a contributing factor in premature mortality. Ozone chemistry is complex and involves more than 80 nonlinear chemical reactions and hundreds of chemical compounds. Ozone cannot readily be evaluated using dilution and dispersion algorithms (TCEQ, 2006). Photochemical computer models are a means of combining meteorology, chemical speciation, temporal, and emissions information to estimate a baseline of ozone concentrations followed by modifications to the input data to assess multiple PAQCS. Only through an iterative process of modifying the input parameters to the model can the state of the science in photochemical modeling be advanced to suggest a reasonable determination as to the value of PAQCS.

CAMx is utilized with the purpose of assessing PAQCS that may reduce ambient ozone concentrations to a certain level. Given that El Paso is currently in attainment of the 2008 8-hour ozone NAAQS of 0.075 ppm, it is not necessary to conduct an attainment demonstration from a regulatory perspective. At some future date, however, the ozone standard may be modified to a range between 0.060 ppm and 0.70 ppm as proposed in 2009. This project affords the opportunity to assess multiple PAQCS and prepare an attainment demonstration that may be integrated into a future SIP.

1.3 Dissertation Objective

The objective of this dissertation is to evaluate the response of a photochemical modeling system to modifications in emissions applied as input data to a modeling simulation. Air pollution emissions from area, point, and mobile sources are the driving forces behind the formation of tropospheric ozone. Point sources include large industrial facilities also identified as “major sources” and defined as a stationary source or group of stationary sources that emit or have the potential to emit 10 tons per year or more of a hazardous air pollutant or 25 tons per year or more of a combination of hazardous air pollutants (42 USC §7491). “Area sources” are any stationary sources that are not major sources. Examples of area sources include gasoline stations, dry cleaners, and automotive paint bodyshops. Mobile sources consist of internal combustion motorized vehicles which may be subdivided into two categories: onroad and nonroad mobile. Onroad mobile sources traverse over local highways and roadways. Nonroad mobile sources include construction equipment, locomotives, and aircraft among others.

The three major source categories (point, area, and mobile) contribute large quantities of atmospheric pollutants which can be assessed by a photochemical modeling system. The focus of this dissertation is to assess photochemical model sensitivity and performance to modifications of Cd. Juárez area source emissions and in turn recommend potential air quality improvement strategies. The expectation for air quality planners is the emissions reductions identified by the photochemical modeling system translate into real reductions in ozone pollution.

1.4 Organization of this Report

This dissertation follows the following format:

- Section 1 outlines this report. Included in section are a description of the PdN region and a discussion on the objectives of this dissertation.
- Section 2 discuss the National Ambient Air Quality Standards (NAAQS) and summarizes potential modifications to the 8-hour average ozone standard. Terminology used in describing compliance with the standard is provided.
- Section 3 provides a summary of PdN air quality with a description of the regional continuous air monitoring stations (CAMS) and the ambient air monitoring network. This section also discusses air quality trends in the PdN region.
- Section 4 discusses the role Volatile Organic Compounds (VOC) and oxides of nitrogen (NO_x) emissions in photochemistry. This section discusses the reactivity of VOCs which play an important role in the formation of photochemical ozone.
- Section 5 discusses State Implementation Plans and the role of air quality planning strategies to improve regional air quality. An historical account of air quality planning strategies conducted in the PdN region over the past 30 years.
- Section 6 provides a discussion on photochemical reactions associated with the formation of tropospheric ozone.
- Section 7 provides an accounting of previous ozone studies conducted across the PdN region.
- Section 8 discusses the Conceptual Model (CM) which is the product of a thorough assessment of air quality conditions within the Paso del Norte airshed.

A CM analyzes the interaction of multiple variables involved in ozone forming reactions. Variables include meteorology, ambient air quality, and emissions.

- Section 9 summarizes the CAMx photochemical model, variables, and input parameters that are considered in building and running the CAMx model.
- Section 10 provides a discussion on emissions inventories and the estimation of emissions from area, point and mobile sources.
- Section 11 discusses the input variables applied to the CAMx modeling simulations conducted for this dissertation. This section discusses the experimental aspect of this dissertation by describing in detail the modeling domain, gridding system, meteorological conditions, and emissions pre-processing for integration into the photochemical simulation.
- Section 12 discusses the modifications to the emissions data and sensitivity analysis applied to evaluate the sensitivity of the photochemical modeling system.
- Section 13 discusses the model simulation outputs and statistical analysis conducted to determine the accuracy and performance of the photochemical model.
- Section 14 provides a discussion on results generated by the photochemical model on each of the simulations conducted for this dissertation.
- Section 15 provides a description and discussion on time-series plots which were developed to further evaluate the sensitivity of the photochemical modeling system. TS plots assist in evaluating whether the model over-predicts or under-

predicts ozone concentrations on an hourly basis due to variations in the emissions applied to each simulation.

- Section 16 provides a discussion on the results and the sensitivity of the photochemical modeling system as well as recommendations for future research.

1.5 El Paso, Juárez, and the PdN Region

The City of El Paso is located at the westernmost edge of Texas. Doña Ana County, New Mexico and the state of Chihuahua in Mexico adjoin El Paso to the west and south respectively. Ciudad Juárez, Chihuahua is contiguous to El Paso, separated by the Rio Grande River which serves as the international boundary. El Paso's elevation is on average approximately 3,800 ft (1,158 m) above sea level (ASL); the elevation at the Rio Grande is approximately 3,300 ft (1,005.8 m) ASL. El Paso is currently the sixth-largest city in Texas and the 22nd largest city in the United States.

El Paso is a geographically isolated metropolitan area, more than 342 miles (550 km) east of the nearest large metropolitan city of Phoenix, AZ. In general, El Paso is a flat desert area with an extensive mountain range known as the Franklin Mountains, which rise to over 3,280 ft (1,000 m) above the surrounding area and are a north-south oriented mountain chain that is approximately 14.4 miles (23.1 km) long and 3.1 miles (5 km) wide (Harbour, 1972). The Franklin Mountains divide El Paso between the western one third of the city and the central and eastern two thirds of the city.

El Paso generally presents an arid, warm climate with very hot summers and mild winters. Nicknamed the "Sun City", El Paso receives a daily average of 7.9 hours of sunshine in December to 12.8 hours of sunshine during June with 85.8% of possible

sunshine per annum. Rainfall averages 9.35 inches per year, most of which predominately occurs from July through September. The record high temperature for El Paso is 114 °F (46 °C) and the record low is -7 °F (-13.89 °C). Temperatures range from an average high of 57.2 °F (14.0 °C) and an average low of 32.9 °F (0.5 °C) in January to an average high of 95.3 °F (35.2 °C) in June and an average low of 72.0 °F (22.2 °C) in July (Li, et al 2011).

The three cities of El Paso, Juárez, and Sunland Park plus surrounding areas are jointly called Paso del Norte (PdN) or “path to the north”. The region has a combined estimated population in excess of 2.6 million, and covers an estimated land area of 13,352 square miles (3 458 152.124 9 hectares - PDNG, 2009). The binational urban core is formed by the central business districts of El Paso and Ciudad Juárez which are separated by the Rio Grande. Air quality in the PdN is considered among the worst along the U.S.-Mexico border although the situation has substantially improved in the past 10 years.

2 Air Quality in the Paso del Norte Region

Air quality conditions in the PdN region have been among the worse along the US-Mexico border. As environmental laws, rules, and regulations began developing, resources have been brought to bear to measure air quality through a regional air quality monitoring network. The network helps determine if improvements have been achieved through implementation of air quality improvement initiatives. Air quality conditions in the PdN region have improved during the past 10 years as a result of air quality improvement initiatives notwithstanding the growth of population and industry.

2.1 Air Quality Standards

The Federal government established air quality standards to protect the environment from the deleterious effects of reduced air quality. Passage of the National Environmental Policy Act (1970) ushered an era of rules and regulations established for the purpose of protecting human health and minimizing damage to other biological systems such as rivers, streams, forests, and agricultural crops

2.2 National Ambient Air Quality Standards

The Federal Clean Air Act (FCAA), last amended in 1990, requires EPA to set National Ambient Air Quality Standards (NAAQS - 40 CFR Part 50) for pollutants considered harmful to public health and the environment. Two NAAQS categories are identified. Primary standards provide public health protection, including protecting the health of "sensitive" populations such as asthmatics, children, and the elderly. Secondary standards provide public welfare protection, including protection against

decreased visibility and damage to animals, crops, vegetation, and buildings (<http://www.EPA.gov/air/criteria.html>).

Six principal “criteria” pollutants, listed in Table 2.1, are specified under the NAAQS. Units of measure for the standards are parts per million (ppm) by volume, parts per billion (ppb) by volume, and micrograms per cubic meter of air ($\mu\text{g}/\text{m}^3$). A Metropolitan Statistical Area (MSA) attains the NAAQS for any of the 6 criteria pollutants if ambient air quality concentrations measured at the federally approved air monitoring stations observe ambient pollutant concentrations which are within parameters specified for each criteria pollutant.

Table 2.1 National Ambient Air Quality Standards

Pollutant [final rule cite]		Primary/ Secondary	Averaging Time	Level	Form
Carbon Monoxide [76 FR 54294, Aug 31, 2011]		primary	8-hour	9 ppm	Not to be exceeded more than once per year
			1-hour	35 ppm	
Lead [73 FR 66964, Nov 12, 2008]		primary and secondary	Rolling 3 month average	0.15 $\mu\text{g}/\text{m}^3$ ⁽¹⁾	Not to be exceeded
Nitrogen Dioxide [75 FR 6474, Feb 9, 2010] [61 FR 52852, Oct 8, 1996]		primary	1-hour	100 ppb	98th percentile, averaged over 3 years
		primary and secondary	Annual	53 ppb ⁽²⁾	Annual Mean
Ozone [73 FR 16436, Mar 27, 2008]		primary and secondary	8-hour	0.075 ppm ⁽³⁾	Annual fourth-highest daily maximum 8-hr concentration, averaged over 3 years
Particle Pollution Dec 14, 2012	PM _{2.5}	primary	Annual	12 $\mu\text{g}/\text{m}^3$	annual mean, averaged over 3 years
		secondary	Annual	15 $\mu\text{g}/\text{m}^3$	annual mean, averaged over 3 years
		primary and secondary	24-hour	35 $\mu\text{g}/\text{m}^3$	98th percentile, averaged over 3 years
	PM ₁₀	primary and secondary	24-hour	150 $\mu\text{g}/\text{m}^3$	Not to be exceeded more than once per year on average over 3 years
Sulfur Dioxide [75 FR 35520, Jun 22, 2010] [38 FR 25678, Sept 14, 1973]		primary	1-hour	75 ppb ⁽⁴⁾	99th percentile of 1-hour daily maximum concentrations, averaged over 3 years
		secondary	3-hour	0.5 ppm	Not to be exceeded more than once per year

as of October 2011

Source: www.epa.gov/air/criteria.html. Accessed February 14, 2013.

2.3 Ozone pollution in the Paso del Norte

El Paso, Texas faces many challenges regarding deteriorated yet improving regional air quality conditions. A process of improving air quality includes development of planning strategies and programs specifically targeted toward each air pollutant. A State Implementation Plan (SIP) is prepared for nonattainment conditions by the state Environmental agency for the EPA or the EPA prepares a SIP in the event a state Environmental agency does not exist or defers to the federal government. Over the past thirty years El Paso has not attained the NAAQS for 1-hour ozone (O_3), particulate matter with an aerodynamic diameter of 10 micrometers (PM_{10}), and carbon monoxide (CO).

2.3.1 Development of the 8-hour Ozone NAAQS

The current 2008 8-hour ozone NAAQS is 0.075 parts per million (ppm) (73 FR 17636). EPA in 2009 proposed a revision of the 8-hour ozone NAAQS to between 0.060 ppm – 0.070 ppm (75 FR 2938). The proposed revision was rescinded in September, 2011 by order of the President thereby leaving the 2008 ozone standard intact.

The 8-hour ozone NAAQS differs from the 1-hour standard in several respects. Aside from extending the standard from 1-hour to 8-hours to reduce prolonged exposure, attainment of the 1-hour standard is based upon the number of exceedances at a given monitor, whereas attainment for the 8-hour standard is determined by a regional ozone design value.

2.3.2 Ozone Design Value (DV) for El Paso

An 'Ozone Design Value' (DV) is defined as the fourth-highest 8-hour average ozone concentration averaged over a consecutive 3-year period. The region demonstrates attainment with the 8-hour standard when the DV for all monitors in the region is equal to or below 0.075 ppm (EPA, NAAQS) or the ozone standard currently in effect. DVs are used not only in determining attainment versus nonattainment, but also in determining the severity of nonattainment.

Above the exceedance value, EPA established 6 Classification Ranges for the 8-hour ozone NAAQS which determine the level of control measures and time provided to comply with the standard. Table 2.2 identifies the NAAQS nonattainment designations and time allowance (as specified in 40 CFR Parts 50 and 51) to comply with the 8-hour ozone standard.

Table 2.2 Classification Ranges for the 8-hour Ozone Standard and Time Allowance for Compliance

Classification	From (ppm)	Up to (ppm)	Time Allowance
Marginal	0.076	0.085	3 Years
Moderate	0.086	0.099	6 Years
Serious	0.100	0.112	9 Years
Severe-15	0.113	0.118	15 Years
Severe-17	0.119	0.174	17 Years
Extreme	0.175	≥0.175	10 Years

§181(D)(2) of the FCAA (42 USC §7511) provides an increasing amount of time from the date of designation to attain the standards for the progressively higher

classifications. Areas in the lower classification levels have fewer and/or less stringent mandatory air quality planning and control requirements than those in higher classifications.

El Paso is currently designated in attainment of the 8-hour ozone standard given the current DV of 0.071 ppm. However, if the potentially revised standard would have been set at 0.070 ppm or lower, El Paso County would be classified as 'marginal' nonattainment and the level of severity would have to be established by EPA at the time it promulgates the new standard.

3 Air Quality Data for the PdN Region

The PdN air quality monitoring network spans 3 states and 2 countries. Air monitoring networks are located in El Paso County, Texas, the municipality of Juárez, and Doña Ana County, New Mexico. Both the El Paso and Juárez monitoring networks are integrated into the TCEQ air quality monitoring system commonly known as the Leading Environmental Analysis and Display System (LEADS).

3.1 Air Quality Parameters

Ambient air quality parameters collected and analyzed for this report include the following surface air quality data from Continuous Air Monitoring Stations (CAMS)

- Ozone (O₃);
- Nitric oxide (NO);
- Nitrogen dioxide (NO₂);
- Oxides of nitrogen (NO_x);
- Carbon monoxide (CO);
- Volatile Organic Compounds;
- Surface and upper air meteorological data from CAMS;
- Barometric Pressure;
- Wind speed resultant;
- Wind direction resultant;
- Sonic detection and ranging (SODAR);
- Radar wind profiler (RWP) soundings;
- Radio Acoustic Sounding System (RASS) virtual temperature (T_v);
- Dew point;
- Relative Humidity;
- Solar radiation; and
- Ultraviolet radiation.

Volatile and semi-volatile organic compounds are measured at both CAMS and Photochemical Assessment Monitoring Stations (PAMS). The following organic components are monitored and sampled:

- C2-C11 volatile organic compounds (VOCs) from automatic gas chromatograph (auto-GC);
- Carbonyls from canister samplers; and
- Semivolatile organic carbon (SVOC) from polyurethane foam (PUF) and canister samplers

3.2 Air Quality Monitoring Network

Table 3.1 identifies each ambient monitoring station in the PdN region. Not all regional CAMS were used in the analysis undertaken for this report. C6CM (Anthony) and C662 (20-30 Club) were not considered for this dissertation due insufficient ozone data from each station. Also, the post—processing application is limited to 14 CAMS when comparing the PREDICTED ozone concentrations to OBSERVED ozone concentrations. This topic will be covered in detail in Section 9.

Table 3.1 Paso del Norte CAMS and Monitored Parameters

List of Paso del Norte CAMS and Monitored Parameters														
CAMS ID	Site Name	City, State	O3	NO	NO2	NOx	CO	WS	WD	GC	UV	SLR	lcpv	lcpy
C12	UTEP	El Paso, TX	✓	✓	✓	✓	✓	✓	✓		✓	✓	-898.604	-865.303
C37	Ascarate	El Paso, TX	✓	✓	✓	✓	✓	✓	✓				-889.572	-868.661
C41	Chamizal	El Paso, TX	✓	✓	✓	✓	✓	✓	✓	✓			-894.296	-866.045
C49	Socorro	El Paso, TX	✓	✓	✓	✓	✓	✓	✓				-881.141	-879.005
C72	Skyline	El Paso, TX	✓	✓	✓	✓	✓	✓	✓				-890.047	-852.124
C414	Ivanhoe	El Paso, TX	✓				✓	✓	✓				-881.708	-865.032
C661	Advanced	Juarez, Chih	✓				✓	✓	✓				-895.199	-874.423
C662	20-20 Club	Juarez, Chih	✓				✓	✓	✓				-895.069	-869.342
C663	SEC	Juarez, Chih	✓				✓	✓	✓				-889.262	-872.561
6CM	Anthony	Anthony, NM						✓	✓				-889.262	-872.561
6O	La Union	La Union, NM						✓	✓			✓	-909.253	-847.365
6ZK	Chaparral	Chaparral, NM	✓					✓	✓			✓	-886.788	-835.992
6ZG	SPCY	Sunland Park, NM	✓					✓	✓			✓	-903.491	-861.551
6ZM	Desert View	Sunland Park, NM	✓	✓	✓	✓		✓	✓			✓	-906.066	-861.389
6ZH	Santa Teresa	Santa Teresa, NM	✓	✓	✓	✓		✓	✓			✓	-915.486	-861.338

3.3 Ozone Conditions in El Paso, Texas

As previously stated, the current ozone standard which became effective in 2008 is 0.075 ppm during an 8-hour averaging period. In order to attain the 2008 8-hour ozone standard, the 3-year average of the fourth-highest daily maximum 8-hour average ozone concentration must be less than or equal to 0.075 ppm. The average is a truncated value.

Figure 3.1 illustrates the trend of ozone DV for El Paso for the period 2001 - 2011. There has been a consistent drop in the ozone DV since 2007. The DV for the 3 year averaging periods ending 2010 and 2011 indicates El Paso attains the 8-hour ozone NAAQS of 0.075 ppm with DVs of 0.071 ppm during both 3 year averaging periods.

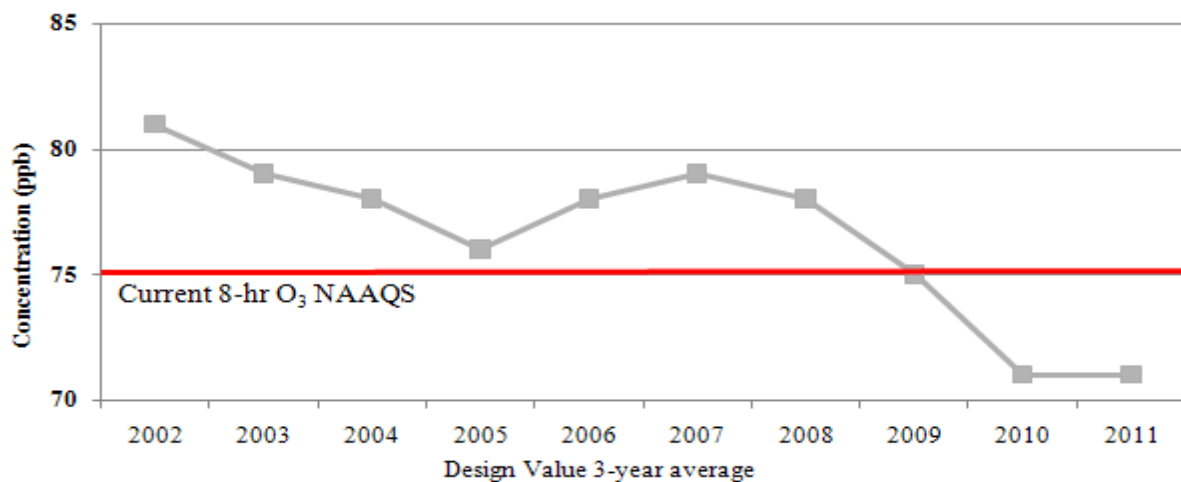


Figure 3.1 Maximum Ozone Design Values for El Paso Between 2002 and 2012

Table 3.2 identifies the ozone 8-hour average 4th highest values by year for the periods 2008 – 2010 as well as the 3-year average which is used to determine the DV for El Paso. Given incomplete data for 2009 and 2010 for CAMS 661 and CAMS 662 respectively in Juárez, those particular years may not be considered in the nonattainment calculation. CAMS 663 provides 3 complete years of data. Notwithstanding, Mexico has not developed an 8-hour ozone standard applicable to Cd. Juárez.

Table 3.2 Ozone 8-Hour Average 4th Highest Value by Year

Monitoring Site	2008	2009	2010	Three-Year Average
El Paso UTEP (C12)	75	66	73	71
El Paso Socorro (C49/F312)	71	70	63	68
El Paso Skyline Park (C72)	72	72	70	71
El Paso Ivanhoe (C414)	78	69	62	69
El Paso Chamizal (C41)	74	65	71	70
El Paso Ascarate Park SE (C37)	73	64	71	69
Ciudad Juárez 20-30 Club (C662)	77	65	73 ^a	71
Ciudad Juárez Delphi (C663)	87	77	75	79
Ciudad Juárez Advance (C661)	80	71 ^a	57	69

^a Incomplete year.

3.4 Air Quality Trends in the PdN Region

The PdN region consists of 3 abutting municipalities sharing one common airshed. El Paso and Sunland Park are located along the northern border, and Juárez is located to the south. The Rio Grande / Rio Bravo is the dividing line between Texas and Mexico. New Mexico's border with Chihuahua runs along latitude 31° 48' until it reaches the boot-heel to the west.

3.4.1 Ambient Air Quality Trends in El Paso, Texas

A Metropolitan Statistical Area (MSA) attains the NAAQS if ambient air quality concentrations measured at the CAMS are within specified parameters for each criteria pollutant. The ozone standard currently in effect is 0.075 ppm which became effective in 2008. In order to attain this standard, the 3-year average of the fourth-highest daily

maximum 8-hour average ozone concentration must be less than or equal to 0.075 ppm. Figure 3.2 illustrates a 10 year trend of ozone exceedance days in El Paso. Additional potential NAAQS exceedance concentrations are provided as an example to provide an indication of the number of exceedances could be observed under different ozone standards.

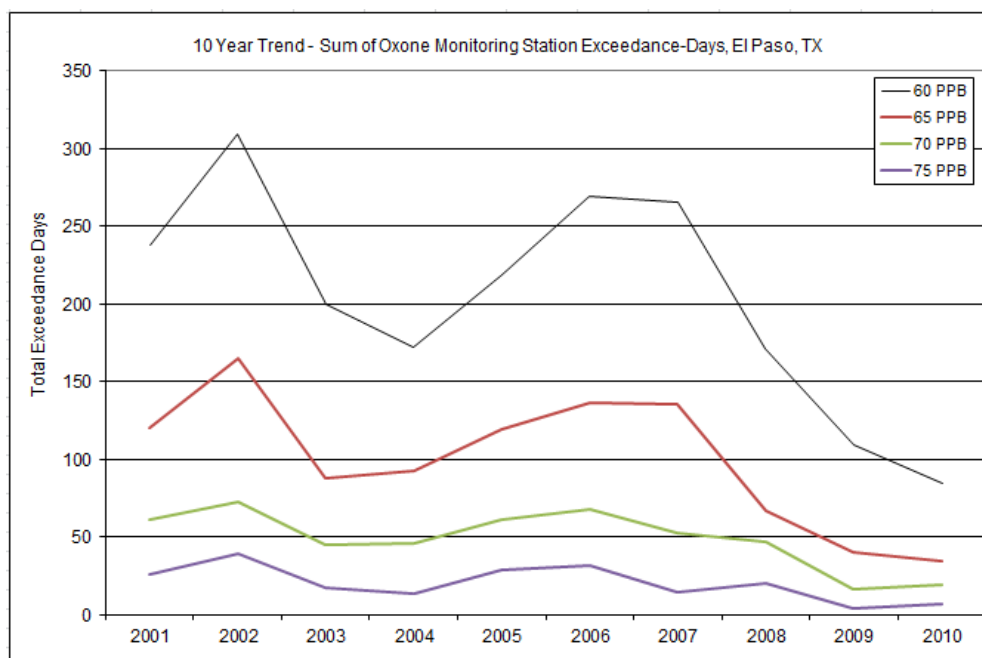


Figure 3.2 10-Year Trend - Sum of Ozone Exceedance-Days at El Paso CAMS

El Paso continues a downward trend in the annual number of exceedance days indicating air pollution reduction strategies are effective at improving air quality. Figure 3.3 illustrates the trend of total non-methane hydrocarbons monitored at CAMS 12, 37, and 41. The solid lines present the annual average, and the dashed lines identify the averages during the summer ozone-season sampling months. TNMHCs are trending downward on a year after year basis.

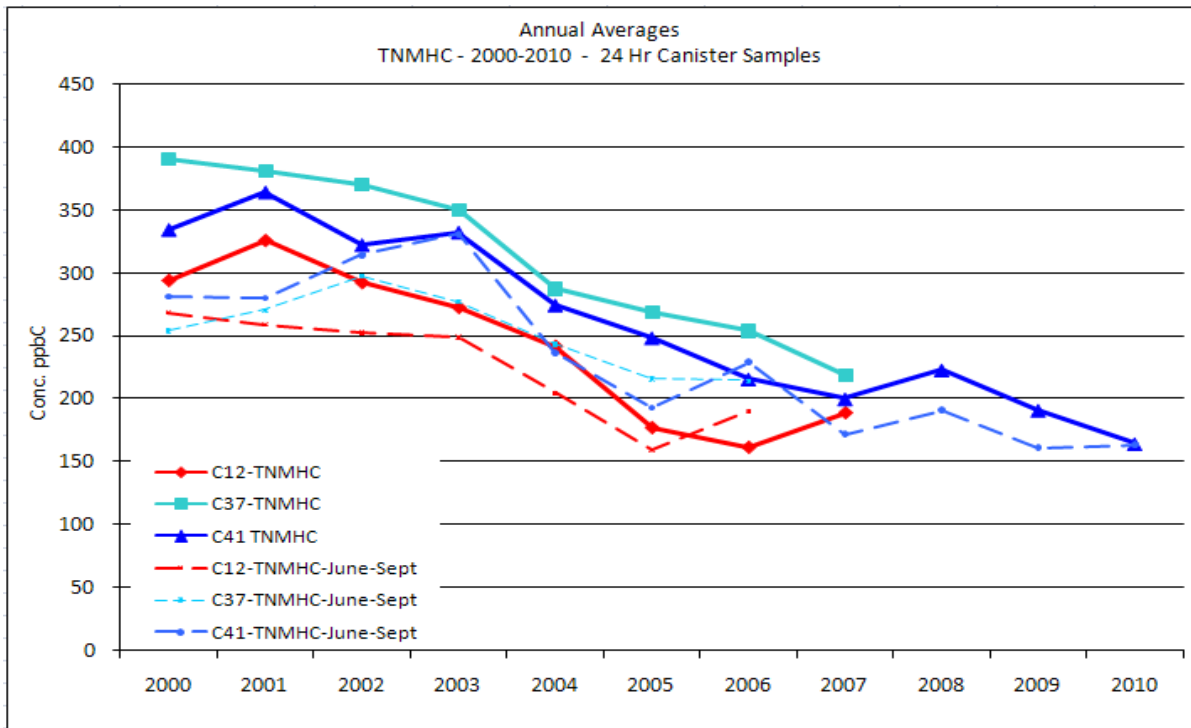


Figure 3.3 10-Year Trend - Annual TNMHC Averages from Canister Samplers

3.4.2 Air Quality Trends in Cd. Juárez, Chihuahua

Continuous ozone monitoring in Juárez city began in 1988 at the Advanced Transformer site, C661, shortly following the signing of Annex V to the La Paz Agreement which established an air quality study area encompassing the El Paso, Juárez, and southern Doña Ana County, NM region. Archived ambient monitoring data became readily accessible in 2003 following integration of the Juárez air monitoring network into the TCEQ LEADS air monitoring network.

In Juarez, the 1st, 2nd, 3rd, 4th, and 5th highest daily maximum 8-hour average ozone concentrations in 2006 were dominated by measurements taken at C663 which is located at an industrial manufacturing facility approximately 2 km from the El Paso-

Juárez international border. Figure 3.4 illustrates an 8-year trend of ozone exceedance days in Juárez.

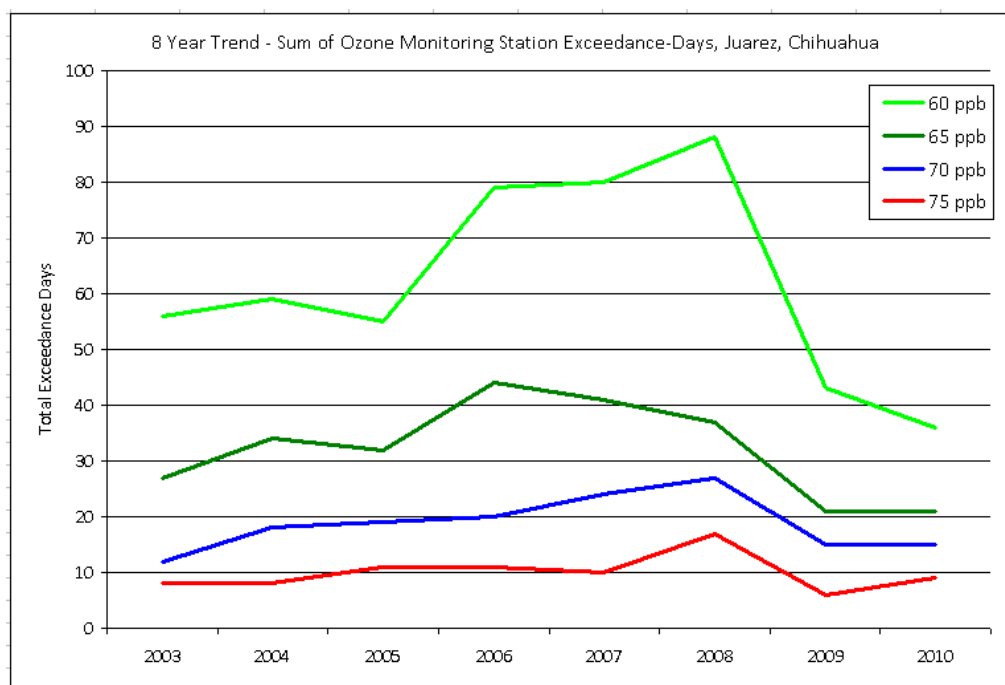


Figure 3.4 8-Year Trend - Sum of Ozone Exceedance-Days, Juárez

On a year after year basis the number of exceedances of the 8-hour ozone design values for Juárez have not improved. Juárez has on average ~10 exceedance days year after year of the 0.075 ppm 8-hour average ozone NAAQS.

3.5 Other Air Pollutants in the PdN

Pollutants for which El Paso has been previously designated nonattainment include carbon monoxide (CO) and particulate matter with an aerodynamic diameter of 10 microns or less (PM10). El Paso was at one time designated nonattainment of the 1-hour ozone standard of 125 ppb, but that standard is no longer applicable to El Paso.

3.5.1 Carbon Monoxide

Figure 3.5 identifies the trend of carbon monoxide concentrations at 2 CAMS which are located both east and west of the US - Mexico Bridge of the Americas in the center of the PdN airshed.

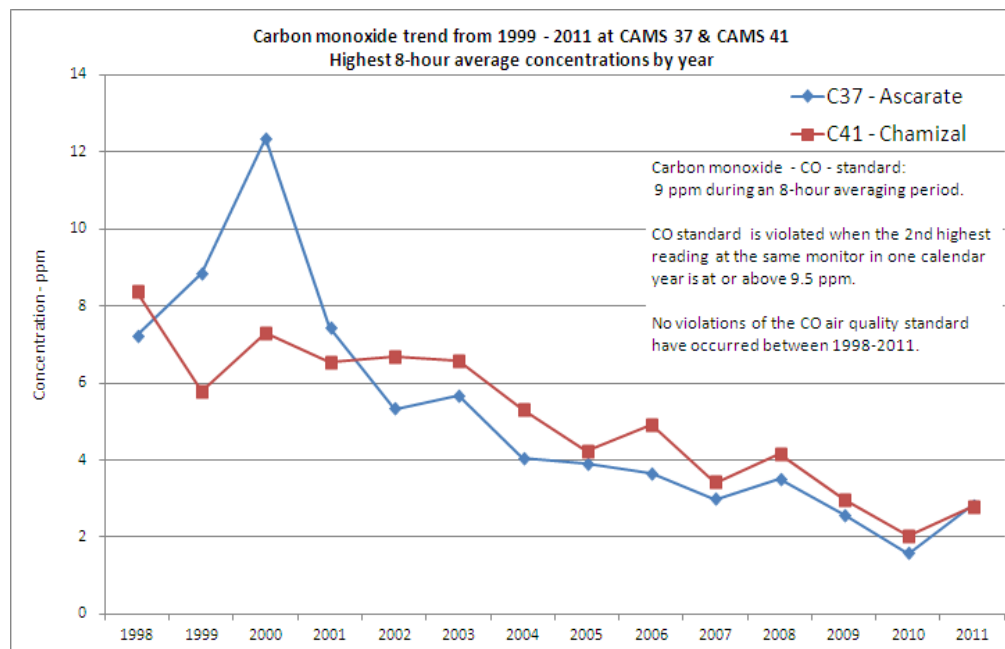


Figure 3.5 Carbon Monoxide Trends at 2 El Paso CAMS

Both C37 and C41 report the highest CO concentrations in El Paso, yet after 2006, the levels are less than 50% of the 9.0 ppm 8-hour average CO NAAQS. El Paso was designated attainment maintenance of the CO standard in 2005. As such all control strategies identified in the CO SIP remain active in order to prevent “backsliding” into nonattainment. CO concentrations were measured during the CAMx simulation. They provide a surrogate tool to assess elevated concentrations from source classifications such as mobile sources and movement of this pollutant to adjacent cells.

3.5.2 Particulate Matter

El Paso is designated nonattainment of the NAAQS for particulate matter with an aerodynamic diameter of 10 microns or less (PM_{10}). Control strategies specified for attainment of the PM_{10} NAAQS include paving all of the public and 2-way industrial roadways in the City of El Paso and street sweeping on a regular basis. El Paso tends to exceed the PM_{10} NAAQS during high-wind events when wind gusts exceed 30 MPH. However, when meteorological conditions form to produce high wind speeds and gusts, an exemption in the PM_{10} SIP allows El Paso to be waived from violating the PM_{10} standard when monitored concentrations exceed the NAAQS which is established at 150 micrograms per cubic meter ($\mu g/m^3$) during a 24-hour averaging period.

PM_{10} consists primarily of geologic material which has been mechanically ground by the contact of vehicle tires over unpaved roadways, at rock quarries, or other similar industrial facilities. However, during high-wind events the dust in the surrounding area may be carried aloft and transported into the El Paso international airshed. The PM_{10} SIP has granted exemptions to El Paso from any exceedances which occur during high-wind events.

El Paso was assessed for compliance with the NAAQS for $PM_{2.5}$ which is particulate matter with an aerodynamic diameter of 2.5 microns or less. The multiple assessments undertaken by TCEQ, UTEP and other institutions indicate that El Paso attains the $PM_{2.5}$ NAAQS. $PM_{2.5}$ has five major precursors that contribute to the development of the aerosol including ammonia, nitrates (NO_x), sulfates (SO_x), VOC, and directly emitted mechanically ground geologic materials. Sources of $PM_{2.5}$ consists of accumulated ultra-fine aerosols such as sulfates and nitrates from industrial and agricultural operations, and diesel exhaust emissions from locomotives, plus heavy- and light-duty vehicles.

4 Reactive Hydrocarbons and Oxides of Nitrogen

Ozone formation is driven by a combination of favorable meteorological factors and a reactive mixture of volatile organic compounds (VOC) and oxides of nitrogen (NO_x). Reactivity in regards hydrocarbons refers to “the potential of a given volatile organic compound to make ozone” (Carter, 1994). Some VOCs make ozone much more effectively than other less reactive VOC.

Photochemical modelers would prefer to have an EI of individual chemical species to place into their models. Unfortunately, the EI is generally not available in that level of detail. Previous research reports that EIs may underreport VOC by 10 to 100-fold (TCEQ, 2006). The purpose of this discussion is to highlight the complexity of addressing VOC emissions in photochemical modeling given the broad array of compounds that form this class of pollutants. As will be noted the role that VOC play in the formation of ozone in the PdN region is far more important than the role of NO_x. Understanding the complexity of this pollutant class may improve the precision in photochemical modeling.

4.1 Speciation of Volatile Organic Compounds

Speciation is the top-down process of breaking a prepared emissions inventory (EI) of criteria pollutants into preferably compound-specific constituents. Historically, photochemical modelers rely on national databases such as SPECIATE or AP-42/FIRE. Annually, and as part of the EI submittal process, industry voluntarily submits speciated emission reports.

A speciation profile for an emission-generating process is a list of constituent compounds and the mass fraction of each. Since many speciation profiles may exist for one type of process or source classification code (SCC), depending on area of the country and the specifics of the process, it is necessary to tie a specific profile to a specific process via cross-reference. It is possible for several units or processes to use the same speciation profile so many units or processes can point to one speciation profile.

Gasoline is a major source of air pollution which has two different speciation profiles. Gasoline vapor emitted through volatilization from storage tanks is very different from combusted gasoline. Additionally, summer gasoline differs from winter gasoline in composition. Gasoline distributed in El Paso during summertime is formulated to reduce both NO_x emissions and volatilization by adding components which reduce the Reid Vapor pressure (RVP). During the summer months this is known as low-RVP gasoline.

4.2 VOC Reactivity

Volatile organic compounds (VOC), as previously stated, are principal components of the photochemical reaction which produces ozone. VOCs containing 2-8 carbon atoms are monitored at Photochemical Assessment Monitoring Stations (PAMS) using an automatic gas chromatograph (auto-GC). Reactivity of the VOCs is associated with the number of double bonds and chemical structure. Double bonds increase the reactivity of the hydrocarbon molecules.

Straight-chain hydrocarbons with single bonds are identified as alkanes and considered saturated. Alkanes are considered to be the least reactive of the nonmethane hydrocarbons given the single bond is much stronger than molecules with double bonds (TCEQ, 2008). VOC reactivity scales such as those identified in Table 4.1 classify the extent to which particular species of VOC promotes the formation of ozone based on maximum incremental reactivities.

4.3 Maximum Incremental Reactivity

Several reactivity scales are in use to express the reactivity of hydrocarbons in the atmosphere. The two most popular are the hydroxyl (OH-) and the maximum incremental reactivity (MIR) scales. MIR is a measure of the maximum amount of ozone that can be formed by adding an incremental amount of a particular VOC to a mixture of NO_x-rich air. Units are grams of ozone produced per gram of VOC injected into the system (TCEQ, 2008).

MIR is calculated from smog chamber experiments and photochemical modeling. William Carter of the University of California at Riverside is the pioneer and leading expert in this field. Table 4.1 presents an excerpt from Carter's MIR reactivity scales (Carter, 1994).

Auto-GC data are available for C41 located at Chamizal National Memorial. The analysis concluded that while some compounds (e.g., alkanes – saturated long-chain hydrocarbons with single carbon bonds) occasionally caused high reactivity, those frequently responsible for high ozone formation days were alkenes (propylene,

ethylene, butenes [1-butene, cis-2-butene, trans-2-butene], and 1,3-butadiene) all of which have double bonds.

Table 4.1 Maximum Incremental Reactivity (IR) Table Excerpt

Compound	MIR
2-Methyl-2-Butene	14.45
trans-2-Butene	13.91
1,3-Butadiene	13.58
cis-2-Butene	13.23
Propene	11.58
1,2,3-Trimethyl Benzene	11.26
1,3,5-Trimethyl Benzene	11.22
Isoprene	10.69
m-Xylene	10.61
1-Butene	10.29
cis-2-Pentene	10.24
trans-2-Pentene	10.23
Ethene	9.08
1-Pentene	7.79
o-Xylene	7.49
Acetylene	1.25
2,3,4-Trimethyl Pentane	1.23
2-Methyl Heptane	1.20
2,3-Dimethyl Butane	1.14
n-Octane	1.11
n-Nonane	0.96
n-Decane	0.83
Benzene	0.82
Propane	0.56
Methane	0.0139

4.4 Maximum Allowable Emissions Rate Tables

From an emissions modeling and industrial permitting perspective, the Maximum Allowable Emission Rate Table (MAERT) is developed to identify HRVOCs emitted by

an industrial facility. The MAERT is primarily a guideline used for SIP planning purposes in order to limit the emissions entering a modeling airshed from an industrial facility and to assist air quality planners in calculating the mass of HRVOC emitted by the facility.

The specific compounds identified within the MAERT are consistent with the definition of an HRVOC under 30 TAC §115.10 and should be identified on an emissions point basis for all process vents, flares, and cooling towers authorized by the permit. As defined in 30 TAC §116.10, a MAERT is included with a preconstruction permit issued under Chapter 116 that contains the allowable emission rates established by the permit for a facility (TCEQ, 2012).

For MAERTs within a flexible permit, the HRVOC emissions from all process vents, flares, and cooling towers under the VOC cap should be separated into individual caps for each species of HRVOC (TCEQ, 2005). TCEQ established a rule change requiring the identification of specific species listed in the MAERT as well as reporting on an annual and hourly basis for the purpose of controlling emissions of highly reactive VOCs (TCEQ, 2005r). Through these procedures it is expected that emission inventory data will be of sufficient accuracy for use in photochemical modeling with improved results.

4.5 Highly Reactive VOCs

As reported in the TexAQS 2000 Field Study (TexAQS, 2000), highly reactive VOC (HRVOC) species were found to be in larger proportion than expected. Ethylene and propylene are generally the most important contributors to total reactivity-weighted concentration in the Houston airshed (TexAQS, 2000). The potential exists for similar

conditions in El Paso due to the operation of a refinery located at the center of the binational community.

4.5.1 Big 12 HRVOCs

Various TCEQ investigations identified the “Big 12 HRVOCs” which play an important role in the rapid formation of ozone in other regions of Texas with petroleum refining activities (Jolly, 2004). The “Big 12 HRVOCs” are listed in Table 4.2. Concentrations of species such as ethylene and propylene in ambient air were often found to be many times larger than could be explained by reported emissions inventories.

Table 4.2 Original "Big 12" HRVOC

HRVOC Name	Potential Source(s)
Propylene	Refineries and plastics
Ethylene	Petroleum refining
Formaldehyde	Combustion & ethylene oxidation
Acetaldehyde	Vehicle emissions
Isoprene	Natural emissions from pine trees
Butenes	Petroleum refining
1,3-butadiene	Petroleum refining
Toluene	Gasoline emissions & refineries
Pentenes	Petroleum refining
Trimethylbenzenes	Gasoline emissions & refineries
Xylenes	Gasoline emissions & refineries
Ethyltoluenes	Gasoline emissions & refineries

Successfully modeling pollutant concentrations observed during the various studies of the Houston-Galveston-Beaumont area necessitated adjustments to reported emissions inventories once again indicating the underreporting of certain HRVOCs in the EI of industrial facilities. (Jolly, 2004)

Adjusting EIs to account for unreported HRVOC emissions and modifying input parameters for photochemical model runs on updated emissions of these specific compounds presented a set of unique challenges to photochemical modelers, since emission processing software typically is not designed to apply adjustments or controls to individual VOC species (Jolly, 2004).

4.5.2 VOC Group Names and Constituents

Continued research into the sources of VOC and EI underreporting established VOC Groups and Constituents (Jolly, 2004). Jolly reports a study that was undertaken to continue assessing the potential underreporting of VOCs in the industrial point source EIs from petrochemical facilities in the Houston shipping channel. The results of this investigation indicate that VOC emission inventories continue to be severely underreported by up to 9-fold while NO_x EIs are assumed to be reported correctly (Jolly, 2004).

The problem with developing accurate EIs apparently continues to be due to fugitive emissions from valves, flares, cooling towers, and spills. It is possible that the current research may also observe underestimated VOC emissions from the local refinery as well as other area sources such as VOC and NO_x emissions generated at the international bridges which are not reported in any emissions inventory.

Table 4.3 identifies VOC Groups and Constituents (Thomas, 2008). This particular study identified VOC species reported by the multiple auto-GC's deployed in Houston and based on wind directions as well as dispersion modeling comparing the emissions inventory to monitored VOC concentrations at specific distances from the sources.

Table 4.3 VOC Group Names and Constituents

Group Name	Constituent(s)
butadiene	1,3-butadiene
butanes	isobutane, n-butane
butenes	t-2-butene, c-2-butene, 1-butene
c5cyclos	cyclopentane, cyclopentene
c6arom	benzene
c6cyclos	methylcyclopentane, cyclohexane
c7c10arom	m/p-xylene, o-xylene, m-ethyltoluene, p-ethyltoluene, o-ethyltoluene, 1,3,5-trimethylbenzene, 1,2,4-trimethylbenzene, 1,2,3-trimethylbenzene, toluene, ethylbenzene, isopropylbenzene, npropylbenzene, m-diethylbenzene, p-diethylbenzene, styrene
c7c11other	methylcyclohexane, 2,4-dimethylpentane, 2-methylhexane, 2,3-dimethylpentane, 3-methylhexane, n-heptane, 2,2,4-trimethylpentane, 2,3,4-trimethylpentane, 2-methylheptane, 3-methylheptane, n-octane, n-nonane, n-decane, n-undecane
ethene	ethene
hexanes	n-hexane, 2,2-dimethylbutane, 3-methylpentane, 2,3-dimethylbutane, 2-methylpentane pentanes isopentane, n-pentane
pentenes	2-methyl-2-butene, t-2-pentene, 3-methyl-1-butene, 1-pentene, c-2-pentene
propene	propene

This Houston study also made broad assumptions requiring additional attention. It assumed that the wind direction was associated with the sources located in the direction from which the winds approached the monitoring stations. This assumption ignores possible mixing and circulating winds within the Houston airshed. A similar situation may exist in the PdN area. Given the complex terrain and the various mountain ranges which trap pollutants within the airshed it is important to assess the sources of VOC emissions across the region.

The VOCs identified in Table 4.3 tend to be produced primarily at refineries and are constituents of vehicular combustion processes. El Paso's refinery located in the center of the binational community plus high motor vehicle volumes at the international Ports of Entry as well as local roadways continue to be major sources of regional VOC and NO_x emissions. On high ozone days the stable atmospheric conditions do not favor the rapid dispersion of point or fugitive emissions from the facility as well as mobile source emissions.

The local mountain ranges also serve to trap most of the regional pollutants causing a build-up of local pollutants. Calm wind conditions from variable directions as will be indicated in the section of this report on wind statistics prevent the dispersion of pollutants. This variability of wind direction may also make it difficult to confirm the exact sources of emissions which contribute to the formation of regional ozone.

Several studies have also reviewed the role of early morning VOC:NO_x ratios. These studies looked at various VOC:NO_x ratios continuing on the assumption that NO_x EIs were correct and VOC EIs were underreported.

4.6 TNMHC / NO_x Ratios

A preliminary assessment of PAMS data in relation to the formation of ozone involves comparing the total non-methane hydrocarbon (TNMHC) and NO_x concentrations. It is important to note that the OH⁻ radical has a key role in the sequence of reactions which form ozone (Seinfeld, et.al., 1998). Equation 4.1 identifies the generalized TNMHC:NO_x ratio:

$$Q = \text{TNMHC}[\text{ppbC}] / \text{NO}_x[\text{ppbV}] \quad \text{Equation 4.1}$$

where Q = the ratio of total nonmethane hydrocarbons to nitrogen oxides.

A $Q < 5$ indicates VOC-limited conditions. The low ratio indicates that variations in NO_x do not significantly influence ozone formation. A $Q > 15$ indicates NO_x-limited conditions. This indicates ozone formation is limited by availability of NO_x rather than VOCs. A ratio where $5 \geq Q \geq 15$ indicates transitional conditions and both NO_x and VOC controls may be more effective at reducing ozone concentrations. The PdN region tends to fall within the transitional zone, and regional air quality may improve through reductions of both NO_x and VOC emissions.

TNMHC from both biogenic and anthropogenic sources are involved in the formation of ozone and are progressively oxidized to CO and CO₂ over periods of hours to weeks (Paulson, 1999). There currently is no consensus regarding the compounds identified in the quantification of TNMHC to calculate the ratio due to the wide variability in incremental reactivity and reaction products formed by oxidation of the hydrocarbons (Thomas, 2008). Some VOC species with double bonds present high incremental

reactivity and are highly reactive while saturated hydrocarbons have significantly slower reactivity and have a limited role in the formation of ozone.

The PdN region is primarily impacted by five types of ozone-precursor emissions of varying reactivities with respect to ozone production ability. These five types of emissions are as follows:

- Highly reactive industrial VOC emissions (HRVOC) from the local refinery in the center of the region;
- Anthropogenic VOC emissions, other than HRVOCs, primarily from mobile sources and other ordinary urban area sources, occurring throughout the PdN region;
- Biogenic emissions from local agricultural operations as well as the natural flora.
- Mobile source NO_x and VOC emissions; and
- Industrial NO_x emissions from sources located both within the urban centers and throughout the binational community.

As a result of the multiple sources of precursor emissions, the TNMHC:NO_x ratios throughout the region vary widely as do the reactivities producing ozone throughout the community. Some species ratios may help identify dominant source categories. Investigating ratios of individual chemical species may help to identify the presence of unique regional sources for a species at a particular monitoring site. Mobile sources for example are a major contributor to hydrocarbon emissions from high roadway traffic areas. Vehicular traffic is ubiquitous across the urban zones and concentrated at the international Ports of Entry and congested roadways.

It is useful to examine ratios of ambient hydrocarbons that are characteristic of motor vehicles and to compare them to the ratios of the same species reported in the emission inventory. Ratios commonly used to identify mobile source emissions include acetylene:benzene, toluene:benzene, xylene:benzene, ethylene:acetylene, CO:benzene, and CO:acetylene (Main et al., 1999).

The “Big 12 VOC” species mentioned above play a major role in ozone formation and summation of TNMHC (Jolly, 2004). There are limitations to consider regarding the value of the TNMHC:NO_x ratio given this method is considered sound, but the following factors should be considered (EPA, 1996).

- Application of TNMHC:NO_x ratios rely upon morning, center-city TNMHC and NO_x measurements;
- The TNMHC:NO_x ratio will vary widely in time and space;
- Ratios delineating NO_x- and VOC-limited regimes vary with time and location and are affected by vertical mixing processes that often are not accounted for in surface meteorological measurements;
- The age of the air mass undergoing photochemical reactions may not have lower concentrations of HRVOC or elevated NO_x which has a longer residence time in the atmosphere than VOC. This may impart different control responses at the same TNMHC:NO_x ratios; and
- Inconsistent and uncertain measurement techniques affect the ratio. These include various interpretations of TNMOC as well as different MIR values for the VOCs considered in the TNMOC concentration.

4.6.1 Empirical Kinetic Modeling Approach

The Empirical Kinetic Modeling Approach (EKMA) was developed to assess limiting factors in the formation of ozone. The EKMA approach is based on the generation of a series of ozone isopleths using a model called the ozone isopleths plotting package (OZIPP). Figure 4.1 illustrates two types of EKMA diagrams. The EKMA model puts forward the concept that maximum afternoon ozone levels are dependent on the morning concentrations and mixing ratios of TNMHC and NO_x (EPA, 1994). The time period between 6 AM to 9 AM is considered most appropriate for assessing precursor levels which lead to production of elevated ozone concentrations.

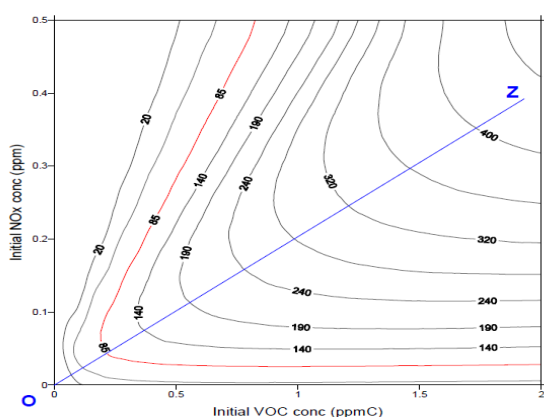


Figure 4.1a

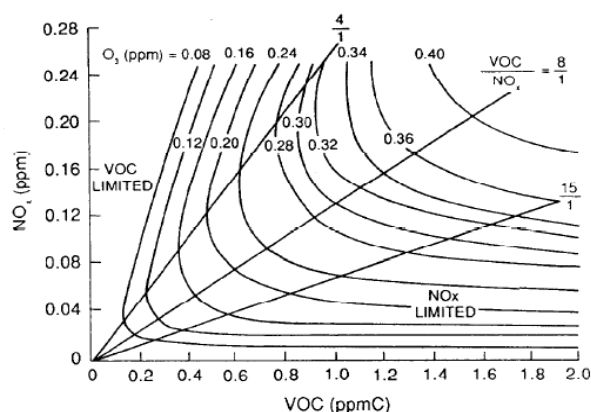


Figure 4.1b

Figure 4.1 Examples of EKMA Diagrams

Mobile source emissions of VOC and NO_x are typically elevated due to the morning commute, and photochemical activity is minimal between 6 AM to 9 AM before sunlight and warm temperatures start accelerating the photochemical reactions. It is important to note that elevated ozone is not due only to precursors but also to regional

transport of ozone into a monitoring domain. This variable is considered in developing the boundary conditions applied to the photochemical model.

Air quality monitoring agencies conduct targeted VOC monitoring utilizing summa canisters and carbonyl cartridges during those specific hours. TCEQ conducts canister sampling in El Paso at several CAMS between 6 AM to 9 AM on days when meteorological conditions favor the formation of ozone. As indicated in Figure 4.1b, three zones can be established on the EKMA chart when plotting TNMHC:NO_x ratios: a NO_x-limited zone, a transitional zone, and a VOC-limited zone.

Higher and lower ratios imply NO_x- and VOC-limiting conditions, respectively. However, depending on whether ozone formation is limited by VOC or NO_x depends on other factors in addition to the TNMHC:NO_x ratio. It is assumed in the EKMA diagrams that ratios greater than >15 were considered NO_x-limited and ratios less than <5 were considered VOC-limited (EPA, 1996).

4.6.2 NO_x-Limited Conditions

A $Q > 15$ indicates NO_x-limited conditions which are conducive to ozone exceedances but which exceedances cannot be prevented through anthropogenic VOC control. At high VOC to NO_x ratios ($Q > 15$), an area is considered NO_x-limited, and VOC controls may be ineffective. Such conditions occur when biogenic VOC emissions alone can cause ozone exceedances. These conditions tend to occur in heavily forested areas where pine trees emit highly reactive isoprene.

Regions which may present a different type of NO_x-limited conditions may be associated with hydrocarbon fracturing (or “fracking”) operations. VOCs in these areas are emitted into the atmosphere as wastewater or drilling fluids are pressurized into the

subsurface strata during drilled for natural gas and petroleum hydrocarbons. Pressurized fluids force VOC and other gases out of the soil strata and to the surface. In general, increasing VOC concentrations may produce elevated ozone concentrations even during cold winter days (NOAA 2011, Carter 2012).

4.6.3 VOC-Limited Conditions

A $Q < 5$ indicates VOC-limited conditions. VOC reductions in VOC-limited regions are most effective in reducing ozone concentrations. The VOC-limited condition indicates that modifications in NO_x concentrations do not significantly influence ozone reductions and NO_x controls may actually lead to ozone increases. VOC-limited conditions are defined to be all those conditions that are not NO_x-limited, that is, conditions conducive to exceedances but where the exceedances can be prevented through control of either VOC or NO_x alone or a combination of both. Increasing NO_x may also lead to either more or less ozone depending on the prevailing TNMHC:NO_x ratio (Seinfeld, 1998).

4.6.4 Transitional Conditions

When TNMHC:NO_x ratios are at intermediate levels ($5 \leq Q \leq 15$), a combination of VOC and NO_x reductions may be warranted. It should be noted that photoreactivity of VOC reduces over the duration of the day as the air mass ages and VOCs are oxidized to CO₂. The TNMHC:NO_x ratio provides a useful perspective for developing local and regional control strategies. The effectiveness of the control strategies may then be assessed over time notwithstanding changes in emissions that develop at future dates.

Strategy development is based entirely on emissions estimates and photochemical model results of questionable or at best unknown accuracy (EPA, 1994). This being the case multiple iterations of the model must be run to achieve the following:

- Assess the effectiveness of the baseline model to obtain a relative response as close to OBSERVED ozone concentrations values as possible.
- Obtain a normalized error (NE) of $\leq 35\%$ which is considered an acceptable level of allowable error (or spread) between OBSERVED and PREDICTED concentrations (ENVIRON, 2012).
- Modify emissions reduction strategies and therefore emissions input data into the model to predict ozone concentrations concurrent with the emissions reductions.
- Properly adjust emissions inputs to account for increases in emissions to properly model future-case ozone scenarios.

Figure 4.2 illustrates daily TNMHC:NO_x ratios observed at C37 in 2006. The data is based on 6-day canister sampling events and comparison of concurrent day and hour NO_x concentrations. Focusing on June 16, 2006, prior to the June 18 ozone event, the ratio exhibited primarily VOC-limited and minimal transitional conditions.

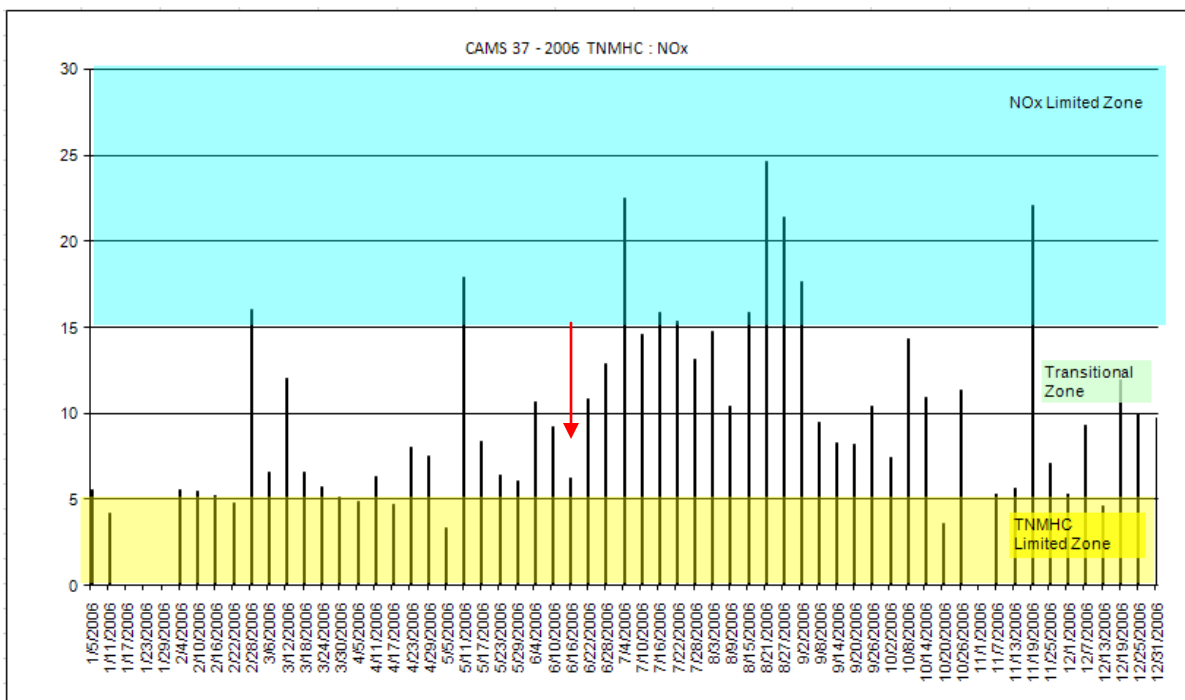


Figure 4.2 2006 TNMHC:NOx Ratios Based on 6-day canister sampling at C37

Figure 4.3 illustrates 24-hour TNMHC:NOx ratios for June 2006. TNMHC:NOx ratios for the most part of the month June 2006 were in the transitional range. Only 6 days of the month were in the NOx-limited zone and only 1 day was in the VOC-limited range. The day of interest in this dissertation, June 18, had only one hour where the TNMHC:NOx ratio was in the NOx-limited range. It should be noted that the hours of 6 AM – 9 AM are used to determine the limiting aspects of ozone formation. The purpose for observing early morning TNMHC:NOx ratio is VOCs have not been oxidized or photochemically reacted compared to TNMHC components as the air mass ages.

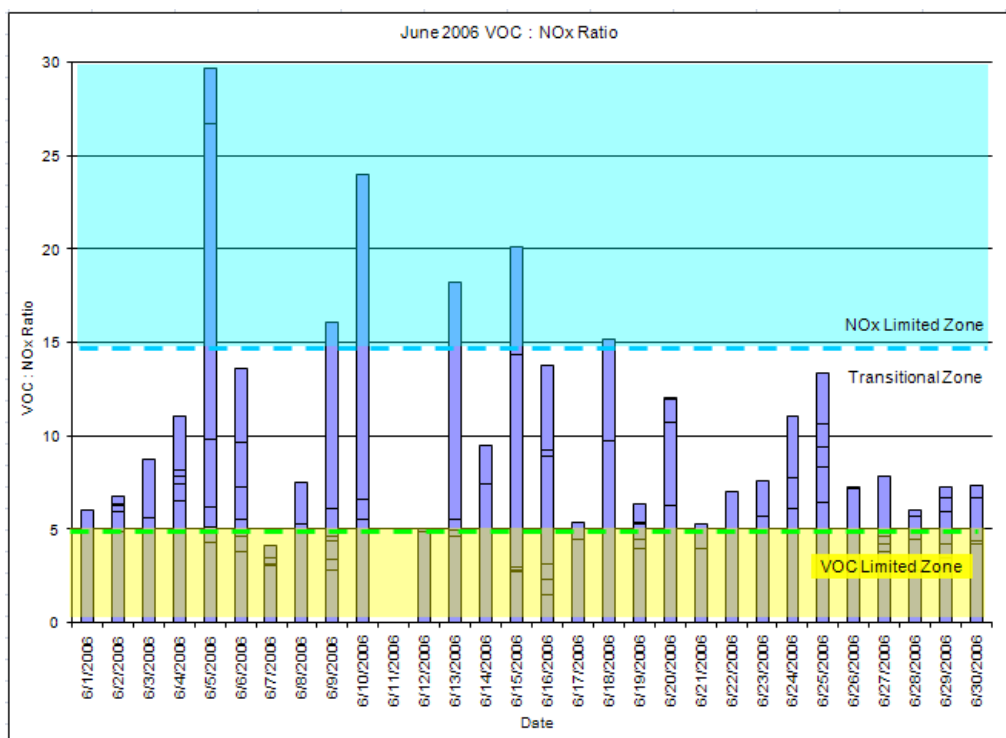


Figure 4.3 June 2006 TNMOC:NOx Ratios at C37

Figure 4.4 shows the diurnal variation of TNMHC:NOx levels for June 18, 2006 ozone event. On this day El Paso and Juárez CAMS observed ozone exceedances at all stations except C12. The highest 8-hour ozone concentration observed in El Paso was 88 ppb at C414 in east El Paso while in Juarez the highest 8-hour ozone concentration reached 94 ppb at C663 in northeast Juárez.

The orange vertical bar in Figure 4.4 indicates the 8-hour average period at which the ozone exceedance began at C37. The specific hour indicating the pollutant reading is based on 5-minute averages reported during the hour moving forward (10:00 to 10:59). During the hours of 7 AM to 9 AM the TNMHC:NOx ratio was in the VOC-limited zone.

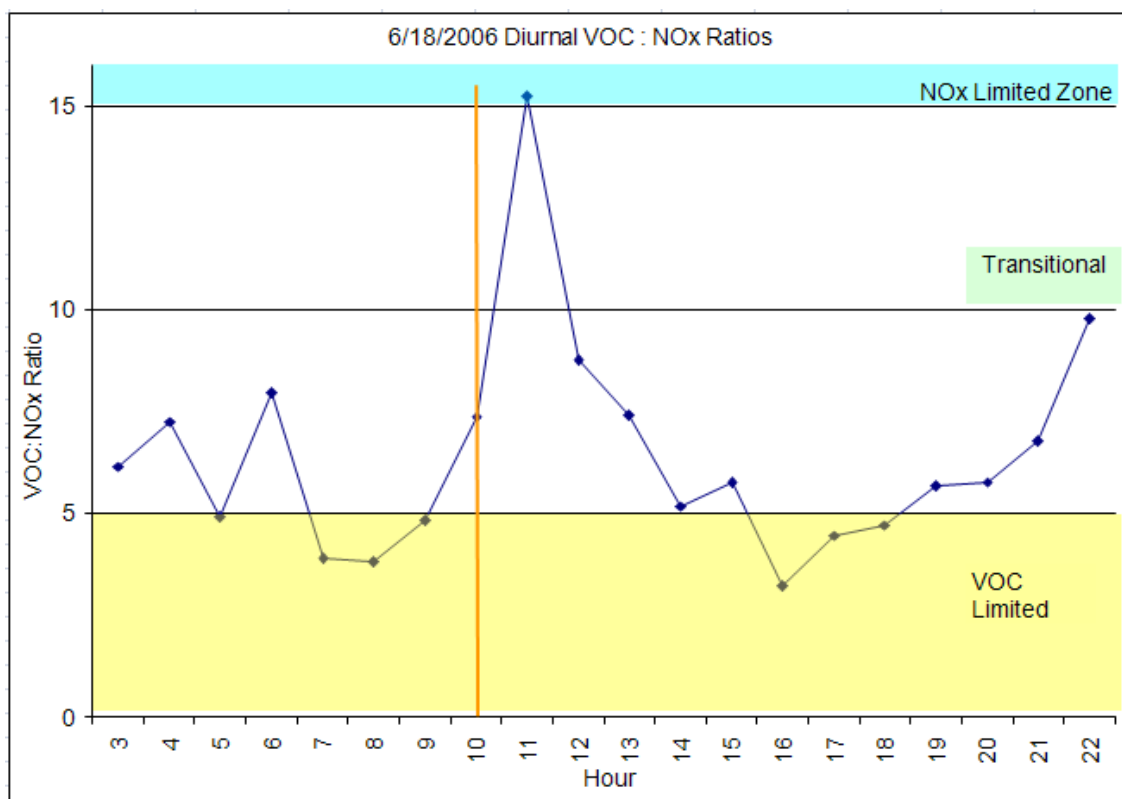


Figure 4.4 June 18, 2006 TNMHC:NOx Ratios

Figure 4.5 presents TNMHC:NOx ratios for July, 2006. NOx-limited conditions occur only 4 days of this month. The majority of the month observes a ratio in the transitional zone. On 10 July, 2006, C37, C49, C661, and C663 observed elevated 8-hour average ozone concentrations of 74 ppb, 81 ppb, 61 ppb, and 81 ppb respectively. On 11 July, 2006, C12, C37, and C41 observed the highest 8-hour ozone concentration of the year with concentrations of 92 ppb, 90 ppb, and 89 ppb respectively.

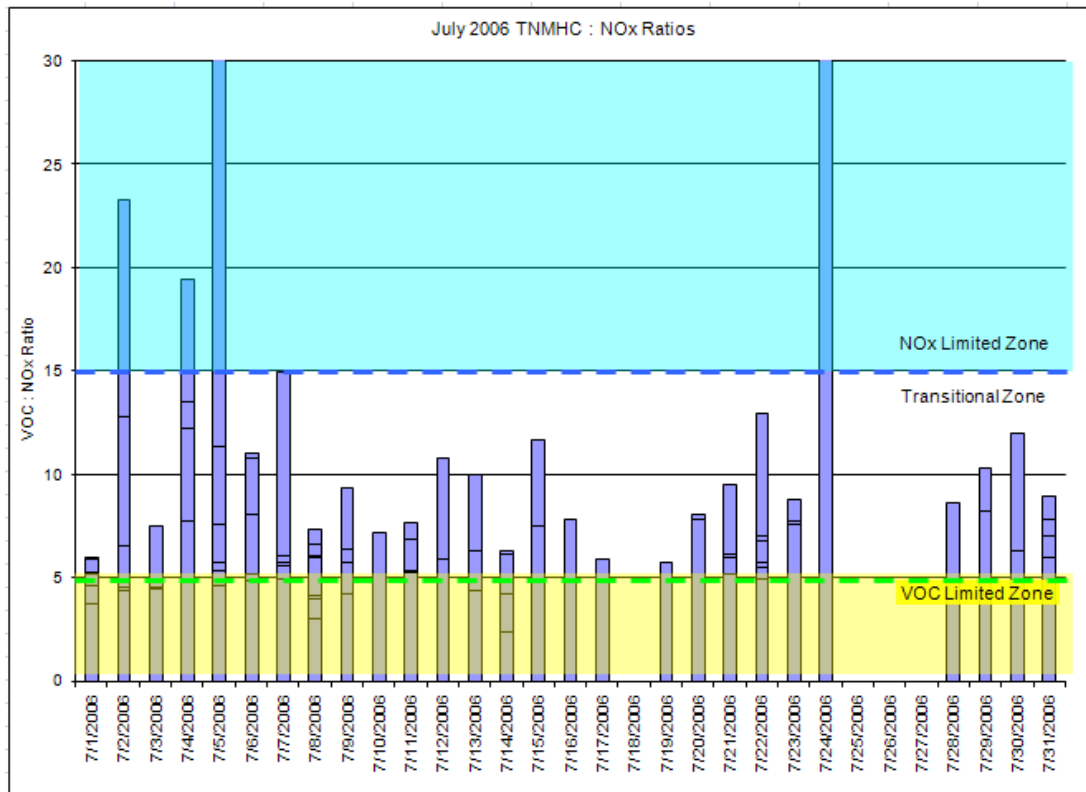


Figure 4.5 July 2006 VOC:NOx Ratios

The hourly diurnal TNMHC:NOx ratios at C37 on 11 July, 2006 are provided in Figure 4.6. Early morning ratios were primarily in the VOC-limited range. A minimal spike in the ratio was observed at 10 AM prior to the hour at which the exceedance was observed. The 8-hour average ozone exceedance was observed at 11 AM at C12, C37, and C72 and 10 AM at C41.

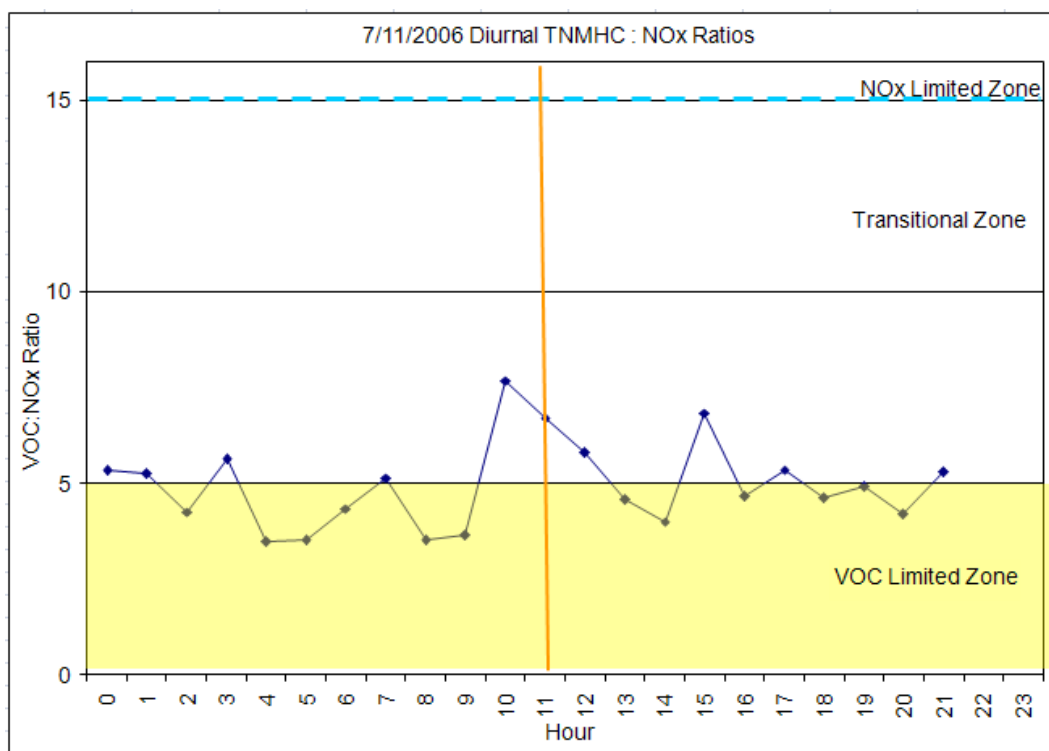


Figure 4.6 Diurnal VOC:NOx ratios during ozone event

4.6.5 CAMx Determination of VOC- or NOx- Limited Conditions

EKMA diagrams are often applied to distinguish VOC-limited from NOx limited conditions and to develop a classification based on VOC-to-NOx ratio observed during the early hours of the diurnal cycle. The EKMA approach classifies VOC- or NOx-limited behavior based on the response of the peak ozone due to the diagram being based on several hours of photochemistry. However, as indicated in the charts above, the day may begin VOC-limited and become 'transitional as the day and photochemical reactions proceed.

4.7 Summary

Ozone formation is driven by a combination of favorable meteorological factors and a mixture of NO_x and reactive VOCs. Of the multiple VOC species generated by point, area, or mobile sources, modelers must determine which are likely to be the most reactive when preparing strategies to reduce ozone concentrations.

The concept of VOC- or NO_x-limiting conditions is constantly reviewed due to the inconsistency associated with the VOC species selected as TNMHC when determining the TNMHC:NO_x ratio. Reactivity in regards hydrocarbons refers to “the potential of a given volatile organic compound to make ozone”. Some VOCs with double carbon bonds make ozone more effectively than other less reactive saturated VOCs.

Photochemical modelers would prefer to have an EI of individual chemical species to place into their models. Unfortunately, the EI is generally not available at that level of detail. Previous research reports that EIs may underreport VOC from 10 to 100-fold (TCEQ, 2006). This consistent error in reported EIs may be due to various factors:

- Industries are charged permit fees based on tons of emissions. Underreporting emissions may save the entity thousands of dollars annually in operating fees;
- The emissions level at which major sources are identified is lower in regions designated nonattainment of the NAAQS. In order to comply with Federal air quality permitting rules and regulations established by the Federal Clean Air Act regarding maximum allowable emissions, entities may underestimate total emissions if doing so prevents the source from being considered a “major source”. Underreporting may be necessary in order to not surpass the maximum allowable emissions limits;
- Fugitive emissions from floating roofs, spills, leaky valves and other unknown factors at industrial facilities are neither accounted for nor reported;

- Lax enforcement of environmental rules and regulations by the a state or federal regulatory entity may allow industry to exceed emissions limits compared to limits allowed by permits;
- Upset / Maintenance rules allow entities to emit large concentrations of VOC emissions in order to achieve a satisfactory or less dangerous operating level;
- The surrogate estimate is not specific when allocating emissions across the population. Populated areas with no business activity may be assigned a portion of all emissions and those with many businesses may have underestimated emissions allocations; and
- Entities which generate air pollution emissions will look for any method of not reporting all emissions generated at their facilities. Doing so is costly due to the per-ton permit fee.

5 State Implementation Plan for Control of Ozone Pollution in El Paso

A State Implementation Plan (SIP) defines a series of air quality improvement strategies which should bring a U.S. county or metropolitan statistical area into attainment of the NAAQS (or standard) which has been violated. For example, the 8-hour and 1-hour ozone standards specify the time at which a violation of the standard occurs.

Emission reduction requirements specified in the FCAA of 1977 and amendments of 1990 require states with ozone nonattainment areas that are classified moderate or greater to reduce ozone precursors an amount of sufficient quantity to attain the standard. The state with the nonattainment area submits a SIP to the EPA defining the series of air quality improvement activities intended to bring the area into attainment of the standard which has or have been violated. EPA, in turn, reports the SIP or SIP revision in the Federal Register formally accepting the plan.

5.1 1-hour Ozone State Implementation Plan

A SIP was established for El Paso County, Texas in March 1979 identifying emissions reductions that could be achieved to reduce ozone forming precursors. The primary purpose of this SIP was to reduce VOC emissions in compliance with the 1977 FCAA. The 1977 FCAA established a statutory deadline of December 31, 1982 for demonstration of air quality planning strategies that would bring communities such as El Paso in compliance of the newly-established 1-hour ozone NAAQS. The Texas Air Control Board (TACB), predecessor to both the Texas Natural Resource Conservation Commission (TNRCC) and the Texas Commission on Environmental Quality (TCEQ)

developed this SIP. In the process, TACB stated a degree of uncertainty that VOC emissions reductions could help achieve compliance with the ozone NAAQS given previous experience in not attaining the standard in Houston, TX (TACB, 1977).

The SIP was developed due to a violation of the 1-hour ozone standard of 0.12 parts per million (ppm) when the “West” monitoring site, currently UTEP C12, had a design value of 0.160 ppm. A violation of the 1-hour ozone standard occurs when the annual average number of exceedances, over a three year period, recorded at a single monitoring site is greater than one. Four exceedances measured during a three-year period at a single air monitoring station equals one violation of the ozone standard. An exceedance of the 1-hour ozone standard is considered to be a monitored value of 0.125 ppm or greater. El Paso was classified as a serious nonattainment area at the time, and the SIP submitted for El Paso demonstrated that a 20% reduction in VOC would bring the city into compliance with the ozone NAAQS.

5.1.1 Empirical Kinetic Modeling Approach

Prior to applying the Urban Airshed Photochemical Model, EPA applied a City-Specific Empirical Kinetic Modeling Approach (EKMA) to determine the amount of VOC emissions that must be reduced to comply with the ozone NAAQS. EPA developed the *Guideline for use of City-Specific EKMA in Preparing Ozone SIPs* (EPA, 1981) which states followed in developing air quality planning strategies for regions or MSAs that were not in compliance with the ozone NAAQS. The planning document required the following variables be considered:

- Emissions inventory development;
- Air parcel trajectories;

- Mixing height;
- Non-methane hydrocarbon (NMHC) to NO_x ratios;
- Initial conditions of NMHC and NO_x;
- Emission fractions;
- Ozone aloft; and
- NO_x reduction.

A thorough explanation of each of these variables applied to the EKMA for regional air quality planning in ozone nonattainment areas is provided in TACB (1985). TACB developed a demonstration using the EKMA specifying a 15% reduction in VOC emissions would bring El Paso in compliance with the 1-hour ozone NAAQS.

§185B(2) of the FCAA (42 USC § 7511f) established studies to assess ozone sensitivity to VOC and NO_x reductions. The studies examined the roles of NO_x and VOC emission reductions, the extent to which NO_x reductions may contribute (or be counterproductive) to achievement of attainment in different nonattainment areas, the sensitivity of ozone to the control of NO_x, the availability and extent of controls for NO_x, the role of biogenic VOC emissions, and the basic information required for air quality models. These studies were instrumental in further development of the EKMA diagrams.

Guidelines provided by EPA require that the 5 days with the highest ozone levels recorded during the 3-year monitoring period at each appropriately sited monitoring station be modeled to estimate the percentage of VOC reduction required. EPA guidelines specify that the 4th highest reduction value estimated for each site be identified and the highest of these reduction values be selected as the “design”

percentage reduction value for the nonattainment area. VOC emissions must be reduced by that percentage (TACB, 1985).

5.1.2 Inspection and Maintenance SIP Revision

In July, 1992, the TACB submitted a SIP revision addressing emissions reductions from motor vehicles. The SIP required visual inspection for installation of emissions control systems such as catalytic converters. A “tailpipe” emissions test was required to assure motor vehicles emissions were within acceptable guidelines for CO and hydrocarbons. A loaded mode 2-speed test was also required to test vehicle emissions under a simulated 30 MPH load. Several other tests are also specified in the 1992 I&M SIP revision but are not applied to the El Paso area.

A SIP developed for El Paso indicated that VOC emissions would be reduced by 15% from 1990 levels and included a demonstration that El Paso County could achieve the ozone standard as a result of the 15% VOC emissions reduction plan. The Urban Airshed Model (UAM), a predecessor of CAMx, was the tool applied to model the attainment demonstration. Among the methodologies El Paso agreed to implement to reduce VOC by 15% were the following:

- Deployment of Stage I and Stage II vapor recovery systems at almost all gasoline stations;
- Distribution of low-Reid vapor pressure (low-RVP) gasoline during the summer ozone season;
- A vehicle inspection and maintenance (I & M) program;
- Solvent control strategies at auto paint body shops; and
- Specified VOC emissions controls at local point sources.

As indicated earlier, El Paso County's proximity to Cd. Juárez affects air quality improvement planning strategies given Mexico's laws, rules, and regulations which are unlike El Paso's. As a result, §818 of the 1990 FCAA Amendments incorporates §179B which contains special provisions for nonattainment areas that are affected by emissions emanating from outside the United States. EPA approved a SIP for El Paso County under §179B when the Texas TNRCC (renamed the TCEQ) established to the EPA's satisfaction that implementation of the plan would achieve timely attainment of the NAAQS "but for" emissions emanating from Cd. Juárez.

5.2 Development of the 8-hour Ozone SIP

What follows is a brief history of the 8-hour ozone NAAQS and its impact on El Paso. A Federal Register notice published April 30, 2004, (69 FR 23858), identified areas designated by EPA as nonattainment of the 8-hour ozone NAAQS. This was a culmination of reviewing MSA's across the country for compliance with the 1997 8-hour standard established at 0.085 ppm. El Paso County was designated attainment with an effective date of June 15, 2004.

On March 27, 2008, EPA strengthened the primary and secondary 8-hour ozone standard to 0.075 ppm (73 FR 16436). On March 10, 2009, the Governor of Texas recommended to EPA that El Paso County be designated in nonattainment of the 2008 ozone standard. In September 2009, EPA announced it would reconsider the 2008 NAAQS. On January 19, 2010, EPA proposed to lower the primary ozone standard to a range of 0.060 – 0.070 ppm (75 FR 2938). EPA also proposed a separate secondary standard based on cumulative seasonal average ozone concentrations. On September

2, 2011, EPA withdrew the proposed revision to the ozone standard at the request of President Barak Obama.

In a memo dated September 22, 2011 from EPA Assistant Administrator Gina McCarthy, EPA announced that it would proceed with initial area designations under the 2008 8-hour ozone standard, starting with the recommendations states made in 2009 and updating the recommendations with the most current, certified air quality data (2008 through 2010). On May 21, 2012, the EPA published in the Federal Register final designations for the 2008 8-hour ozone standard (77 FR 30088). El Paso County was designated attainment / unclassifiable under the 2008 8-hour ozone NAAQS, effective July 20, 2012. This designation, however, requires El Paso to continue applying the air quality planning strategies established by all previous SIPs in deference to what are considered the “anti-backsliding provisions” (40 CFR 51.905(c)).

5.3 8-Hour Ozone Maintenance SIP Revision

EPA’s Phase I Implementation Rule for the 8-hour ozone standard directed that areas designated nonattainment for the 1-hour ozone standard but designated attainment for the 8-hour standard submit a maintenance plan for the 1997 8-hour ozone standard by June 15, 2007 (69 FR 23951). The maintenance plan had to demonstrate that the area was attaining the 8-hour and 1-hour standards and would continue to attain the 8-hour ozone standard through 2014; maintenance could be demonstrated by projecting lower NO_x and VOC emissions in future years.

The plan was required to include ambient air quality monitoring data and analysis, an attainment inventory, and a contingency plan. The TCEQ submitted this

maintenance plan to the EPA on January 20, 2006. On January 15, 2009, the EPA proposed approval of the El Paso ozone maintenance plan SIP revision (74 FR 2387) which became effective on March 16, 2009. On October 20, 2010, the EPA published a final rule in the Federal Register (75 FR 64675) clarifying the EPA's approval of the 1997 8-hour ozone maintenance plan. This SIP revision included the following:

- Data from 2002, 2003, and 2004 indicate attainment of the 1-hour standard;
- An attainment inventory for 2008 was submitted indicating compliance with the 15% VOC emissions reduction requirement; and
- Control strategies are deployed which include low-RVP gasoline program, an I&M program, continued compliance with all previously specified control strategies, and point source VOC controls among others.

5.4 Summary

Initial air quality planning strategies applied EKMA to recommend ozone reduction strategies and demonstrate attainment with the 1-hour ozone standard. The state of the science regarding controlling ozone formation focused primarily on reductions in VOC emissions. State Environmental planning agencies such as the TACB could demonstrate attainment of the 1-hour ozone NAAQS by focusing on large reductions of VOC and small reductions in NO_x.

The TACB focused primarily on VOC reductions as indicated by the content of SIPs prepared beginning in 1979. Attention was given to reduce VOC through Stage I & Stage II vapor recovery systems, industrial VOC emissions reductions through control of fugitive emissions, I&M programs which specified limits on hydrocarbon emissions, 15%

VOC emissions reduction strategies, and VOC controls primarily in the petrochemical industry located in the Houston, TX shipping channel but also included a petroleum refinery in El Paso.

The ozone SIP for El Paso also focused primarily on controlling VOC emissions. Since the first ozone SIP in 1979 which recommended installation of Stage I vapor recovery systems to the current 8-hour ozone SIP revision, El Paso has focused on VOC controls, and it is possible further VOC controls can be achieved but at much greater cost.

Cd. Juárez, however, does not require stringent air quality planning strategies for the control of VOCs which are not a critical component of Mexico's emissions inventory system. Air quality assessments focus on industrial combustion processes and NO_x emissions as well as other combustion components such as CO, CO₂ and PM_{2.5}. Industrial and commercial VOC emissions information is voluntarily provided.

This research is an opportunity to recommend VOC control strategies which can be substantiated through greater detail provided in emissions inventories and applied to photochemical modeling. By understanding the role which certain species of VOC play in the formation of ozone it is possible to direct emissions reduction strategies to effectively reduce ozone.

Understandably some technologies such as Stage I and Stage II vapor reductions have shown to be effective as well as cost-effective at reducing emissions contributing to ozone formation. However, a better understanding of VOC emissions from light industrial sources such as the maquiladoras in Juárez will assist air quality

planners in recommending emissions reduction strategies in this part of Mexico which lacks stringent VOC emissions reduction strategies.

6 Basic Principles of Ozone Chemistry

Ozone, also known as photochemical smog, is an atmospheric pollutant that produces severe eye irritation, distressed respiratory symptoms, and poor visibility among other physical effects. The following three elements are necessary for the formation of ozone: the electromagnetic energy from a light source with a wavelength in the ultraviolet region, volatile organic carbons (VOC), and nitrogen oxides (NO_x). VOCs and NO_x are primarily produced by fossil fuel combustion.

6.1 Ozone Formation Processes

Figure 6.1 identifies a schematic on ozone formation (Stanley, 2005). The process initiates at the bottom of the schematic with production of nitric oxide (NO) and reactive hydrocarbons, also known as volatile organic carbon (VOC), formed primarily by the fossil fuels combustions. NO reacts with tropospheric ozone or a hydrocarbon radical (RO₂) to produce nitrogen dioxide (NO₂). NO₂ absorbs solar energy ($h\nu$) to produce NO and atomic oxygen, O. Atomic oxygen reacts with molecular oxygen (O₂) to form tropospheric ozone, which feeds back into the NO_x system.

Atomic oxygen can also react with hydroxyl radicals (OH[•]) and ozone to form the reactive hydrocarbon radicals utilized in the NO_x system. These radicals also react to form other components such as peroxyacetyl nitrate (PAN) and aldehydes (RC=OH where R is a hydrocarbon chain).

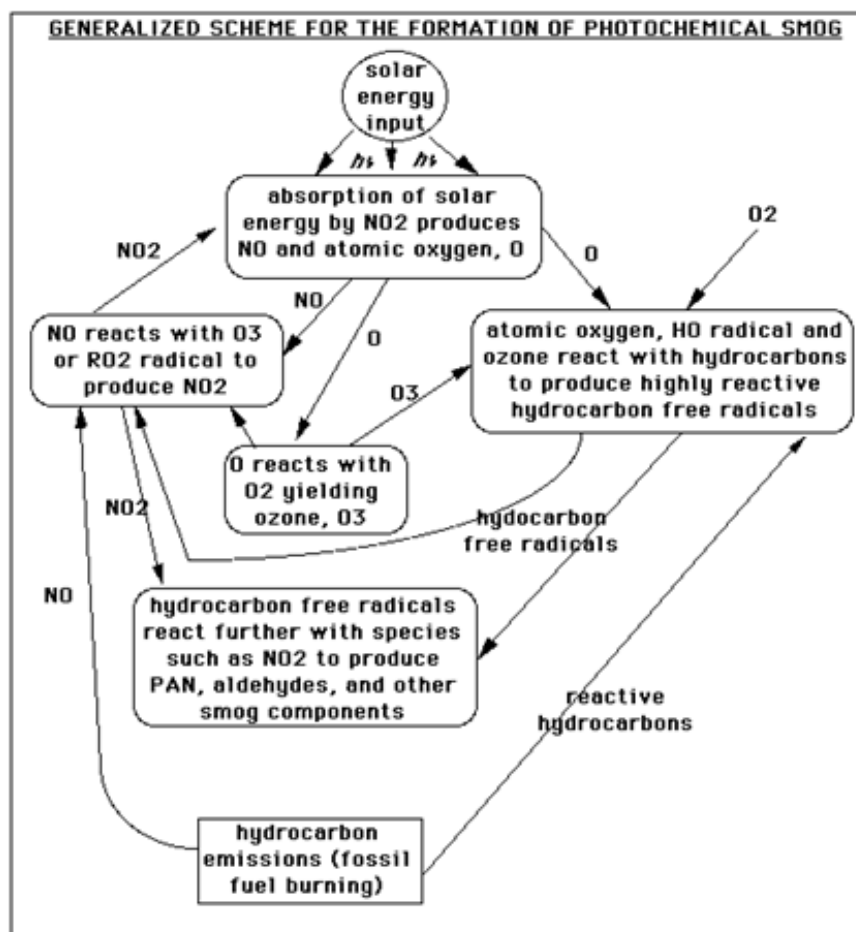


Figure 6.1 Generalized Ozone Formation Pathways
(From Smog Photochemistry in the Troposphere - undated)

6.1.1 The Chapman Mechanism

The primary photochemical reactions involved in the formation of tropospheric ozone are driven by nitrogen oxides produced through high temperature combustion processes. Table 6.1 illustrates the Chapman Mechanism proposed by Stanley Chapman in 1930. The Chapman Mechanism posits a theory on the formation of ozone in the stratosphere at an altitude above ~30 km (Seinfeld, 1998). The Chapman Mechanism posits that the ozone layer originates from the photolysis of atmospheric O_2 .

Table 6.1 Major Steps of the Chapman Mechanism

$O_2 + h\nu \rightarrow O + O(^1D)$	$\lambda < 240\text{nm}$	Reaction 6.1
$O_2 + O + M \rightarrow O_3 + M$		Reaction 6.2
$O_3 + h\nu \rightarrow O_2 + O$	$240\text{nm} \geq \lambda \geq 320\text{nm}$	Reaction 6.3
$O_3 + O \rightarrow O_2 + O_2$		Reaction 6.4

The Chapman Mechanism is explained as follows:

- Reaction 6.1: At an altitude above 30km molecular oxygen (O_2) absorbs a photon and photodissociates. This is also referred to as photolysis. Only photons with wavelength (λ) less than 240 nanometers (nm) can dissociate O_2 .
- Reaction 6.2: The oxygen atom (O) reacts rapidly with O_2 in the presence of a third body (a catalyst denoted M) to form ozone.
- Reaction 6.3: Ozone absorbs solar radiation with λ between 240nm and 320nm and decomposes back to O_2 and O.
- Reaction 6.4: Ozone can also react with atomic oxygen (O) to regenerate O_2 .

Ozone formation also involves the participation of NO_x and VOC. Table 6.2 identifies chemical reactions associated with NO_x .

Table 6.2 NO_x participation in Ozone Formation

$\text{NO}_2 + h\nu \rightarrow \text{NO} + \text{O}$		Reaction 6.5
$\text{NO} + \text{O}_3 \rightarrow \text{NO}_2 + \text{O}_2$		Reaction 6.6

Reactions in Table 6.2 can be generalized as follows

- Reaction 6.5: Nitrogen dioxide (NO₂) absorbs a photon and dissociates into nitric oxide (NO) and atomic oxygen.
- Reaction 6.6: Nitric oxide reacts with ozone to form nitrogen dioxide and molecular oxygen

6.2 Kinetics of Ozone Formation

Ozone formation can also be observed from a kinetic perspective. Kinetics involves the rate at which reactions take place. In the topic at hand kinetics addresses the rate at which ozone, NO, NO₂, and NO_x form and decompose as well as oxidation processes for VOCs. Table 6.3 identifies key reactions and the rate constant affecting the speed at which the reactions take place.

Table 6.3 Kinetic Reactions in Ozone Formation

Reaction	Rate Constant (or comment)	Reaction Number
$\text{NO}_2 + h\nu \rightarrow \text{NO} + \text{O}$	Dependant on light intensity	Reaction 6.7
$\text{O} + \text{O}_2 + \text{M} \rightarrow \text{O}_3 + \text{M}$	$6.0 \times 10^{-34} (\text{T}/300)^{-23} \text{ cm}^3 \text{ molecule}^{-1} \text{ sec}^{-1}$	Reaction 6.8
$\text{NO} + \text{O}_3 \rightarrow \text{NO}_2 + \text{O}_2$	$2.2 \times 10^{-12} \exp^{(-1430/\text{T})} \text{ cm}^3 \text{ molecule}^{-1} \text{ sec}^{-1}$	Reaction 6.9
$\text{O}_3 + h\nu \rightarrow \text{O}({}^1\text{D}) + \text{O}_2$	$0.0028k_1$	Reaction 6.10
$\text{O}({}^1\text{D}) + \text{M} \rightarrow \text{O} + \text{M}$	$2.9 \times 10^{-11} \text{ cm}^3 \text{ molecule}^{-1} \text{ sec}^{-1}$	Reaction 6.11
$\text{O}({}^1\text{D}) + \text{H}_2\text{O} \rightarrow 2\text{OH}\cdot$	$2.2 \times 10^{-10} \text{ cm}^3 \text{ molecule}^{-1} \text{ sec}^{-1}$	Reaction 6.12
$\text{CO} + \text{OH}\cdot \rightarrow \text{CO}_2 + \text{HO}_2\cdot$	$2.2 \times 10^{-13} \text{ cm}^3 \text{ molecule}^{-1} \text{ sec}^{-1}$	Reaction 6.13
$\text{HO}_2\cdot + \text{NO} \rightarrow \text{NO}_2 + \text{OH}\cdot$	$3.7 \times 10^{-12} \text{ cm}^3 \text{ molecule}^{-1} \text{ sec}^{-1}$	Reaction 6.14
$\text{OH}\cdot + \text{NO}_2 \rightarrow \text{HNO}_3$	$1.1 \times 10^{-11} \text{ cm}^3 \text{ molecule}^{-1} \text{ sec}^{-1}$	Reaction 6.15

Ozone formation reactions are described as follows:

- Reaction 6.7: Nitrogen dioxide (NO_2) reacts with a photon, $h\nu$, to form nitric oxide (NO) and a singlet oxygen atom - O. The reaction rate depends on how much light energy strikes the surface of the planet on a sunny day versus a cloudy day.
- Reaction 6.8: Singlet oxygen reacts with the oxygen molecule (O_2) in the presence of a catalyst "M" to form ozone. "M" also represents any mass which participates in the ozone formation or destruction reactions. The catalyst M

remains unchanged as it should. The reaction rate depends on ambient temperature.

- Reaction 6.9: Ozone reacts with NO to produce more NO₂ and O₂ which feed back into Reactions 6.7 and 6.8 ensuring steady ozone production. The rate of this reaction is dependent on ambient temperature.
- Reaction 6.10: Ozone is degraded by light energy forming a charged form of singlet oxygen, O(1D) and molecular oxygen. This reaction proceeds at a much slower rate than Reaction 1.
- Reaction 6.11: The charged oxygen reacts with a catalyst (M) to return to its normal state.
- Reaction 6.12: Some of the charged oxygen reacts with water in the atmosphere to form a hydroxyl radical, OH[•]. Radicals are fragments of molecules that have at least one unpaired electron and are highly reactive. OH[•] is responsible for the majority of atmospheric chemical reactions during the day. Other radicals take control at night-time when there is no sunlight to drive the reactions.
- Reaction 6.13: Atmospheric CO produced by fossil-fuel combustion reacts strongly with OH[•] to form CO₂ and hydroperoxy (HO₂) radicals.
- Reaction 6.14: The HO₂ radicals formed in Reaction 6.13 react with the extra NO to form more NO₂ and more OH[•]. The reaction rate is dependent on ambient temperature.
- Reaction 6.15: OH[•] reacts with NO₂ to form nitric acid, HNO₃, which is eventually washed out of the atmosphere. This reaction plays an important role in

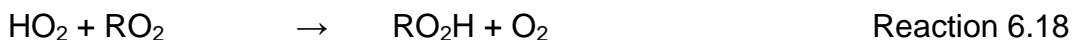
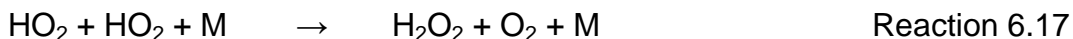
determining the limiting conditions behind ozone formation as will be discussed later in this report.

6.3 Sensitivity of Ozone Formation to VOCs and NO_x

The sensitivity of ozone formation to VOCs and NO_x during the photochemical reaction process is attributable to the fate of radicals. The radical pool consists primarily of hydroxyls (HO_x) which are the sum of OH, HO₂ and RO₂ radicals. When NO_x is plentiful, the main radical termination (i.e., HO_x removal) pathway is nitric acid (HNO₃) formation. The final step is important in identifying the limiting factors associated with formation of ozone.



If NO_x is plentiful the reaction will produce HNO₃ and the conditions under which ozone forms are considered VOC-Limited. M is catalyst which is not consumed or modified in the reaction. Under conditions where NO_x concentrations are minimal the radical-radical reactions dominate HO_x removal, e.g.:



When NO_x concentrations are low, the formation of ozone is limited by the availability of NO to react with HO₂ and RO₂ radicals. This scenario describes a NO_x-

limited condition. HO_2 and RO_2 radicals that do not react with NO participate in peroxide formation. Peroxide formation (H_2O_2 = hydrogen peroxide, or RO_2H = organic hydroperoxides) is indicative of scarce NO_x and NO_x -limited ozone formation. Useful indicators of VOC- vs. NO_x -limited ozone formation are based on the ratio of H_2O_2 production to HNO_3 production – $\text{H}_2\text{O}_2:\text{HNO}_3$.

ENVIRON (2011) reports that Sillman (1999) developed a convenient method of making a determination of ozone limiting conditions in an airshed. This determination may be conducted by reviewing data generated as a product of a CAMx simulation. Obtaining the data involves extracting particular variables from the output files generated by this photochemical modeling system. H_2O_2 and HNO_3 are 2 of several chemical species generated as output from the CAMx simulation. Other species include isoprene (C_5H_8) or nitrous acid (HONO) for example.

If the ratio between H_2O_2 and HNO_3 exceeds 0.35 then ozone formation is NO_x -limited. Ozone formation is VOC-limited when this ratio is less than 0.35. Output generated by the CAMx RUN is assessed to determine the ratio and recommend PAQCS. A more complete discussion on the $\text{H}_2\text{O}_2:\text{HNO}_3$ ratio is provided in Section 12.

6.4 Summary

Ozone formation is dependent upon solar radiation, atmospheric stability, and VOC and NO_x source emissions. Motor vehicle emissions produce NO_x and VOC, and emissions from multiple source categories contribute to the precursor mix. On warm days during stable atmospheric conditions and a sufficient mix of emissions, photolytic reactions occur to form tropospheric ozone. NO_2 decreases as sunlight converts it to

NO and O which is free to react with O₂ to form ozone. Shortly thereafter, oxidized VOC reacts with NO to increase NO₂ by midmorning causing a reduction in NO and increase in ozone.

The purpose of modeling is to consider the multiple chemical reactions and meteorological conditions involved to produce output which predicts output ozone concentrations close to observed. Normalized bias of $\pm 15\%$ and normalized error of $\leq 35\%$ are considered acceptable (ENVIRON, 2012) when comparing PREDICTED and OBSERVED ozone concentrations. Baseline modeling is followed by modifications to input data to generate output indicating an increase or reduction in ozone concentrations in relation to emissions entering a modeled airshed. However, prior to developing control strategies, it is important to develop as good a baseline as possible to minimize error and bias.

7 Previous Photochemical Ozone Studies in the PdN Region

Several photochemical modeling studies have been conducted for the PdN region prior to this research. This dissertation is an expansion on a baseline model developed for UTEP (ENVIRON, 2012). Prior to this research, only 3 ozone modeling projects have been conducted in the PdN region. The following sections are also referred to in the Conceptual Model for El Paso (Li, 2012).

7.1 The 1991 and 1994 Ozone Studies

The Texas Natural Resource Conservation Commission (TNRCC), predecessor to the TCEQ, conducted 2 ozone modeling studies (Teche 1991; TNRCC 1994). Yocke (2000) reported the Urban Airshed Model IV (UAM-IV) was applied to the studies. UAM-IV ozone modeling was conducted for a 2-day ozone episode of Aug. 15-16, 1986. Hourly ozone concentrations of up to 0.150 ppm were observed at 1 of the 3 monitors in El Paso; NO₂ was recorded at 1 CAMS. Ozone was reasonably modeled although the simulated results were found to lag behind the observed data. Unrepresentative temporal ozone variation was attributed to the uncertainties involved in the Cd. Juárez emissions, VOC reactivities, and upper air meteorology.

In a 1994 study, 4 ozone episodes (Feb. 9-10; June 23-24; July 1-3; and Oct. 11-4) were modeled by the TNRCC (TNRCC 1994). Emissions from Cd. Juárez were not added to the modeled emissions inventory. This study was eventually considered inaccurate and not reported due to the lack of emissions from Juárez. Notwithstanding the lack of Juárez emissions, the TNRCC in June, 1994, petitioned the EPA requesting

that the El Paso ozone nonattainment area be exempted from the NO_x control requirements of §182(f) of the FCAA as amended in 1990.

The exemption request was based on a photochemical grid modeling which showed that the El Paso nonattainment area would attain the 1-hour ozone NAAQS by the FCAA mandated deadline without the implementation of additional NO_x controls required under §182(f), “but for” emissions emanating from outside the United States. On November 21, 1994, the EPA conditionally approved this exemption request, conditioned upon the EPA approving the modeling portion of the El Paso attainment demonstration SIP (CFR 2010).

7.2 The 1996 PdN Ozone Study

In 1996, the EPA conducted an extensive ozone study in El Paso partly to fulfill the accords set forth by Annex V of the La Paz Agreement aimed at evaluating air quality improvement strategies (MacDonald et al 2001) and partly to address the ozone nonattainment situation in El Paso. The objective of the study was to understand the chemical and physical processes that influence high ozone concentrations in the PdN region. The study included multiple research groups conducting tasks ranging from emission inventory development to photochemical modeling to meteorological data acquisition conducted aloft.

7.2.1 Photochemical Modeling

The photochemical modeling study conducted by MacDonald et al (2001) focused on the ozone episode of August 12-14, 1996. An ozone event was observed August 13 when the maximum 1-hour ozone concentration reached 0.137 ppm at C41.

This event had similar synoptic characteristics to most events observed from 1985 to 1996. The meteorological characteristics observed to be similar amongst events are summarized as follows:

- A 500 mb ridge to the west of the PdN;
- High surface temperatures;
- Strong sunlight with few clouds;
- Elevated concentrations of ground-level ozone precursors during morning hours;
- Aloft air warming;
- Atmospheric stability;
- Weak surface pressure gradients;
- Low wind speeds (<1.5 m/sec) commonly from the southeast;
- Strong nocturnal inversion; and
- Slow mixed layer growth rates (MGR).

MacDonald also observed that carryover of ozone or precursor concentrations did not have a significant effect on elevated ozone concentrations. Of note are days with slow MGR but higher wind speeds (>1.5 m/s) where ozone concentrations were not as high as days with low wind speeds. However, concentrations were widely spread across the region during the sampling period.

7.2.2 Meteorological Modeling

The 1996 study included extensive meteorological modeling and upper air monitoring. Brown et al (2001) simulated the meteorology during the August 13, 1996 ozone episode using the Higher-Order Turbulence Model for Atmospheric Circulation

(HOTMAC) meteorological model. The modeling domain was a nested mesh of 4 grids with dimensions of 1km, 2km, 4km, and 8 km centered at the El Paso and Cd. Juárez area.

The investigation focused on the vertical structure and evolution of the atmospheric boundary layer for the period from August 12-14. This period was characterized by a slowly-evolving high pressure system over the region, a persistent upper-level jet at 2,500-3,500 m above ground level (AGL), deep daytime mixed layer heights with depth of 3,500 m, and unusually deep nighttime stable layers extending up to 2,500 m AGL.

7.2.3 Emissions Inventory Development

A concurrent ozone precursor emissions inventory conducted for the 1996 study was compiled and evaluated by Funk et al (2001). Point, area, and mobile source emission data were obtained from local government agencies and spatially and temporally allocated to a gridded domain using region-specific demographic and land-cover information. The inventory was processed using the Emissions Processor System version 2.0 (EPS2) which generates emissions files compatible with the UAM.

This study compared emission inventory ratios of nonmethane hydrocarbon NMHC:NO_x and carbon monoxide (CO):NO_x ratios to corresponding ambient ratios. It was reported that the NMHC and NO_x concentrations both peaked in the early morning at C662 (the 20/30 Club site at Cd. Juárez) and rapidly diminished 8 AM. The NMHC:NO_x ratio at C662 remained high (~14 at 6 AM and ~24 at 12 PM) during the day indicating NO_x-limited conditions.

Concurrent levels of NMHC and NO_x observed in downtown El Paso were comparable to those measured at C662 except in the early morning hours between 6 AM and 8 AM. Both NMHC and NO_x levels at C662 were approximately twice the levels observed in downtown El Paso at 6 AM, but dropped rapidly at both locations to approximately the same level by noon. This EI recommended the following:

- On-road and off-road mobile sources, and area sources should be examined based on activity data, emission factors, and spatial and temporal allocation of emissions sources, and
- The NMHC speciation profiles used in compiling the inventory should be replaced with local data with the emphasis placed on the mobile and area source components of the inventory.

7.2.4 Canister Sampling

Ambient air samples were collected by summa canisters and reported by Funk, et al (2001). Fujita (2001) and Seila et al (2001) conducted this sampling and built source profiles of motor vehicles, gasoline, liquefied petroleum gas (LPG), and commercial natural gas (NG) for the PdN. Ambient VOC samples were collected at surface air quality monitoring sites, near sources of interest and aloft on the city of El Paso and Cd Juárez during a six-week monitoring campaign for the 1996 ozone study.

Toluene and propane were the most abundant hydrocarbons found in El Paso and Cd. Juárez. Acetaldehyde, acetone, and formaldehyde were the most abundant carbonyls collected by the samplers. Fujita (2001) performed a source apportionment study using the Chemical Mass Balance (CMB) receptor model and found that the major contributor to NMHC in the PdN during the study period was on-road vehicle emissions

and that gasoline vehicle exhaust accounted for half to two-thirds of NMHC in central Cd. Juárez and El Paso. The highest gasoline vehicle exhaust contributions were observed to coincide with vehicular traffic during the morning and afternoon peak hours.

The diurnal patterns of gasoline contributions suggested that these were associated with tailpipe emissions rather than evaporative emissions from stationary sources. Emissions from diesel exhaust contributed approximately 2-3% of NMHC in Cd. Juárez and less than 2% in El Paso. Surface coatings contributed 1.8% of NMHC whereas biogenic emissions were not significant sources within PdN.

The research team eventually provided a summary of the CAMx modeling for the 1996 PdN ozone study (Emery et al 2000; Yocke et al. 2000; Roberts 1997). The key difference in ozone pollution between the PdN and other urban areas is that the ozone production rates were high in the morning and peaks were reached before noon in the PdN. A conceptual model was developed (Yocke et al. 2000) for future studies in the PdN with the following recommendations:

- The mixed layer growth rate was suppressed after 1000 Mountain Standard Time (MST) on Aug 13, and perhaps the same or slightly faster before 1000 MST than on typical cleaner days; and
- The precursor cloud was very compact and was centered near downtown El Paso/Juárez.

Higher NO_x and VOC concentrations in the early pre-dawn hours of Aug. 13 1996 were likely the result of the following:

- A shallower than normal nocturnal surface layer;

- Lighter than normal winds;
- Perhaps locally higher VOC emissions (although VOC canister data were rather ambiguous on this issue);
- A shallow nocturnal layer may have allowed 50-80 ppb ozone aloft (possibly due to regional recirculation) to penetrate to the surface at higher concentrations soon after sunrise, as the mixing depth first began to grow;
- The early arrival of ozone at the surface on Aug. 13 may have provided a ready source of OH⁻ radicals promoting ozone photolysis;
- The early OH⁻ plus higher early morning precursor concentrations, and potentially higher than normal morning NMHC/NO_x ratios, may have sustained relatively high ozone production rates until about noon;
- Urban ozone clouds were fairly compact suggesting localized ozone production centers. After about noon, the ozone production may have been limited by the availability of NO_x or may have been overcome by vertical dilution rates, and the ozone cloud was simply transported away by the afternoon winds; and
- The ozone cloud was transported downwind to the north by 1300 MST Aug. 13 and seemed to have remained largely intact (coherent).

As stated by Emery et al (2000), a key challenge during the model preparation is the minimization of interpolation / averaging error caused by the use of different projections for the emissions and meteorological grids. In addition, evaporative emissions from resting motor vehicles should be included in the emission inventory.

This issue was considered insignificant by Fujita (2001). Three limitations were also identified as follows:

- NO_x concentrations were over predicted;
- Vertical diffusivities were not properly characterized; and
- The Juárez emission inventory appeared inaccurate.

Such limitations prompted a sensitivity analysis that strongly suggested the Juárez emissions have a strong influence on ozone production in the PdN. To reduce this bias, Juárez VOC emissions were increased by a factor 4, NO_x emissions reduced by a factor of 2, and measured vertical diffusivities were forced on the model. The considerable adjustment required for VOC emissions suggest the following:

- VOC emissions were considerably underestimated;
- The speciation profiles were inadequate, and / or the existence of highly reactive species was unaccounted for during the emission inventory preparation.

7.3 Studies after 1996

Research related to the PdN ozone formation conducted after 1996 focused on meteorology partly due to the fact that El Paso was designated in attainment of the ozone NAAQS in 2004.

7.3.1 Addressing Uncertainties of the 1996 Ozone Study

Limited ozone modeling was performed by Nagaraj (2002) focusing on uncertainties identified in the 1996 study. Nagaraj (2002) performed a sensitivity study

for the 1996 ozone episode using CAMx 3.0 and emission and meteorological data retrieved from the 1996 ozone study.

NO_x emissions were reduced or increased by a factor of 2 during this sensitivity analysis to evaluate the impact on ozone and NO_x concentrations. Based on the CAMx modeling results for three ozone episode days (Aug. 11-13, 1996), Nagaraj concluded that conditions regarding PdN ozone formation are NO_x-limited. Increasing NO_x emissions resulted in increase in ambient NO_x concentrations which in turn resulted in a significant decrease in ozone concentrations. The effect was more pronounced in Cd. Juárez than in El Paso.

7.3.2 Community Multiscale Air Quality Modeling

Lu et al. (2008) applied a different air quality modeling system that includes the Community Multiscale Air Quality (CMAQ) chemistry and transport model, the Sparse Matrix Operator Kernel Emissions (SMOKE) emissions processing model, and the Weather Research and Forecasting (WRF) mesoscale numerical meteorological model to investigate the same August, 1996 ozone episode. Lu's results indicated that the modeling system exhibited the capability to simulate high ozone occurrence in 1996.

Different sensitivity tests were conducted to identify the contributions to high surface ozone concentration from eight VOC subspecies, biogenic and anthropogenic VOCs, and long-range transport of ozone and its precursors. This study determined that reductions of the ethene, isoprene, paraffin, olefin, and formaldehyde help mitigate the surface ozone concentration. In addition, biogenic VOCs and the long-range transport of ozone and its precursors appeared to produce an insignificant contribution in the control of surface ozone.

As indicated in previous sections of this report, having a better understanding of the VOC groups in an airshed improves the ability to develop air quality planning strategies. Simply modifying VOC emissions in a model provides the approach the planning strategy can pursue if in fact ozone concentrations can be reduced. However, translating the modification of a VOC functional group to actual emissions sources requires a good knowledge of both emissions inventory development and facilities generating specific modeled VOC emissions.

7.3.3 Western U.S. Border-Region Ozone Study

Additional related ozone study was found in a study performed by Shi et al. (2009) for the western US border region. Their goal was to determine the primary contributing processes for the simultaneous ozone episodes in San Diego, Imperial Valley, and El Paso in June 1-4, 2006. CMAQ was employed and a backward air trajectory analysis was performed.

It was found that the CMAQ model under-predicted the multi-site observed ozone concentrations for El Paso. The mean normalized bias (MNB) for 1-hour and 8-hour ozone concentrations were 22.8% and 22.1%, respectively. For El Paso, the model predicted 1-hour peak levels within a factor of 2 of observed levels. By using a process analysis (PA) technique (Jang et al 1995) it was found that the major contributors to surface ozone concentrations in El Paso were the chemistry processes and both the vertical and horizontal advection.

Horizontal advection occurred mainly during the night and early morning hours (0600). Elevated ozone concentrations in El Paso were primarily induced by photochemical production, vertical diffusion, and vertically advection. Horizontal

advection was also responsible for a net outflow of ozone during daytime hours. An interesting observation was that during the daytime the photochemical process is dominant by the depth of the boundary layer (4,000 m) while at nighttime titration of NO_x is limited to the lowest 100 m. Backward air trajectory analysis indicated that the mass of air that moving into the PdN region during a June 3, 2006 ozone event came from the east (from northern Texas and specifically from Oklahoma City).

7.3.4 MM5 Mesoscale Meteorological Modeling

Meteorological modeling focusing on the PdN has been performed by various research groups. Pearson and Fitzgerald (2001) studied the meteorology over the complex terrain of El Paso by running the time-dependent, 3-D mesoscale MM5 model. The meteorological results obtained with the MM5 model were compared to field data reported by TNRCC. It was found that the dispersion of pollutants by wind plays an important role on the days of low peak ozone concentration.

Lee and Fernando (2003) employed the same MM5 model to simulate the synoptically influenced local winds in the PdN for the Aug. 14, 1996 episode (summer case) and a Dec. 14, 1998 (winter case) event. Lee and Fernando reported that local thermal dynamic forcing (which leads to local thermal circulation) and synoptic forcing (which is dominated by partly stagnant high pressure conditions) characterized the summer event. Synoptically influenced local mountain / valley circulation was well predicted and agreed with field data. The mixed layer height predicted by the model agreed with the observations for the summer case.

7.4 Summary

Several air quality studies have been conducted in the PdN region to assess the conditions leading to ozone formation. Most of the modeling campaigns have generated results indicating the need for improved modeled emissions inventories. The comprehensive 1996 ozone study continued to reiterate the need for improved emissions inventory for Juárez. The 1994 TNRCC study lacked the Juárez emissions inventory altogether. Results by Funk (2001) indicate the need for better activity data plus spatial and temporal information which more accurately reflects the Juárez profile. Methods applied to develop the EI for Juárez are based on US emissions factors and methods. Activity data, spatial and temporal allocations all follow the US model which likely introduces error in the photochemical modeling exercise.

MacDonald reports lag of several hours between the predicted and observed ozone peaks which could indicate the input parameters applied to emissions processing may have the incorrect time zone. Potentially activity data applied to emissions processing may also need to be adjusted if predicted peaks are several hours behind observed.

8 Conceptual Model

The conceptual model (CM) is a review of ambient air quality data, meteorology, and emission inventories. This is an important first step prior to selecting a ozone episode to model. It examines the factors associated with the formation of ozone in an area such as the City of El Paso. The CM may also observe regional-level ozone conditions such as occurs over the PdN metroplex consisting of El Paso County, Texas, southern Doña Ana County, New Mexico, and the municipality of Juárez, Chihuahua, Mexico. The CM also considers the potential transport of air pollutants into a region in which case external sources may contribute to degraded air quality. Based on results obtained during development of the CM, a 10-day ozone modeling episode was selected which ran from 6 June to 21 June, 2006.

8.1 The Conceptual Model for the Paso del Norte Region

Tropospheric ozone is produced by the reaction of volatile organic compounds (VOCs) with hydroxyl radicals (OH^\cdot) in the presence of nitrogen oxides (NO_x). Ozone formation chemistry initiated by OH^\cdot is well documented and understood (Finlayson-Pitts and Pitts, 2000; Seinfeld and Pandis, 1998). Ozone formation CMs provide a characterization of ozone trends, precursors, formation, and transport of air pollution into the region of interest. This information is then compiled and developed into a comprehensive picture of not only where and when ozone forms, but also how and why ozone forms in a geographic area. Conceptual models can be used as tools for selecting modeling episodes or qualitatively evaluating and assessing photochemical modeling results.

The CM posits 12 questions which provide air quality planners the opportunity to evaluate the results of their research and the potential determinants of ozone formation within an area monitored for ozone. Among the questions are included the following:

1. Is the nonattainment problem primarily a local one, or are regional factors important?
2. Are ozone and/or precursor concentrations aloft also high?
3. Do violations of the NAAQS occur at several monitoring sites throughout the nonattainment area, or are they confined to one or a small number of sites in proximity to one another?
4. Do observed 8-hour daily maximum ozone concentrations exceed 75 ppb frequently or just on a few occasions?
5. Is there an accompanying characteristic spatial pattern or is there a variety of spatial patterns when 8-hour daily maxima in excess of 75 ppb occur?
6. Do monitored violations occur at locations subject to mesoscale wind patterns which may differ from the general wind flow?
7. Have there been any recent major changes in emissions of VOCs or NO_x in or near the nonattainment area?
8. Are there discernible trends in design values or other air quality indicators which have accompanied a change in emissions?
9. Is there any apparent spatial pattern to the trends in design values?
10. Have ambient precursor concentrations or measured VOC species profiles changed?
11. What past modeling has been performed and what do the results suggest?
12. Are there any distinctive meteorological measurements at the surface or aloft which appear to coincide with occasions with 8-hour daily maxima greater than 75 ppb?

These questions were answered in the CM developed for the PdN region (Li, 2011) and assist the decision-making process in the selection of a modeling episode.

Several models are applied when developing the CM. Mesoscale meteorological modeling using a limited-area, non-hydrostatic, primitive-equation Weather Research and Forecasting (WRF) model and backward air trajectory analysis using the National Oceanic and Atmospheric Administration (NOAA) Hybrid Single-Particle Lagrangian Integrated Trajectory (HYSPLIT) model are applied to understand factors and conditions during ozone episodes and identify areas which may transport ozone or precursors to El Paso.

8.2 Mesoscale Meteorological Conditions

The Weather Research and Forecasting (WRF) mesoscale model (Skamarock et al. 2001) provides an assessment of continent-scale meteorological conditions. Meteorology plays an important role in ozone formation. To understand the meteorological factors and synoptic conditions leading to an ozone episode, a simulation using WRF was prepared for the period June 12 - 21, 2006. An ozone event occurred on June 18 during this ozone episode.

A “warm run” for the PdN region provides a preliminary assessment of the meteorological factors inputted into WRF to determine if adequate and reasonable outputs can be generated. The model is run over three domains centering at El Paso, TX. The spatial resolutions for coarse, medium and fine domains are 36-km, 12-km and 4-km respectively where 35 sigma vertical levels were implemented. Figure 8.1 illustrates the domain coverage established by the WRF model.

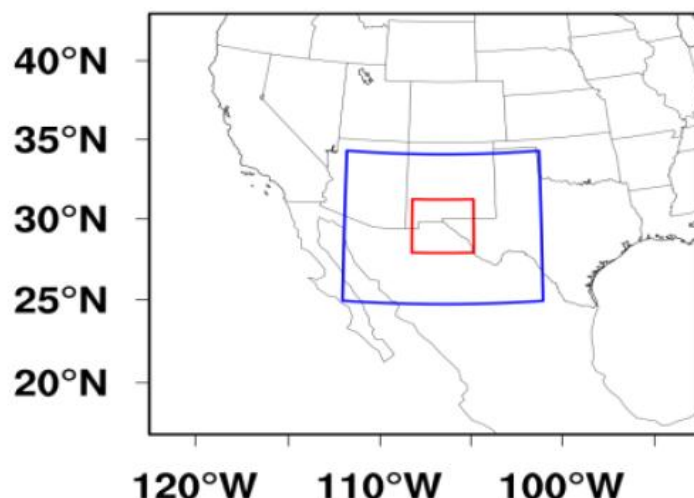


Figure 8.1 Domain Coverage by the WRF Model

The data incorporated into the WRF model as initialization and lateral boundary conditions were obtained from the National Center for Weather Prediction (NCEP) Final (FNL) dataset with a 6 hour interval. Previous studies have reported that ozone episodes for the PdN region during which times the elevated ozone concentrations are usually characterized by stagnated weak winds and stagnant air over the region, few limited frontal movements, no precipitation, clear skies, slow-moving high barometric pressure systems, clear skies, and high temperatures (Lu, et al 2008; Brown, et al, 2001).

8.3 HYSPLIT Model

The Hybrid Single Particle Lagrangian Integrated Trajectory Model (HYSPLIT) model is applied to assess the movement of a particle (or a parcel of air) within a region of interest. HYSPLIT generates either a forward- or back-trajectory indicating the direction a parcel of air travels or a back-trajectory to estimate the origin of the parcel of

air respectively. Mesoscale meteorological modeling using WRF and HYSPLIT models identify large-scale wind patterns and backward trajectories respectively of air parcels flowing to the PdN region.

Figure 8.2 presents a backward trajectory analysis conducted for the summer 2006 ozone episode. It represents the percentage of the arriving direction of winds to the PdN region during the summer of 2006.

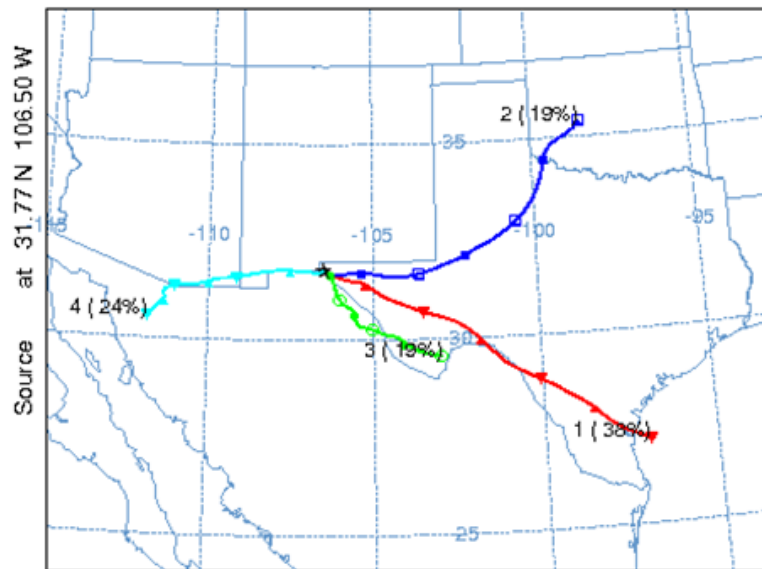


Figure 8.2 Backward Trajectories by Predominant Direction - Summer 2006

Mesoscale modeling of the wind patterns during the 2006 ozone episode identified the following meteorological conditions favor elevated ozone concentrations:

- Low mixing height;
- High temperature;
- Low humidity;
- Low wind conditions; and
- Prevailing east-west winds.

These conditions are consistent with the findings from surface meteorology. Multiple 72-hour backward air trajectory analyses of air mass movements during 2006 identified that 1) pollution sources including transport ozone located to the east and west of El Paso were more likely to be transported into the city; and 2) ozone and/or precursors originated hundreds of miles from El Paso ranging from the Baja California to the Gulf of Mexico. Figure 8.3 presents a 24-hour backward trajectory of a parcel of air arriving at C37 at 00 UTC on 12 July.

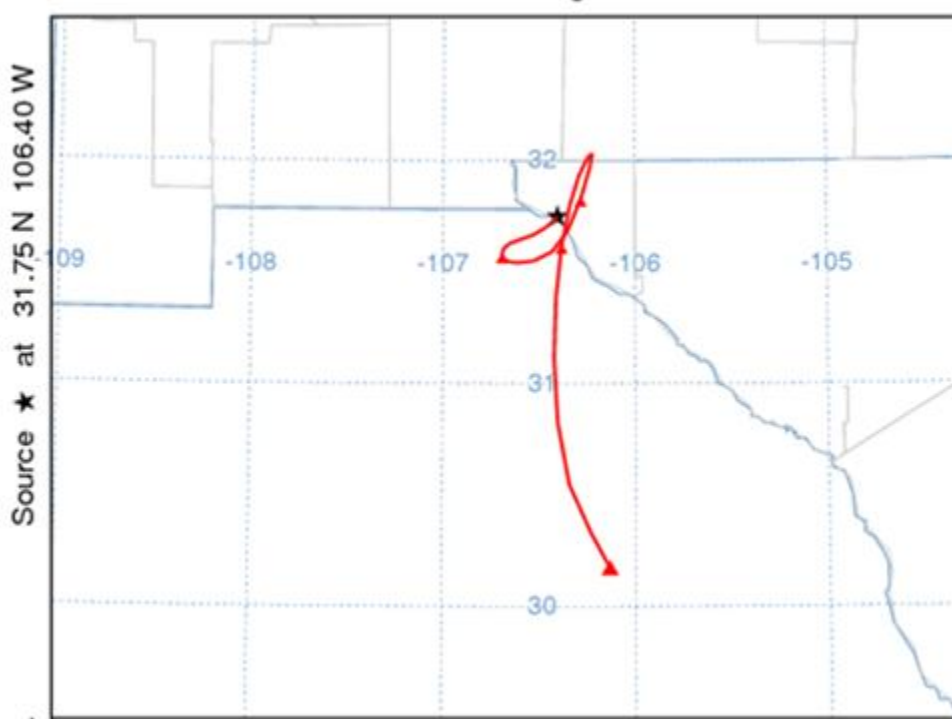


Figure 8.3 24-hour backward trajectory arriving at C37 on 00 UTC on 12 July, 2006

The trajectory of the parcel indicates that emissions from both El Paso and Juárez were sufficiently mixed upon arrival at C37 and any elevated ozone concentrations may not necessarily be attributed to Cd. Juárez.

Figure 8.4 illustrates a backward trajectory of the air mass arriving at C37 at 00:00 on June 19, 2006. The flow of the air mass into the region is identified as from the south and southwest. This would indicate that Juárez is the regional source of emissions observed at C37. The particular area may be influenced by emissions generated at the international port of entry as vehicles queue to cross into the U.S.

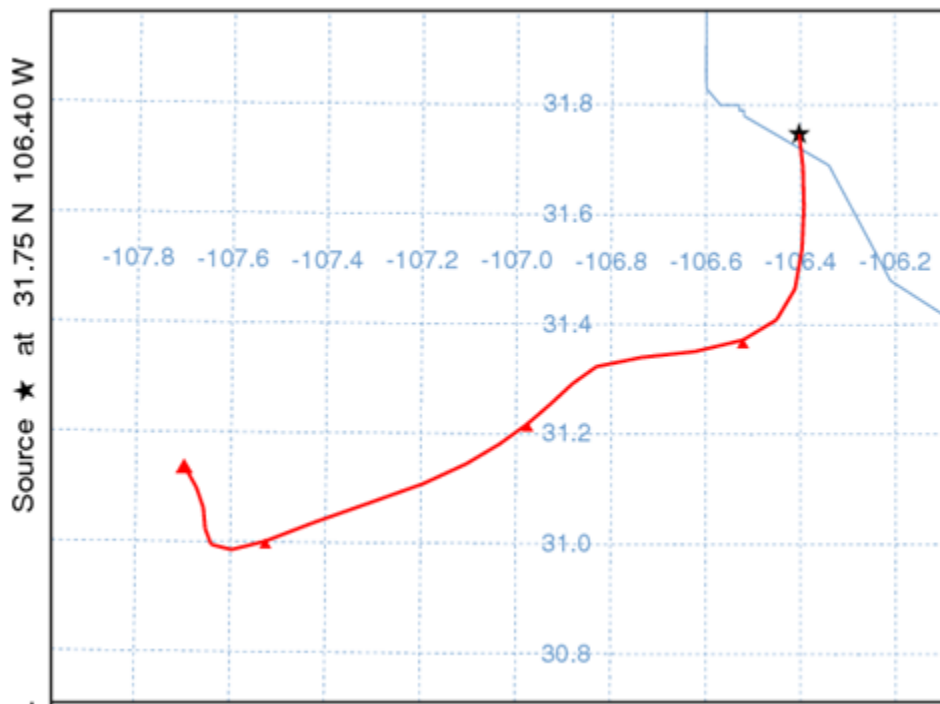


Figure 8.4 Backward trajectory arriving at C37 on 19 June, 2006

8.4 Surface Wind Characteristics

Wind roses are the graphical presentation of the frequency of occurrence of wind direction and wind speed categories at a monitoring station. Wind roses are a common method of reporting surface meteorological conditions. Surface wind statistics indicated by wind roses consist of hourly wind speed and wind direction data which are two

critical parameters in understanding the fate and transport of atmospheric pollutants (Li, 2011).

An important statistic of wind roses in regards the ozone formation potential of an area surrounding the CAMS is calm winds identified in the inner-most ring of the wind rose. Calm conditions are defined as wind speeds below 1 m-sec⁻¹. An area is more prone to generate elevated ozone concentrations over an extended period of time when a higher percentage of calm conditions are observed.

8.4.1 Wind Statistics During Ozone Seasons

Surface wind patterns in the PdN region vary dramatically among the various ambient air monitoring stations due to significant geological features such as the Franklin Mountains which bisect El Paso, the Juárez Mountains to the south, Mount Cristo Rey to the west, and the Hueco Mountains to the east. The following figures present the wind roses for the years 2006 and 2008 at CAMS located in the 3 different communities of the PdN region. Important similarities in wind direction can be found between the CAMS during specific observation periods. However, at any particular moment the winds can be blowing in any direction due to the region's complex terrain.

Figure 8.5 identifies the “key” to understanding wind roses. Each wind speed bin is identified by its own graphical representation ranging from a simple black bar for the slowest wind speed bin ranging from 1.01 to 1.54 meters per second (mps) to the large blue rectangle for wind speeds ≥ 10.8 mps.

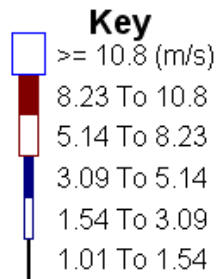


Figure 8.5 Wind Speed Key

The wind rose bar represents the direction from which the winds approach the monitoring station.

C12 is located adjacent to the University of Texas at El Paso in the southwest corner of the City of El Paso. Ozone-season wind statistics for 2006 and 2008 at C12 are indicated in Figure 8.6.

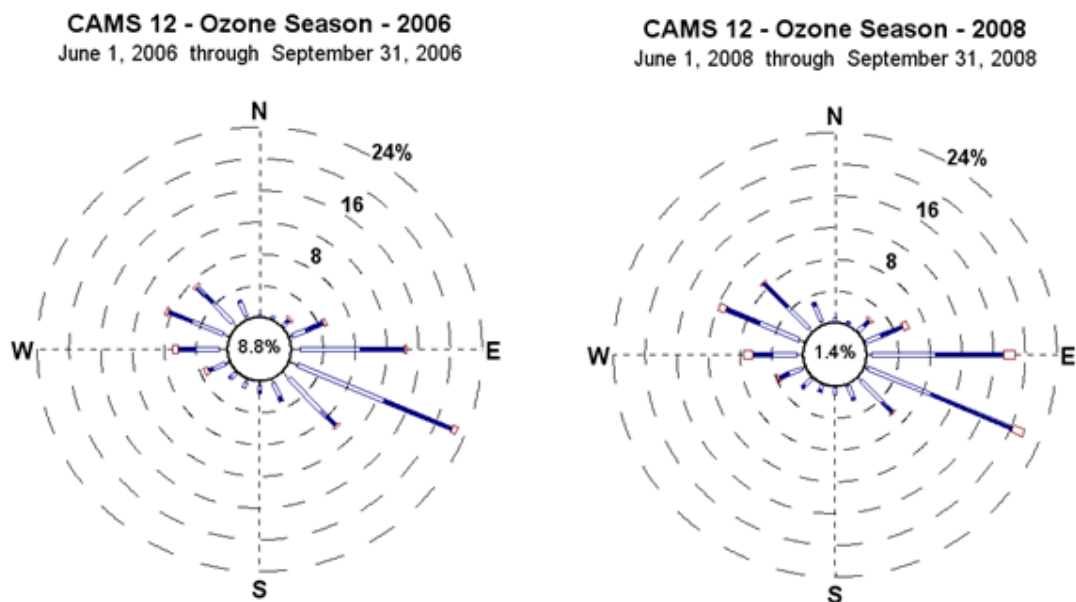


Figure 8.6 Wind Roses for the 2006 & 2008 Ozone Seasons at C12

Wind vectors were nearly identical and predominantly from the south southeast (SSE) during the 2006 and 2008 ozone season. Calm wind conditions were observed >8% and >1% of the time at C12 during the ozone season of 2006 and 2008 respectively.

Figure 8.7 presents the ozone season wind rose for CAMS 6ZN which is located at Sunland Park City Yard near the foot of Mt. Cristo Rey. SSE winds at C6ZN consistently dominated the wind field with a high percentage of calm condition >9% and >12% in 2006 and 2008 respectively. Wind statistics at C12 and C6ZN are very similar.

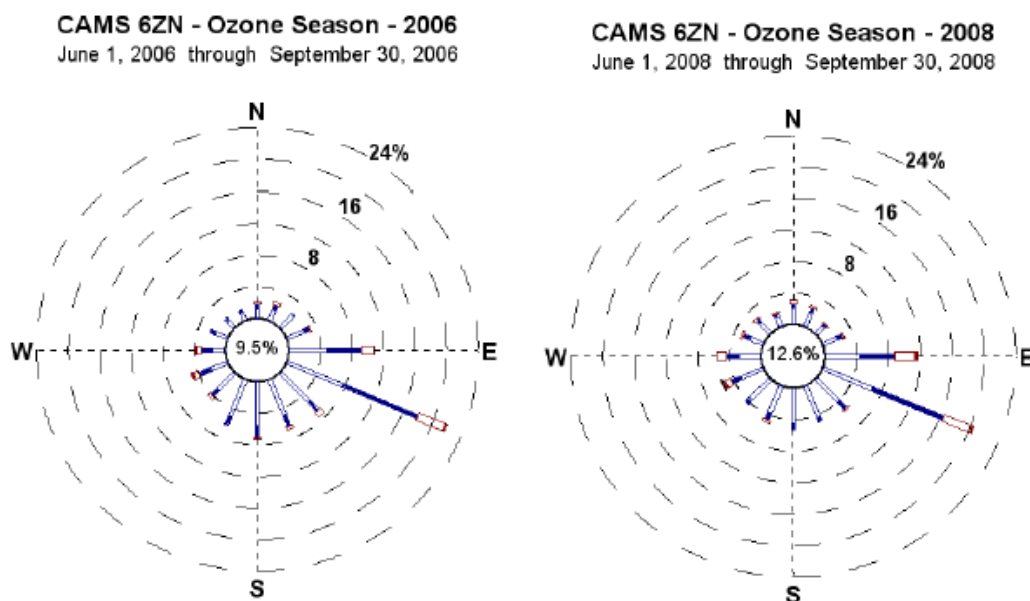


Figure 8.7 Wind Roses for the 2006 & 2008 Ozone Seasons at 6ZN

Figure 8.8 shows the ozone season wind roses for C663 in Juárez. This station is located in the parking lot of a maquiladora in northeast Juárez. Easterly winds consistently dominated the wind field with a very high percentage of calm conditions

>43% and 22% in 2006 and 2008 respectively. C663 behaved less predictably with a high percentage of calm hours.

The wind pattern was dominated by easterly winds and low winds that prevailed at other times. It is possible that the wind pattern at this station was influenced by buildings or obstacles in the vicinity of the monitoring station which is surrounded on all sides by the 20' tall walls of the industrial building structures where it is deployed.

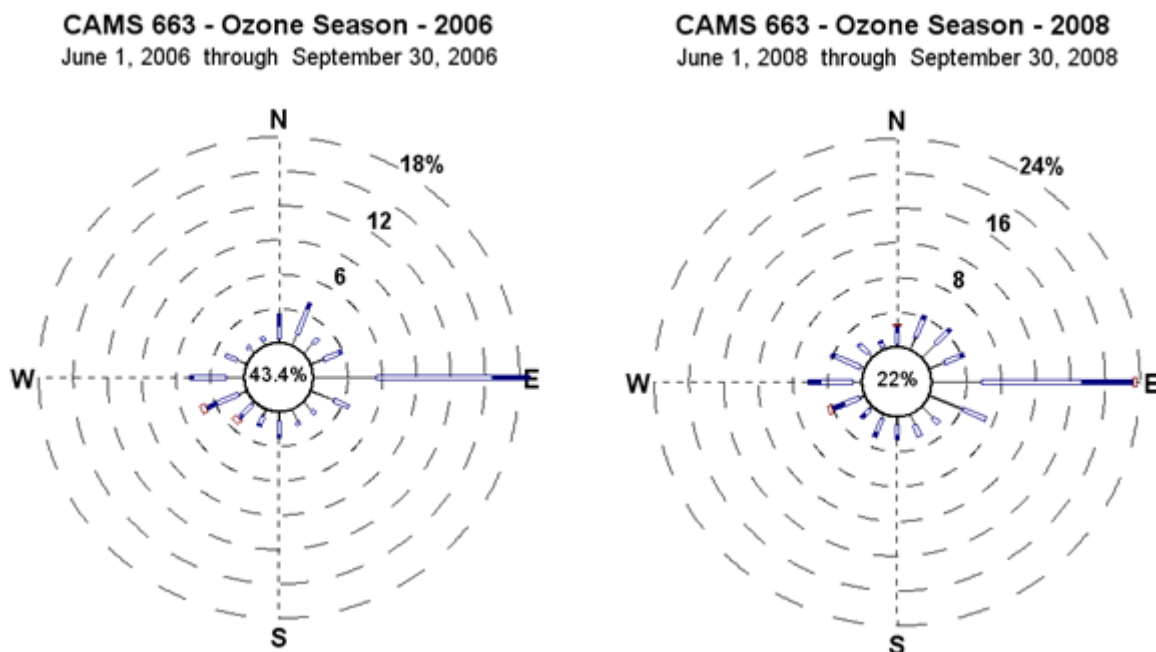


Figure 8.8 Wind \Roses for the 2006 & 2008 Ozone Seasons at C663

C72 is located at Skyline Park near the foothills of the Franklin Mountains in northeast El Paso. This site is located a distance of over 10 miles from the river valley. Figure 8.9 presents the wind roses at C72 for 2006 and 2008. Ozone season winds were variable with downslope gusts and a marked north and south component.

C72 experiences wind statistics that are different from those observed at other monitors deployed near the river valley. C72 is highly influenced by the north-south winds along the ridgeline of the Franklin Mountains and the downslope wind gusts from the eastern slopes of the Mountains.

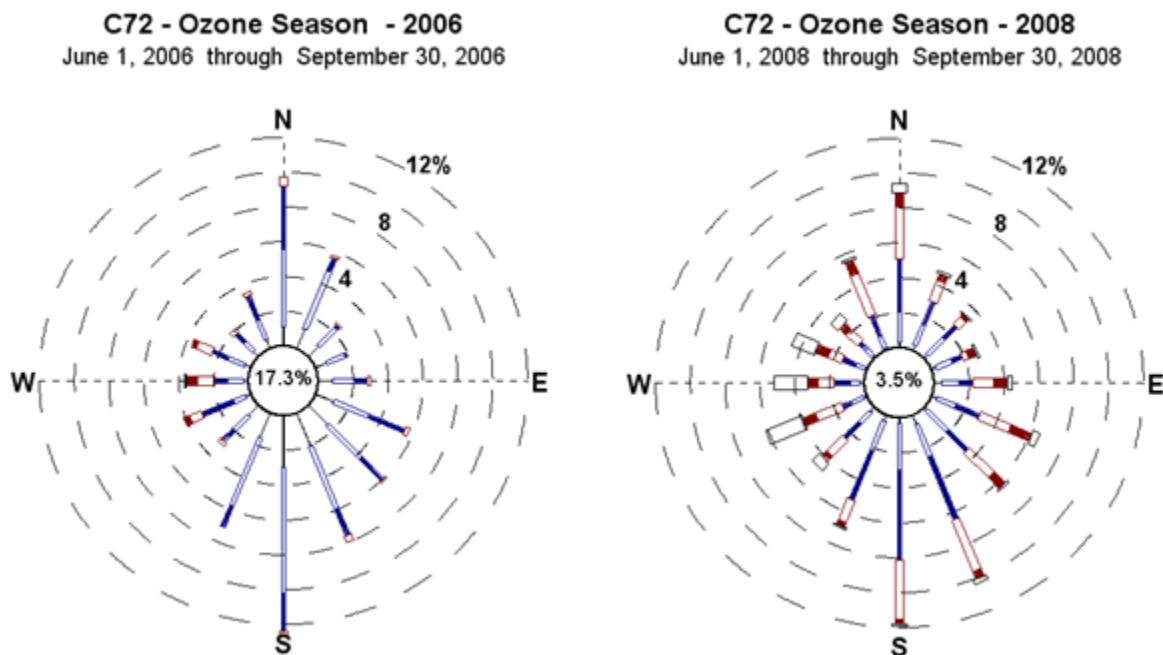


Figure 8.9 Wind Roses for the 2006 & 2008 Ozone Seasons at C72

C37 is located at the southeast corner of Ascarate Park just across the Border Highway from Cd. Juárez. The site is approximately 2 miles east of the Bridge of the Americas Port of Entry. The station is in an open space with no structural obstructions nearby. Figure 8.10 shows 2006 and 2008 ozone season wind roses at C37. ESE winds are the predominant wind direction at C41 in 2006. 2008 shows more variability in wind direction. Calm conditions occurred 7% and ~22% of the time during the 2006 and 2008 ozone seasons respectively.

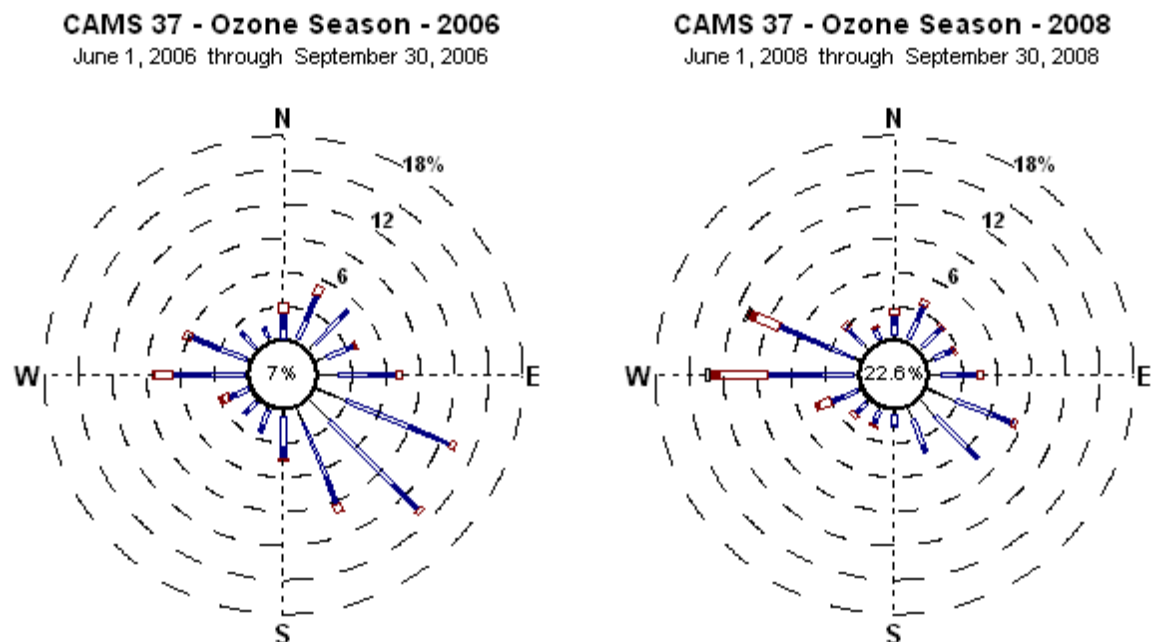


Figure 8.10 Wind roses for the 2006 & 2008 Ozone Seasons at C37

C41 is located at the Chamizal National Memorial in an open space with no structural obstructions or trees nearby. Figure 8.11 shows 2006 and 2008 ozone season wind roses at C41. ESE winds are the predominant wind direction at C41. Both easterly and westerly winds also occurred more frequently at this site. Calm conditions occurred 13% of the time during the ozone seasons

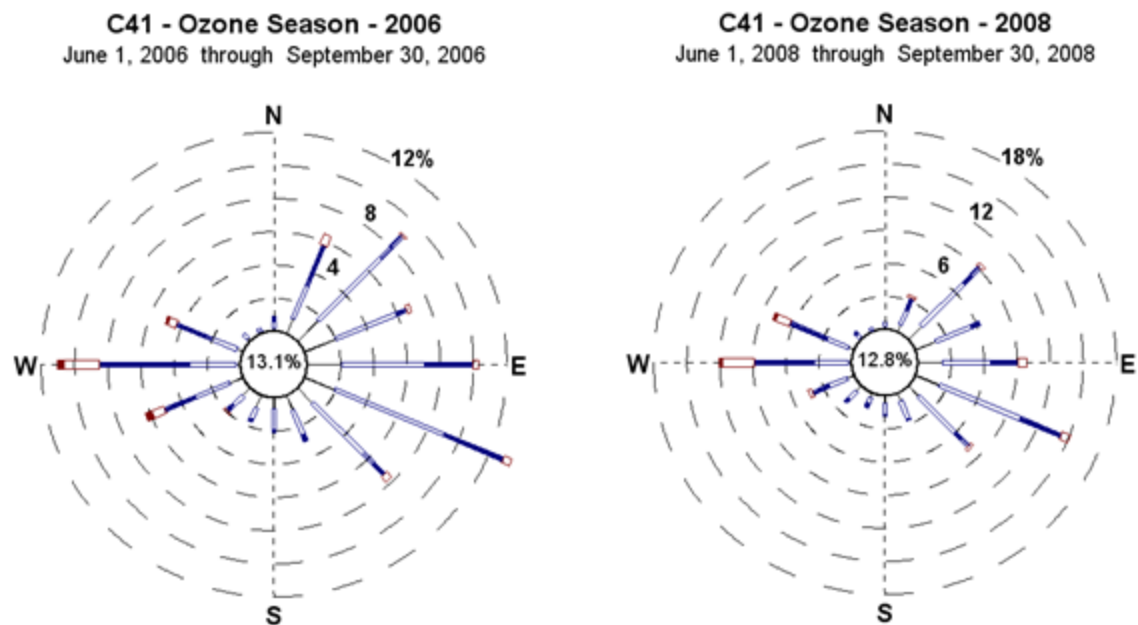


Figure 8.11 Wind roses for the 2006 & 2008 Ozone Seasons at C41

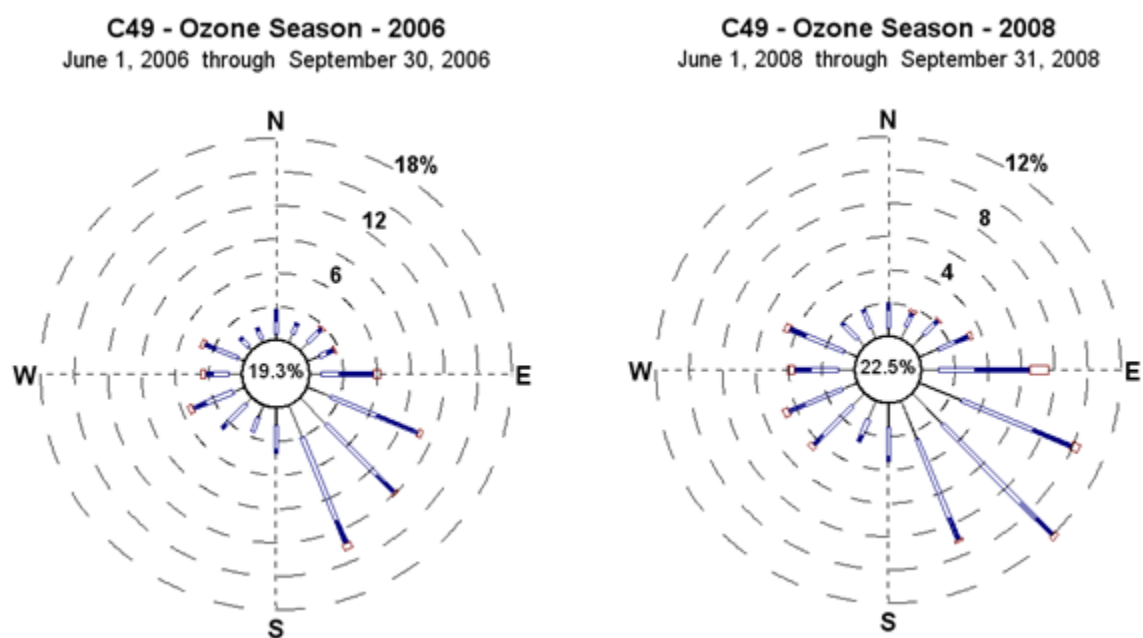


Figure 8.12 Wind roses for the 2006 & 2008 Ozone Seasons at C49

C49 is located in Socorro which is in southeastern El Paso County. Figure 8.12 presents wind roses for the ozone season during 2006 and 2008 at C49. The station is located in a residential neighborhood of primarily one story structures. Wind vectors at C49 are predominantly from the southeast during both ozone seasons. Calm conditions prevailed >19% and >22% for 2006 and 2008 respectively during the 4 month ozone season. Variable light breezes also approached this station during the remainder of the ozone season.

C414 is located on Ivanhoe Dr. in the eastside of El Paso near U.S. Highway 62/180. The station is deployed at a fire station a short distance from Lee Trevino Blvd. Figure 8.13 presents wind roses for the 2006 and 2008 ozone seasons at C414.

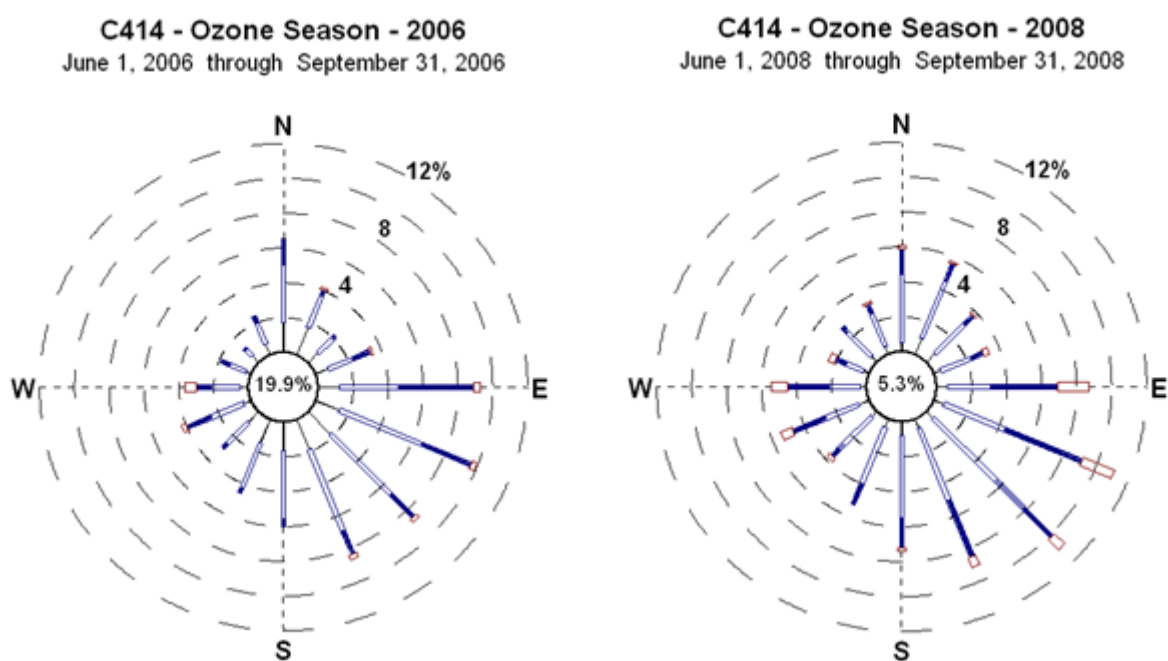


Figure 8.13 Wind Roses for the 2006 & 2008 Ozone Seasons at C414

This site observes predominantly SE and easterly winds. C414 observed much calmer breezes during 2006 than in 2008. This station observes a higher percentage of elevated wind speeds compared to other sites. The elevated winds also exhibit a southeast and easterly direction.

8.4.2 Wind Statistics During Ozone Episodes

The following figures show wind roses during ozone episodes. An ozone episode occurs on a 10 day period during which time ozone concentrations exceed the NAAQS. During ozone episodes the percentage of calm regional winds tends to be lower due to the passage of a low pressure front which is followed by a high pressure system which may last several days.

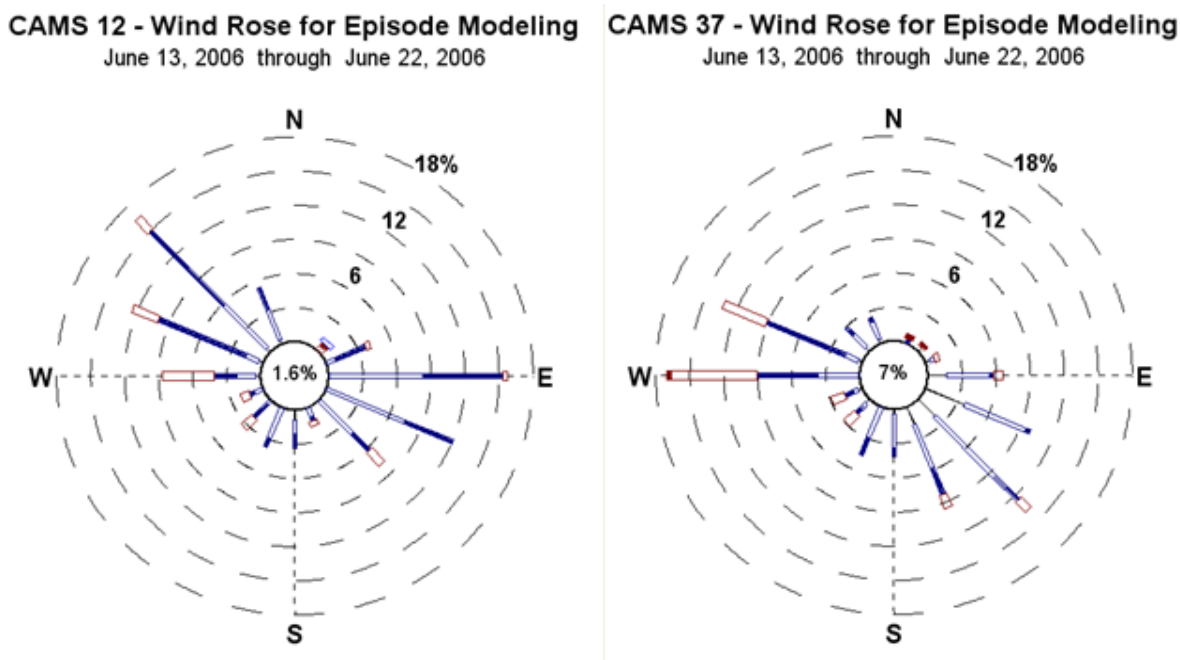


Figure 8.14 Wind Roses for ozone Modeling Episodes

The June 12 - 21, 2006 ozone episode will be modeled in this investigation. Figure 8.14 presents wind roses for C12 and C37 during an ozone episode established as June 12 – 21, 2006. During this period the PdN region observed a high degree of wind variability as well as elevated wind speeds. Predominant winds approached the region from the west, northwest, east, and southeast directions. Westerly winds tended to have the highest speeds. A low percentage of calm conditions occurred during the 10 day episode.

8.4.3 Wind Statistics During Ozone Events

Air quality statistics for wind speed and wind direction indicate that stable atmospheric conditions are favorable for the formation of elevated ozone. Stable atmospheres are characterized by low wind speeds and very few frontal systems near the center of a regional high pressure system which may cover hundreds of square miles. The high pressure system coupled with low mixing height establishes the stable conditions to allow the rapid formation of ozone.

Wind roses for the June 18, 2012 ozone event indicate a high degree of variability regarding the wind vectors approaching the PdN region. Figure 8.15 illustrates wind roses for C12 and C37 during the 6/18 ozone event. This ozone event shows that the prevailing breezes were not from the same direction. At C12 the predominant breezes came from the northwest and southwest. Slight breezes also approached C12 from the easterly and westerly directions. C37 indicates the predominant winds approached from southeast. Calm wind conditions were observed 12% of the time at both sites. The high variability of the winds during the 24 hour period must be further examined to assess regional wind patterns.

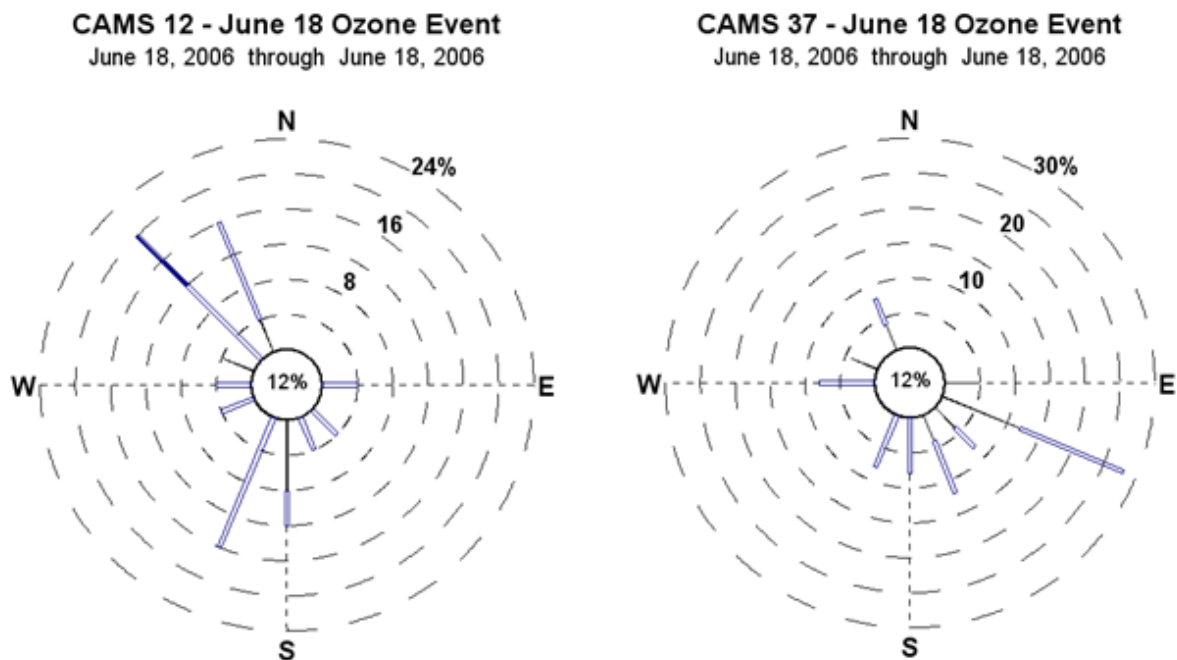


Figure 8.15 C12 and C37 Wind Rose for June 18, 2006 Ozone Event

C41 and C414 observed the highest concentrations on the US side during the June 18 ozone event. Figure 8.16 shows wind roses for C41 and C414. A marked difference between C41 and C414 compared to C12 and C37 is the high percentage of calm conditions. Calm conditions were observed 32% and 44% of the time at C41 and C414 respectively on 6/18. Breezes at C41 came predominantly from the SE and SW. Slow breezes occurred at this site for the entire 24 hour period. C414 also observed predominantly southerly breezes.

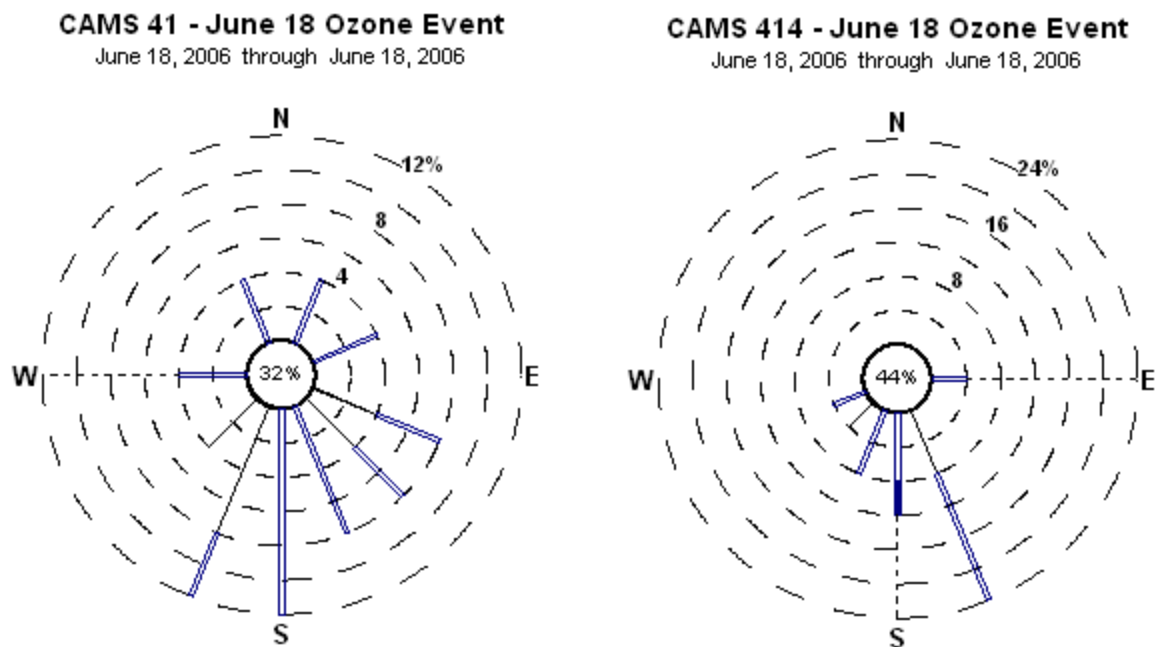


Figure 8.16 C41 and C414 Wind Rose for June 18, 2006 Ozone Event

Figure 8.17 presents wind roses during ozone events that occurred at C12 on 8/26 and 7/11, 2006. Of note is the low percentage of calm conditions on 8/26 which is the day with the highest 8-hour average ozone concentration in 2006. Wind vectors on 8/26 were predominantly from the southeast and northwest. On 7/11 wind vectors approached C12 primarily from the easterly direction. Both 7/11 and 8/26 observed slight breezes throughout the day.

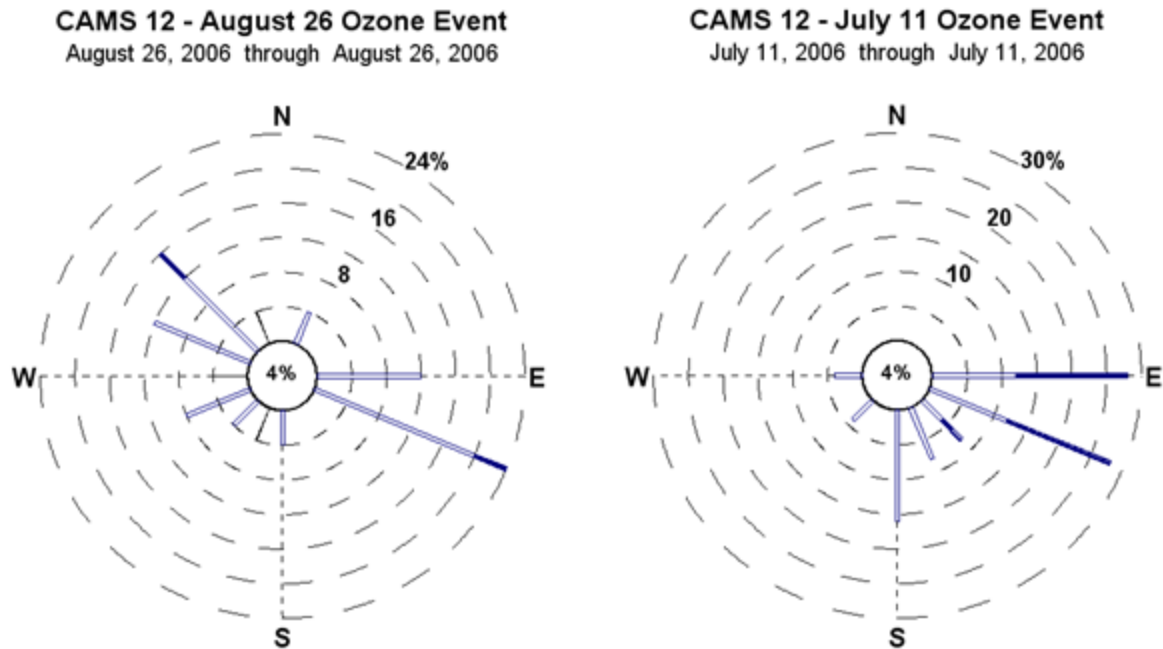


Figure 8.17 Wind Roses for Ozone Events at C12 on 7/11 and 8/26, 2006

8.5 Selection of Photochemical Modeling Episode

The primary purpose of the CM is to accumulate and assess the multiple variables associated with elevated ozone concentrations. This process is followed by development of a photochemical model focusing on the ozone episode and event.

Several ozone exceedances occurred in the PdN region during 2006, which is the year the TCEQ selected to conduct photochemical modeling across the State of Texas as part of the Rider 8 air quality improvement initiative. Table 8.1 presents the 4 highest 8-hour average ozone concentrations observed during 2006 at the El Paso and Juárez monitoring sites. The highest 8-hour average ozone concentration of 99 ppb was observed at C663 in Juárez on 8/26. An ozone event also occurred on 6/18. This day

was selected for development of modeling simulations for this report. An 8-hour average high of 94 ppb was observed at C663.

Table 8.1 Top 4 Ozone Exceedance Days During 2006

	Date	Value-H1	Date	Value-H2	Date	Value-H3	Date	Value-H4
C12	7/11/2006	92	6/3/2006	86	8/23/2006	85	7/4/2006	84
C37	7/11/2006	90	8/26/2006	88	6/18/2006	81	7/10/2006	74
C41	7/11/2006	89	6/18/2006	88	8/23/2006	79	6/4/2006	78
C49	8/26/2006	92	7/10/2006	81	6/18/2006	81	9/10/2006	73
C72	6/18/2006	78	7/11/2006	77	8/23/2006	76	7/12/2006	73
C414	6/18/2006	88	8/26/2006	82	7/11/2006	78	6/4/2006	77
C661	6/18/2006	69	7/11/2006	67	7/10/2006	61	6/12/2006	61
C662	6/18/2006	87	8/23/2006	76	8/26/2006	72	7/4/2006	72
C663	8/26/2006	99	6/18/2006	94	7/11/2006	86	7/10/2006	81

It should be noted that the highest frequency of elevated ozone concentrations occurred on 6/18 when 8 CAMS observed elevated ozone concentrations above the 0.075 ppm exceedance threshold. The highest 8-hour average concentration observed in 2006 was 0.099 ppm at C663 in Cd. Juárez on 8/26.

8.6 Summary

The purpose of the meteorological modeling is to support future ozone air quality modeling in the PdN region. The 8-hour ozone standard was exceeded throughout the state of Texas during the June 2006 episode. The purpose of building a properly performing meteorological simulation is to apply the same meteorological model during the extent of all modeling runs. A properly performing meteorological model needs to be prepared only one time after which it will be repeatedly applied for future modeling exercises.

Meteorology plays a major role in ozone formation and transport. Wind speed and wind direction provide a good indicator of the source of emissions which contribute to the formation of ozone. The wind roses for the PdN region indicate that the predominant wind vectors approach from the westerly and easterly directions.

On 8-hour exceedance days in the PdN region, the afternoon winds are typically light and come primarily from the east and southeast. These mid-morning and afternoon wind patterns help to explain the location of the highest 8-hour ozone design values, which, based on 2006 data, occurred in the central portion of the PdN area primarily along the El Paso-Juárez international border.

In El Paso, C12 tends to observe the highest ozone concentrations perhaps since the air parcels transported towards this station include emissions from the international bridges, the central business districts of both El Paso and Juárez, and the local refinery. As the light afternoon winds cross through the area from the east and southeast towards the westernmost monitor in El Paso on 8-hour exceedance days, the ozone concentrations increase until the highest levels are detected at C12.

9 The CAMx Photochemical Modeling System

The Comprehensive Air Quality Model with Extensions (CAMx) is an Eulerian photochemical dispersion model that allows for an integrated 'one-atmosphere' assessment of gaseous and particulate air pollution over scales ranging from sub-urban to continental (ENVIRON, 2009). CAMx was developed by ENVIRON International Corporation (ENVIRON) for the EPA. TCEQ and EPA rely on CAMx as the air quality model of choice for State Implementation Plan (SIP) demonstrations in Texas. CAMx was selected as the photochemical air quality modeling system evaluated by this dissertation.

CAMx Version 5.40 (CAMx v5.40) is the current version of the modeling system. This version has been extensively utilized by TCEQ for baseline, basecase, and future-case modeling. Applying this version also maintains consistency with CAMx simulations for Houston, Dallas-Fort Worth, Austin, San Antonio, and other potential nonattainment regions of Texas.

The focus of this dissertation is to evaluate modifications to a baseline modeling scenario which was developed with the best available information. Modifications to the baseline scenario will be observed to assess their impact on ozone concentrations. VOC and NO_x emissions, which as previously indicated are the primary chemical drivers in the formation of ozone, will be modified for this evaluation of the CAMx modeling system. ENVIRON (2009) reports the following variables affect photochemical air quality modeling results:

- Spatial (vertical and horizontal) and temporal distribution of anthropogenic and biogenic emissions;

- Chemical composition of the emitted emissions NO_x, VOC, CO, and PM_{2.5};
- Spatial and temporal variations in wind fields;
- Dynamics of the boundary layer, including stability and mixing;
- Chemical reactions involving VOC, NO_x, CO, and other important compounds;
- Diurnal variations of solar radiation and temperature;
- Loss of ozone and ozone precursors by dry deposition; and
- Ambient background concentrations of VOC, NO_x, CO, and other pollutants within, immediately upwind of, and above the study region.

Each variable reported above must be documented both spatially and temporally for regional conditions when developing the configuration files required for a CAMx simulation. Variables and output must also be assessed early when running the simulations to confirm the input variables or the model do not generate spurious data.

9.1 The Continuity Equation

CAMx simulates the emission, dispersion, chemical reaction, and removal of pollutants in the troposphere by solving the pollutant continuity equation for each chemical species (*i*) on a system of nested three-dimensional grids. The Eulerian continuity equation describes the time dependency of the average species concentration (*c_i*) within each grid cell volume as a sum of all of the physical and chemical processes operating on that volume. This equation is expressed mathematically in terrain-following height (*z*) coordinates:

$$\begin{aligned} \frac{\partial c_l}{\partial t} = & -\nabla_H \cdot V_H c_l + \left[\frac{\partial(c_l \eta)}{\partial z} - c_l \frac{\partial}{\partial z} \left(\frac{\partial h}{\partial t} \right) \right] + \nabla \cdot \rho K \nabla (c_l / \rho) \\ & + \left. \frac{\partial c_l}{\partial t} \right|_{Emission} + \left. \frac{\partial c_l}{\partial t} \right|_{Chemistry} + \left. \frac{\partial c_l}{\partial t} \right|_{Removal} \end{aligned} \quad \text{Equation 9.1}$$

where V_H is the horizontal wind vector, η is the net vertical “entrainment rate”, h is the layer interface height, ρ is atmospheric density, and K is the turbulent exchange (or diffusion) coefficient.

The first term on the right represents horizontal advection, the second term represents net resolved vertical transport across an arbitrary space- and time-varying height grid, and the third term represents sub-grid scale turbulent diffusion. Chemistry is treated by simultaneously solving a set of reaction equations defined from specific chemical mechanisms such as those identified in CB6. Pollutant removal includes both dry surface uptake (deposition) and wet scavenging by precipitation.

CAMx can perform simulations on three types of Cartesian map projections: Universal Transverse Mercator (UTM), Rotated Polar Stereographic (RPS), and Lambert Conic Conformal (LCC). CAMx also offers the option of operating on a curvilinear geodetic latitude / longitude grid system as well. The vertical grid structure is defined externally, so layer interface heights may be specified as any arbitrary function of space and/or time. This flexibility in defining the horizontal and vertical grid structures allows CAMx to be configured to match the grid of any meteorological model that is used to provide Environmental input fields.

The continuity equation is numerically marched forward in time over a series of time steps. At each step, the continuity equation is replaced by an operator-splitting approach that calculates the separate contribution of each major process (emission,

advection, diffusion, chemistry, and removal) to concentration change within each grid cell. The specific equations that are solved individually in the operator-splitting process are shown in order below.

$$\left. \frac{\partial c_i}{\partial t} \right|_{\text{Emission}} = m^2 \frac{E_i}{\partial x \partial y \partial z} \quad \text{Equation 9.2}$$

$$\left. \frac{\partial c_i}{\partial t} \right|_{\text{X advection}} = - \frac{m^2}{A_{yz}} \frac{\partial}{\partial x} \left(\frac{u A_{yz} c_i}{m} \right) \quad \text{Equation 9.3}$$

$$\left. \frac{\partial c_i}{\partial t} \right|_{\text{Y advection}} = - \frac{m^2}{A_{xz}} \frac{\partial}{\partial y} \left(\frac{v A_{xz} c_i}{m} \right) \quad \text{Equation 9.4}$$

$$\left. \frac{\partial c_i}{\partial t} \right|_{\text{Z transport}} = \frac{\partial(c_i \eta)}{\partial z} - c_i \frac{\partial}{\partial z} \left(\frac{\partial h}{\partial t} \right) \quad \text{Equation 9.5}$$

$$\left. \frac{\partial c_i}{\partial t} \right|_{\text{Z diffusion}} = \frac{\partial}{\partial z} \left[\rho K_v \frac{\partial(c_i/p)}{\partial z} \right] \quad \text{Equation 9.6}$$

$$\left. \frac{\partial c_i}{\partial t} \right|_{\text{XY diffusion}} = m \left\{ \frac{\partial}{\partial x} \left[m \rho K_x \frac{\partial(c_i/p)}{\partial x} \right] + \frac{\partial}{\partial y} \left[m \rho K_y \frac{\partial(c_i/p)}{\partial y} \right] \right\} \quad \text{Equation 9.7}$$

$$\left. \frac{\partial c_i}{\partial t} \right|_{\text{Wet Scavenging}} = - \Lambda_i c_i \quad \text{Equation 9.8}$$

$$\left. \frac{\partial c_i}{\partial t} \right|_{\text{Chemistry}} = \text{Mechanism - specific Reaction Equations} \quad \text{Equation 9.9}$$

where c_i is species concentration ($\mu\text{mol}/\text{m}^3$ for gases, $\mu\text{g}/\text{m}^3$ for aerosols), E_i is the local species emission rate ($\mu\text{mol}/\text{s}$ for gases, $\mu\text{g}/\text{s}$ for aerosols), Δt is timestep length (s), u and v are the respective east-west (x) and north-south (y) horizontal wind components (m/s), A_{yz} and A_{xz} are cell cross-sectional areas (m^2) in the y-z and x-z planes, respectively, m is the ratio of the transformed distance on the various map projections to

true distance ($m=1$ for curvi-linear latitude/longitude coordinates), and Λ_l is the wet scavenging rate (s^{-1}).

The injection of emissions from all sources for a given grid is the first process in each time step. CAMx then performs horizontal advection, but alternates the order of advection in the x and y directions for each master time step.

9.2 Domain Grid Cells

Pollutant concentrations are specified at the center of each grid cell volume, representing the average concentration over the entire cell. Meteorological fields are supplied to the model to quantify the state of the atmosphere in each grid cell for the purposes of calculating transport and chemistry. Gridded configurations address the movement of pollutants and meteorology both into and out of each grid cell. As such the horizontal and vertical advection and diffusion of pollutants must be considered.

CAMx internally carries the variables indicated above in an “Arakawa C” grid configuration as indicated in Figure 9.1. This configuration illustrates that horizontal wind components u and v are staggered from each other to facilitate the solving of the transport equations in “flux form”. Figure 9.1 also shows the horizontal cell indexing convention used in CAMx. Each cell is defined by the index pair (i,j) , where i ranges from 1 to nx (the number of cells in the east-west direction), and j ranges from 1 to ny (the number of cells in the north-south direction).

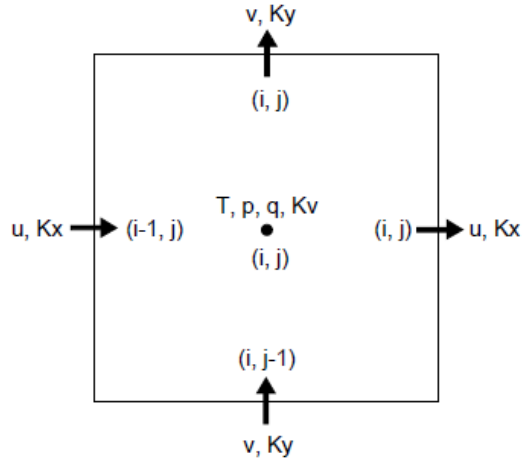


Figure 9.1 Horizontal Grid Cell Indexing Convention

Addressing the vertical aspects of the grid cell configuration, most variables are carried at each layer midpoint (defined as exactly half way between layer interfaces). Any exceptions are those variables that describe the rate of mass transport across the layer interfaces, which include the vertical diffusion coefficient K_v and the rate of vertical transport η . These variables are carried in the center of each cell horizontally, but are located at the top layer interface in the vertical direction.

As previously stated, the center of each grid cell volume is the location where all chemical reaction mechanisms are applied. The grid center assimilates the average concentration over the entire cell thus minimizing computing time for each time-step progression of the simulation.

Meteorological variables such as temperature, pressure, water vapor, and cloud water are specified at the grid cell center. Wind components and diffusion coefficients are specified at the grid cell interfaces where mass in and out of each cell is accounted.

9.2.1 Grid Nesting

As indicated in the CAMx User Guide (ENVIRON, 2011), the model incorporates two-way grid nesting which means that pollutant concentration information propagates into and out of all grid nests during model integration. Any number of grid nests can be specified in a single run, while grid spacing and vertical layer structures can vary from one grid nest to another. The nested grid capability of CAMx allows cost-effective application to large regions in which regional transport occurs, yet at the same time providing fine resolution to address small-scale impacts in selected areas.

9.2.1.1 Horizontal Grid Nesting

Each grid nest is defined over a subset of master (or coarse) grid cells. The range of master grid row and column indices that define the coverage of each nested grid must be specified in the run control file. An integer number of nested grid cells must span one master grid cell; this number is referred to as a “meshing factor”. “Buffer” cells are added around the perimeter of each nested grid to hold boundary conditions and are added automatically within.

All nested grid output files contain data for the entire array of computational and buffer cells; however, buffer cell concentrations are considered invalid and should be ignored. Additionally, all nested grid input files must contain data for the entire array of computational and buffer cells. An example of a horizontal nesting arrangement is shown in Figure 9.2 (from ENVIRON, 2011).

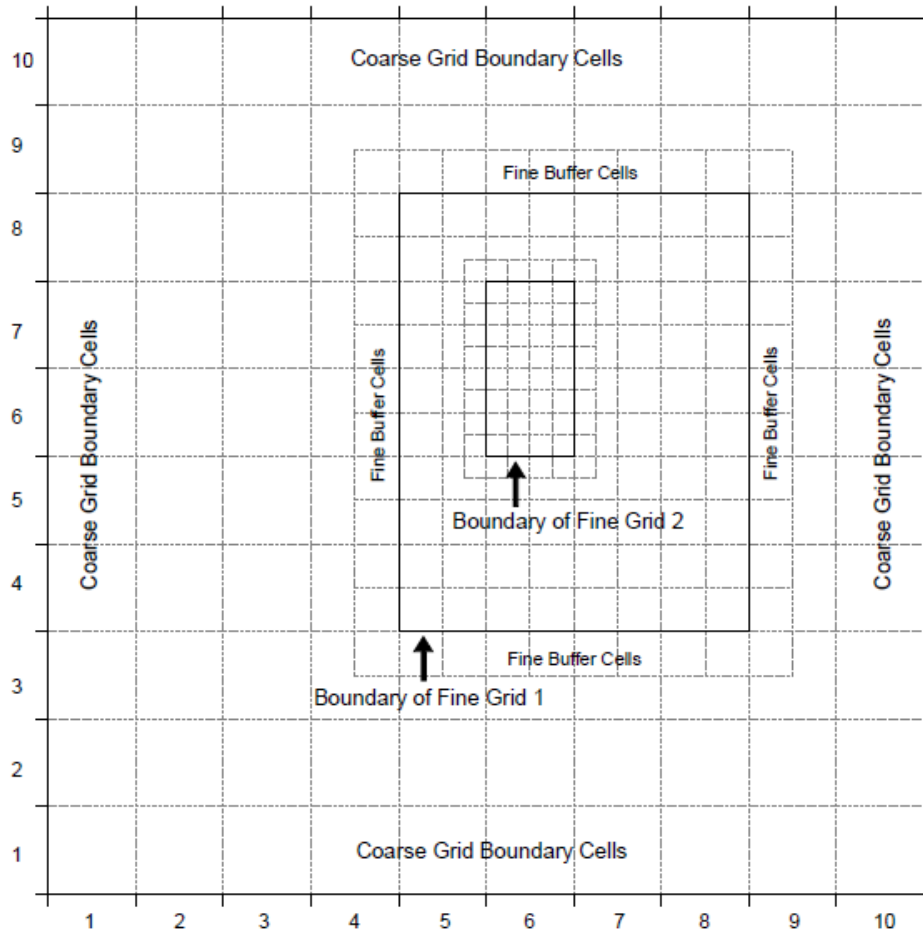


Figure 9.2 Horizontal Grid Nesting Arrangement

The horizontal grid nesting arrangement presented above illustrates two telescoping nested grids within a 10x10 cell master grid. The outer nest identified as “Boundary of Fine Grid 1” contains 10x12 cells (including buffer cells to hold internal boundary conditions), and the inner nest identified as “Boundary of Fine Grid 2” contains 6x10 cells (including buffer cells). A meshing factor of 2 spanning master grid cells (5,4) to (8,8), and one with a meshing factor of 4 spanning master grid cells (6,6) to (6,7). In the model to be developed for this study, this gridding system may be identified

as the 36-12-4 gridded configuration. This is better defined as the 36 km coarse grid with a 12 km nested grid, and a 4 km fine grid.

9.2.1.2 Vertical Grid Nesting

Nesting in the vertical is allowed only by sub-dividing parent grid layers into a series of finer layers. To maximize flexibility in the vertical grid structure, each parent grid layer may be individually split into a unique set of fine layers or not split at all. The vertical layer division is defined by the input height/pressure file for each grid. Figure 9.3 presents an example of how layers may be defined for a master grid and two fine grid nests.

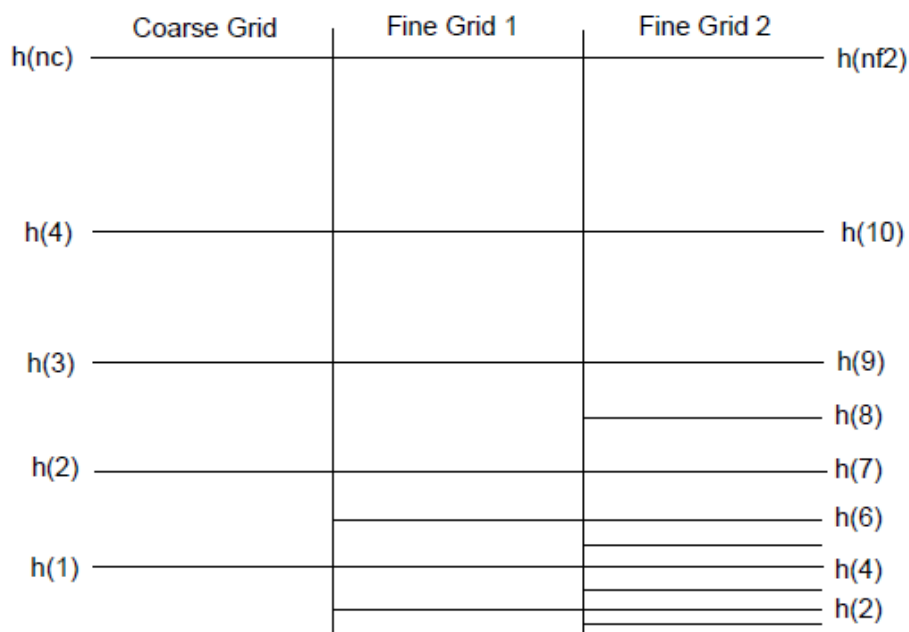


Figure 9.3 Vertical Layer Configuration and Nesting

Vertical nesting is not recommended because it can lead to mass consistency errors. The indexing convention in the vertical is also shown in Figure 9.3, where the top

of layer k is referenced as interface k . Index $k=0$ is at the ground. The lowest 2 master (coarse) grid layers are split into 4 layers in nested Fine Grid 1. The lowest 5 layers of Fine Grid 1 are split into 9 layers in nested Fine Grid 2. The nested grids include a matching layer interface for every parent grid layer interface.

9.2.1.3 Gridded Nests Data Requirements

The following FORTRAN binary input / output (I/O) files must be provided for the master grid, and optionally provided for each nested grid:

- Gridded surface emissions;
- Fractional land-use distribution;
- Height / pressure (defines the layer interface structure);
- Horizontal wind components;
- Temperatures;
- Vertical diffusivities;
- Water vapor; and
- Clouds and precipitation

Any of these input files may be supplied for each nested grid or none at all. If any of these files are not supplied for a particular nested grid, the Flexi-Nest algorithm within CAMx interpolates the missing fields from the parent grid. It is desirable to provide nested grid data whenever possible. However, the ability to interpolate data is useful for testing sensitivity to grid configurations or for situations when it is not possible to run a meteorological model for all grid nests. The Flexi-Nest option also allows users to redefine the nested grid configuration at any point in a simulation.

Nested grids can be introduced or removed only at the time of a model restart since a new CAMx user control file must be used to redefine the grid configuration. For example, the user may wish to “spin-up” the model using a regional-scale master grid and a single nest over an area of interest for two days. Starting at 6 AM on the third day, the user may introduce one or more nests within the original nested grid for more detailed analysis. This would require that the model be restarted at 6 AM of the third day with a new control file that defines the position of the new nests provides any additional input fields for these grids. CAMx will internally reconcile the differences in grid structure between the nested grid restart files and the new user control file, and then interpolate any data fields not supplied to CAMx for the new nests from the parent grid(s).

9.2.2 4-Kilometer Gridding Surrogates

Spatial gridding surrogates were developed from Land-use / Land-cover (LULC), population and transportation network data. These data are processed with Geographic Information System (GIS) software by overlaying the 4-km modeling grid definition and outputting the various gridded surrogate fields to an EPS3-ready file format.

LULC data are obtained from the USGS EROS Data Center web site and comprise a subset of the National Land Cover Dataset (NLCD). This dataset provides dominant land use data for each state at a spatial resolution of 30 meters. The dataset includes 21 LULC categories based on a Modified Anderson Level 2 categorization scheme indicated in Table 9.1. These data also form the basis of the GIS data layers used by the EPA in the development of emissions surrogates.

Table 9.1 NLCD Land Cover Classification Codes

Code	Description
11	Open Water
12	Perennial Ice/Snow
21	Low Intensity Residential
22	High Intensity Residential
23	Commercial/Industrial/Transportation
31	Bare Rock/Sand/Clay
32	Quarries/Strip Mines/Gravel Pits
33	Transitional
41	Deciduous Forest
42	Evergreen Forest
43	Mixed Forest
51	Shrubland
61	Orchards/Vineyards/Other
71	Grasslands/Herbaceous
81	Pasture/Hay
82	Row Crops
83	Small Grains
84	Fallow
85	Urban/Recreational Grasses
91	Woody Wetlands
92	Emergent Herbaceous Wetlands

Population-based surrogates are prepared using a high resolution global population database called LandScan 2006. The LandScan 2006 database was developed by Oak Ridge National Laboratory for the United States Department of Defense. The LandScan database is obtained as raster GIS data sets for the entire world at a spatial resolution of 30 arc seconds and processed using GIS scripts to generate gridding surrogates for the 4-km modeling domain.

Transportation related gridding surrogates for emissions were developed from the EPA's GIS databases assembled for use in EPS3 emissions preprocessing system. The data are derived from the 2000 U.S. Census TIGER-Line files, which provide the

appropriate roadway surrogates for emission inventory development. Also, data obtained from EPA are re-coded and assigned to the 4 road classes commonly used in emissions processing systems. The original features codes, designated by the Census Feature Class Code (CFCC) in the GIS datasets, were also retained. Table 9.2 shows the mapping of NLCD codes to the EPS-3 surrogate codes and description of the surrogate.

Table 9.2 Mapping of NCLD codes to the EPS3 Surrogate Codes

Surrogate #	Surrogate Code	NLCD Code	Description
1	TCA	11,12,21,22,23,31,32,33,41,42,43,51,61,71,81,82,83,84,85,91,92	Total County Area
2	TPP	100	Total Population
3	UPP	101	Urban Population
4	RPP	102	Rural Population
5	THU	200	Total Housing Units
6	TRU	21,22	Total Residential land
7	LDR	21	Low-density Residential
8	HDR	22	High-density Residential
9	TRL	21,22	Total Residential Land
10	HDU	10,22,23,85	High-density Residential; Commercial / Industrial /Transportation; Urban/Recreational Grasses
11	TRC	21,22,23	Total Residential; Comm / Industrial/ Trans
12	RCG	21,22,23,85	Total Residential; Comm / Indust / Transp / Urban / Recreational Grasses
13	AGL	61,81,82,83,84	Agricultural lands
14	ANO	81,82,83,84	Agricultural lands w/o Orchards
15	ORC	61	Orchards
16	TFL	41,42,43	Total Forest Land
17	EFL	42	Evergreen Forest Land
18	H2O	11,12	Water
19	BQM	31,32,33	Barren / Quarries / Mines
20	CIT	23	Commercial / Industrial / transport
21	RLA	31,32,33,41,42,43,51,61,71,81,82,83,84,91,92	Rural Land Area
22	TRD	All roads-301,302,303,304	All Roadways
23	PRD	Primary roads-301,302	Primary roads
24	SRD	Secondary roads-303,304	Secondary roads
25	URD	Urban roads-301,303	Urban roads
26	RRD	Rural roads-302,304	Rural roads
27	UPR	Urban Primary roads-301	Urban Primary roads
28	USR	Urban Secondary roads-303	Urban Secondary roads
29	RPR	Rural Primary roads-302	Rural Primary roads
30	RSR	Rural Secondary roads-304	Rural Secondary roads
31	TRR	401,402	Total Railroads
32	RC1	401	Class 1 Railroads
33	R23	402	Class 2 & 3 Railroads
34	AIR	501	Airports
35	PRT	502	Ports
36	GLF	601	Golf Courses
37	WWT	701	Waste Water Treatment Plants

9.3 CAMx Photochemical Modeling System Components

CAMx functions as a system integrating several components to generate a product useful for air quality planning. The modeling simulation involves a series of time steps which function by integrating a number of components indicated below:

- Meteorology;
- Emissions inventories;
- Chemical Mechanisms defined by the Carbon Bond Model version 6 (CB6);
- Initial and boundary conditions; and
- Post-processing.

9.3.1 Meteorological Inputs

TCEQ recently initiated the use of WRF meteorological model 5-day blocks with an overlapping period between blocks to account for model spin-up. The WRFCAMx pre-processing program extracts data from the hourly WRF outputs and creates CAMx-ready meteorological input files for the episode modeling period as indicated by the following steps:

- WRFCAMx extracts data from the WRF grids to the corresponding CAMx grids;
- Performs mass-weighted vertical aggregation of data for CAMx layers that span multiple WRF layers; and
- Applies diagnostic analysis techniques to derive key variables required by CAMx that are not directly output by WRF.

CAMx requires meteorological input data for the parameters described in Table 9.3. The following input data are derived from the WRF results. WRF-CAMx performs several functions:

Table 9.3 CAMx Meteorological Input Parameters

CAMx Input Parameter	Description
Layer interface height (m)	3-D gridded hourly time-varying layer heights
Winds (m/s)	3-D gridded hourly wind vectors (u,v)
Temperature (K)	3-D gridded hourly temperature 2-D gridded surface temperature
Pressure (mb)	3-D gridded hourly pressure
Vertical Diffusivity (m ² /s)	3-D gridded hourly vertical exchange coefficients
Water Vapor (ppm)	3-D gridded hourly water vapor mixing ratio
Cloud Cover	3-D gridded hourly cloud and precip water contents
Land-use Distribution	2-D gridded static land-use/land-cover distribution

9.4 Model-Ready Emissions

An important component in photochemical modeling discussed in previous ozone studies is preparation of an accurate emissions inventory. Pollutant emissions are treated in two basic ways within CAMx:

- Low-level (gridded) emissions that are released into the lowest (surface) layer of the model; and
- Elevated stack-specific (point) emissions with buoyant plume rise that can be emitted into any model layer.

Emissions are injected into each cell of every grid at every time step during the simulation. Gridded and point emissions are provided to CAMx in separate source-specific input files. External emission processing systems such as the Emissions Processing System - Version 3 (EPS3) are used to develop gridded and point, time- and space-resolved, chemically-speciated input files for CAMx.

9.4.1 Gridded Emissions

As indicated in the CAMx v5.40 user guide, two-dimensional gridded low-level emissions are defined by space- and time-varying rates for each individual gas and PM species to be modeled. Gridded emissions represent sources that emit near the surface and that are not sufficiently buoyant to reach into the upper model layers. Such emission categories include the following:

- Low-level stack (point) emissions that are too small to result in plume rise above the model surface layer;
- Other non-point industrial sources (fugitive leaks, tanks, etc.);
- Mobile sources (cars, trucks, non-road vehicles, railroad, marine, aircraft, etc.);
- Residential sources (heating, cooking, consumer products);
- Commercial sources (bakeries, refueling stations, dry cleaners);
- Biogenic sources; and
- Natural sources (small fires, wind-blown dust).

The spatial distribution of each individual source within these categories is defined by the modeling grid. Information such as population distribution, housing density, roadway networks, vegetative cover, etc. is typically used as a surrogate to distribute regional emission estimates for each source to the grid system. Processing

tools are used to combine emissions from all sources into a single input file for each grid.

9.4.2 Elevated Point Emissions

Elevated point emissions are also defined by space- and time-varying rates for each individual gas and PM species to be modeled. As indicated earlier, CAMx can also be applied to model the dispersion of aerosols such as $PM_{2.5}$. The only difference elevated point emissions and area source emissions is that these sources primarily emit from individual stacks with buoyant rise that may take them into upper model layers. These types of sources are almost always associated with large industrial processes, such as electric generators, smelters, refineries, large factories, etc. The spatial distribution of these points is specifically given by the coordinates of the stacks themselves (grid locations are determined within CAMx).

Plume rise is determined within CAMx as a function of stack parameters (height, diameter, exit velocity and temperature) and ambient meteorological conditions, so the point source file provides speciated time-resolved emission rates and stack parameters for each individual source. A single point source file provides the definition of all stacks and their emissions over the entire modeling domain. Plume rise is calculated using the multi-layer stability-dependent algorithm of Turner et al. (1986). This approach calculates the momentum and buoyant plume rise energy from the stack, takes the larger of these two values, and determines the dissipation of that energy via mixing with ambient air according to the meteorological conditions through the host model layer.

If sufficient energy remains to reach into the next model layer, the calculation for buoyant rise repeats for the meteorological conditions of that layer, and so on, until a

layer is found where the plume cannot rise any farther. All emissions from this source are then injected into the grid cell directly above the stack at this layer height.

This algorithm was adopted for CAMx because it provides a more realistic handling of stable layers aloft that can trap plume rise, whereas this effect would not be realized based on meteorological conditions at stack top alone. The mathematical parameters associated with management of the plume data is further described in section 2 of the CAMx v5.40 User Guide. However, regardless of the ability of the model to calculate the dispersion of a plume into the upper volume of cells, the TCEQ recommends maintaining emissions as low-level gridded emissions to confine chemical interactions of point source emissions in the first layer (email communication with TCEQ modeling team manager, Nov. 2012).

9.4.3 Initial and Boundary Conditions

Date-specific, hourly, spatially-varying initial and boundary conditions (IC/BC) of Carbon Bond Mechanism 2006 (CB6) species were developed for a 4 km modeling grid. CB6 concentrations for the 2006 episodes were prepared by ENVIRON from ozone season - chemically speciated EI data.

9.4.4 Photolysis Rates and Related Inputs

CAMx requires an input file that contains the spatial and temporal distribution of ultraviolet (UV) surface albedo, total atmospheric haze turbidity, and total atmospheric ozone column. These parameters are used to define the variations of photolysis rates across the domain and throughout the duration of the simulation. The albedo / haze / ozone (AHO) file is generated using the CAMx AHOMAP pre-processor - Version 3.

Within AHOMAP, the UV albedo is assigned according to the definition of land-use distribution generated for the modeling domain. Haze turbidity is set to a constant value representing typical rural background levels. CAMx ozone is not particularly sensitive to this parameter. A total integrated ozone column is processed from satellite-derived Ozone Monitoring Instrument (OMI) data downloaded from the following website: <http://jwocky.gsfc.nasa.gov>. AHO data are categorized into 5 bins each for albedo, 3 bins for haze, and bins for ozone.

9.4.5 Total Ultraviolet Visible Radiative Transfer Model

The Total Ultraviolet Visible (TUV) radiative transfer model is used to create a lookup table of photolysis rates to be used in the CAMx runs. TUV calculates the spectral irradiance, the spectral actinic flux, and photo dissociation coefficients (reaction rates). Rates are computed for different solar zenith angles and altitudes for the CB6 chemical mechanism using all combinations of the albedo, haze, and ozone column categories produced from the AHOMAP program. Altitudes range from ground level to 10 km. Early June is applied to estimate the sun-earth distance (ENVIRON, 2011). AHOMAP data are obtained from the TCEQ Rider 8 website.

Tropospheric ultraviolet (UV) radiation is the driving force for all photochemical processes in this layer of the atmosphere. Photons in the UV wavelength have the potential to break fairly stable molecules into very reactive fragments (photolysis) and thus initiate reaction chains which are otherwise unlikely to occur. UV radiation is harmful to living organisms and detrimental to human health. High doses of UV radiation are considered the major contributing factor for the development of skin cancer or

cataracts. UV radiation can weaken the human immune system and affect crop yields and phytoplankton activity among other potential effects.

Some questions of interest might be: What factors influence the amount of UV radiation available? What is the vertical structure of the radiative field? What sort of feedbacks (e.g., increased or decreased photolysis rates) can be expected from perturbations that - directly or indirectly - affect UV radiation? What are some of the health-related effects that can be expected from changes in atmospheric composition?

TUV outputs a clear-sky photolysis lookup table that is directly input to CAMx. The table defines photolysis rates for several Carbon Bond Mechanism Version 6 (CB6) photolytic reactions over a range of solar zenith angles, altitudes, ozone column, surface UV albedo, and haze turbidity. CAMx internally adjusts the photolysis rates for cloud cover according to the cloud inputs provided to CAMx (from WRF via WRFCAMx).

9.5 Carbon Bond Mechanism Version 6

CB6 describes tropospheric oxidant chemistry in a manner suitable for use in 3-dimensional atmospheric models such as CAMx. CB6 was developed by ENVIRON in coordination with the TCEQ which applies CAMx exclusively for ozone SIP development. The chemical mechanism is a critical component in ozone SIP development as it forms the linkage between NO_x and VOC emissions and ozone concentrations in the photochemical model. Carbon bond mechanisms (CBMs) address photolysis rates which are the rate at which a photon dissociates molecules. CBMs also address chemical reaction rates such as the typical oxidation chemistry involved in the formation and destruction of ozone.

An important factor of CBMs is the manner in which organic reactivity is treated. Earlier versions of the Carbon Bond mechanism, namely CB3 (EPA, 1984), focused on organic functional groups as indicated in the following:

- Single bonded carbon atoms consisting of paraffinic carbon molecules (PAR);
- Reactive double-bonded carbon compounds such as olefins (OLE);
- Slow double bond carbon molecules such as ethylene (ETH);
- Reactive aromatic rings such as benzene, toluene, and xylene (ARO);
- Carbonyl compounds such as ketones and aldehydes (CARB); and
- Highly photolytic α -dicarbonyl compounds - methyl glyoxal and biacetyl (DCRB).

As the 8-hour ozone NAAQS is modified and strengthened, photochemical modeling is required to focus on lower ozone concentrations and improved sensitivity to photochemical reactions. CB6 addresses these issues by building on the number of chemical species and reactions which are evaluated during a CAMx simulation. Closer examination of the many photochemical reactions which take place in the formation and destruction of ozone must be considered. The following aspects of CB6 address more stringent needs:

- Several organic compounds that are long-lived and relatively abundant, namely propane, acetone, benzene and ethyne (acetylene), are added explicitly in CB6 to improve oxidant formation from these compounds as they are slowly oxidized; and

- Attention is given to the fate of organic nitrates and the extent to which their degradation produces NO_x that may then actively participate in oxidant formation.

CB6 defines the kinetics with which the various compounds involved in the formation and destruction of ozone react. As the state of the science in photochemistry evolves additional chemical reactions are built into the carbon bond mechanism to address reactions which were previously not considered. Table 9.4 (from Emery, 2010) compares the expansion of CB6 versus Carbon Bond Mechanism version 5 (CB05).

Table 9.4 Comparison of CB6 and CB05 chemical mechanisms

	CB6	CB05
Gas-phase reactions	218	156
Photolysis reactions	28	23
Gas-phase species	77	51
Emissions species for ozone	21	16

Issues which are emerging in the science of photochemistry involve the formation and destruction of secondary organic aerosols and gas-phase chemistry, which influences PM formation by producing aerosol precursors including sulfuric acid (H₂SO₄), nitric acid (HNO₃), and semi-volatile organic compounds (SVOC). Sulfur dioxide (SO₂) can be oxidized to H₂SO₄ by hydrogen peroxide (H₂O₂) and organic hydroperoxides (RO₂H), in which R is any organic functional group. CB6 updates peroxy radical chemistry to improve formation of peroxides.

Updates to reactions of dinitrogen pentoxide (N_2O_5) with water vapor will affect nighttime formation of HNO_3 which is an end product of the ozone formation and destruction reactions. Secondary organic aerosol (SOA) formation is complex and uncertain. To address this complexity, a variety of modeling approaches have been implemented for SOA, but SOA formation is not a major focus of CB6. The main updates from earlier versions of the CBM to CB6 are as follows:

- Incorporating new scientific information released since the previous mechanism update in CB05 especially as evaluated by the International Union of Pure and Applied Chemistry (IUPAC - Atkinson et al., 2010) and NASA (Sander et al., 2006) review panels;
- Reviewing and updating reactions for alkanes, alkenes and aromatics with the most changes resulting for isoprene and aromatics;
- Adding explicitly several long-lived VOCs that form ozone at regional scales, specifically propane, benzene, acetone and other ketones;
- Adding explicitly acetylene and benzene because they are precursors to SOA formation and useful as anthropogenic emission tracers; and
- Adding explicitly VOC degradation products that can produce SOA via aqueous-phase reactions, specifically glyoxal, glycolaldehyde and methylglyoxal.

By focusing on certain reactions such as acetylene, benzene, and other long-lived VOCs, CB6 is able to more accurately calculate the chemical reaction rates and improve model sensitivity. In the process the state of the science in photochemical modeling improves.

9.6 CAMx Input Files and Run Configuration

Ozone is a secondary pollutant that forms through a complex series of photochemical reactions driven by meteorology and gaseous precursor pollutants. Photochemical modeling with CAMx involves a process of integrating ambient air quality data, emissions inventories, meteorology, and other variables with the goal of obtaining results that correspond to ambient data observed at local air quality monitoring stations. The goal with modeling is to minimize the bias between computed (predicted) outputs and observed ambient data measurements.

The following databases require preprocessing to operate CAMx for the ozone modeling episodes selected for this project:

- Three-dimensional hourly meteorological fields generated by the Weather Research and Forecasting (WRF) model via the WRFCAMx interface tool;
- Land-use distribution fields;
- Three-dimensional hourly emissions generated by the Emissions Processing System - Version 3 (EPS3);
- Initial conditions and boundary conditions (IC/BC); and
- Photolysis rates inputs, including ultraviolet (UV) albedo, haze opacity, and total atmospheric ozone column fields.

9.7 CAMx Post-Processing Tools

CAMx includes a suite of utilities which are assembled as part of CAMxPOST. The suite is a group of post-processing tools that extract data from the binary output files generated during the simulation, concatenate the extracted data to assist in

preparation of 8-hour average ozone data, combine observations and predictions, and calculate statistics. The utilities must be applied in a specific order for correct post-processing of the simulation output file.

9.7.1 CAMxTRCT

CAMxTRCT extracts two-dimensional concentration fields for one or more chemical species from the raw grid-specific CAMx output average files. This utility is written as a c-shell script and can be modified to extract as a group of chemical species of interest. For this dissertation O_3 , NO_x , NO , H_2O_2 , HNO_3 , $HONO$, and isoprene were extracted by CAMxTRCT. Two separate CAMxTRCT files were prepared in order to segregate the directories in which the data was placed. CAMxTRCT output files are in binary format.

9.7.2 AVGCAT

AVGCAT concatenates several CAMx AVERAGE files to provide continuous hourly model output data in a single file to simplify the process of calculating running n-hour averages (e.g., 8, 24, etc.) over multi-day simulations. The program only operates on UAM formatted files. AVGCAT processes simulation output for COARSE grid data.

If data from a FINE grid is to be processed by AVGCAT, then the CAMxTRCT post-processing utility needs to be run on the CAMx FINE grid output to generate files with the COARSE grid format. The AVGCAT executable offers the option for processing COARSE or FINE gridded data. AVGCAT assumes that all files to be concatenated contain the same grid configuration, and the same number and order of chemical species.

9.7.3 OBSCAT

OBSCAT concatenates several OBSERVATION data files together into a single file with the purpose of providing continuous hourly measurement data in a single file to simplify the process of calculating running n-hour averages (e.g., 8, 24, etc.) over multi-day simulations. OBSCAT assumes that all input OBSERVATION files contain identical numbers of hourly records (e.g., 24 hours per site) and identical lists of monitoring sites. Generally, separate OBSERVATION files are developed for the CAMx post-processing system for each day of a multi-day simulation episode. However, the system will also work for a single OBSERVATION file across the entire episode. The output of OBSCAT could also be used for all subsequent operations of the CAMx post processing system.

The OBSCAT executable produces a text file which is read during the CAMxPOST process. The observed data provided by OBSCAT must be a non-negative integer. Otherwise CAMxPOST generates a binary output file which becomes tedious to open.

9.7.4 CAMxPOST

CAMxPOST prepares files for statistical evaluation and/or to generate 1-, 8-, or 24-hour mean predicted concentration fields. CAMxPOST reads the AVGCAT output and processes layer 1 from the input file. Separate c-shell scripts can be prepared specifying the species to process; this function operates on only one chemical species requiring multiple files for each species one wishes to process. The program provides the following capabilities:

- Generates a running n-hourly file in COARSE GRID AVERAGE format;
- Generates a maximum n-hourly file in COARSE GRID AVERAGE format;

- Pairs predictions and observations and generates an ASCII running n-hourly prediction-observation file for further processing of statistics;
- Provides the minimum and maximum predicted concentrations within a nine-cell area around each monitoring location; and
- Generates an ASCII file of maximum observations at each site where "n-hourly" refers to averages over 1 to several hours (e.g., 8, 24, etc.).

For purposes of determining the VOC- or NO_x-Limited ozone formation conditions, additional CAMxPOST scripts were prepared for HNO₃ and H₂O₂. In the previous section it was stated that the OBSCAT file must be a non-negative integer. The reason is CAMxPOST pairs the predicted and observed data for statistical analysis or additional processing such as preparing time-series plots. If a series of negative integers are read by CAMxPOST the procedure fails and generates a binary file.

9.7.5 CAMxSTAT

CAMxSTAT reads an n-hourly PREDOBS file generated by CAMxPOST and calculates the following statistics:

- Unpaired (time and space) peak prediction accuracy;
- Space-paired, time-unpaired peak prediction accuracy by site;
- Space-paired, time-unpaired peak bias and error over all sites;
- Space-paired, time-unpaired bias and error in peak timing;
- Space-paired, time-paired peak bias and error over all sites;
- Mean prediction;
- Mean observation;

- Difference and normalized difference in mean pred and mean obs;
- Absolute, normalized, and fractional bias;
- Absolute, normalized, and fractional error; and
- Root mean square error.

CAMxSTAT produces statistics written to an ASCII report file. CAMxSTAT operates on the contents of the input PREDOBS paired file which extends for the duration of the simulation runtime. The CAMxSTAT script offers a user-entry to indicate a threshold predicted concentration for comparing PREDICTION-OBSERVATION pairings, which for this dissertation was set at 0.040 ppm.

Output generated by CAMxSTAT includes a listing of the PEAK OBSERVED and PEAK PREDICTED values generated during the simulation. The grid cell in which the maximum predicted value occurs is also reported. The PEAK OBSERVED value is provided by the OBSCAT dataset. The file includes a listing of the PEAK PREDICTED values for all the monitoring stations in the modeling domain which have been integrated into the OBSCAT dataset.

9.7.6 EXSTAT

EXTSTAT reports important statistics from a series of report files generated by CAMxSTAT for importation into a spreadsheet and preparation of graphical summaries. Statistics that are reported are the following:

- Unpaired peak prediction accuracy (UPPA);
- Bias in paired peak accuracy among all valid sites (APPA);
- Error in paired peak accuracy among all valid sites (EPPA);

- Bias in peak timing (PTB);
- Normalized bias (NB); and
- Normalized error (NE).

Unpaired Peak Prediction Accuracy (UPPA) compares the peak concentration modeled throughout the selected area against the peak ambient concentration anywhere in the same area. UPPA tests the model's ability to reproduce the highest observed value anywhere in the region (Doty, 2002). The difference of the peaks (model - observed) is normalized by the peak observed concentration" (EPA, 2007). UPPA is calculated as follows:

$$UPPA = \frac{Cp(x, t) - Co(\hat{x}, \hat{t})}{Co(\hat{x}, \hat{t})} \cdot 100\% \quad \text{Equation 9.10}$$

Bias in paired peak accuracy among all valid sites (APPA) is paired in time and space with the observed ozone value. APPA compares the PEAK OBSERVED 1-hour or 8-hour ozone concentration from each regional CAMS included in the simulation with the co-located PEAK PREDICTED value according to Equation 9.11.

$$APPA = \frac{Cp(\hat{x}, \hat{t}) - Co(\hat{x}, \hat{t})}{Co(\hat{x}, \hat{t})} \cdot 100\% \quad \text{Equation 9.11}$$

APPA quantifies the difference between the magnitude of the peak 1-hour or 8-hour ozone concentrations observed at a monitoring station (C_o) and the PEAK PREDICTED ozone concentrations C_p , at the same space and time (\hat{x}, \hat{t}). Model

estimates and observations are thus "paired in space and time." The paired peak estimation accuracy is a stringent model evaluation measure. It quantifies the model's ability to reproduce, at the same time and location, the highest observed ozone concentrations during the simulation. APPA does not have specifications regarding acceptable limits.

Bias in Peak Timing (PTB) indicates the difference in time between the time of day of PEAK OBSERVED and PREDICTED PEAK as indicated in Equation 9.12. For example, if the simulation observes the peak at 1400 hours and the peak observed in the monitoring network occurs at 1200 hours the PTB = 2.

$$PTB = Hour\ of\ Predicted\ PeakObs - Hour\ of\ PeakObs \quad \text{Equation 9.12}$$

Mean Normalized Bias (MNB): This performance statistic averages the model / observation residual, paired in time, normalized by observation, over all monitor times and locations. A value of zero would indicate that the model over predictions and model under predictions exactly cancel each other out. NB describes the ability of the model to over-predict or under-predict ozone concentrations. The calculation of this measure is shown in Equation 9.13.

$$NMB = \frac{\sum_1^N (Model - Obs)}{\sum_1^N (Obs)} \cdot 100\% \quad -15\% \leq NB \leq +15\% \quad \text{Equation 9.13}$$

Normalized Mean Error (NME or NE) (%) indicated in Equation 9.14 is used to normalize the mean error relative to the observations. This statistic averages the absolute sum of the difference (Predicted - Observed) over the sum of Observed values. Normalized mean error is a useful model performance indicator because it avoids over inflating the observed range of values (EPA 2007). NE observes the scatter of the entire dataset generated by CAMx during the simulation for all sites and observations. The goal is to minimize NE to $\leq 35\%$.

$$NME = \frac{\sum_1^N |Model - Obs|}{\sum_1^N (Obs)} \cdot 100\% \quad NE \leq 35\% \quad \text{Equation 9.14}$$

9.8 Limitations of Photochemical Modeling

A major finding in several photochemical modeling studies indicates emission inventories (EIs) grossly underestimate VOC precursors (TexAQS 2000, Yarwood 2005, Funk 1999, Thomas 2008). Modelers conduct multiple simulations and modify input parameters in order to minimize the error between predicted and observed atmospheric parameters. Noor (2008) also reports that grossly under-estimated highly reactive volatile organic compounds (HRVOC) in the EIs of industrial point sources are a major cause of error in photochemical modeling used in the SIP planning process.

HRVOCs which tend to be underestimated include ethene and propene. Both were grossly under-estimated in the EIs of industrial (primarily petrochemical) point sources in the Houston-Galveston-Brazoria (HGB) area (Thomas, 2008). This was a major cause of error in photochemical modeling used in the SIP modeling and planning process. The potential exists for gross estimation of similar HRVOC in the PdN region which would be emitted at the petrochemical refinery in the center of this binational community.

The EIs pointed to small emissions of HRVOC compared to NO_x, leading to relatively slow initial chemistry of such emissions during the CAMx simulations. It was found that these sources emit comparable and substantial amounts of both NO_x and HRVOC causing very rapid O₃ production in the point source plumes (Thomas, 2008, TexAQS, 2000). This being the case, modelers continually modify the model input parameters to reduce the error and bias between observed and predicted ozone concentrations.

The nonlinear interactions among NO_x, VOC, and the role of intermediate radicals that drive oxidant chemistry are difficult to evaluate from the concentration output fields generated by CAMx (Thomas, 2008). The model includes a Process Analysis (PA) tool which assists in the analysis of the significant oxidant pathways in different chemical regimes as a function of space and time. Through PA, multiple iterations and varied input parameters can help define a mix of emissions and identify which emissions reductions may help achieve attainment of the ozone NAAQS. The PA tool was not applied to this dissertation. It should also be noted that this dissertation did not assess the sensitivity to specific VOC species. This study provides a foundation

from which future photochemical modeling simulations may be undertaken for the PdN region.

9.9 Summary

CAMx is an intuitive photochemical model which takes into consideration meteorology, emissions, and boundary conditions associated with ozone formation. The variables which tend to add a high level of error into the modeling process appear to be those involving human judgment from the perspective of emissions inventory development. EIs are derived from emission factors applied to multiple sources and source categories and tend to rely on surrogate data to estimate a regional dataset.

Applying surrogate data to estimate emissions which are inputted into a photochemical model integrates error into the parameters assessed by CAMx. CAMx relies on surrogate data for a portion of the input data processed during the simulation. Point source emissions data should also be as accurate as possible. Failure in accuracy leads to the insertion of error in the photochemical modeling simulation. Such is the importance of developing emission inventory improvement programs to reduce the variance between modeled and actual emissions data.

10 Emissions Inventories

Emission inventories are a summary of air pollutants generated by multiple sources. As the term indicates, an inventory is an accounting of air pollution emissions from the four major source categories consisting of area, onroad mobile, nonroad mobile, and point. This section discusses results obtained from emissions inventories developed by the TCEQ in compliance with FCAA requirements for SIP development.

10.1 Baseline Emissions Inventories

The base year inventory is the primary inventory from which the other three required ozone SIP inventories are derived. The FCAA requires that the base year inventory be a comprehensive, accurate, and current inventory of actual emissions in the nonattainment area (§182(a)(I)). The EI includes emissions of VOC, NO_x, and CO from stationary point and area sources, on-road mobile sources, and non-road mobile sources. Both anthropogenic and biogenic emission sources are included.

Emissions are based on conditions that exist during the peak ozone season which generally extends from June through August. Industrial activity, population, VMT, etc. and emissions must represent a typical peak ozone season day for the base year.

10.1.1 Ozone Season Emissions Inventory

TCEQ developed an ozone season EI from which the modeled EI is prepared. The term "typical ozone season day" refers to activities that occur during the three-month period at which the highest ozone exceedances occur, averaged on a daily basis. For example, if during the summer weekdays (Monday – Friday, June – August)

of any particular year a manufacturing process produces 12,000 tons of material, and this period includes 13 weeks, 5 operating days per week, then the average or "typical" ozone season day activity would be: $12,000 / (13 \times 5) = 185$ tons/day. This value would then be multiplied by the emission factor, control factor, and rule effectiveness factor, if applicable, to calculate the typical ozone season day emissions.

A review of the Texas Air Emissions Repository (TexAER) which contains emissions inventories for Texas provided a simple proportion applied by TCEQ for determining ozone season emissions. Ozone season emissions were 28.8% of annual emissions. Based on this ratio, it is simple to calculate daily emissions applied to the modeled emissions inventory.

10.2 Area Source Emissions

Area sources are those air pollution sources considered too small and too numerous to be handled individually as point source emissions. Area sources are primarily subdivided into two groups characterized by the emission mechanism: 1) evaporative emissions, and 2) fuel combustion emissions. Sources of evaporative losses include gasoline service stations, solvent use, such as dry cleaning, degreasing, surface coating operations, automotive paint shops, architectural coatings, and leaking underground storage tanks. Fuel combustion sources include stationary source fuel combustion in residences, industrial processes, commercial operations, forest fires, structural fires, and solid waste disposal by burning (TCEQ, 2002).

10.2.1 Review of El Paso Area Source Emissions

Area source emissions inventories (ASEIs) are prepared at three-year intervals by the TCEQ. ASEIs for the years 2002, 2005, and 2008 were obtained from Texas Air Emissions Repository (TexAER) website (TCEQ, accessed August, 2011). TCEQ's 1999 ASEI is a comprehensive baseline of area source emissions data from which follow-up ASEIs are updated.

The 2002 ASEI provides comprehensive information which builds off of the 1999 ASEI using EPA's Economic Growth Analysis System (EGAS-4) for most of the SCCs. EGAS-4 is an emissions activity forecast software model that provides State and local governments with an EPA-approved set of emissions activity growth factors. Table 10.1 identifies summary data obtained from TexAER. Seven primary categories are presented as 2-digit Source Classification Codes (SCC).

Table 10.1 Two-digit source classification categories

SCC	Source Classification
21xxxxxxx	STATIONARY SOURCE FUEL COMBUSTION
22xxxxxxx	MOBILE SOURCES
23xxxxxxx	INDUSTRIAL PROCESSES
24xxxxxxx	SOLVENT UTILIZATION
25xxxxxxx	STORAGE AND TRANSPORT
26xxxxxxx	WASTE DISPOSAL - TREATMENT AND RECOVERY
28xxxxxxx	MISCELLANEOUS AREA SOURCES

Ten-digit SCCs present a detailed description of air pollutant emitters and facilities. This project reports data to the 7-digit level which is a high-level of detail for

ASEI information. A list of the most important area sources in the PdN Region identified by 7-digit SCC with brief descriptions is provided in Appendix I.

Table 10.2 summarizes the 2002 area source emissions in TPY based on 2-digit SCCs. As indicated, “Solvent Utilization” comprises the highest VOC emission source category. Nitrogen oxides are the highest emissions source for “Stationary Source Fuel Combustion”. PM₁₀ comprises the largest component of criteria pollutant area source emissions in 2002. Road Construction, Paved Road (fugitive) emissions, and Heavy Construction contribute the major portion of this pollutant.

Table 10.2 2002 El Paso Area Source Emissions Inventory Summary (in TPY)

Source Classification	VOC	N0x	CO	SO ₂	PM ₁₀	PM _{2.5}	NH ₃
STATIONARY SOURCE FUEL COMBUSTION	480	1,174	1,642	404	443	334	14
MOBILE SOURCES	-	-	-	-	3,726	280	-
INDUSTRIAL PROCESSES	109	<0.10	69		9,244	1,980	-
SOLVENT UTILIZATION	5,524	-	-	-	-	-	-
STORAGE AND TRANSPORT	1,052	-	-	-	-	-	-
WASTE DISPOSAL - TREATMENT AND RECOVERY	706	21	4,251	4	601	595	<0.10
MISCELLANEOUS AREA SOURCES	15	2	221	4	1,713	392	2,577
TOTALS	7,887	1,198	6,183	412	15,727	3,582	2,591

Figure 10.1 illustrates 2002 criteria pollutant emissions for El Paso described in Table 10.2. PM₁₀ comprises the bulk of area source emissions due primarily to the amount of unpaved roads in the PdN region. VOCs, however, comprise the majority of gaseous emissions in this region.

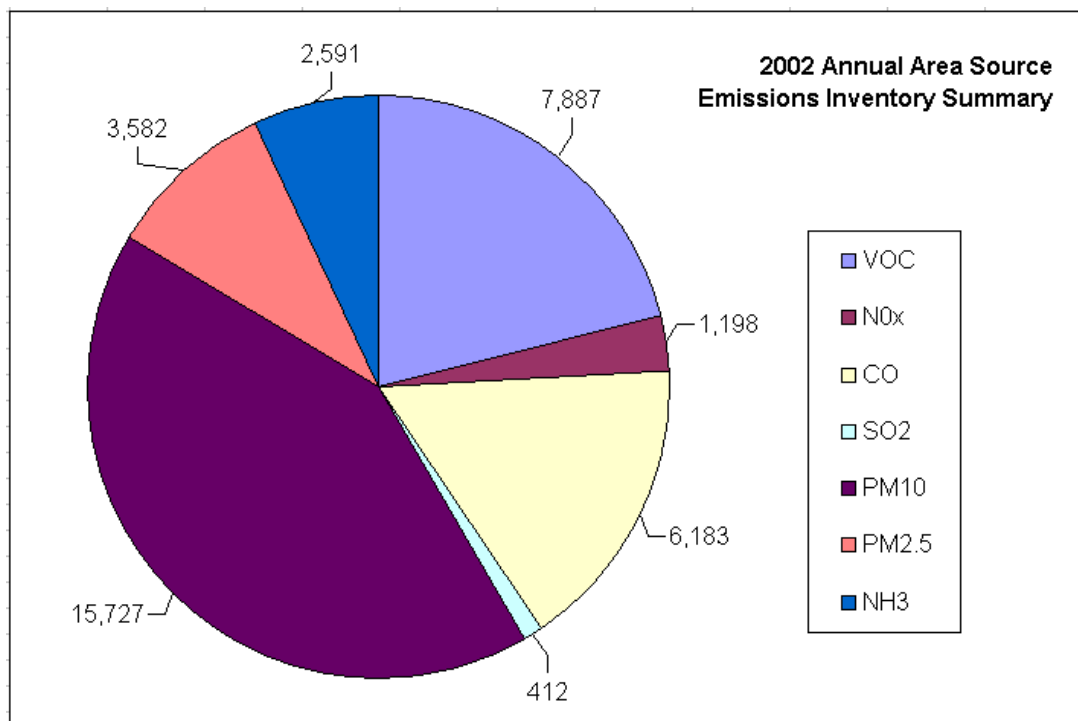


Figure 10.1 2002 El Paso Area Source EI Criteria Pollutants

Table 10.3 summarizes 2005 El Paso area source emissions based on broad category 2-digit SCCs. Data indicates growth from 2002 in VOC, NOx, CO, NH₃, and SO₂ emissions and a significant reduction in PM₁₀ and PM_{2.5} emissions. Figure 10.2 provides a graphical format for 2005 El Paso area source emission. VOC, CO and PM₁₀ are the top three criteria pollutants reported under this source category.

Table 10.3 2005 El Paso Area Source Emissions Inventory Summary (in TPY)

Source Classification	VOC	NOx	CO	SO ₂	PM ₁₀	PM _{2.5}	NH ₃
STATIONARY SOURCE FUEL COMBUSTION	478	1,196	1,644	405	286	279	14
MOBILE SOURCES	-	-	-	-	1,957		
INDUSTRIAL PROCESSES	115	<0.10	72		4,794	1,096	
SOLVENT UTILIZATION	5,938	-	-	-	-	-	-
STORAGE AND TRANSPORT	1,020	-	-	-	-	-	-
WASTE DISPOSAL - TREATMENT AND RECOVERY	740	23	4,465	4	280	280	<0.10
MISCELLANEOUS AREA SOURCES	18	3	236	4	946	232	2,809
TOTALS	8,308	1,221	6,417	413	8,263	1,887	2,823

Figure 10.2 illustrates 2005 criteria pollutant emissions for El Paso described in Table 10.3. VOC and PM₁₀ comprise the bulk of area source emissions due primarily to the amount of unpaved roads in the PdN region. VOCs comprise the majority of gaseous emissions in this region.

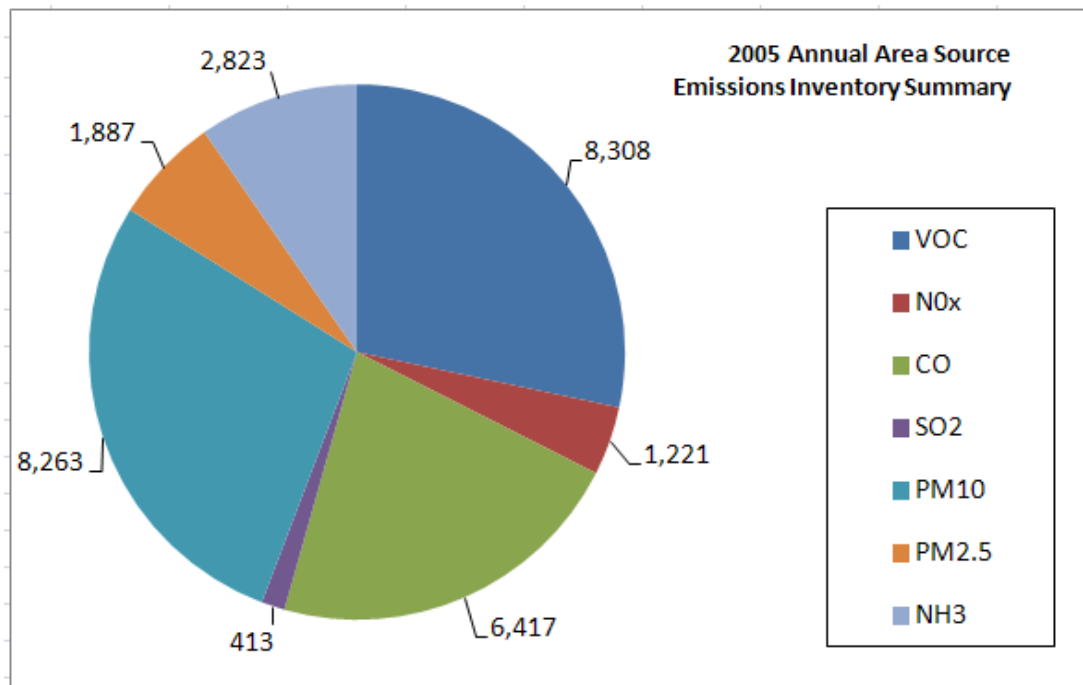


Figure 10.2 2005 Area Source EI Criteria Pollutants (TPY) – El Paso

Table 10.4 summarizes 2008 El Paso area source emissions based on the broad category 2-digit SCCs. Data indicate continued growth from 2005 in VOC, NO_x, CO, NH₃, PM₁₀, and SO₂ emissions. PM_{2.5} emissions are roughly the same. The data is grown from 2005 ASEI data using EGAS-4, contractor updates, implementation of control strategies and other methods.

Table 10.4 2008 Area Source Emissions Inventory Summary (in TPY)

Source Classification	VOC	NO _x	CO	SO ₂	PM ₁₀	PM _{2.5}	NH ₃
STATIONARY SOURCE FUEL COMBUSTION	485	1,214	1,738	414	206	199	20
MOBILE SOURCES					2,041		
INDUSTRIAL PROCESSES	156	<0.10	76		4,863	1,101	
SOLVENT UTILIZATION	6,871						
STORAGE AND TRANSPORT	1,226						
WASTE DISPOSAL - TREATMENT AND RECOVERY	759	23	4,656	4	292	292	<0.10
MISCELLANEOUS AREA SOURCES	17	3	237	4	1,035	253	3,108
TOTALS	9,513	1,240	6,707	422	8,437	1,844	3,128

Figure 10.3 presents the 2008 area source emissions inventory. VOCs, CO, and PM10 represent the top 3 pollutant emissions in El Paso. VOCs consistently present the bulk of emissions. NO_x tends to maintain a ratio of 20% of VOC, but the data indicate the ratio is much lower.

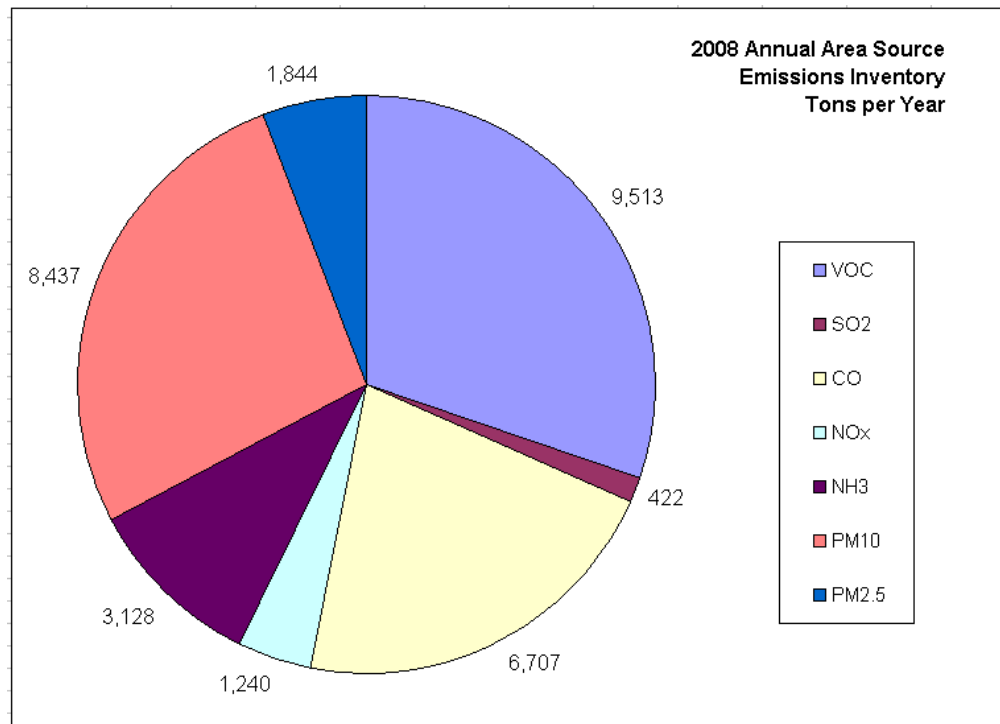


Figure 10.3 2008 Area Source Emission Inventory (TPY) – El Paso

Figure 10.4 summarizes criteria pollutant emissions for the years 2002, 2005, and 2008. EI data indicate an increase of over 1,000 tons (~14%) in the “solvent utilization” category. The increase in VOC in the area source category will be assessed using CAMx. The other categories, CO, PM₁₀, NH₃, and NO_x showed a general increase that was likely estimated using EGAS. Major changes in emissions inventory values are usually due to modifications in the method of calculating emissions or new surveys completed after several years of standardized modifications using default values.

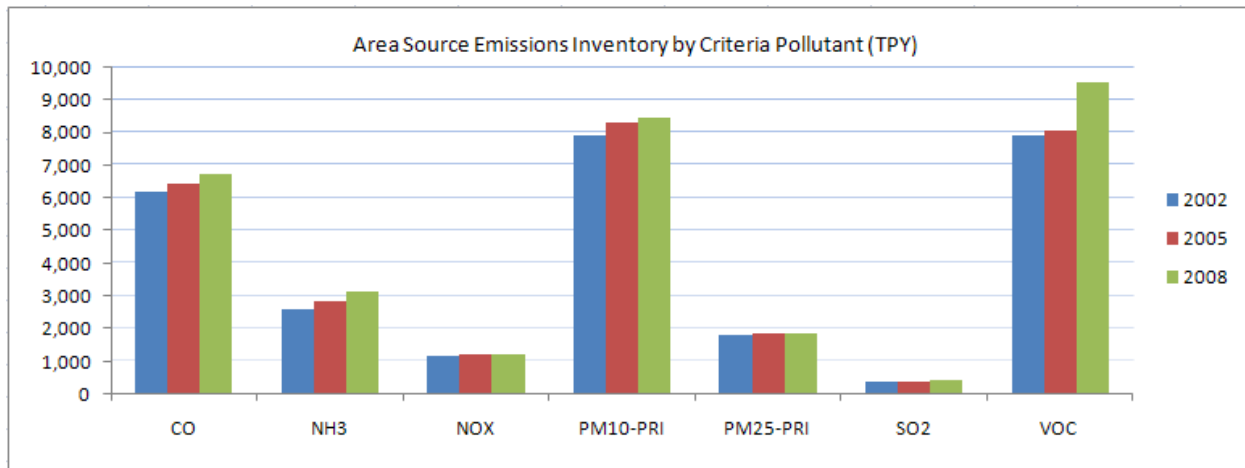


Figure 10.4 El Paso Source Emissions by Criteria Pollutant (TPY) - 2002, 2005, 2008

A high degree of success has been achieved in reducing and controlling VOC emissions by installing Stage 1 & 2 VRS in all El Paso County gasoline stations in compliance with air pollution control strategies established in the SIPs prepared for El Paso. Additional control strategies include the requirement to distribute low-Reid vapor pressure (Low-RVP) gasoline in summer as well as requiring the sale of low-VOC paints for surface-coating applications. However, Figure 10.4 data indicate consistent increases in VOC emissions in the 2002, 2005, and 2008 area source EI while the City of El Paso observes year over year improvements in the ozone DV.

10.2.2 Review of Emission Development Methodology

The 2002 PEI (TCEQ, 2004) provides descriptions of several methodologies applied to the development of the ASEIs. The U.S. EPA's 2002 National Emissions Inventory (NEI) was the starting point for the 2002 PEI. NEI categories and emissions were reviewed and updated with current methodologies and activity data where it was deemed significant to do so. This resulted in the 2002 PEI being compiled from multiple

sources such as TCEQ staff, contractors, and local Councils of Government (COGs). (TCEQ, 2004) EGAS-4 is used to develop 2002 categories not covered by contracted work.

10.2.3 Review of Activity Data

Activity data is described in the Periodic Emissions Inventory reports prepared by TCEQ (TCEQ, 2002 & 2005). Activity data is obtained from multiple sources to include the following:

- Texas Comptroller of Public Accounts;
- Texas Department of Transportation;
- Texas Department of Agriculture;
- Texas Workforce Commission industrial employment data;
- State projected population data;
- Contractor information;
- Mobile 6;
- AP-42; and
- Previous year EIs.

The 2002 Final Periodic Emissions Inventory for Area, Nonroad Mobile, and Biogenic Sources provides a comprehensive discussion on ASEI activity data. (TCEQ, 2002)

10.2.4 Review of Cd. Juárez Area Source Emissions Inventories

Previous reports on Cd. Juárez area source emissions inventories indicate the EI for this city are inaccurate (Emery, 2000) or emissions required substantial modification (Nagaraj, 2002). Sullivan (2012) provided an EI with a 2008 base year. For the most part the 2008 EI for Juárez is based on surrogate data which grows the 1999 national emissions inventory (NEI) developed by Eastern Research Group (ERG). ERG also prepared the 1999 NEI for EPA. Figure 10.5 illustrates the 2008 area source EI for Juárez.

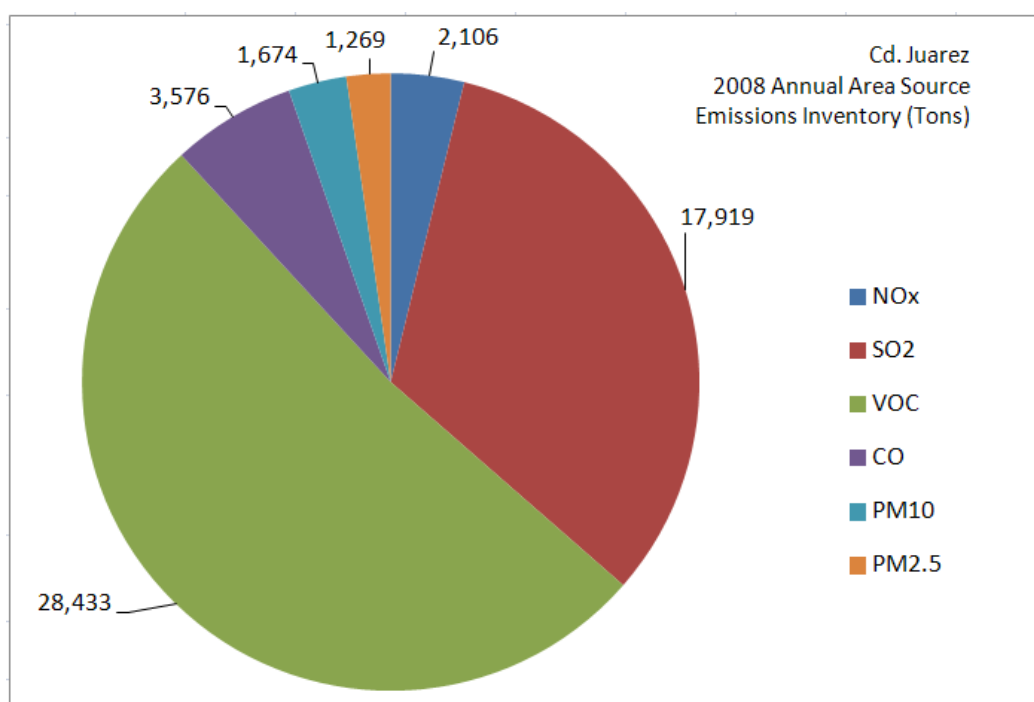


Figure 10.5 2008 Cd. Juárez Annual Area Source Emissions Inventory (TPY)

10.3 Point Sources

Under the current attainment status of El Paso for the ozone NAAQS, the Texas Administrative Code (TAC) Title 30, Part 1, §101.10 (30 TAC §101.10) requires any owner or operator of a stationary emission source to submit an emission inventory (EI) to TCEQ if emissions are equal to or exceed 100 tons per year (TPY) for any contaminant, including VOC, for which a NAAQS has been issued.

Sources that have submitted an initial emission inventory (IEI) are required to submit an annual emissions inventory update (AEIU) that consists of actual and allowable emissions. Owners and operators must supply a certifying statement for each EIs to attest that the information in the inventory is true and accurate. The regional point source EI is compiled by TCEQ from all source-specific EI submissions required by 30 TAC §101.10. TCEQ publishes the most current regional point source EI and updates on an annual basis.

10.3.1 Regional Point Source Contributions and Trends

Point source emission inventories from 1999, 2002, 2004, 2005, 2008, and 2009 were reviewed to evaluate the Standard Industrial Classification (SIC) specific emission contributions and emission trends in El Paso County. All inventories were obtained from the TCEQ website.

The 2009 inventory is the most current EI available from the TCEQ website. Table 10.5 presents VOC and NO_x emissions for the years indicated above. A graphical representation of point source VOC and NO_x data is presented in Figure 10.6.

Table 10.5 Point Source Emissions in El Paso (TPY)

Year	VOC			NOx		
	Sources #	Emissions TPY	Change* %	Sources #	Emissions TPY	Change* %
1999	29	1322	-	20	4495	-
2002	28	780	-41%	19	3695	-18%
2004	25	803	-39%	18	3339	-26%
2005	17	961	-27%	14	3397	-24%
2008	24	1056	-20%	21	4687	4%
2009	18	991	-25%	14	2980	-34%

* the relative change was computed using 1999 as the base year

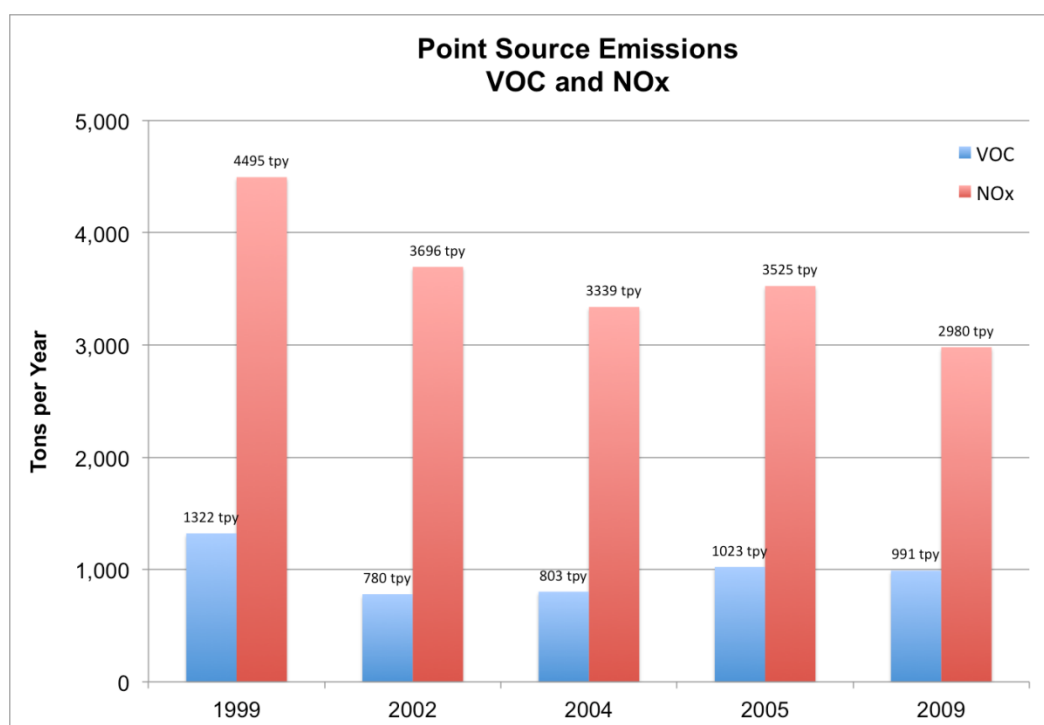


Figure 10.6 El Paso Point Source VOC and NOx Emissions (TPY)

10.3.2 Point Source VOC Emissions in El Paso County, Texas

As defined by the 30 TAC §101.10, in 1999 there were 29 VOC point sources in El Paso with total emissions of 1,322 TPY. By 2009 the number of VOC point sources reduced to 18 and total VOC emissions were 991 TPY. Considerable VOC emissions reductions were achieved by 2004 when emissions totaled 803 TPY, 39% less than in 1999. However, VOC emissions increased to 1,023 TPY in 2005 and dropped to 991 TPY by 2009; 25% less than in 1999.

Major point source emissions categories are Steel Works (SIC 3312), Electric Services (SIC 4911), Petroleum Bulk Stations (SIC 5171) and National Security (SIC 9711). Combined, these five major source categories constituted, on average, 89% of the total regional VOC point source emissions during the last decade as indicated in Table 10.5. The contribution of VOC emissions from Petroleum Refining to the regional point source total was 56% in 2009. The source category with the greatest increase in VOC emissions during the last decade was Steel Works (SIC 3312). SIC 3312 emissions increased nine fold from 13 TPY in 1999 to 118 TPY in 2009.

Figure 10.7 illustrates annual point source VOC emissions categorized by SIC. In El Paso the dominant VOC emission source category was Petroleum Refining (SIC code 2911), which on average contributed 64% of the VOC point source emissions during the last decade. This quantity is indicative of the petroleum refinery located in the center of the PdN community.

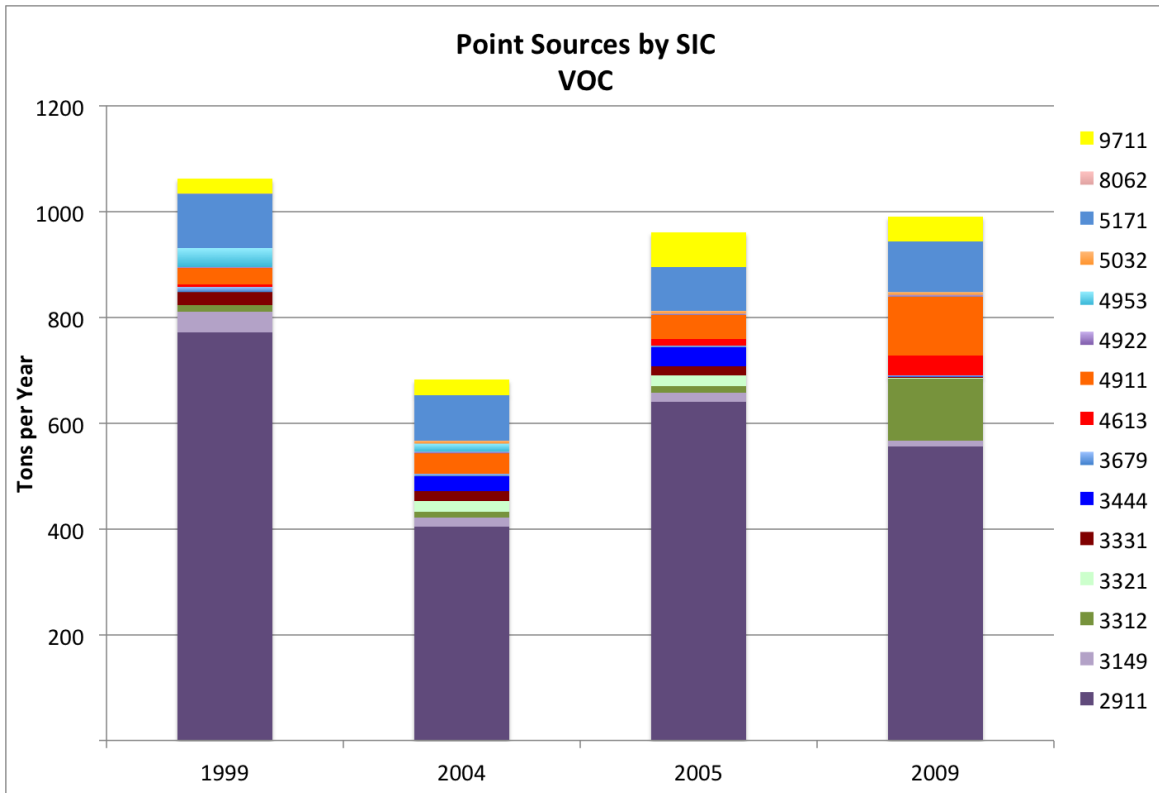


Figure 10.7 VOC Point Source Emissions by SIC (TPY)

Figure 10.8 illustrates annual point source VOC and NOx emissions for the years 1999, 2002, 2004, 2005, and 2009. This data was obtained from the TCEQ website

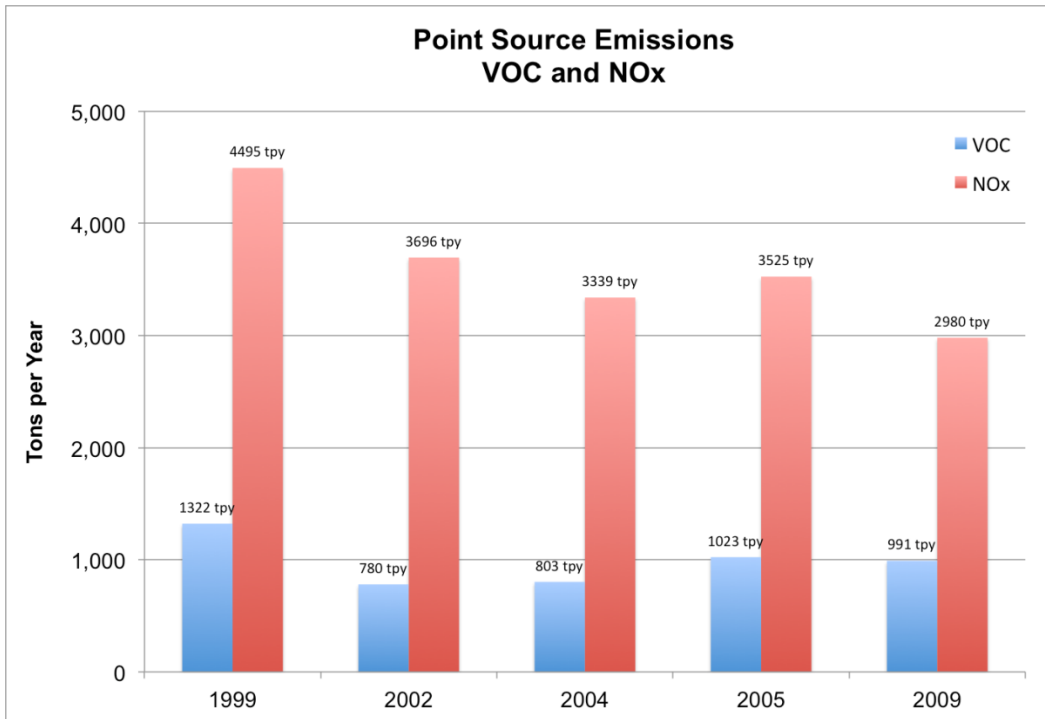


Figure 10.8 El Paso VOC and NOx Emissions 1999-2009 (TPY)

10.3.3 Point Source NOx Emissions in El Paso County, Texas

In 1999 El Paso had 20 NOx point sources with total emissions of 4,495 TPY. By 2009 the number of point sources reduced to 14 and NOx emissions were 2,980 TPY, 34% less than in 1999. Table 10.6 identifies the top 4 point source NOx emissions by source category.

Table 10.6 Top 4 NOx Sources in El Paso, TX by Industrial Classification

Category	SIC	1999	2004	2005	2009	Average
Petroleum Refining	2911	27%	39%	37%	26%	32%
Steel Works	3312	3%	2%	0%	7%	3%
Electric Services	4911	61%	51%	51%	58%	55%
Natural Gas Transmission	4922	3%	3%	4%	5%	4%
	Top 4	95%	95%	93%	96%	95%

Electric Services (SIC 4911) is the source category with greatest emissions. SIC 4911 contributes on average ~55% of the total point source NO_x emissions from 1999-2009. Other major NO_x sources in El Paso are Petroleum Refining (SIC 2911), Steel Works (SIC 3312), and Natural Gas Transmission (SIC 4922).

Combined, the four major source categories mentioned above constituted, on average, 95% of the total point source NO_x emissions during the last decade. Brick, Stone, and Related Construction Materials (SIC 5032) generated the greatest increase in NO_x emissions during the last decade. There was a three-fold increase from 32 TPY in 1999 to 104 TPY in 2009.

10.3.4 Nonroad Mobile Source Emissions

Nonroad mobile sources are, collectively, vehicles that do not normally operate on roads and highways. These are various types of equipment propelled by combustion engines using various fuels. They are used for purposes such as in agricultural operations, construction, lawn and garden maintenance, industry, and recreation. The category also includes aircraft, locomotives, recreational boats, and commercial marine vessels. The fuels used by nonroad mobile sources are gasoline, diesel, compressed natural gas, and liquid petroleum gas LPG (TCEQ, 2004). Table 10.7 identifies the various nonroad mobile source pollutants in TPY.

Table 10.7 Non Road Mobile Source Emissions (TPY)
El Paso, TX (2002, 2005, 2008)

Year	NOx	VOC	CO	SO2	PM10- PRI	PM25- PRI	CO ₂
2002	2,897	1,712	25,412	269	189	184	207,095
2005	2,875	1,547	22,516	49	191	163	214,967
2008	2,381	1,376	19,563	50	200	194	304,649

10.3.5 Aviation Emissions

Aviation emissions are calculated using the Emissions Dispersion Modeling System (EDMS) which is required by the Federal Aviation Administration (FAA) for air quality analysis involving aviation sources. Aircraft, auxiliary power units (APU), and ground service equipment are included as aviation sources modeled by EDMS (FAA, 2005). EDMS was developed in the mid-1980s as a complex source microcomputer model designed to assess the air quality impacts of proposed airport development projects. FAA elevated the status of EDMS to a required model when conducting air quality analysis for aviation sources. This was done to ensure consistency and quality in aviation-related air quality analyses.

Aviation emission algorithms and data used in EDMS are well established and are EPA developed and/or recommended. EDMS includes emission factors for the various airport sources. For example, it incorporates all aircraft engine emissions data contained in the internationally accepted International Civil Aviation Organization (ICAO) Exhaust Emissions Data Bank representing nearly two-thirds of EDMS's aircraft engine emissions data. The remaining third of EDMS's aircraft engine emission data originate from other sources. EDMS also includes vehicle emission factors from EPA's on-road

model, MOBILE5A3. Version 4.1 marked the first phase of migration towards EPA's draft NONROAD model for ground support equipment incorporating NONROAD derived emission factors.

10.3.6 Review of Emissions

The emission inventories of nonroad mobile sources for the years 2002, 2005, and 2008 were obtained from Texas Air Emissions Repository (TexAER) website (TCEQ, accessed August, 2011). Three years of data were reviewed to evaluate the Periodic Emission Inventory (PEI) and check for potential discrepancies in the inventories which could be improved through further investigation.

There is a declining trend in ozone precursor NO_x, VOC, and CO emissions. The reduction of VOC and CO may be due to improved internal combustion engine technologies deployed in recent years, while the reduction of NO_x may be caused by efficient control measures.

10.4 Summary

As reported in Section 9 emissions inventories tend to be inaccurate. Perhaps this is due to the degree of estimation and surrogacy applied to developing the EI. Area source EIs tend to have a high level of estimation due to the large number of emissions sources and the method of allocating emissions across the population or other methods of applying activity data. This matter must be taken into consideration when applying an estimated emissions inventory to a photochemical model.

It should be noted that the modeled EI to be described in the following sections is not based on the EI reported in this section. The EI reported in this section is the official

EI used by TCEQ for air quality planning purposes. The EI applied to photochemical modeling evaluated in this report is unlike the official EI. The author cannot explain this discrepancy. TCEQ provided the EI for 2006 applied to the BASELINE CAMx modeling as well as the EI data provided in this section. The discrepancy is substantial regarding Juárez point sources emissions and may require additional attention.

11 CAMx Modeling

CAMx simulates air quality over many geographic scales. It handles a variety of inert and chemically active pollutants, including ozone, particulate matter, inorganic and organic PM_{2.5} and PM₁₀, mercury, and other toxics. CAMx was developed by ENVIRON as a publicly available air quality model for application in State Implementation Plan development.

This report documents several CAMx simulations developed for an ozone episode during which time meteorological conditions were favorable for the formation of elevated ozone concentrations. Photochemical modeling simulations were conducted for 12 distinct emissions scenarios for the period ranging from June 12-21, 2006. An ozone event occurred on Sunday, June 18. Each simulation was evaluated to assess the impact on ozone concentrations due to variations in NO_x and VOC emissions.

11.1 CAMx Modeling Domain

Figure 11.1 presents the initial modeling grid established for this study. A 36-12-4 kilometer grid was established by the TCEQ for the simulations to provide a wide area of emissions which could potentially impact the State of Texas as well as the PdN region. This domain encompasses the eastern two-thirds of the continental U.S. Nested within the 36 km U.S. grid is the 12 km grid which extends over the State of Texas. A 4 km grid was established as the modeling domain for the CAMx simulation pertinent to the PdN airshed.

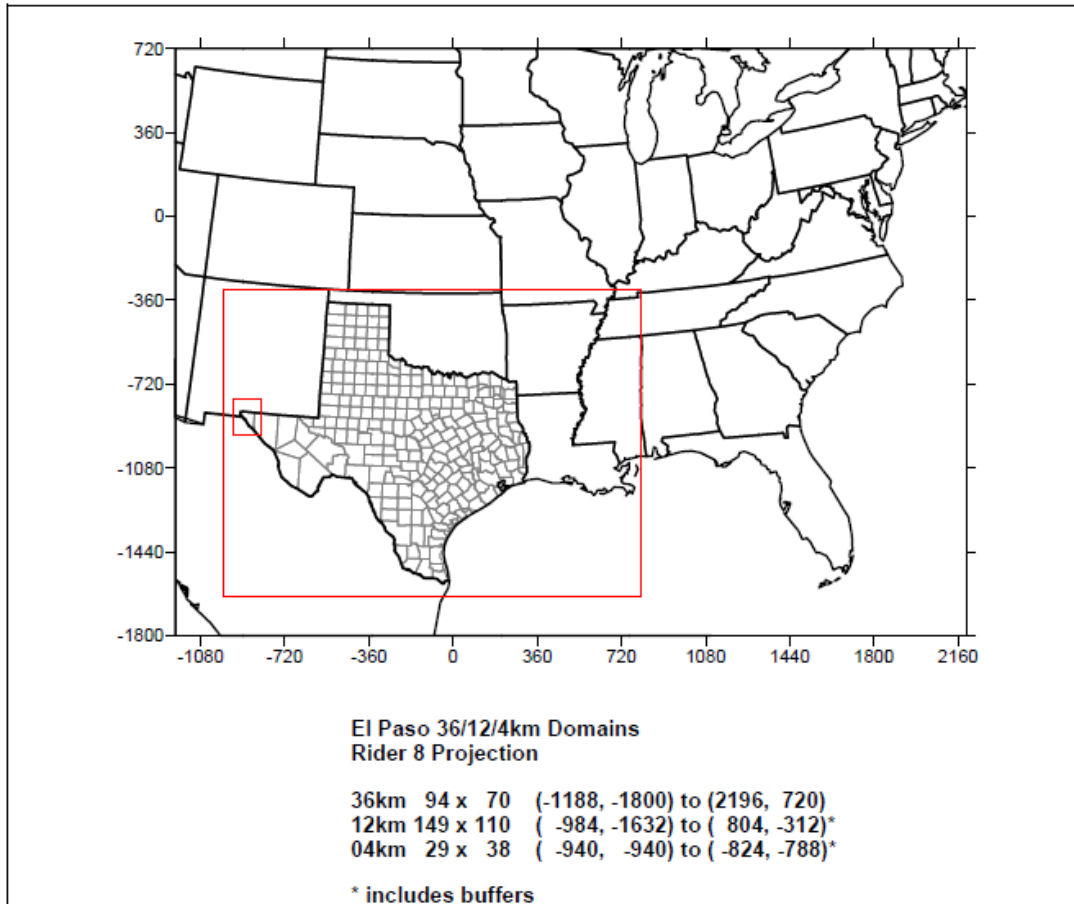


Figure 11.1 36-12-4 kilometer Modeling Grid

11.1.1 Nested Grids

The author considered the 36 km grid spatially over-expansive. Simulation run-time also exceeded 3.5 days. A compact regional domain is necessary given the extensive time requirements to run a simulation. Evaluations for the 12 simulations are focused on the 4 km gridded domain encompassing the PdN region and not a continent-wide domain or the 12 km domain for the state of Texas. A 4 km grid was established to accomplish expedited run-times applied to each simulation. Simulation RUNs were completed in ~1.5 hours.

Figure 11.2 illustrates the 4 km domain established for the PdN region. Care should be taken to not confuse the dashed grid lines on Figure 11.2 with the bold oblique rectangle which represents the 4 km domain. The dashed grid lines are artifacts obtained from the TCEQ website where the image was obtained.

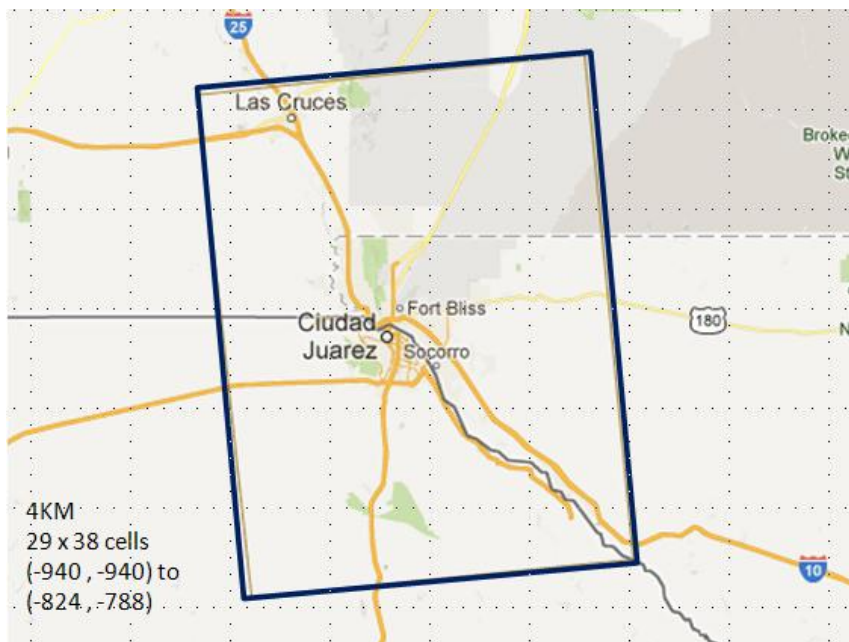


Figure 11.2 Paso del Norte 4-Kilometer Modeling Domain

The PdN domain encompasses El Paso and Hudspeth Counties in Texas, Doña Ana and Otero Counties in New Mexico, and the Municipality of Juárez, Chihuahua, Mexico. The 4 km domain definition was recommended by the TCEQ. Dimension and extent of the 4 km domain was established to include all potential source areas in the PdN area that contribute emissions to the airshed.

The CAMx 4 km domain consists of a grid system with 1,102 cells and encompasses 4,408 km². Figure 11.3 presents the grid cell configuration for the 4 km

domain over census tracts of the PdN community. Each grid cell is enumerated beginning with the bottom left grid cell which is identified as (1,1). Numbering follows a Cartesian coordinate system for rows in the u (east-west) direction and columns in the v (north-south) direction.

The purpose of presenting census tracts instead of a centerline street map is that CAMx applies surrogate data to allocate pollutants across a modeling domain. Each grid cell is allocated a percentage of total population within the MSA. For example, area sources such as residential fuel consumption are calculated according to population as are emissions from dry cleaners or gasoline stations. This method of applying population spatial surrogates simplifies allocating emissions across the modeling domain, yet it contributes to modeling error.

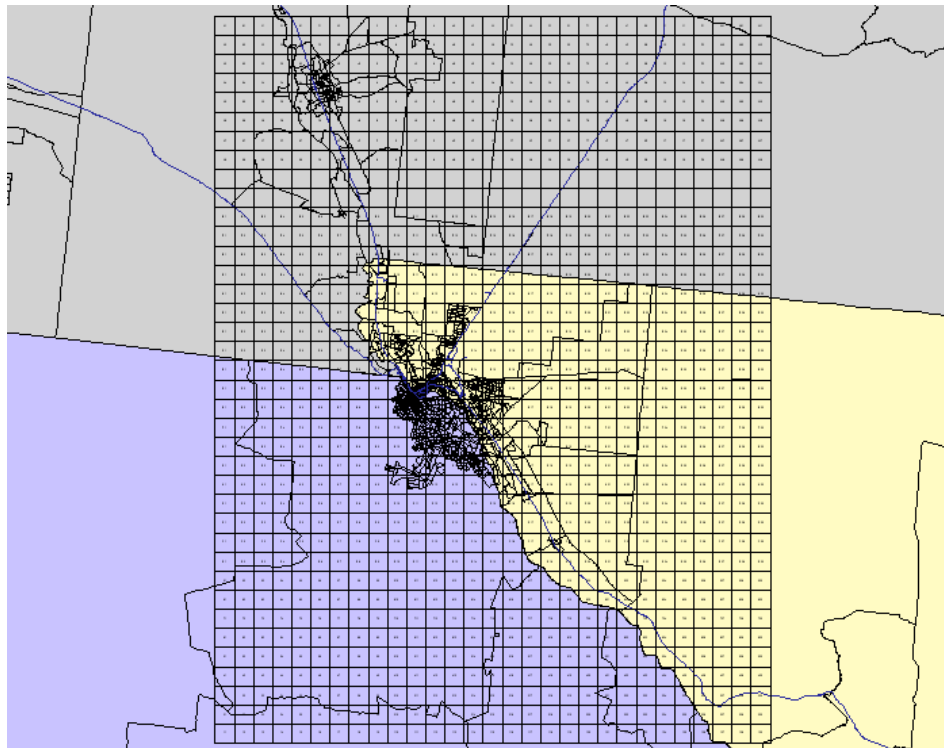


Figure 11.3 Grid Cells of the 4 km Modeling Domain

11.2 CAMx Modeling Inputs

CAMx simulations require a 3-dimensional gridded system to account for the advection of pollutants into atmospheric layers above the surface grid cells. The model calculates the fate of pollutants entering a gridded volume of air. All calculations concerning the fate of pollutants are conducted within the center of the grid cell while the physical transport of the air masses is conducted for the boundaries of each gridded volume (ENVIRON, 2011). However for purposes of this report only a 2-dimensional gridded system has been modeled.

Variables such as meteorology, emissions, landuse, and Carbon Bond chemistry mechanisms are provided as inputs for CAMx modeling. Each variable is developed as a FORTRAN-based c shell script. As indicated earlier in regards the modeling domain, a 4 km gridded domain is applied to this project in order to reduce simulation runtime.

11.2.1 Landuse

Surface land cover distributions are specified in CAMx using a binary file containing time-invariant fields of landuse fractions and leaf area index (LAI) in each grid cell. Section 9 provided a description of NCLD landuse categories. This report applies the Zhang dry deposition scheme. Under this scheme the fractional distributions of 26 landuse categories required for each grid cell are used to define surface characterization for dry deposition calculations and to set default surface roughness lengths. Table 11.1 provides the CAMx landuse categories specific to Zhang.

Table 11.1 CAMx landuse categories for the Zhang dry deposition scheme

Category Number	Land Cover Category
1	Water
2	Ice
3	Inland Lake
4	Evergreen Needle-leaf Trees
5	Evergreen Broadleaf Trees
6	Deciduous Needle-leaf Trees
7	Deciduous Broadleaf Trees
8	Tropical Broadleaf Trees
9	Drought Deciduous Trees
10	Evergreen Broadleaf Shrubs
11	Deciduous Shrubs
12	Thorn Shrubs
13	Short Grass and Forbs
14	Long Grass
15	Crops
16	Rice
17	Sugar
18	Maize
19	Cotton
20	Irrigated Crops
21	Urban
22	Tundra
23	Swamp
24	Desert
25	Mixed Wood Forests
26	Transitional Forest

11.2.2 Biogenic Emissions

A variable to consider regarding landuse is the contribution of biogenic emissions and their role in photochemical reactions in the airshed being modeled. While a detailed discussion on landuse variables is provided in ENVIRON (2012) this section discusses the method of determining biogenic emissions using the leaf area index (LAI) and plant functional types (PFT). The Model of Emissions of Gases and Aerosols from Nature

(MEGAN) established by Guenther et al (Guenther, 2012), was developed by the Biological Atmospheric Interactions group of the Atmospheric Chemistry Division at the National Center for Atmospheric Research (NCAR) for determination of biogenic emissions.

MEGAN is applied to derive net emissions of gases and aerosols from the planetary surface into the atmosphere. MEGAN obtains specific meteorological parameters to determine emissions for plant functional types (PFTs) as a function of temperature, solar radiation, LAI, and leaf age. Landcover data is reviewed to compute fractional coverage for each PFT and vegetation-specific emission factors (EFs). LAI is defined as the ratio of total upper leaf surface area of vegetation divided by the surface area of land on which the vegetation grows (Guenther, 2012).

Temperature effects on leaf emissions are computed as a function both of the current temperature and the average temperature over the previous 15 days (Guenther, 1999). Leaf age factors into the calculation of biogenic emissions as does the amount of solar insolation reaching the surface of the planet. Leaf age fractions for new, young, mature, and old leaves are estimated for each model grid square from local LAI and temperature changes (Guenther, 2012). Biogenic emissions were not modified for the project simulations. LAI data can be obtained from the following URL:

<http://acd.ucar.edu/~guenther/MEGAN/MEGAN.htm>.

MEGAN generated biogenic emissions primarily along the Rio Grande valley running from the northern point of the 4 km modeling domain, through the El Paso / Juárez international boundary and proceeding to Hudspeth County adjacent to the eastern border of El Paso County.

11.2.3 Landuse Data Processing Procedures

GIS and PERL-based processors were utilized to develop landcover and LAI input data for CAMx. Arc Macro Language (AML) scripts were used to process the raster-based and vector-based GIS data and to export ASCII data for subsequent processing with PERL scripts and compilation in FORTRAN. User-defined options specify parameters such as the output modeling domains, map projection parameters, input LULC, and MEGAN LAI data. The CAMx landuse file was prepared for the 4 km modeling domain.

11.2.4 Albedo-Haze-Ozone

The AHOMAP program is utilized to create a text file containing surface UV albedo, total atmospheric haze turbidity, and total atmospheric ozone column data (AHO) which is used to calculate photolysis rates for the simulation period of June 12-21, 2006. The program reads CAMx landuse files for the 4 km domain (or the domain to be modeled if a larger domain is selected) and a global ozone column dataset. The dataset can be downloaded from <http://ozoneaq.gsfc.nasa.gov/OMIOzone.md>.

As indicated in Section 9, AHO generates an output file with 5 categorical bins for albedo, 3 for haze, and 5 for ozone. AHOMAP was modified for the 4 km modeling domain from AHO data previously developed by TCEQ. Each grid cell was assigned a bin number associated with the AHO categorical values. Since regional haze is considered uniform across an airshed, all grid cells are assigned a bin number of 2 for haze. For ozone, each 36 km grid cell in the TCEQ AHO dataset that contained the El Paso 4 km domain was expanded into 81 (9x9) 4 km grid cells. Each of the 81 cells was

assigned the same value as the 36 km cell from which it was derived. For albedo, bin values were developed according to the 4 km CAMx landuse files.

11.2.5 Total Ultraviolet Visible

The TUV program reads the categorical values in each AHO file and creates a FORTRAN lookup table listing photolysis rates for each combination of the categorical AHO values at various solar angles and heights above the ground. The amount of solar energy incident on the surface of the planet is dependent on the angle of the sun given the thickness of the atmosphere a photon must travel to arrive to the mixing layer where the photochemical reactions occur. The TUV files were obtained from the TCEQ. A more complete description of the TUV program is provided in Section 9.

11.2.6 Initial and Boundary Conditions

Initial Conditions and Boundary Conditions (IC/BC) must be applied for the coarsest grid. IC/BC were extracted from the 12 km grid data developed for the 36-12-4 km domains. This is accomplished by the BNDEXTR program. This process applied to the vertical structure weighted concentrations based on the thickness of all UTEP layers in the 4 km domain within each TCEQ 36-12-4 km layer. BNDEXTR generates a binary file of hourly lateral boundary conditions for each data and a 3-dimensional initial condition file (Environ, 2012).

11.3 Emissions Processing

Photochemical modeling by CAMx requires a series of emissions processing steps in order for the model to read the datasets that are inputted into the simulation.

11.3.1 Emissions Processing System - Version 3

The Emissions Processor System - Version 3 (EPS3) was developed by ENVIRON. EPS3 converts emissions from multiple source categories such as point, area and mobile sources. It integrates chemical species and temporal and spatial emissions allocations into a two-dimensional gridded dataset. This application is the foundation for processing atmospheric emissions which are then processed by CAMx.

EPS3 converts the resolution of emissions inventory data to the resolution needed by an air quality model such as CAMx. Emission inventories are typically prepared to provide data with an annual total emissions quantity for each emissions source. TCEQ provides emissions inventory information at the Texas Air Emissions Repository (TexAER): www.tceq.texas.gov/airquality/areasource/TexAER.html. TexAER also provides emissions inventory data for ozone seasons emissions which are roughly 28.8% - 29.4% of annual emissions depending on source classification codes (SCC) discussed in Section 10.

EPS3 allocates pollutant emissions such as VOC, NO_x, CO and SO₂ into the chemical classes employed by the model. Emissions data are spatially allocated to grid cells for each hour of the modeling episode. Specificity of EI data can be modified to meet the resolution required by CAMx by modifying chemical species entering the grid cell, modifying the temporal resolution, or modifying population values indicated for each grid cell. EI data are developed as either daily average or annual-total emissions. CAMx requires emission data on an hourly basis for each model grid cell given the model simulation functions as a series of hourly time-steps.

Figure 11.4 illustrates the steps that EPS3 applies to process the different source categories. EPS3 transforms EI data by temporal allocation, chemical speciation, spatial allocation, and layer assignment if necessary in the event a stack emits a plume at an elevated height.

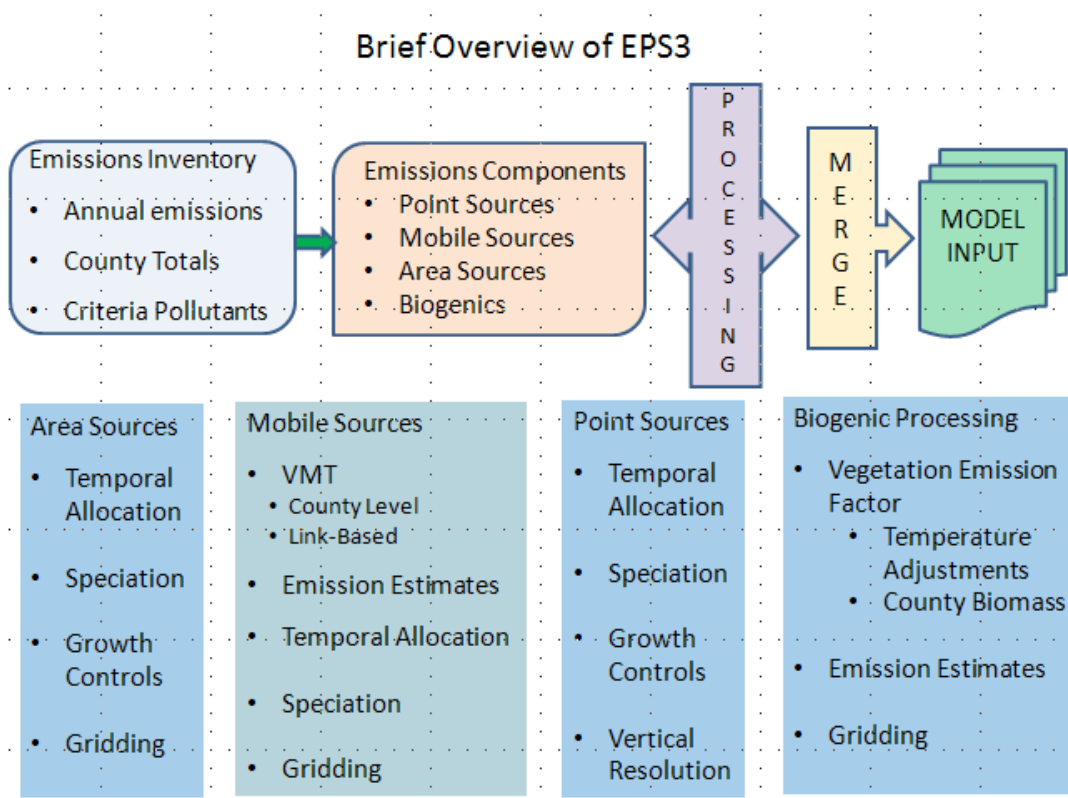


Figure 11.4 EPS3 Flow Diagram

EPS3 reads ASCII text files with daily or annual emissions and calculates emissions for weekday, Friday, Saturday, and Sunday. Chemical species are allocated according to the types of source. Model-ready gridded emissions were processed by EPS3 from point, county-level surrogate area sources, and link-level mobile emission inventories and biogenics emissions processed by MEGAN. TCEQ provided speciated EI data for El Paso and Cd. Juárez point sources.

11.3.2 Emission Inputs

EPS3 generated CAMx model-ready emissions at 4 km grid resolution. Files processed by EPS3 for elevated point sources are prepared from the AIRS Facility Subsystem (AFS) format which is identified as a CAMx-ready flat file. Each row of data represents a record and each space or group of spaces in the row represents a specific variable of the AFS format. The data is processed through a temporal allocation procedure which assigns emissions to a specific set of time segments during a 24-hour period. Finally, data is allocated into specific grids over the modeling domain. The last step generates the gridded emissions dataset. Table 11.1 specifies the source categories processed by EPS3 and the jurisdictional information to which the source categories belong.

Table 11.1 Source Categories processed by EPS3

Source Categories	Jurisdictional data sources
Area Sources	<ul style="list-style-type: none"> • Juárez Area Sources • New Mexico Area Sources • Texas Area sources • Oil and Gas Drilling • Drilling Rigs
Point Sources	<ul style="list-style-type: none"> • Juárez Point Sources • New Mexico Point Sources • Texas Point Sources
Mobile Sources	<ul style="list-style-type: none"> • Juárez Mobile Sources • New Mexico Mobile Sources • Texas Mobile Sources <ul style="list-style-type: none"> ○ Highway Performance Monitoring System ○ Idling emissions
Nonroad or Offnetwork Sources	<ul style="list-style-type: none"> • Juárez Point Sources • New Mexico Point Sources • Texas Point Sources • Linehaul locomotives

Each jurisdiction for which emissions were processed requires its own set of emissions data. The EPS3 program also generates a series of log files which can be reviewed to assess if the proper treatment of the emissions inventories was provided. The EPS3 for all intents and purposes provides a suite of information allowing one to determine the daily modeled emissions inventory and assess if any spurious data is being applied to the model before the time-consuming simulation is initiated.

11.4 CAMx Processes

Information referenced above is summarized in Figure 11.5. The 1st step in the process, which should be understood, is development of the modeling domain. The following steps are distinct to themselves but are eventually merged during the CAMx simulation.

An emissions inventory is a fairly extensive process, and it tends to introduce the most error into the modeling effort due to the surfeit of surrogate data that is estimated for the source categories that comprise the point, area, biogenic, and mobile sources. As will be indicated in the next section, the modeled EI and the actual EI are very different. The actual EI is based on what is likely the best available information based on emissions factors and emissions growth factors (EGAS) methods that may or may not take into consideration the most accurate data. However given the extensive data that must be considered in preparing the EI, it should be assumed that this is the best available information. The modeled EI attempts to build from the actual EI, but some emissions sources are unavailable such as idle vehicles at the Ports of Entry, which is a major source of VOC and NO_x emissions.

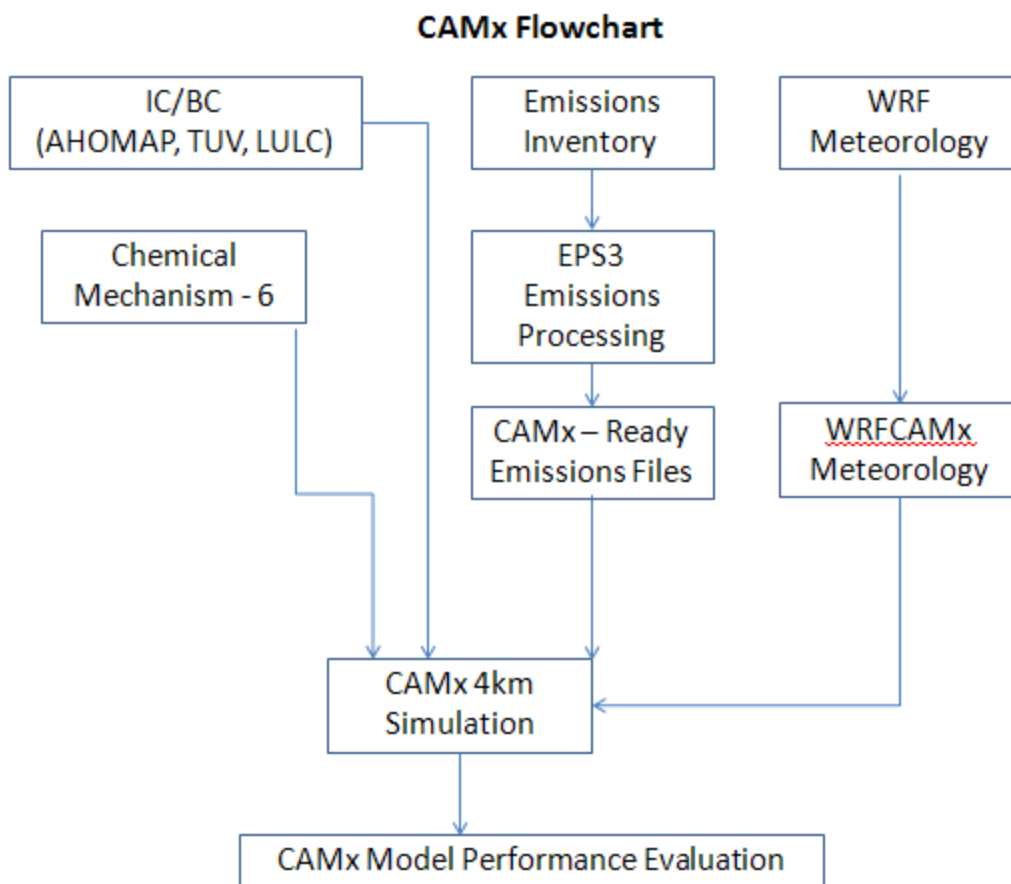


Figure 11.5 CAMx Data Processing Flow Chart

Initial and boundary conditions include total ultraviolet, albedo, haze, and column ozone (AHO), and land use / land cover. The CB6 chemical mechanism continues improvement as more stringent NAAQS require improved sensitivity to predict ozone at lower concentrations. The Chemical Mechanism has improved from calculating emissions for functional groups to improved chemical kinetics for specific chemical species such as the highly reactive volatile organic compounds.

Weather Research and Forecasting (WRF) modeling may introduce error in the CAMx simulation given the WRF developer's assessment of model performance for the

various atmospheric physics options that may be simulated before selecting an adequate WRF simulation. Additionally, the thickness of each layer selected by the WRF modeler may also introduce variability in the results. As indicated earlier, 2 WRF layers were assessed to attempt to interpolate the layer thickness between both, but the difference in layer thickness was extensive requiring selection of only one. Eventually it is the modeler's discretion to determine the WRF simulation with the best performance statistics when compared to OBSERVED data. Selection of the most accurate meteorological conditions is of most importance since, once selected, it remains unmodified for the duration of any sensitive analysis as well as future-case modeling.

WRF data is processed by WRFCAMx and emissions are processed by EPS3. Following EPS3 processing the emissions files are merged. The IC/BC files, CB6, meteorology, and emissions are processed by CAMx to generate simulation results which can be evaluated as discussed in the following sections.

12 The CAMx Simulation

Photochemical modeling for this report employed CAMx v.5.40 (ENVIRON, 2011) to simulate physical and chemical processes governing the formation and transport of ozone with CB6 gas phase chemistry. For consistency with State of Texas modeling efforts, the 4 km simulation was run with the same user-selected options as the TCEQ Rider 8 modeling campaign. This section describes the specific emissions data applied to evaluate the model for sensitivity to variations in VOC and NO_x emissions.

12.1 The Modeled Emissions Inventory

The emissions inventory developed for a simulation consists of daily source category emissions reported in tons per day (TPD). The model processes 17 separate data files representing point, area, mobile, and biogenic emissions for all 3 jurisdictions. All the emissions (except biogenics) and meteorological data provided for this report was obtained from TCEQ. The single 4 km gridded domain was developed by ENVIRON (2012) as part of a separate project

12.1.1 EPS3 and Biogenic Emissions

Output generated by EPS3 software and PTAR2IOAPI program (which specifically processes MEGAN data) is processed as gridded emissions data. This data is processed through the MRGUAM program which merges the 17 EPS3 and biogenic emissions files into a single binary file representing one modeled day's set of input data that is run during the simulation. 10 files are produced, one each for the 10 day ozone episode modeling simulation. The CAMx merging procedure produces an ASCII text space-delimited log file denoted MRGUAM, which can be viewed with standard

spreadsheet or text editing software. The purpose of the MRGUAM log file is to review the emissions data to confirm the correct emissions values are processed during the simulation. The MRGUAM log file provides an important quality check to confirm the emissions inventory data processed by EPS3 or PTAR2IOAPI (for biogenic emissions) is correct, confirms each source category is properly specified, and no spurious data have been created. The MRGUAM log file generates multiple types of datasets such as the following:

- Total daily emissions;
- Total source category emissions;
- Total emissions by species; and
- Total emissions by each of the 17 data files, to name a few.

12.1.2 Daily Modeled Emissions

Emissions modeled by CAMx must be compiled in tons per day (TPD). NO_x and VOC are the two pollutants of interest for this series of simulations since they play a major role in the formation or destruction of ozone. Figure 12.1 presents the total NO_x and VOC emissions that are modeled for the PdN region. 542 TPD of VOC and 154 TPD of NO_x comprise the BASELINE modeled EI dataset. The BASELINE modeled EI was developed by ENVIRON for UTEP.

This data is considered the most accurate modeling emissions dataset available as it was prepared by TCEQ and ENVIRON for a statewide photochemical modeling campaign. The BASELINE simulation for this dissertation represents the foundation from which all further sensitivity modeling is conducted. Given the purpose of this dissertation is to evaluate the performance of the model due to modifications in either VOC or NO_x emissions for Cd. Juarez area source emissions, the BASELINE

represents the results from the unmodified dataset. As such, the table below represents the BASELINE dataset applied to the BASELINE simulation.

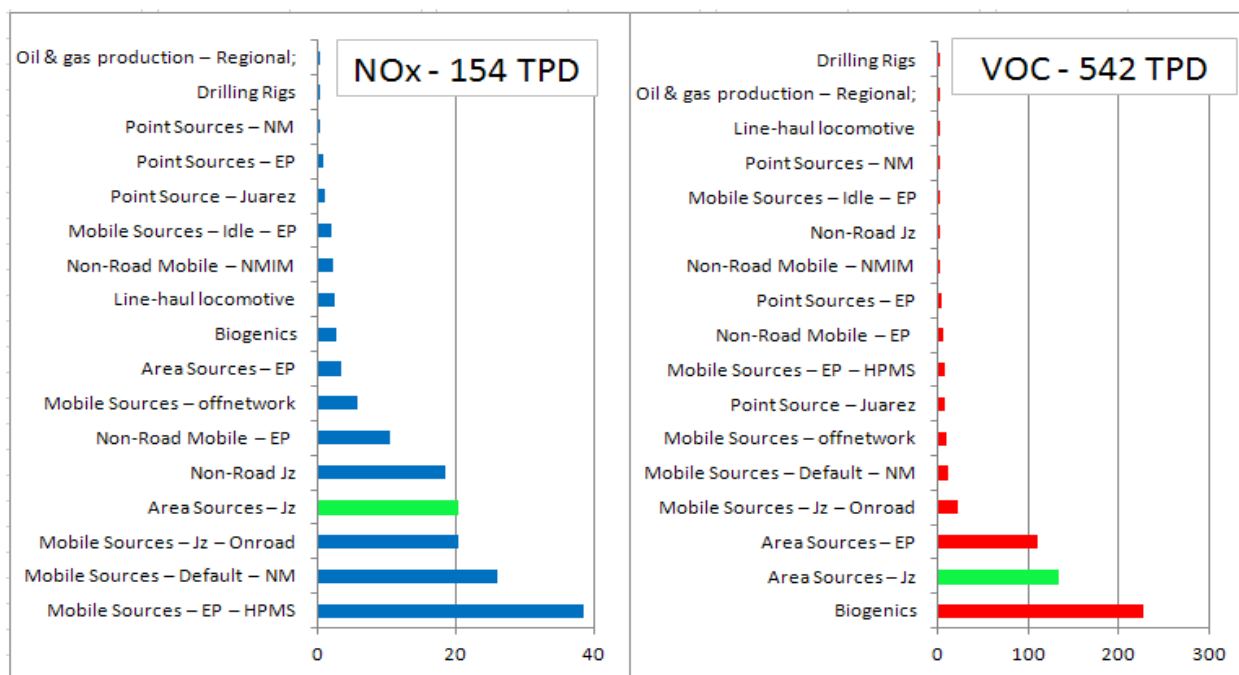


Figure 12.1 Total Emissions Processed by CAMx (TPD)

The green bar in both the VOC and NOx charts identifies the area source emissions for each pollutant. in the BASELINE data for Cd. Juárez. Area source VOC and NOx emissions will be modified and processed in a series of simulations to assess the sensitivity of the CAMx model to modifications in these 2 pollutants.

There are several reasons for evaluating the impact of modifications to Cd. Juárez area source NOx and VOC emissions.

- Juárez area source NOx emissions are among the highest compared to mobile sources which represent the three highest NOx emissions in all three jurisdictions in the PdN;

- Juarez area source VOC emissions are roughly half of biogenic VOC emissions. However, biogenic emissions in the PdN region have low reactivity (ENVIRON, 2012), and very little may be done to reduce this emissions source. Juarez area sources VOCs represent the greatest anthropogenic emissions in the region. This provides an opportunity to assess the impact on ozone formation due to modifications of this pollutant; and
- El Paso area source VOC emissions are the third highest, yet it may be assumed that due to air pollution reduction strategies implemented in the SIP, further reductions may be difficult or costly to achieve.

Table 12.1 presents daily modeled VOC and NOx emissions for regional source categories that are modeled in the BASELINE simulation. Of note in the datasets are the low point source NOx emissions.

Table 12.1 Daily Modeled VOC and NOx Emissions for Regional Source Categories

Source Category	Weekday	Saturday	Sunday
NOx (TPD)			
Area	23.4	21.8	20.7
Nonroad	33.5	21.4	19.7
Onroad	92.3	75.9	67.5
Point	1.9	1.6	1.3
Biogenics	2.8	2.2	2.6
VOC (TPD)			
Area	242.5	230.2	223.2
Nonroad	10.4	13.8	11.9
Onroad	50.6	43.9	41.2
Point	11.8	9.6	7.2
Biogenics	226.9	199.7	230.4

ENVIRON (2012) reports 43.7 TPD of NOx for Weekday emissions. However, when the BASELINE MRGUAM file for this report is reviewed, only 1.9 TPD of NOx are indicated. This discrepancy is not explained, and it needs to be thoroughly investigated.

Figure 12.2 identifies modeled VOC emissions by source category. The modeled VOC EI indicates area sources and biogenics comprise 242.5 TPD (45%) and 227 TPD (42%) of total emissions respectively. ENVIRON (2012) reports that biogenic VOC contributions in the PdN region consist primarily of monoterpenes which have low reactivity insofar as participation in tropospheric photochemical reactions is concerned.

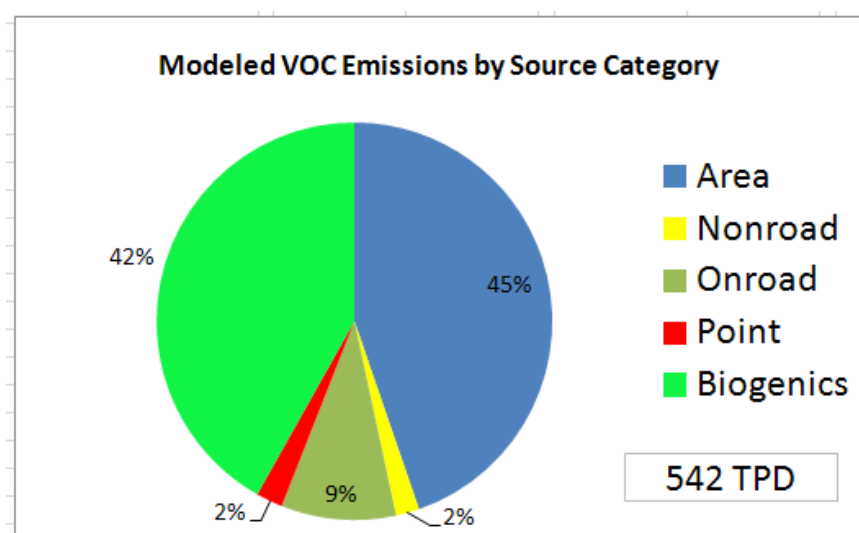


Figure 12.2 Modeled VOC Emissions in TPD Processed by CAMx

Figure 12.3 presents the daily modeled NO_x emissions which are processed during the CAMx simulation. Onroad and nonroad mobile sources emissions comprise 60% and 22% respectively of total NO_x emissions.

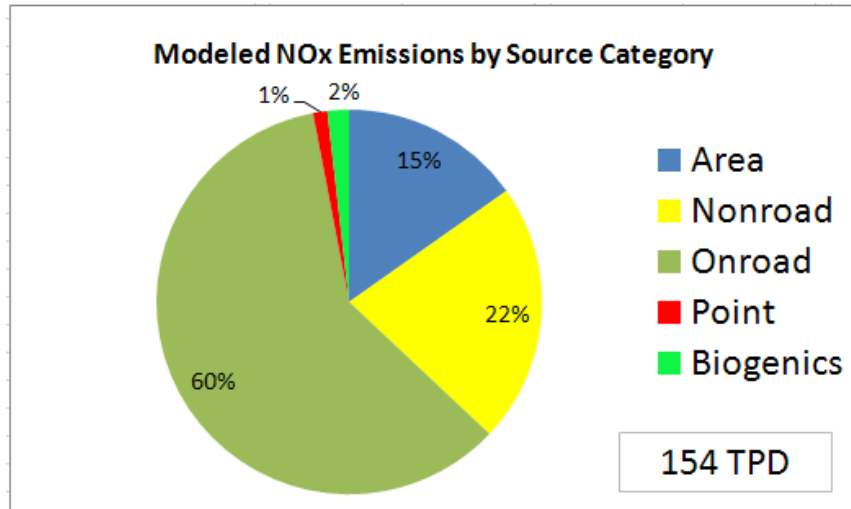


Figure 12.3 Modeled NOx Emissions in TPD Processed by CAMx

12.1.3 Regional Modeled Emissions

Table 12.2 identifies modeled VOC and NO emissions by source category and jurisdiction. Of note regarding inputs entering the modeling simulations are the very low point source NOx emissions in both El Paso and Juárez. Point source NOx emissions of 1.9 TPD for a community of 2.6 million inhabitants is likely inaccurate. Given biogenic emissions are ubiquitous throughout the airshed, the total biogenics amount (226.9 TPD) was split between the 2 communities. Biogenics were the only binational emissions dataset. The remaining 16 emissions files were specific to the jurisdiction. Future modeling endeavors should consider establishing single regional emissions datasets for each source category.

Table 12.2 Modeled VOC and NO_x Emissions by Source Category and Jurisdiction (TPD)

	EP NO _x	EP VOC
Area	3.3514	110.049
Nonroad	12.9113	6.0629
Onroad	66.4417	18.6152
Point	0.964	3.9927
Biogenics	1.38245	113.4382
TOTALS	85.05085	252.158
	Jz NO _x	Jz VOC
Area	20.0853	132.4435
Nonroad	18.5067	1.7355
Onroad	20.2795	22.2122
Point	0.8963	7.808
Biogenics	1.38245	113.4382
TOTALS	61.15025	277.6374

Figure 12.4 identifies modeled VOC emissions by source category in Cd. Juárez. Area sources comprise 132 TPD (48%) of VOC emissions modeled by the CAMx simulation. Biogenics comprise 113 TPD (41%) of VOC emissions generated in Juárez that are modeled by CAMx. Considering the very low reactivity of biogenic emissions, one may stipulate that if just the VOCs from anthropogenic sources were considered by the simulation then area sources comprise almost 90% of all VOC emissions generated in Cd. Juárez. Table 12.2 indicates 7.8 TPD of VOC point sources emitted from Juárez. Examination of the point source dataset which is processed by EPS3 indicated the PEMEX terminal in Cd. Juárez provided the bulk of these emissions.

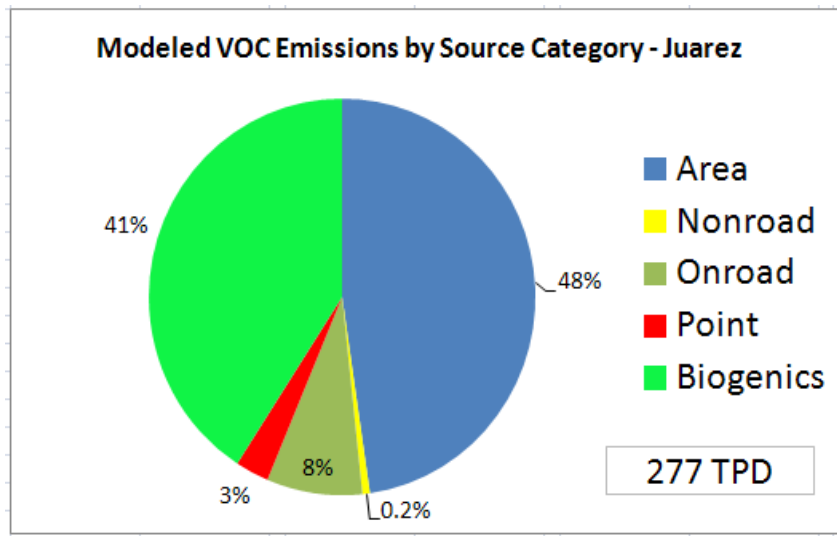


Figure 12.4 Modeled VOC Emissions by Source Category - Juárez

Figure 12.5 presents the modeled NO_x emissions for Cd. Juárez. Mobile sources constitute ~63% of NO_x emission totaling 38.7 TPD for the BASELINE simulation.

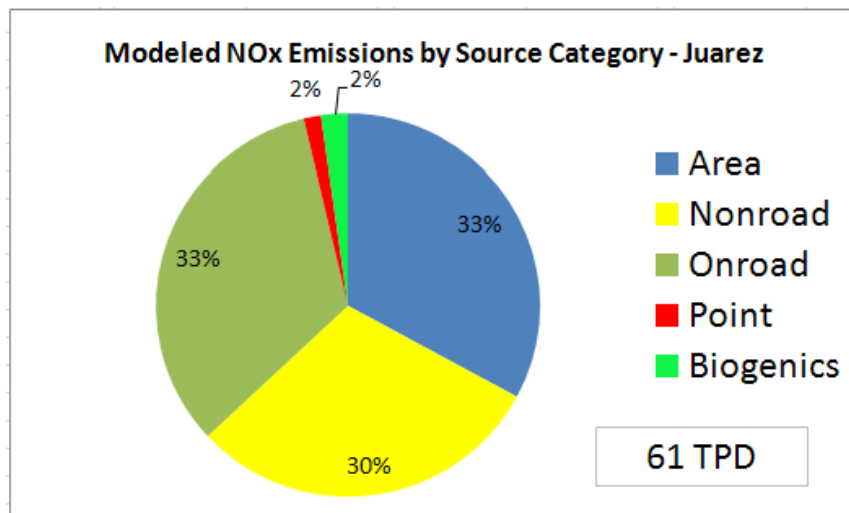


Figure 12.5 Modeled NO_x Emissions by Source Category - Cd. Juárez

Biogenic NO_x is generated by soil nitrification which occurs below the soil surface and is emitted into the atmosphere. The total emitted volume of this pollutant is minimal. It should be noted that the 2 Electric Generating stations in Juárez were listed as emitting minimal VOC's notwithstanding the electric generating facilities (EGF) are fired by #6 diesel fuel (bunker oil), have no emissions control equipment, and utilize no stacks.

Figure 12.6 presents modeled VOC emissions by source category for El Paso and south-central New Mexico (SC-NM) which consists of Doña Ana and Otero Counties. Given Doña Ana County accounts for the majority of emissions due to both population and industrial activity, the SC-NM region will henceforth be identified as DAC.

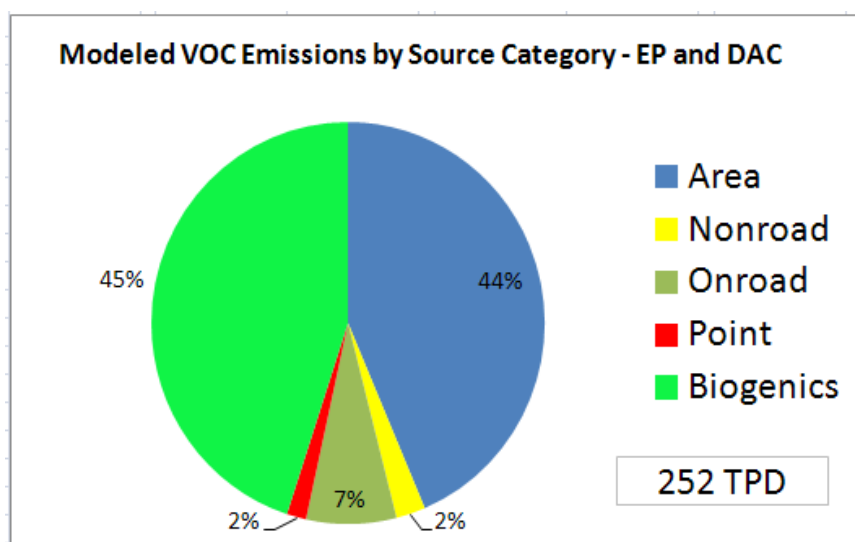


Figure 12.6 Modeled VOC Emissions by Source Category – EP and DAC

Modeled emissions for the BASELINE “Weekday” simulation indicate 252 TPD of VOC are generated in El Paso and DAC or ~25 TPD fewer emissions than Juárez.

Solvent utilization is the highest source of VOC emission from area sources. Mobile sources account for 9% of total emissions with modeled point source VOC emissions accounting for only 2% of total modeled VOC emissions.

Figure 12.7 illustrates modeled NO_x emissions for the BASELINE simulation. Onroad and nonroad mobile sources account for 93% of total mobile source NO_x emissions generated in El Paso and DAC. Area sources contribute 4% of NO_x emissions. Point sources are likely underreported as 1% of total regional NO_x emissions.

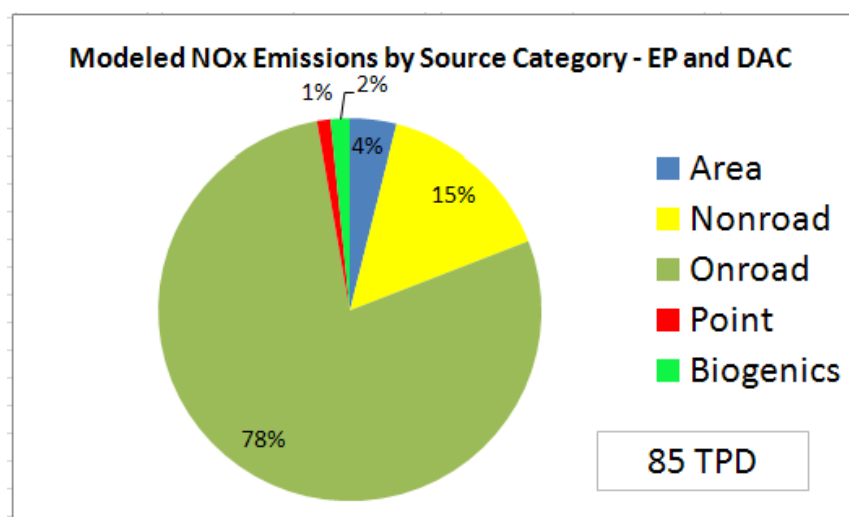


Figure 12.7 Modeled NO_x Emissions by Source Category - EP & DAC

Table 12.3 specifies the daily modeled NO_x and VOC emissions in TPD for the BASELINE simulation. Of note are the modifications in daily emissions based on Weekday, Friday, Saturday, and Sunday simulation days.

Table 12.3 BASELINE Daily Modeled Emissions in the PdN (TPD)

Date		NOX	VOC
12-Jun-06	Monday	153.9	559.4
13-Jun-06	Tuesday	153.9	558.3
14-Jun-06	Wednesday	154.0	553.5
15-Jun-06	Weekday	154.0	542.2
16-Jun-06	Friday	156.5	499.3
17-Jun-06	Saturday	123.0	497.2
18-Jun-06	Sunday	111.8	514.1
19-Jun-06	Monday	153.9	520.0
20-Jun-06	Tuesday	154.0	501.4
21-Jun-06	Wednesday	154.0	519.0

EPS3 generates a temporal output dataset which is processed by the MRGUAM function. The c-shell script integrated into the EPS3 c-shell job for each processed source category determines the day of the week to assign to each Julian date. This file naming format is indicated in the c-shell scripting language as yyyyjjj (e.g. yyyy = 2006 and jjj = 168 which results in 2006168).

Regarding day-of-week NO_x emissions, simulated emissions for Friday are ~1.2% greater than Weekday simulated emissions. Saturday emissions are ~20.7% less than Weekday emissions. Sunday emissions are ~28% lower than Weekday emissions.

Regarding day-of-week VOC emissions, simulated emissions for Friday are ~10% lower than Weekday emissions, Saturday emission are ~0.5% less than Friday emissions, and Sunday emissions are ~7% less than Weekday emissions. Similar proportions are maintained for all sensitivity runs.

12.1.4 Sensitivity Analysis Emissions Assignments

Table 12.4 is a matrix of modifications applied to Juárez area source emissions data in order to conduct sensitivity analysis using the CAMx photochemical modeling system. The BASELINE Cd. Juárez area source emissions that are modified for this report are identified in Table 12.2. BASELINE NO_x is 20.08 TPD and BASELINE VOC is 132.4 TPD. The purpose of the 12 distinct simulations was to assess the variation in the results compared to the BASELINE simulation. From this perspective one may identify potential air quality control strategies (PAQCS) that could be recommended.

Table 12.4 Matrix of Area Source Emissions Modifications for CAMx Simulations

	1	2	3	4	5	6	7	8	9	10	11	12
NO _x	↑ 50%	↓ 50%			↑ 50%	↓ 50%	↑ 75%	↓ 75%			↑ 75%	↓ 75%
VOC			↓ 50%	↑ 50%	↑ 50%	↓ 50%			↑ 75%	↓ 75%	↑ 75%	↓ 75%

For each RUN identified in Table 12.4, an arrow pointing up indicates emissions increase. An arrow pointing down indicates emissions decrease. The number which follows indicates if BASELINE emissions for the specific pollutant are modified by 50% or 75% in the specified direction. Simulations are described as follows:

- Run 1 and Run 2: Increase and decrease NO_x respectively by 50%;
- Run 3 and Run 4: Decrease and increase VOC respectively by 50%;
- Run 5: Increase both NO_x and VOC by 50%;
- Run 6: Decrease both NO_x and VOC by 50%;
- Run 7 and Run 8: Increase and decrease NO_x respectively by 75%;
- Run 9 and Run 10: Increase and decrease VOC respectively by 75%;

- Run 11: Increases both NO_x and VOC by 75%; and
- Run 12: Decreases both NO_x and VOC by 75%.

12.2 Procedure for Preparing the Emissions Data Files

The Juárez BASELINE area source database was modified according to the parameters established for each simulation indicated in Table 12.4. The modified emissions file, which is in ASCII space-delimited text format, was then processed by EPS3. No other source category files described in Table 11.4 were modified or processed by EPS3. However, for future modeling exercises it is recommended that the point source data sets for the 3 jurisdictions be thoroughly reviewed and modified to more accurately reflect regional point source NO_x and VOC emissions. The EPS3-processed Cd. Juárez area source file is then merged by the MRGUAM utility and the CAMx executable is initiated.

12.2.1 CAMx Simulation Emissions

Figure 12.8 illustrates the modeled emissions for Weekday, Friday, Saturday and Sunday for all CAMx simulations undertaken by this dissertation. Juárez area source emissions account for ~12.9% of daily regional simulated NO_x emissions and 24.3% of daily regional simulated VOC emissions in the BASELINE scenario. VOC emissions for BASELINE and all 12 simulations are the larger quantities of each pair indicated for the BASELINE and each RUN or all values above 200 TPD in Figure 12.8.

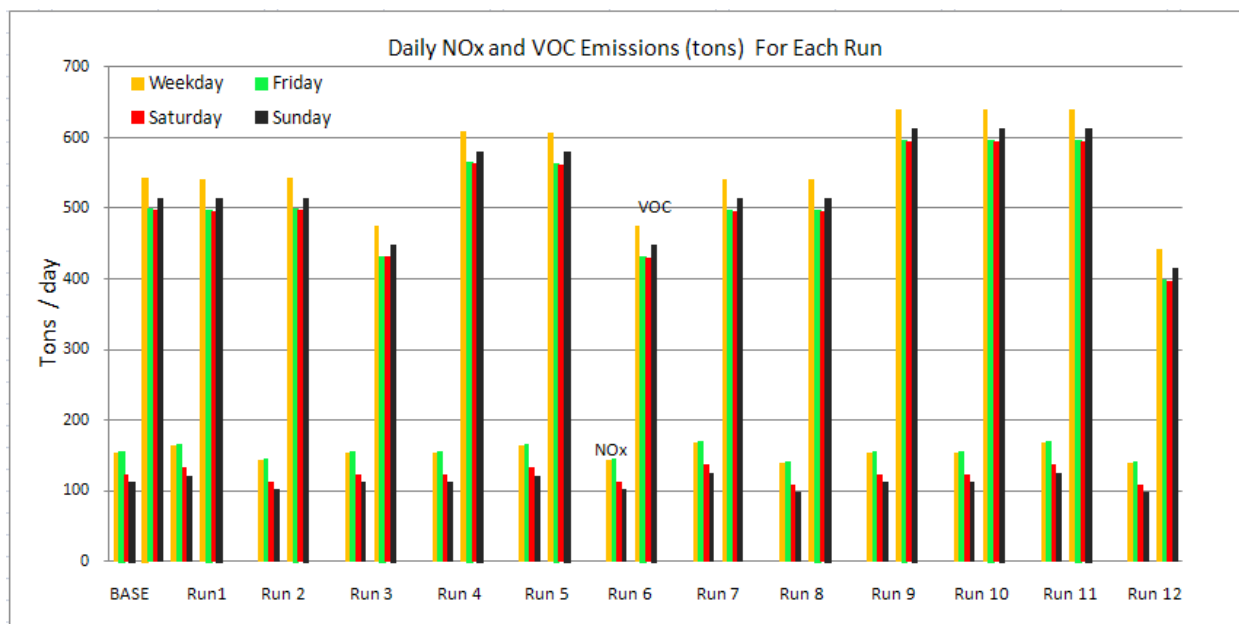


Figure 12.8 VOC and NOx Emissions for BASELINE and Sensitivity Analysis

Figure 12.9 provides a better resolution format for viewing the emissions simulated during each of the 12 sensitivity analysis RUNS. Close examination of Figure 12.9 indicates El Paso area source emissions remain unchanged while the Juárez area source emissions for the 2 pollutants increase or decrease based on the scenario specifications.

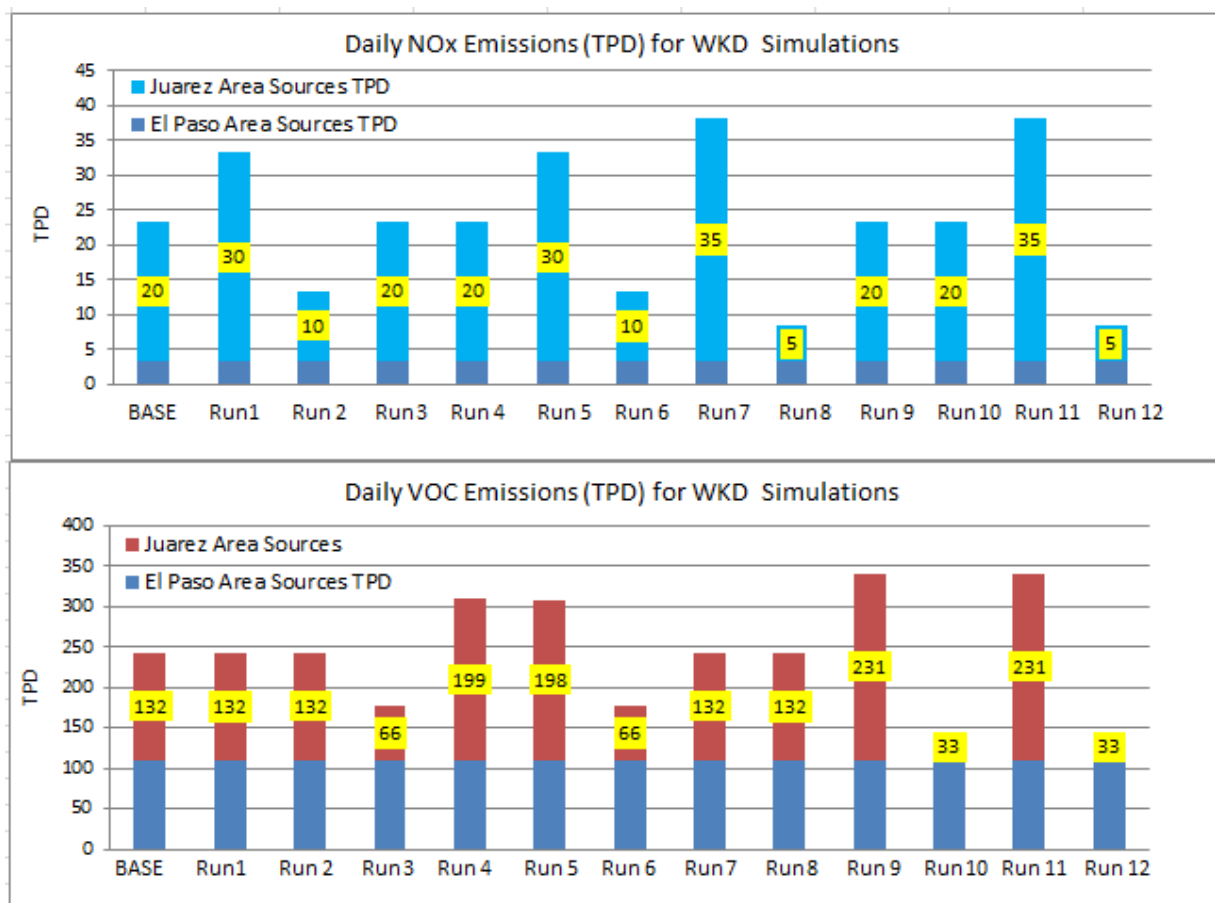


Figure 12.9 Modifications to the Juárez Area Source Daily Emissions Simulation for both NOx and VOC

Figure 12.9 provides only Weekday (WKD) emissions. The values reported are obtained from the MRGUAM log file which as indicated earlier provides a quality check allowing the modeler to confirm all modifications to the simulation run files are according to specification and no spurious data have been added.

13 CAMx Simulation Results and Model Performance

CAMx simulations were developed for 12 scenarios which modified Cd. Juárez area source VOC and / or NO_x emissions. Model performance was evaluated for 1-hour and 8-hour ozone. Comparisons were made of the PREDICTED ozone concentrations vs. ozone concentrations OBSERVED at the regional CAMS across the modeled domain. Only 1 CAMS, C662, was not included in this assessment due to the current limitations in the OBSCAT, which is one of the CAMx post-processing tools.

This section discusses CAMx simulation results for 18 June, 2006 (6/18). While simulations involved the entire 10-day ozone episode, the results of primary concern regarding the evaluation conducted on CAMx focus on 18 June which was the day of the ozone event. Photochemical modeling relies on a suite of statistics to determine model performance. Each of the 12 simulations produced a set of results to assess potential air quality improvement strategies based on modifications to NO_x or VOC emissions. More importantly, CAMx includes a suite of statistical tools to determine if the emissions modifications fall within acceptable parameters regarding model performance as discussed in Chapter 9.

On 6/18, C663 observed the highest 8-hour ozone concentration among the 8 CAMS observing an exceedance of the 8-hour ozone NAAQS. C663 also observed the highest 8-hour ozone concentrations in the PdN region during 2006, 0.099 ppm on 26 August, 2006 as indicated in Table 8-1. On the US side of the border, C12 at UTEP tends to observe the highest ozone concentrations and multiple exceedances during the year.

13.1 Model Performance Goals

Each simulation must generate results that are within acceptable parameters for Normalized Bias (NB) and Normalized Error (NE) as air quality models in order to be acceptable for NAAQS modeling purposes (EPA, 2007). NB and NE are important statistics in assessing the accuracy of the model to predict ambient ozone. Model performance goals for NB and NE are $\pm 15\%$ and $\leq 35\%$ respectively (ENVIRON, 2012). Positive NB indicates over-prediction of ozone and negative NB indicates under-prediction of ozone. NE and NB are based on all predicted and observed values in the modeling simulation for the entire 4 km domain. Equation 9.13 is applied to calculate NE, and equation 9.14 is applied to calculate NB.

13.2 Model Performance Definitions

Table 13.1 presents model performance results and statistics for 1-hour ozone. PEAK OBSERVED (PeakObs) and PREDICTED PEAK (PredPeak) ozone plus the suite of statistics generated by CAMx are identified. The maximum PeakObs on 6/18 was 120.7 ppb.

Table 13.1 Results and Statistics for 1-Hour Ozone Simulations for 18 June, 2006

Date ID		BASELINE	1201-0000	1201-0900	1201-1100	1201-1300	1201-2100	1201-2300	1202-1000	1202-1300	1202-1500	1202-1800	1202-2330	1203-0200
RUN ID			1	2	3	4	5	6	7	8	9	10	11	12
Model Output and Statistics	Cell	13,18	13,18	13,17	11,26	13,17	13,18	13,18	13,18	13,17	13,17	11,26	13,17	11,26
	PredPeak	103.3	102.1	102.4	91.7	113.9	113.0	92.7	100.1	102.3	119.7	86.8	118.8	87.8
	PeakObs	120.7	120.7	120.7	120.7	120.7	120.7	120.7	120.7	120.7	120.7	120.7	120.7	120.7
	PairPred	99.3	89.1	98.4	86.7	107.8	108.7	89.1	95.2	97.6	112.1	80.1	113.6	83.3
	UPPA	-14.4	-23.2	-15.1	-24	-5.6	-6.4	-23.2	-17.1	-15.3	-0.9	-28.1	-1.6	-27.2
	APPA	-1.5	-8.7	-2.1	-10	4.8	5.2	-8.7	-3.6	-2.7	7.8	-14.6	8.6	-12.8
	EPPA	12.2	14.4	11.9	15.3	13.1	13.2	14.4	13.3	11.9	15.2	17.2	15.2	16
	PTB	4	4	3	4	3	4	4	4	3	3	4	4	4
	NB	-3.3	-6.7	-2.1	-8.7	1.2	0.1	-6.7	-6.3	-1.8	3.1	-11.5	1.8	-8.7
	NE	25.6	23.2	24.2	24.2	27.1	28.1	23.2	26.3	23.3	27.8	23.9	29.5	22.4
	NOX		↑ 50%	↓ 50%			↑ 50%	↓ 50%	↑ 75%	↓ 75%			↑ 75%	↓ 75%
	VOC				↓ 50%	↑ 50%	↑ 50%	↓ 50%			↑ 75%	↓ 75%	↑ 75%	↓ 75%
Difference between Peaks (%)	PredPeak BL-PredPeak		-1.1	-0.8	-11.2	10.3	9.4	-10.3	-3.1	-1.0	15.8	-16.0	15.0	-15.0
	PairPred BL-PairPred		-10.3	-0.9	-12.7	8.6	9.5	-10.3	-4.1	-1.7	12.9	-19.3	14.4	-16.1
	PredPeak Peak Obs		-15.4	-15.1	-24.0	-5.6	-6.4	-23.2	-17.1	-15.3	-0.9	-28.1	-1.6	-27.2
Difference between Peaks(ppb)	PredPeak BL-PredPeak		-1.2	-0.9	-11.6	10.6	9.7	-10.6	-3.2	-1.0	16.4	-16.5	15.5	-15.5
	PairPred BL-PairPred		-10.2	-0.9	-12.6	8.5	9.4	-10.2	-4.1	-1.7	12.8	-19.2	14.3	-16.0
	PredPeak Peak Obs		-18.6	-18.3	-29.0	-6.8	-7.7	-28.0	-20.6	-18.4	-1.0	-34.0	-1.9	-32.9

Mid-Table 13.1 presents the difference between RUNS with modified emissions compared to BASELINE results. This indicates the sensitivity of the model to the emissions modification. The table also identifies the difference between the PREDICTED PEAK and PEAK OBSERVED value. This indicates whether the modification is closer or further from the OBSERVED value. Further consideration may be given as to whether a reduction in PREDICTED ozone is appropriate for specific potential air quality control strategies. The following defines the calculations identified in Table 13.1.

- PredPeak | BL-PredPeak indicates the difference between the PredPeak for the specific RUN and BASELINE PredPeak;

- PairPred | BL PairPred indicates the difference between the PAIRED PREDICTED PEAK value and the BASELINE PAIRED PREDICTED PEAK. The PairPred Peak represents the peak value predicted by CAMx that is paired to the specific CAMS observed value. CAMx generates a PredPeak value for each grid cell for each time-step and interpolates a predicted ozone concentration at the CAMS within the grid cell taking into consideration the concurrent time-step ozone values at the adjacent cells for the purposes of interpolating an ozone concentration value at the specific CAMS; and
- PredPeak | PeakObs indicates the difference between the PREDICTED PEAK and the PEAK OBSERVED value for each RUN. The PeakObs value does not change given this is the peak 1-hour ozone concentration on 6/18. This variable helps determine the model performance by indicating the variation between predicted and observed peaks and the impact on ozone concentrations due to emissions modifications.

13.3 Model Performance Summary for 1-Hour Ozone

Comparing each RUN to BASELINE data in Table 13.1 indicates that modifying VOC emissions generated the greatest variability in 1-hour ozone. Modifications to NO_x generated minimal variability in 1-hour ozone. Comparing PredPeak | BL-PredPeak indicates that increasing only NO_x by 50% (RUN 1) or 75% (RUN 7) results in reduced 1-hour ozone by 1.1 ppb and 3.1 ppb respectively. Reducing only NO_x by 50% (RUN 2) or 75% (RUN 8) reduced 1-hour ozone 0.8 ppb and 1.1 ppb respectively. NO_x tends to titrate ozone albeit minimally as compared to the BASELINE results.

Increasing only VOC by 50% or 75% resulted in improved bias by 2% compared to BASELINE. Increasing or decreasing both VOC and NOx combined did not produce results significantly different from VOC-only modifications. Modifications to NOx emissions, at existing concentrations, are insignificant contributors to improvements or further degradation of air quality. These results indicate that the PdN region ozone formation conditions are VOC-limited as will be discussed for each RUN in the following section.

Figure 13.1 presents the PAIRED PREDICTED PEAK for 1-hour ozone CAMx simulation RUNS for 6/18. The yellow bar at the base of the graph represents results identified as BASELINE. The PAIRED PREDICTED PEAK for 1-hour compares ozone concentrations observed at the CAMS to a concentration predicted by CAMx.

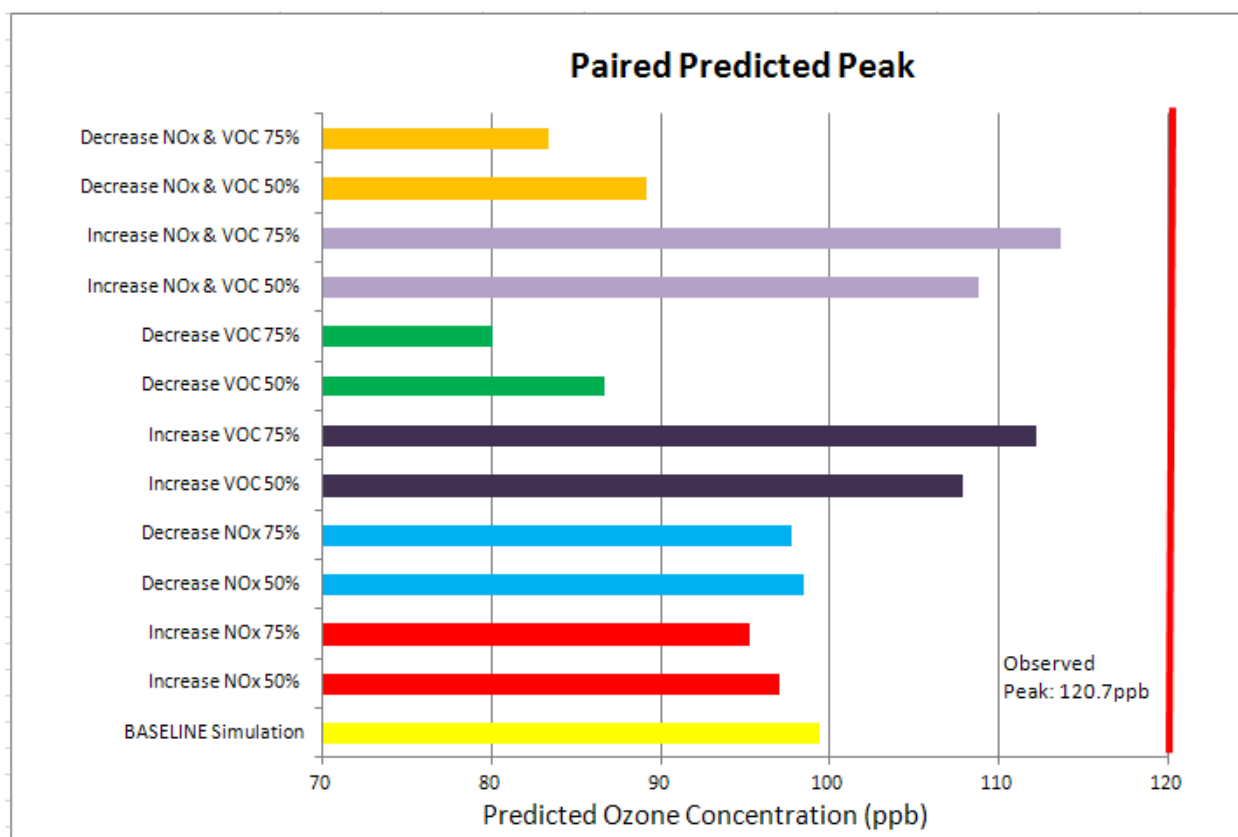


Figure 13.1 Paired Predicted Peak for CAMx Simulations and 1-Hour Ozone for 18 June, 2006

Figure 13.2 presents the PREDICTED PEAK 1-hour ozone concentrations for 6/18. This value represents the maximum ozone concentration within any particular grid cell in the modeling domain regardless of location within the cell. As can be observed in either Figure 13.1 or Figure 13.2, the greatest variability in 1-hour ozone concentrations occurs when VOC emissions are modified.

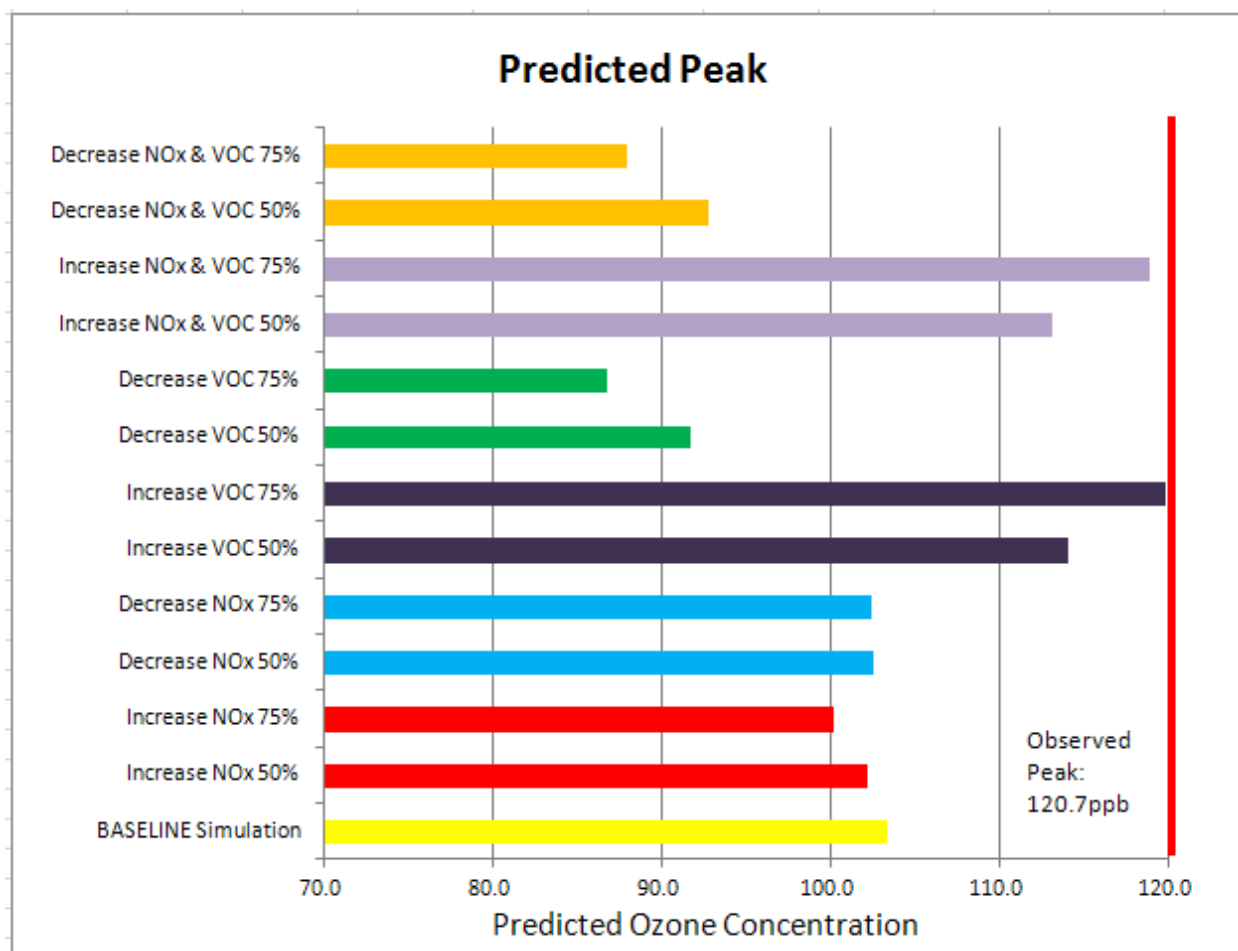


Figure 13.2 PREDICTED PEAK for CAMx Simulations and 1-Hour Ozone for 18 June, 2006

All simulations consistently under-predict the PEAK OBSERVED 1-hour ozone concentrations. Modifying VOC emissions tends to generate predicted 1-hour ozone peaks closer to the PEAK OBSERVED concentration. Increasing or decreasing combined NOx and VOC emissions vary little from modifications to VOC emissions alone.

13.4 Results and Statistics for 8-Hour Ozone

Table 13.2 presents the results and statistics for 8-hour ozone simulations for 18 June. PEAK OBSERVED and PREDICTED PEAK ozone plus the suite of statistics generated by CAMx are also indicated. 8-hour ozone results varied significantly from 1-hour ozone results. The maximum 8-hour PEAK OBSERVATION on 6/18 was 95.1 ppb.

Table 13.2 Results and Statistics for 8-Hour Ozone Simulations for 18 June, 2006

Date ID		BASELINE	1201-0000	1201-0900	1201-1100	1201-1300	1201-2100	1201-2300	1202-1000	1202-1300	1202-1500	1202-1800	1202-2330	1203-0200
RUN ID			1	2	3	4	5	6	7	8	9	10	11	12
Model Output and Statistics	Cell	13,18	13,18	13,17	11,27	13,17	13,18	13,18	14,17	13,17	13,17	11,27	13,17	11,27
	PeakObs	95.1	95.1	95.1	95.1	95.1	95.1	95	95.1	95.1	95.1	95.1	95.1	95.1
	PredPeak	93	90.11	94.05	83.22	102.9	101.8	84.49	89	93.28	107.1	80.51	106.3	80.71
	PairPred	92.1	83.6	92.6	80.3	100.5	100	83.6	88.3	86.9	103.7	73.8	104.1	78.8
	UPPA	-2.1	-11.1	-1	-12.4	8.3	7.1	-11.1	-5.2	-7	12.7	-15.3	11.9	-15.1
	APPA	2.5	-3.9	3	-5.9	9	8.5	-3.9	0.6	-0.7	11.6	-10.5	11.7	-7.6
	EPPA	9	8.3	9.5	8.9	14.3	13.7	8.3	8.5	8.5	16.6	12.1	16.4	9.5
	PTB	3	3	3	3	3	3	3	3	3	3	3	3	3
	NB	3.9	0.4	5.4	-1.8	8.8	7.4	0.4	1.8	0.6	10.8	-4.8	9.2	-1.6
	NE	23.7	22.1	22.4	23	24.4	25.4	22.1	24.3	24.5	24.8	22.8	26.5	21.5
	NOx		↑ 50%	↓ 50%			↑ 50%	↓ 50%	↑ 75%	↓ 75%			↑ 75%	↓ 75%
	VOC				↓ 50%	↑ 50%	↑ 50%	↓ 50%			↑ 75%	↓ 75%	↑ 75%	↓ 75%
Difference between Peaks (%)	PredPeak BL-PredPeak	-3.1	1.1	-10.5	10.6	9.4	-9.2	-4.3	0.3	15.1	-13.4	14.3	-13.2	
	PairPred BL-PairPred	-9.2	0.5	-12.8	9.1	8.6	-9.2	-4.1	-5.6	12.6	-19.9	13.0	-14.4	
	PredPeak Peak Obs	-5.2	-1.1	-12.5	8.1	7.0	-11.1	-6.4	-1.9	12.6	-15.3	11.8	-15.1	
Difference between Peaks(ppb)	PredPeak BL-PredPeak	-2.9	1.1	-9.8	9.8	8.8	-8.5	-4.0	0.3	14.1	-12.5	13.3	-12.3	
	PairPred BL-PairPred	-8.5	0.5	-11.8	8.4	7.9	-8.5	-3.8	-5.2	11.6	-18.3	12.0	-13.3	
	PredPeak Peak Obs	-5.0	-1.1	-11.9	7.8	6.7	-10.5	-6.1	-1.8	12.0	-14.6	11.2	-14.4	

Comparing each RUN to the BASELINE data indicate that modifying VOC emissions generates the greatest variability in 8-hour ozone concentrations. Model performance statistics presented in Table 13.2 are generated by comparing 8-hour predicted averages to 8-hour average observed ozone.

Modifications to NO_x generated minimal variability in 8-hour ozone. NE and NB improved by 1.6% and 0.7% when NO_x emissions increase or decrease by 50% respectively when compared to the BASELINE. The variability in 8-hour ozone was sufficient to quality modifications to NO_x emissions as a potential air quality control strategy if only a 1 or 2 ppb reduction in ozone is required to attain a modified 8-hour ozone NAAQS. As reported earlier, El Paso's design value in 2011 was 71 ppb. Reducing the NAAQS to a hypothetical concentration of 70 ppb, for example, would cause El Paso to be designated nonattainment of the new NAAQS. As reported by ENVIRON (2012), elevated NO_x concentrations in the PdN ambient air tends to titrate ozone albeit minimally.

Increasing only VOC by 50% or 75% produced results which did not significantly change the NE or NB. Increasing or decreasing both VOC and NO_x combined did not produce results which significantly differ from modification on RUNs with only VOC modifications. This indicates that modifications to NO_x emissions, at existing concentrations, are insignificant contributors to improvements or further degradation of air quality when coupled with modification to VOC. It should be noted that Cd. Juárez comprises 83.4% of regional area source NO_x emissions (20.1 TPD vs. 3.35 TPD for El Paso). Juárez area sources comprise roughly 33% of all Cd. Juárez NO_x emissions considering only the modeled emissions inventory. As has been indicated, the regional modeled EI requires substantial modifications insofar as point source NO_x emissions are concerned.

It should also be noted that NE for all simulations was $\leq 35\%$ which is within acceptable parameters. NB for all simulations was between $\pm 15\%$ which is also within

acceptable parameters. A discussion on the specific runs is provided in the following section. Figure 13.3 presents the PAIRED PREDICTED PEAK for CAMx simulations and 8-hour ozone for June 18, 2006.

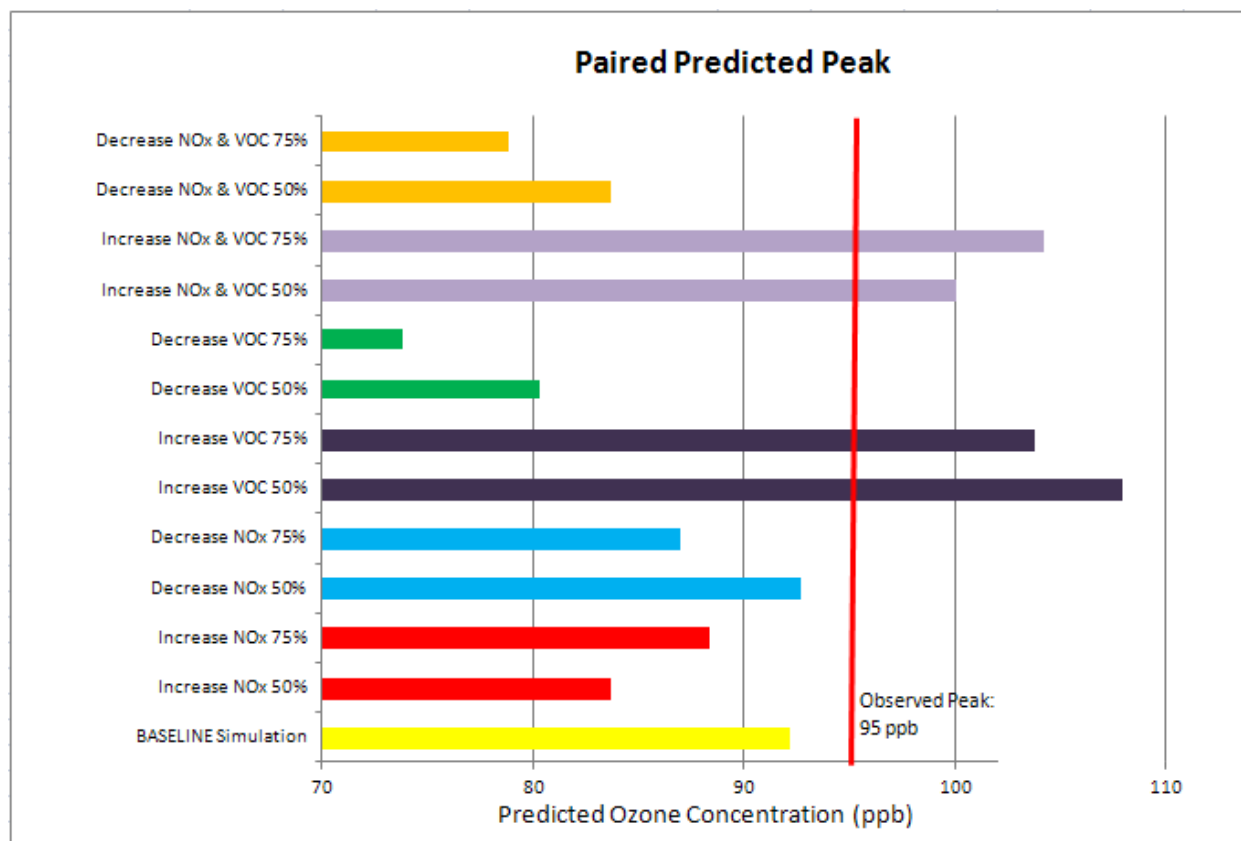


Figure 13.3 Paired Predicted Peak for CAMx Simulations and 8-Hour Ozone on 18 June, 2006

The yellow bar at the base of the graph represents BASELINE results. The greatest variability in 8-hour ozone concentrations occurs when VOC emissions increase or decrease.

Figure 13.4 illustrates the PEAK PREDICTED 8-hour ozone concentration generated by the CAMx simulations. Most of the simulations under-predict 8-hour ozone. Results indicate the model over-predicts the PEAK OBSERVED 8-hour ozone

concentration in simulations where VOC emissions were increased either 50% or 75% either alone or in combination with concurrent increases in NO_x.

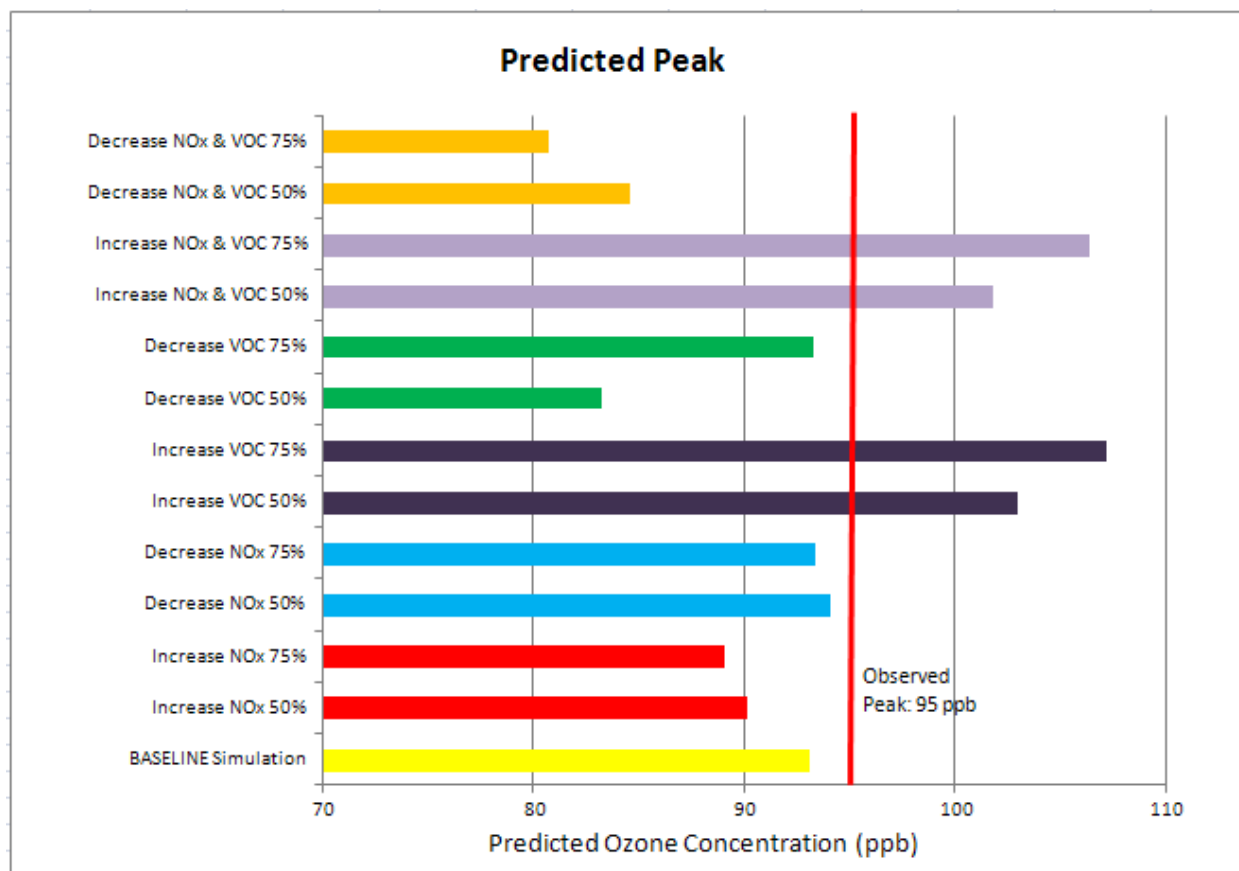


Figure 13.4 PREDICTED PEAK for CAMx Simulations and 1-Hour Ozone on 18 June, 2006

Of note are increases in NO_x tend to reduce 8-hour ozone compared to BASELINE results due to the ability of NO_x to titrate ozone. Decreases in NO_x did very little to change 8-hour ozone concentrations. The greatest decreases in 8-hour ozone occurred when both NO_x and VOC were reduced 50% and 75%.

14 Model Performance Evaluations for Each Simulation.

Model performance was evaluated for 1-hour and 8-hour ozone concentrations only at the regional CAMS which were included in the modeling simulation. This section addresses the diurnal formation and destruction of ozone on 6/18 which is the day of the ozone exceedance.

Each RUN including the BASELINE provides model performance data and the model's ability to predict ozone within acceptable benchmarks. The BASELINE model performance was discussed in ENVIRON (2012) and will briefly be discussed in this section. Model performance statistics for all RUNs are compared to the BASELINE.

As indicated in the previous section the model should obtain NE $\leq 35\%$ and NB $\pm 15\%$. Tables 13.1 and 13.3 indicate model performance parameters were achieved for all simulations. Varying NO_x and VOC either improved or diminished model performance, but NE and NB were within acceptable modeling performance parameters on all simulations.

This section presents model performance statistics as bar graphs for PEAK OBSERVED and PAIRED PREDICTED ozone concentrations. The maximum observed 1-hour and 8-hour ozone concentrations are plotted along with co-located daily maximum 8-hour and 1-hour ozone among all sites. The following statistics are measures of model performance (ENVIRON, 2011):

- Average paired peak accuracy (APPA);
- Normalized Error (NE); and
- Normalized Bias (NB).

14.1 BASELINE Model Performance

Figure 14.1 depicts daily BASELINE model statistics, the highest 8-hour ozone PEAK OBSERVED among all sites in the PdN region, and the co-located daily PAIRED PREDICTED PEAK. The model under-predicts 1-hour ozone on 9 of 10 simulation-days. Model performance was acceptable on 6/18, the ozone exceedance day. The positive APPA on 6/14 indicates several other CAMS over-predicted maximum 1-hour ozone.

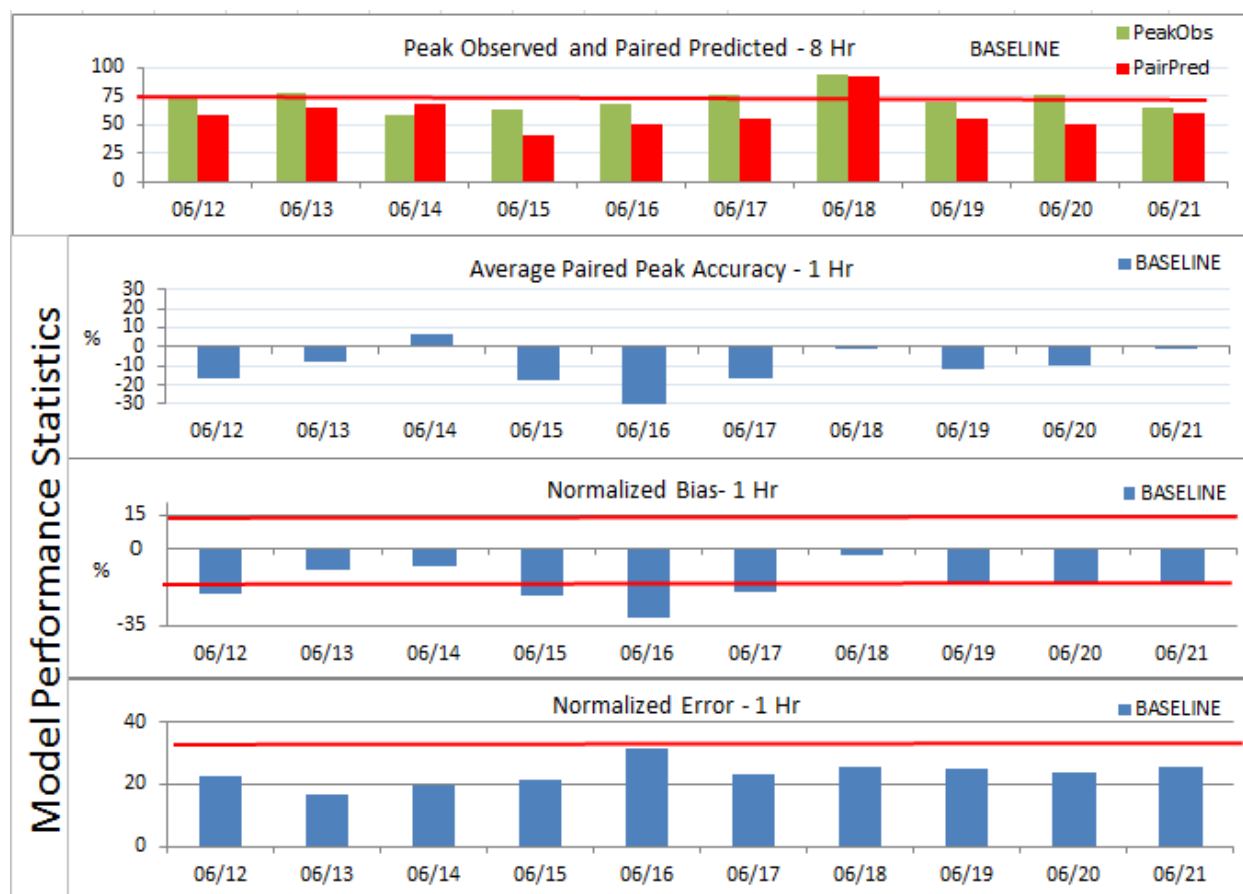


Figure 14.1 Model Performance Statistics – BASELINE

The very low APPA (-29.8%) on 6/16 is validated by the very low NB and NE (-31.2% & -31.5% respectively) indicating a very strong under-prediction. On 6/18 the model performed very well regarding NB & NE notwithstanding under-prediction of the maximum peak. The APPA on 6/18 was very good at -1.5% indicating minimal under-prediction of ozone concentrations.

Figure 14.2 illustrates the diurnal variability in 1-hour ozone comparing the OBSERVED and PREDICTED diurnal values.

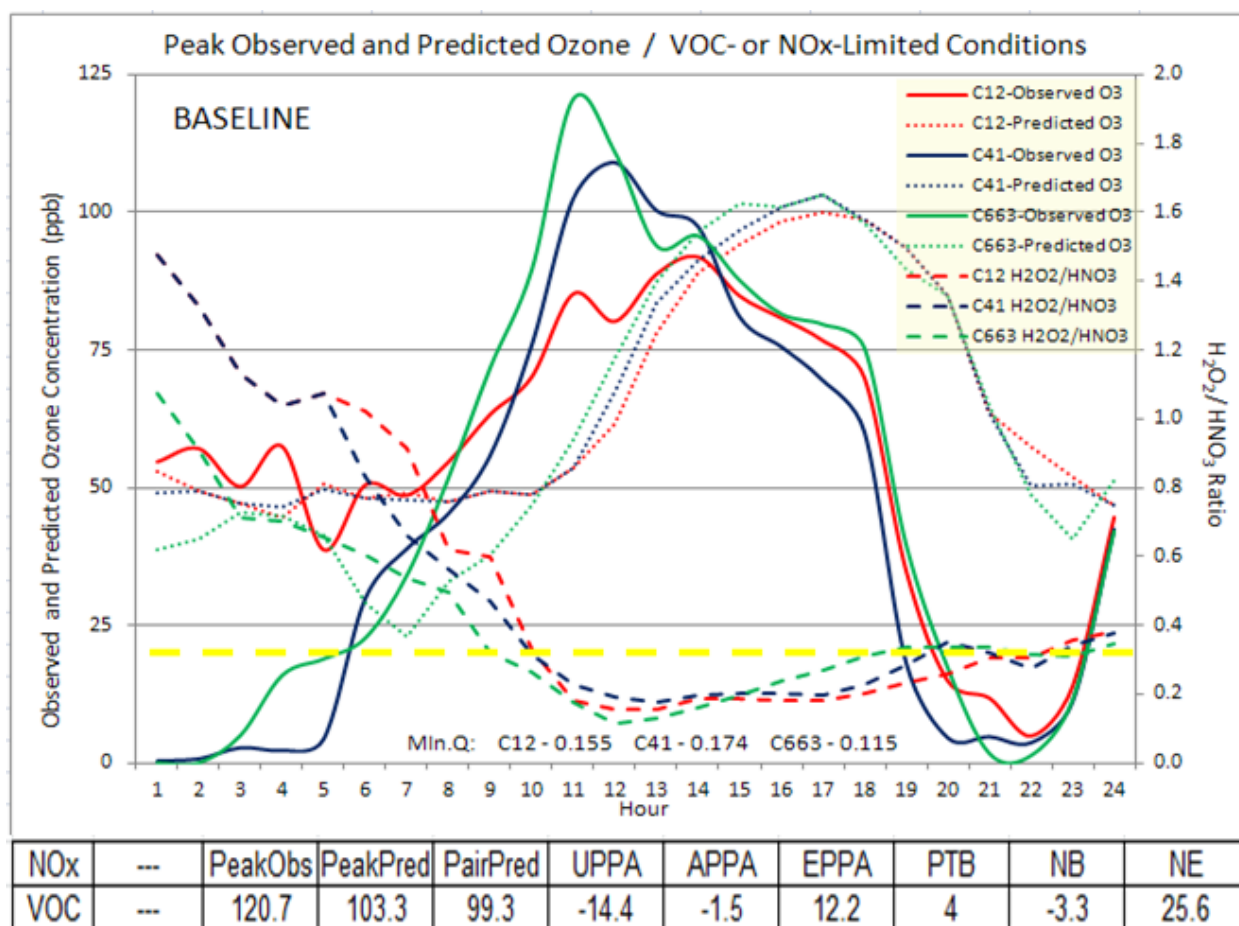


Figure 14.2 Diurnal Predicted and Observed 1-Hour Ozone (ppb) / H₂O₂:HNO₃ Ratios – BASELINE

Predicted hourly ozone is presented as dotted lines, and observed hourly ozone is presented as solid lines. The $\text{H}_2\text{O}_2\text{:HNO}_3$ ratio is presented as a dashed line. The difference between the occurrence of the PeakObs and PredPeak is indicted as PEAK TIME BIAS (PTB), which for the BASELINE simulation is 4 hours.

Three stations are presented in Figure 14.2. The purpose of plotting the $\text{H}_2\text{O}_2\text{:HNO}_3$ ratios for the 3 stations (C663, C12, and C41) is C663 observes the daily maximum 1-hour ozone across the PdN region, C12 at UTEP is the site in El Paso observing the most exceedances on the US side of the border, and an Auto-GC is deployed at C41 providing the opportunity to observe hourly TNMHC concentrations and prepare TNMHC/NO_x ratios as discussed in Section 4 regarding ozone limiting conditions in association with the model's production of H_2O_2 and HNO_3 . The diurnal ozone formation graphic includes the $\text{H}_2\text{O}_2\text{:HNO}_3$ ratio which helps in determining whether ozone formation conditions are NO_x- or VOC-limited. A ratio ≥ 0.35 indicates NO_x-limited conditions while a ratio < 0.35 indicates VOC-limited conditions (ENVIRON, 2011).

Figure 14.3 illustrates the diurnal variability in 8-hour ozone comparing the OBSERVED and PREDICTED concentrations. PREDICTED 8-hour ozone is presented as dotted lines; observed 8-hour ozone is presented as solid lines. The $\text{H}_2\text{O}_2\text{:HNO}_3$ ratio is presented as dashed lines and provides a general reference given 8-hour average $\text{H}_2\text{O}_2\text{:HNO}_3$ ratio is not applicable to this analysis. A red line is set at 75ppb indicating the 8-hour ozone NAAQS.

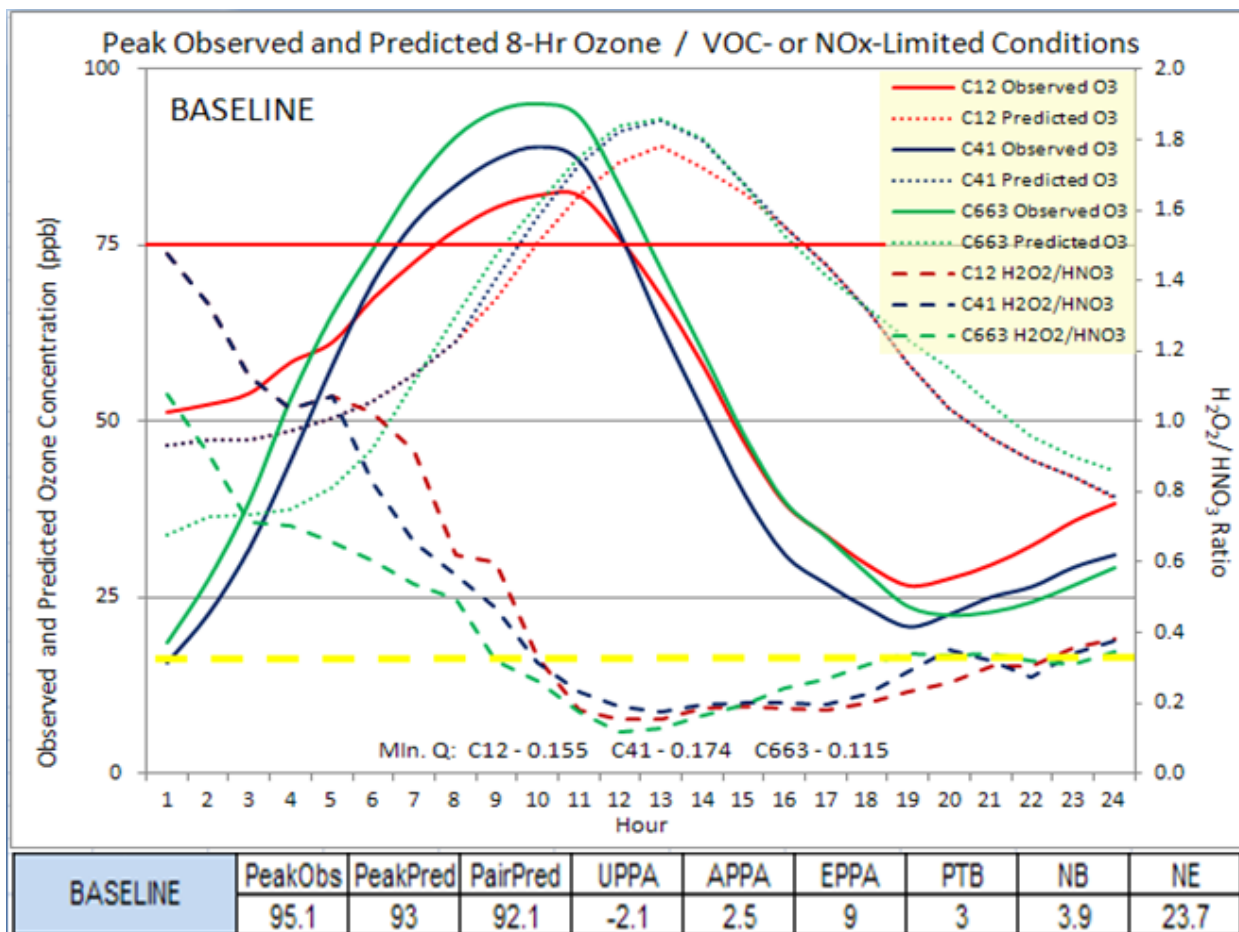


Figure 14.3 Diurnal Predicted and Observed 8-Hour Ozone (ppb) / H₂O₂:HNO₃ Ratios – BASELINE

8-hour ozone data indicate the PTB is slightly improved to 3 hours compared to 1-hour ozone. CAMx under-predicts the peak ozone (93 ppb) and the PAIRED PREDICTED (92.1 ppb) 8-hour average ozone concentration. NB (3.9%) and NE (23.7%) are within acceptable model performance parameters.

14.2 RUN 1 Model Performance Evaluation

Figure 14.4 presents performance statistics for RUN 1, 8-hour ozone PEAK OBSERVED, and co-located daily PAIRED PREDICTED PEAK among all sites in the PdN region. The model under-predicts 8-hour ozone on 9 of 10 simulation-days as indicated by negative APPA. On 6/14 the 8-hour PAIR PREDICTED concentration at several CAMS exceeded the OBSERVED 8-hour ozone concentration. The worse under-prediction occurred on 6/16 with APPA (-30.1%) and NB (-31.8%). NE (32%) was within acceptable parameters for this statistic.

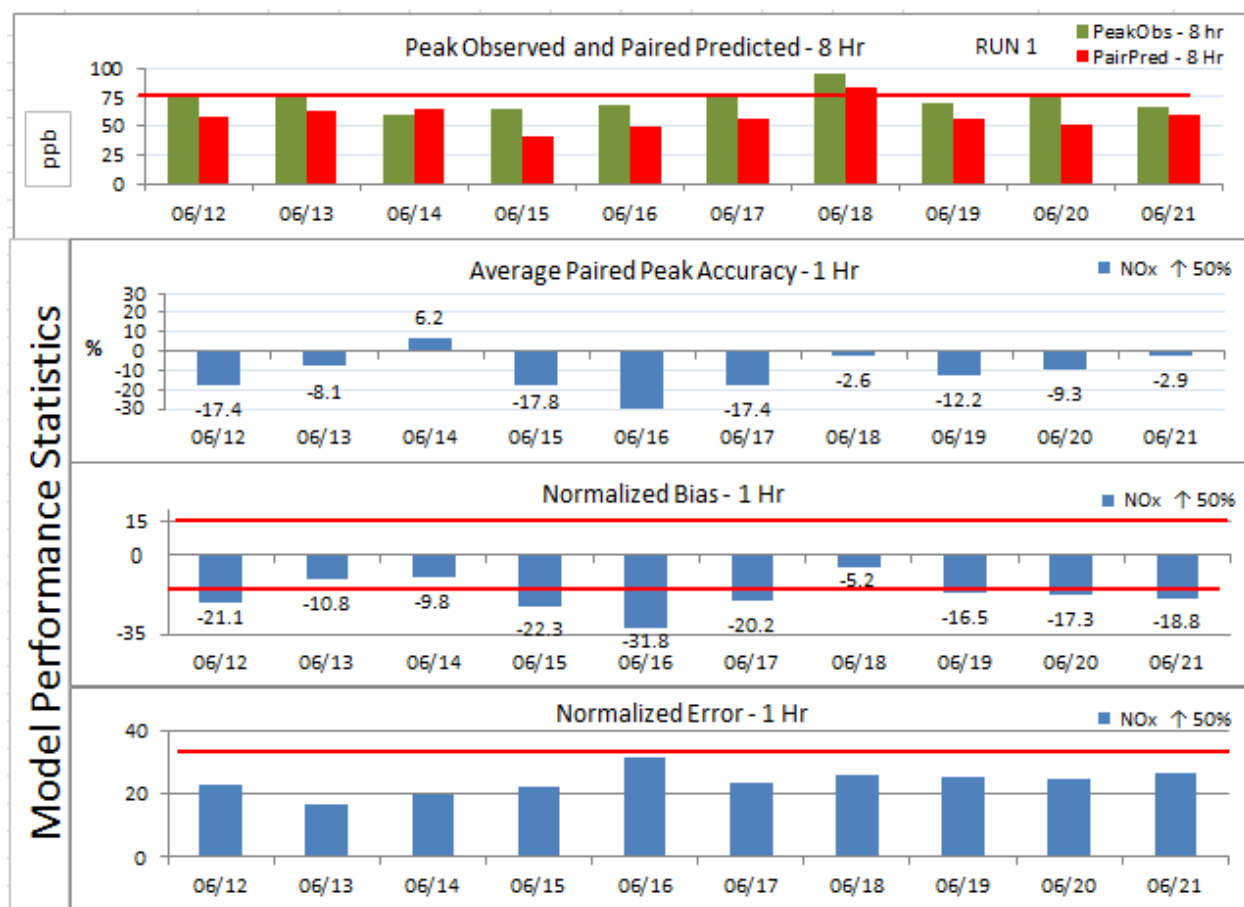


Figure 14.4 Model Performance Statistics – RUN 1

Figure 14.5 depicts RUN 1 diurnal PREDICTED and OBSERVED 1-hour ozone concentrations. Overall NB achieved acceptable model performance parameters of $\pm 15\%$ on 7 or 10 days. NE for all 10 simulation days was acceptable and within the $\leq 35\%$ threshold. On 6/18 the model performed well regarding NB & NE where both increased compared to BASELINE (1.9% and 0.6% respectively). PTB is comparable to BASELINE at 4 hours. PredPeak 1-hour ozone is reduced slightly compared to BASELINE. PAIRED PREDICTED 1-hour ozone is reduced by 2.4 ppb.

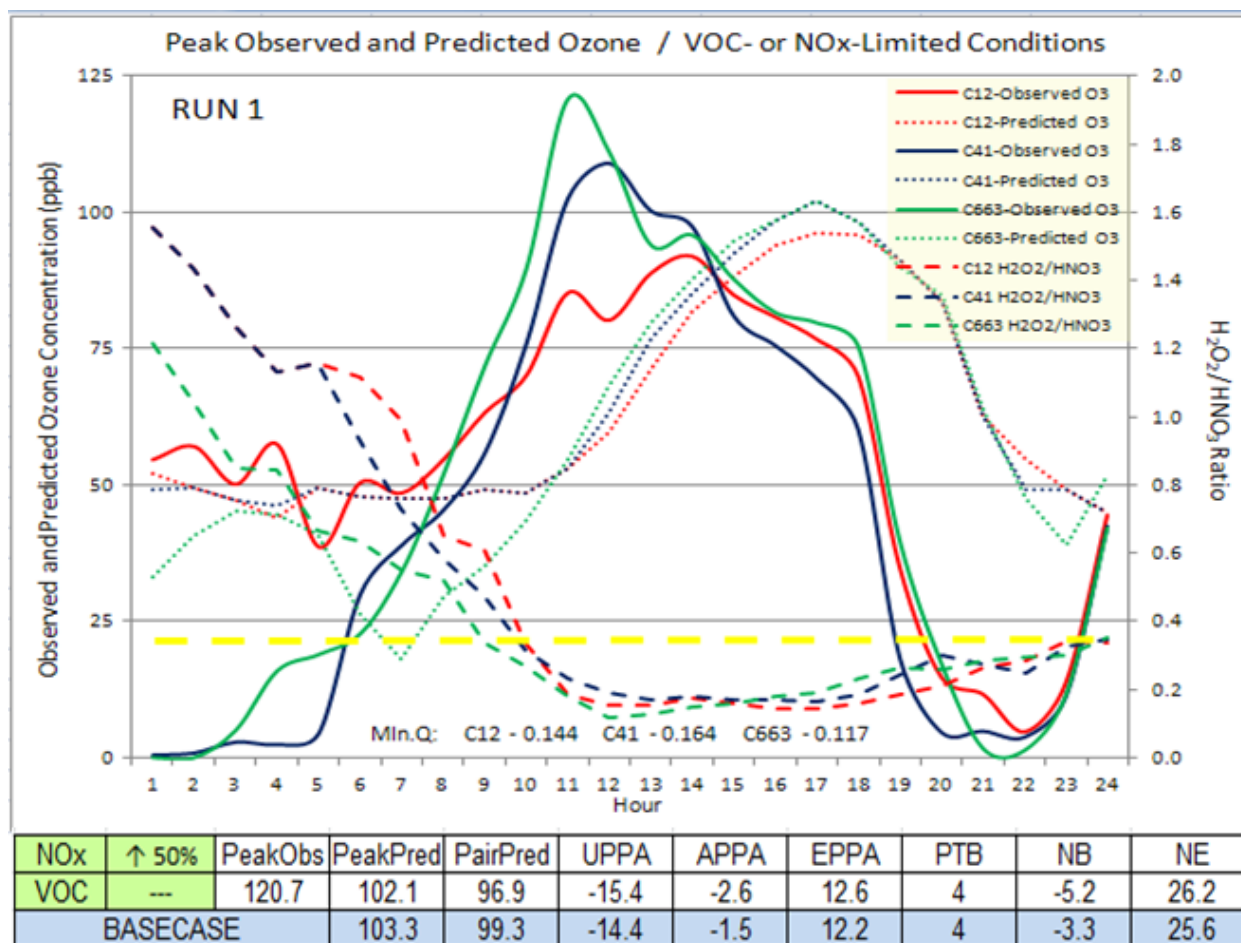


Figure 14.5 Diurnal Predicted and Observed 1-Hour Ozone (ppb) / H₂O₂:HNO₃ Ratios–6/18/2006 – RUN 1

The diurnal $\text{H}_2\text{O}_2:\text{HNO}_3$ ratio indicates NO_x -limiting conditions exist during the early morning hours. As photochemistry increases and HNO_3 production accelerates a VOC-limiting condition develops for the duration of the elevated ozone event on 6/18. The shift from NO_x -limited to VOC-limited conditions occurs at 0900hrs however given the PTB of 4 hours it is possible the VOC-limited condition developed 4-hours earlier.

Figure 14.6 illustrates diurnal OBSERVED and PREDICTED 8-hour average ozone concentrations. $\text{H}_2\text{O}_2:\text{HNO}_3$ ratios are provided as reference.

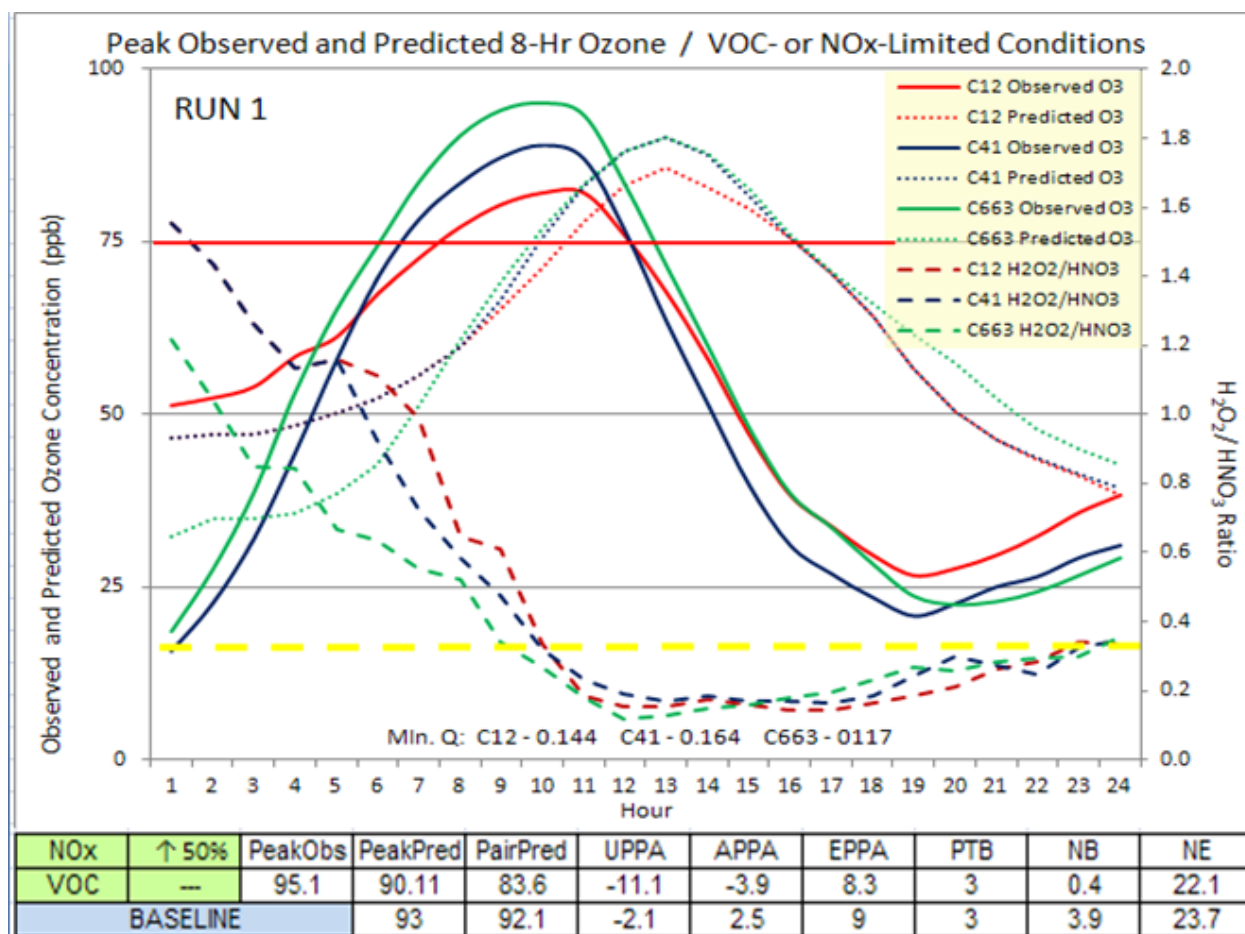


Figure 14.6 Diurnal Predicted and Observed 8-Hour Ozone (ppb) / $\text{H}_2\text{O}_2:\text{HNO}_3$ Ratios – RUN 1

PTB between PEAK OBSERVED and PEAK PREDICTED 8-hour averages is 3 hours. PEAK PAIRED PREDICTED 8-hour average ozone is 83.6 ppb. Both OBSERVED and PREDICTED 8-hour ozone exceeds the 75 ppb NAAQS for several hours.

Of interest during this simulation is the reduction of ozone compared to the BASELINE simulation with the 50% increase in NO_x emissions. This occurs when NO_x titrates ozone due to the abundance of this pollutant. However this may be observed, reducing ozone by increasing NO_x is not a good air quality improvement planning strategy.

14.3 RUN 2 Model Performance Evaluation

RUN 2 decreases NO_x emissions by 50%. Figure 14.7 presents performance statistics for RUN 2, 8-hour ozone PEAK OBSERVED, and co-located daily PAIRED PREDICTED PEAK among all sites in the PdN region.

The model under-predicts 8-hour ozone on 9 of 10 simulation-days. On 6/14 the 8-hour PAIRED PREDICTED PEAK concentration at 6 CAMS exceeds the OBSERVED 8-hour ozone. The worse under-prediction occurred on 6/16 observing APPA (-29.4%), NB (-30.5%). NE (30.9%) was with acceptable limits for this statistic. 6/18 simulation results indicate good model performance with minimal NB (-2.1%) for 8-hour ozone.

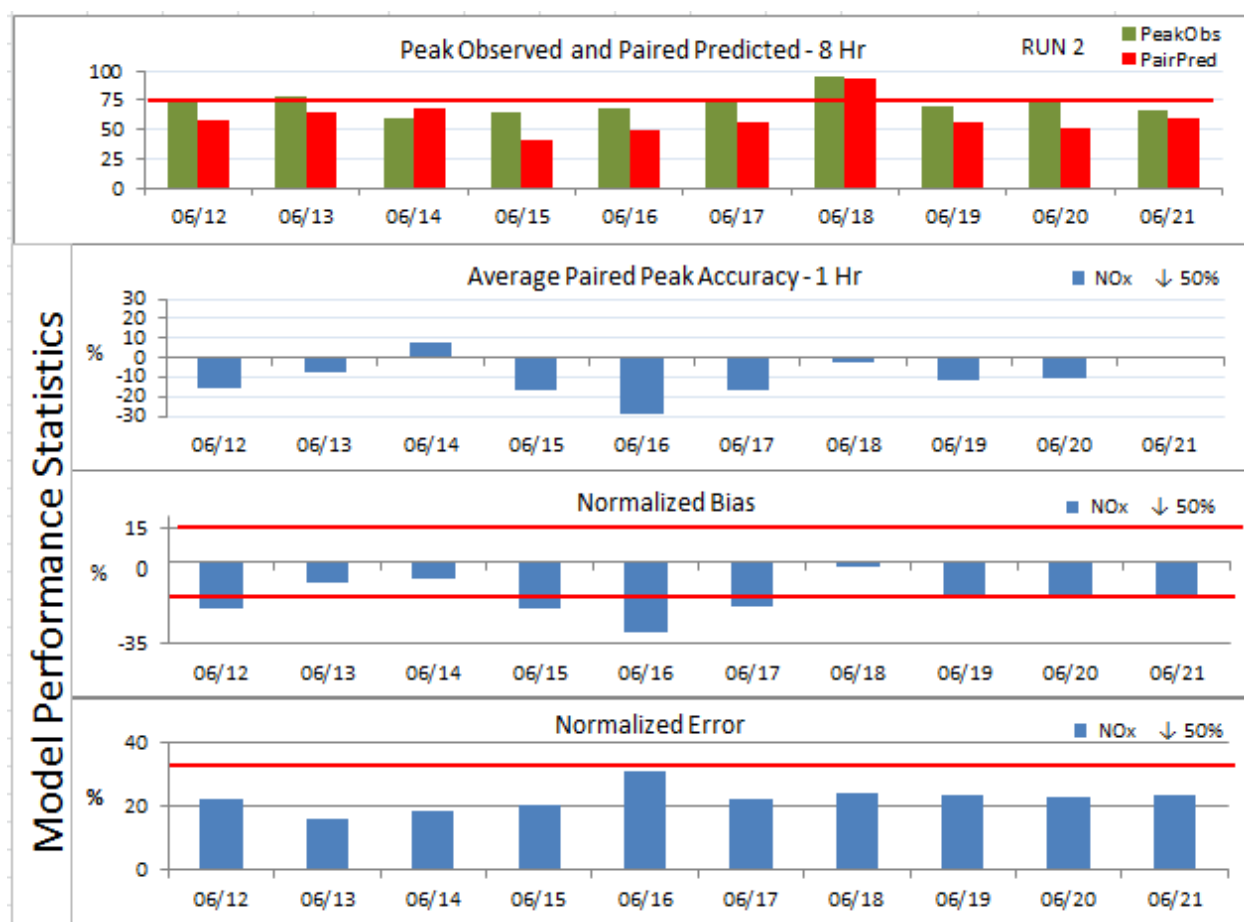


Figure 14.7 Model Performance Statistics – Run 2

The model under-predicts 1-hour ozone on 8 of 10 simulation-days regarding APPA. On 6/14 the PREDICTED PEAK 1-hour ozone was 0.5 ppb below BASELINE. The positive APPA for 6/14 indicates several other CAMS over-predicted maximum 1-hour ozone. APPA on 6/16 (-29.4%) indicates very poor model performance which is confirmed by low NB (-30.5%). APPA (+0.5%) on 6/21 indicates slight over-prediction accuracy among all co-located paired sites. PEAK PREDICTED 1-hour ozone (102.4 ppb) on 6/18 is 0.9 ppb less than the BASELINE PEAK PREDICTED. The negative NB for all days indicates the model under-predicts 1-hour ozone across all co-located sites compared to observed 1-hour ozone concentrations.

NE (30.9%) on 6/16 was within acceptable parameters regardless of the very low NB (-30.5%) on this day. On 6/18 the model performed very well regarding NB (-2.1%) & NE (24.2%) where both statistics improved slightly compared to BASELINE. The model performed within acceptable NE parameters on RUN 2 for 1-hour ozone.

Figure 14.8 depicts RUN 2 diurnal PREDICTED and OBSERVED 1-hour ozone concentrations. The diurnal variation for 1-hour ozone on 6/18 presented in Figure 14.8 indicates an improved PTB which shifts to 3 hours compared to 4 hours in the BASELINE. $\text{H}_2\text{O}_2:\text{HNO}_3$ ratios indicate early morning NO_x limited conditions becoming VOC-limited at ~9 AM for C663 observations. C663 also generated a predicted minimum $\text{H}_2\text{O}_2:\text{HNO}_3$ ratio (0.121) compared to C12 and C41 $\text{H}_2\text{O}_2:\text{HNO}_3$ ratios (0.158 and 0.186 respectively).

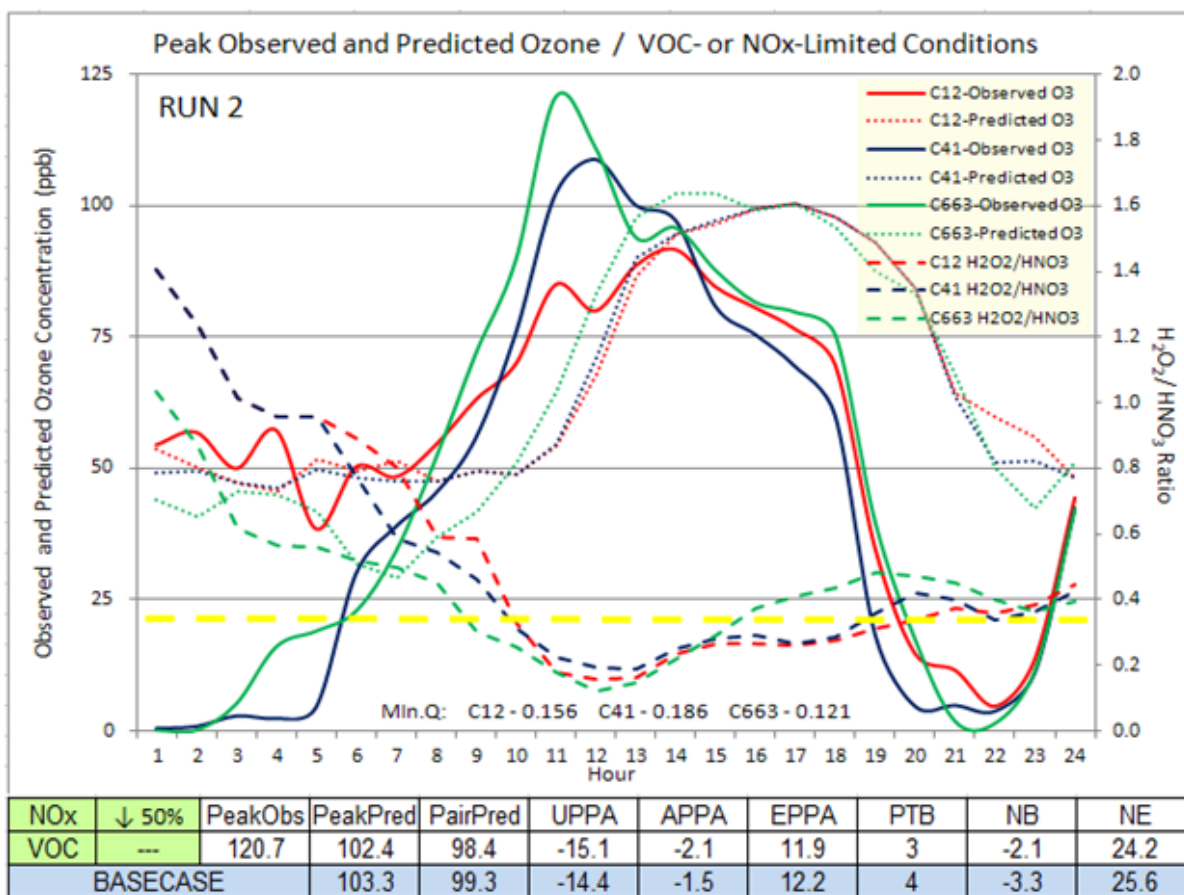
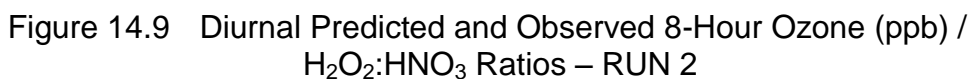


Figure 14.8 Diurnal Predicted and Observed 1-Hour Ozone (ppb) /
H₂O₂:HNO₃ Ratios – RUN 2

Figure 14-9 illustrates diurnal OBSERVED and PREDICTED 8-hour average ozone concentrations. H₂O₂:HNO₃ ratios are provided as reference. The PTB between OBSERVED and PREDICTED 8-hour averages is unchanged (3 hours) compared to BASELINE. PEAK PAIRED PREDICTED 8-hour average ozone is 92.6 ppb. PREDICTED 8-hour ozone exceeds the 75 ppb standard for several hours on 6/18. 8-hour ozone increases 1 ppb compared to BASELINE. Of interest during this simulation is the increase of ozone compared to the BASELINE given the 50% decrease in NO_x emissions.



14.4 RUN 3 Model Performance Evaluation

RUN 3 involved reducing area source VOC emissions in Juárez by 50%. Figure 14.10 presents performance statistics for RUN 3, 8-hour ozone PEAK OBSERVED, and co-located daily PAIRED PREDICTED PEAK among all sites in the PdN region.

The model under-predicts 1-hour ozone on all 10 simulation days. The difference between this and previous RUNs is the over-prediction occurs on 6/13. The simulation presented failing NB on 7 of 10 days. The PREDICTED PEAK on 6/18 for 1-hour ozone was 91.7 ppb indicating good model response to modifications in VOC emission.

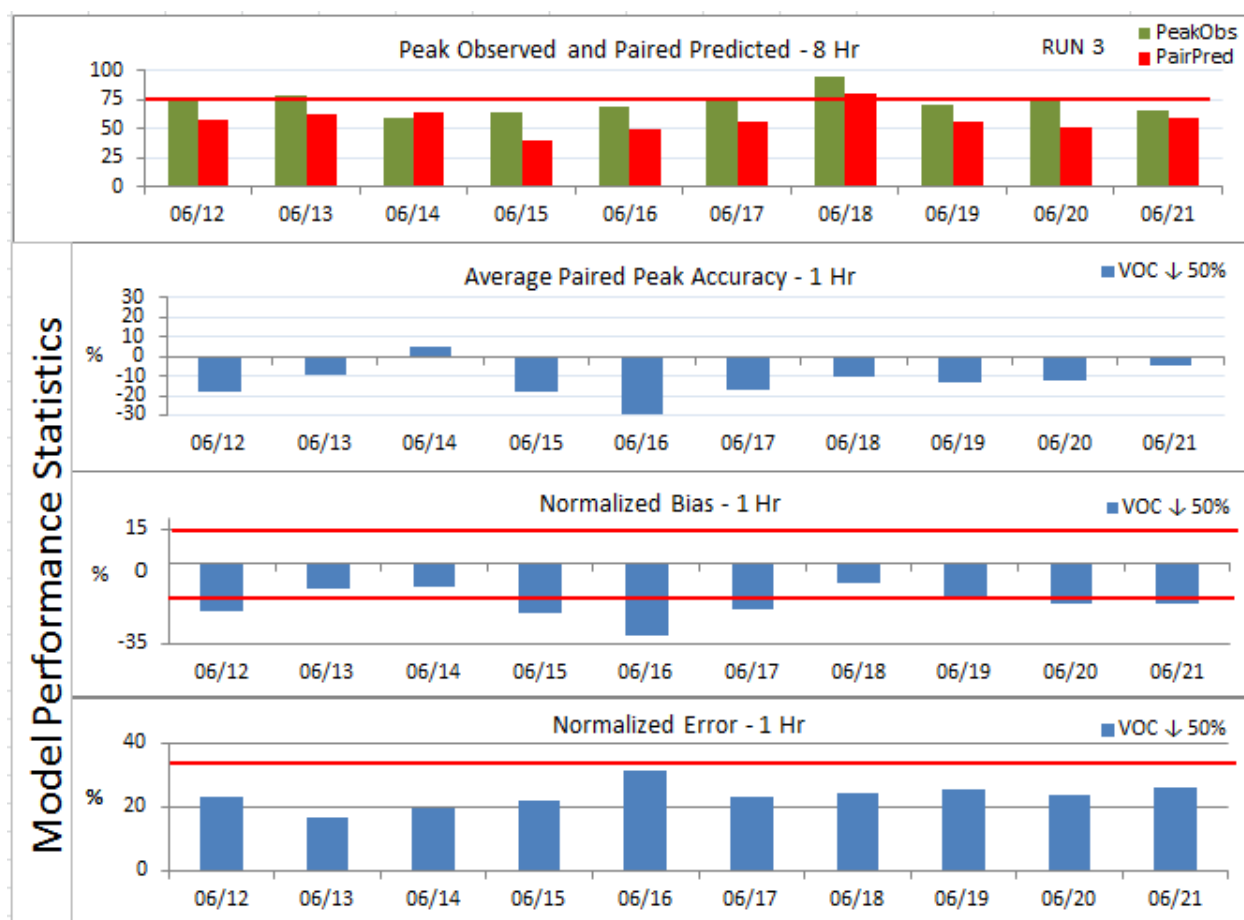


Figure 14.10 Model Performance Statistics – Run3

Figure 14.11 presents diurnal OBSERVED and PREDICTED 1-hour ozone and H₂O₂:HNO₃ ratios. The PAIRED PREDICTED PEAK 1-hour ozone (86.7 ppb) is 12.6 ppb less than BASELINE. The PTB is unchanged from BASELINE at 4 hours. NE improves from 25.6% to 24.2%. NB (-8.7%) decreases from BASELINE.

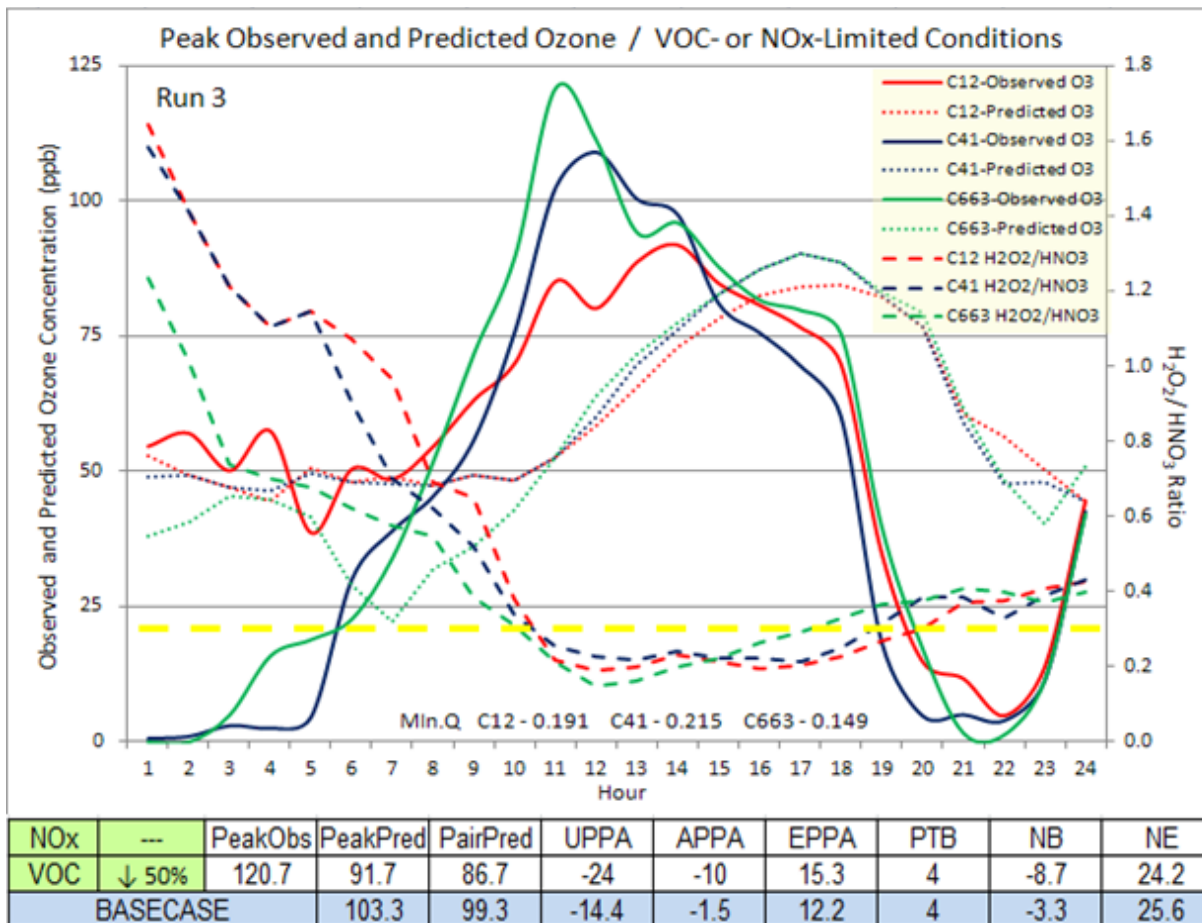


Figure 14.11 Diurnal Predicted and Observed 1-Hour Ozone (ppb) / H₂O₂:HNO₃ Ratios – RUN 3

Figure 14.12 presents diurnal PREDICTED and OBSERVED 8-hour ozone and H₂O₂:HNO₃ Ratios. The PAIRED PREDICTED PEAK 8-hour ozone is 80.3 ppb and the PREDICTED PEAK 8-hour is 83.2 ppb. This simulation shows good response to the

50% reduction in VOC emission. NB (-1.8%) indicates minimal under-prediction, and NE (23%) indicates the simulation is relatively unchanged from BASELINE and operating within acceptable parameters for these statistics.

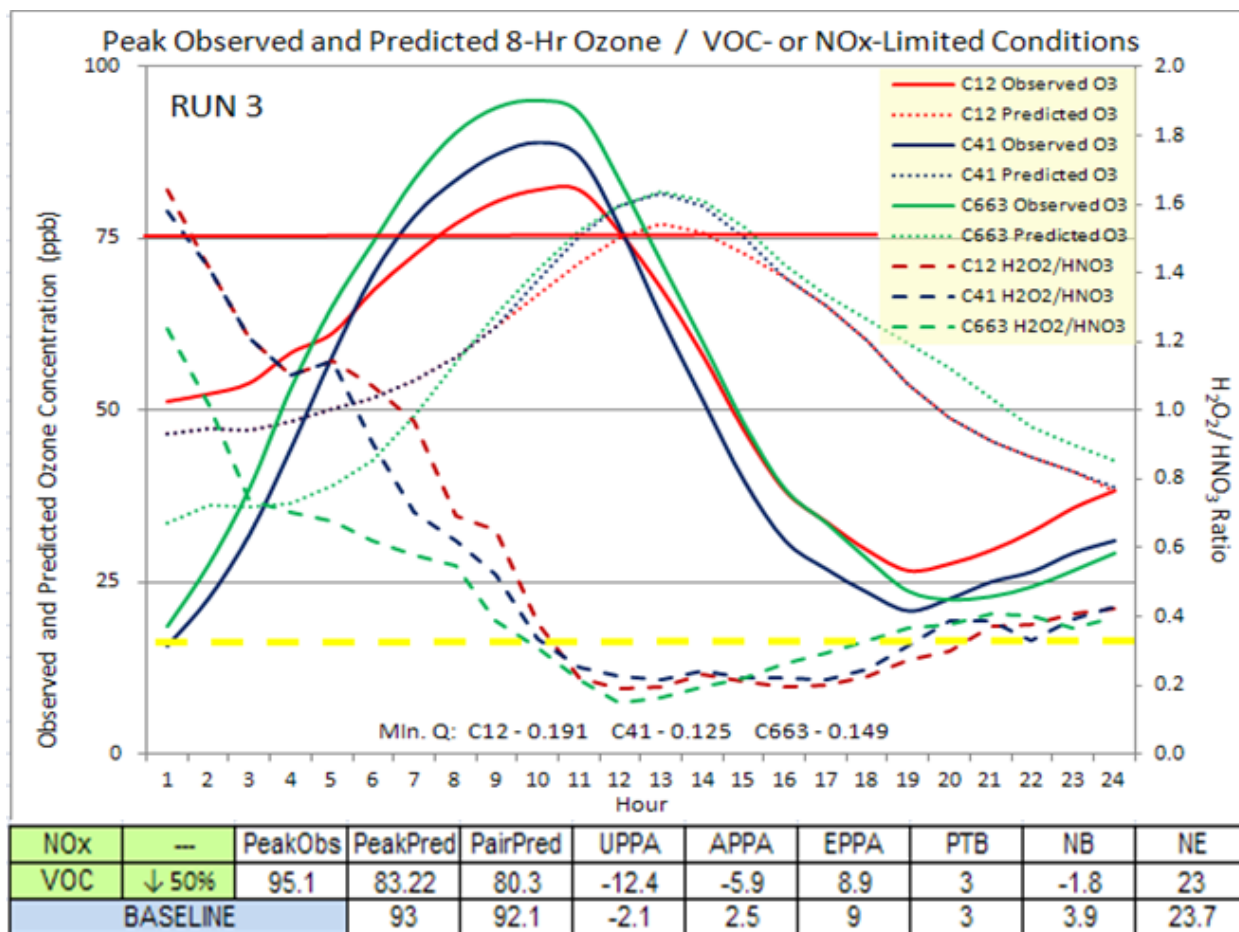


Figure 14.12 Diurnal Predicted and Observed 8-Hour Ozone (ppb) / H₂O₂:HNO₃ Ratios – RUN 3

14.5 RUN 4 Model Performance Evaluation

RUN 4 involved increasing area source VOC emissions in Juárez by 50%. Figure 14.13 presents performance statistics for RUN 4, 8-hour ozone PEAK OBSERVED, and co-located daily PAIRED PREDICTED PEAK among all sites in the PdN region.

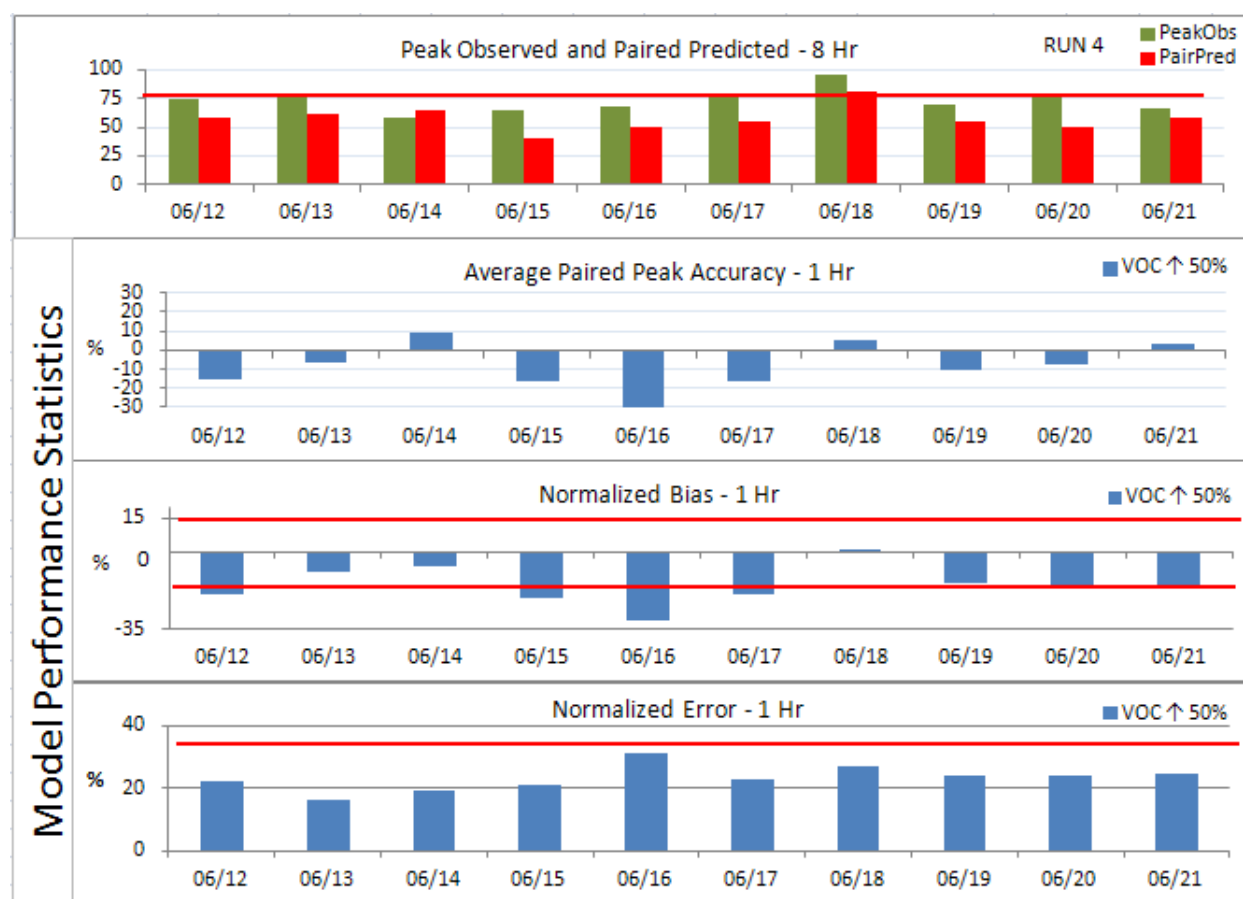


Figure 14.13 Model Performance and Statistics - RUN 4

The model under-predicts 1-hour ozone on 9 of 10 days. On 6/18 the model slightly over-predicts OBSERVED ozone as indicated by NB (1.2%). The simulation failed NB on 4 of 10 days where NB was <-15%. The PAIRED PREDICTED PEAK

which occurred at C663 was 107.8 ppb. Figure 14.14 presents diurnal PREDICTED and OBSERVED 1-hour ozone and H₂O₂:HNO₃ ratios.

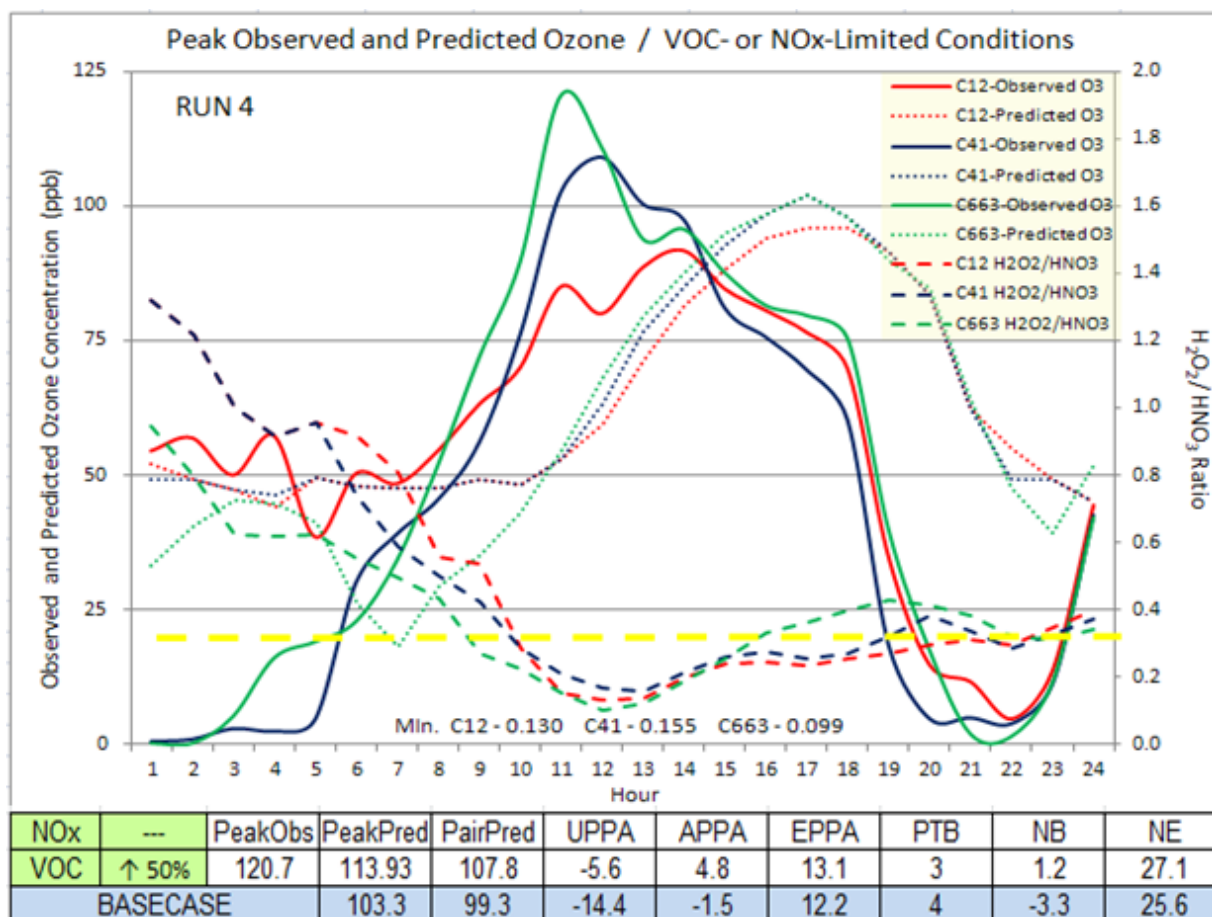


Figure 14.14 Diurnal Predicted and Observed 1-Hour Ozone (ppb) /
H₂O₂:HNO₃ Ratios – RUN 4

An increase of 50% in area source VOC emissions increased the PREDICTED PEAK 1-hour ozone ~113.9 ppb or ~10.6%. The increase is 10 ppb greater than BASELINE and continues to be less than 10 ppb below the PEAK OBSERVED. PTB improves (3 hours) compared to the BASELINE (4 hours). NE is reduced by 1.5 percentage points. H₂O₂:HNO₃ ratios indicate a NO_x-limited condition exists in the early

morning hours and a shift to VOC-limited conditions at ~9 AM remaining VOC-limited for the duration of the ozone event. Figure 14.15 presents diurnal predicted and observed 8-hour ozone and $\text{H}_2\text{O}_2:\text{HNO}_3$ ratios.

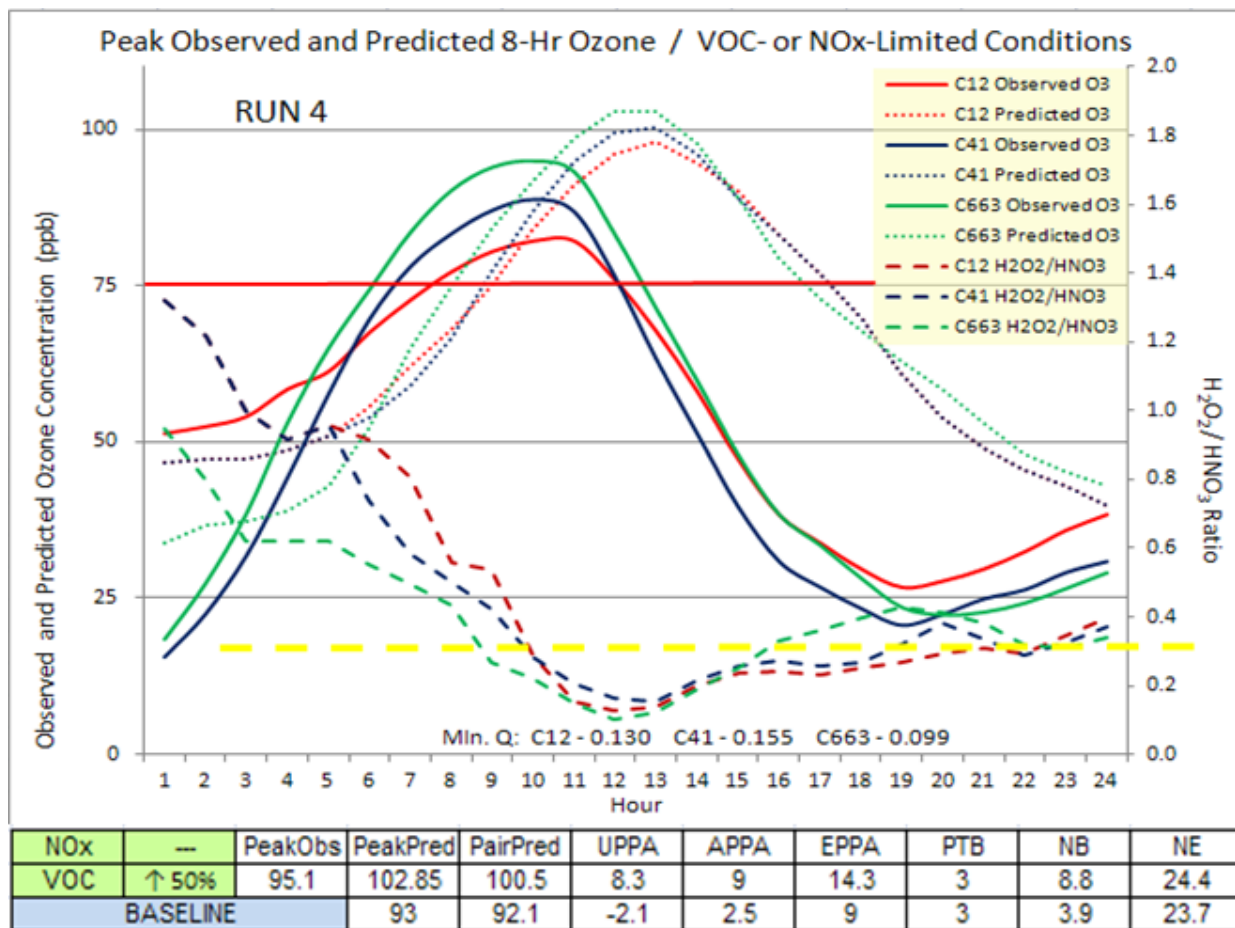


Figure 14.15 Diurnal Predicted and Observed 8-Hour Ozone (ppb)
 $\text{H}_2\text{O}_2:\text{HNO}_3$ Ratios – RUN 4

8-hour ozone PAIRED PREDICTED PEAK (100.5 ppb) and 8-hour ozone PREDICTED PEAK (102.85 ppb) over-predict OBSERVED 8-hour ozone and indicate good model response to increased VOC emissions. Positive NB (8.8%) indicating the

over-prediction and NE (24.4%) indicate the simulation is operating within acceptable parameters for these statistics.

14.6 RUN 5 Model Performance Evaluation

RUN 5 involved increasing Juárez area source NO_x and VOC emissions by 50%. Figure 14.16 presents performance statistics for RUN 5, 8-hour ozone PEAK OBSERVED, and co-located daily PAIRED PREDICTED PEAK among all sites in the PdN region.

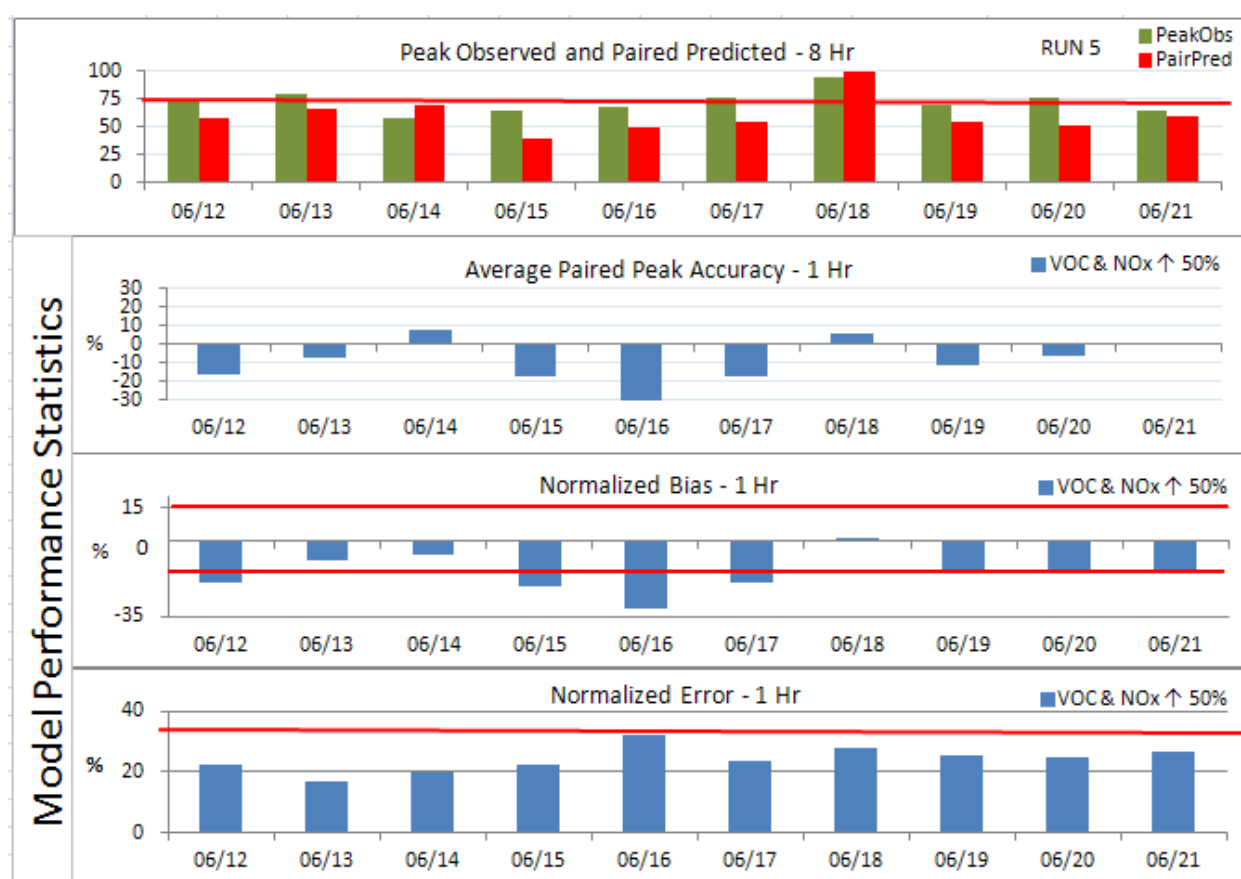


Figure 14.16 Model Performance Statistics – RUN 5

The model under-predicts 1-hour ozone on 9 of 10 days. The model over-predicts OBSERVED 1-hour ozone on 6/18 as indicated by NB (0.1%). The simulation

presented failing NB on 7 of 10 days where NB was <-15%. There was minimal improvement of NB with 2 days (6/19 and 6/20) reaching -15.9%. The 1-hour ozone PREDICTED PEAK on 6/18 (113 ppb) indicates good model response to increased VOC and NOx emissions. The PAIRED PREDICTED PEAK (108.7 ppb) occurred at C663. It should be noted that the increase in both VOC and NOx emissions significantly increased the PEAK PREDICTED 1-hour ozone by 9.7 ppb.

Figure 14.17 presents diurnal PREDICTED and OBSERVED 1-hour ozone and H₂O₂:HNO₃ ratios for RUN 5.

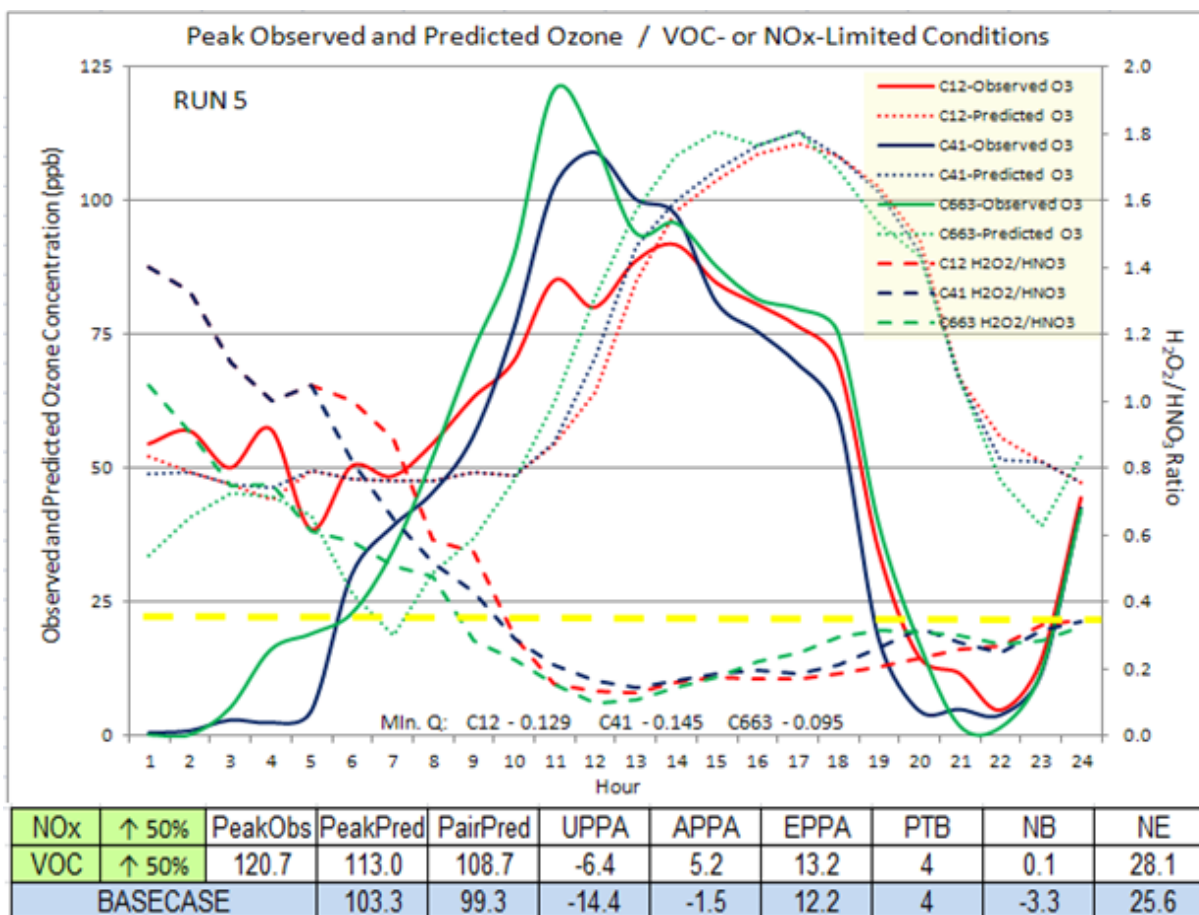


Figure 14.17 Diurnal Predicted and Observed 1-Hour Ozone (ppb) / H₂O₂:HNO₃ Ratios – RUN 5

An increase of 50% in Juárez area source VOC emissions increased the PREDICTED PEAK 1-hour ozone (113 ppb or ~9.4%). The increase in 9.7 ppb greater than BASELINE continues to be 6.3 ppb below the OBSERVED PEAK. The PTB (4 hours) remained unchanged compared to BASELINE. NE (28.1%) increased by 2.5 percentage points from BASELINE. The model performed within acceptable NB (0.1%) and NE (28.1%) parameters. Figure 14.18 presents diurnal PREDICTED and OBSERVED 8-hour ozone and H₂O₂:HNO₃ ratios for RUN 5.

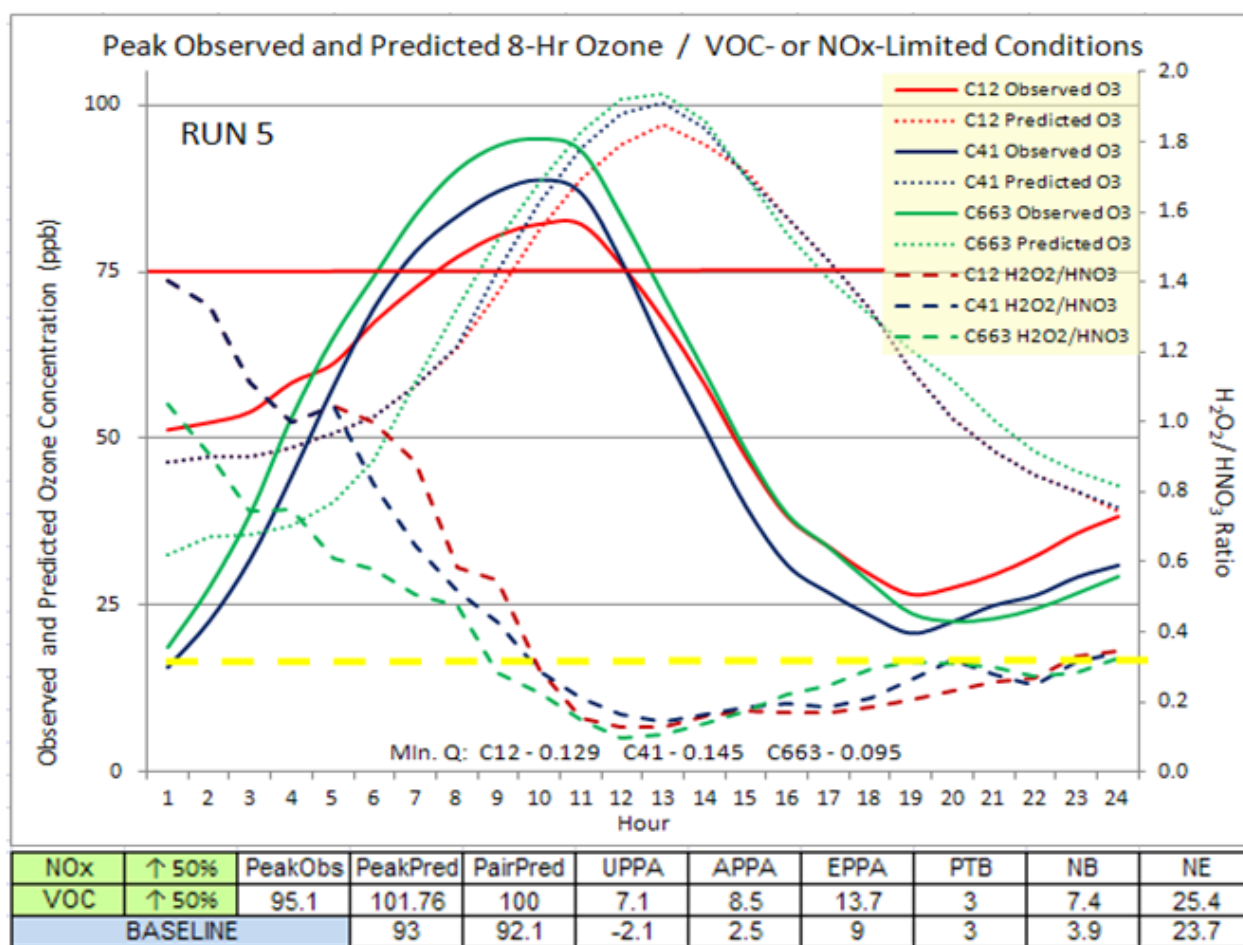


Figure 14.18 Diurnal Predicted and Observed 8-Hour Ozone (ppb) / H₂O₂:HNO₃ Ratios – RUN 5

The PAIRED PREDICTED PEAK 8-hour ozone (100 ppb) and the PREDICTED PEAK 8-hour (102.76) ppb indicate good model response to increased emissions. It should be noted that RUN 5 with 50% increase in both VOC and NO_x generated an 8-hour ozone PREDICTED PEAK 1 ppb below RUN 4 which increased just VOC area source emissions by 50%. Both PREDICTED PEAK and the PAIRED PREDICTED PEAK over-predict OBSERVED 8-hour ozone and indicate good response to the 50% increase in Juárez area source VOC and NO_x emissions. The positive NB (7.4%) substantiating the over-prediction and NE (25.4%) indicates the simulation generated results within acceptable parameters for these statistics.

H₂O₂:HNO₃ ratios indicated early morning NO_x-limited conditions converting to VOC-limited conditions at 9 AM as photochemistry and HNO₃ production begins. The H₂O₂:HNO₃ ratio (0.095) is the lowest observed during the series of simulations and is closely associated with PREDICTED PEAK ozone concentrations. The minimum Q is observed at 12 PM. Of note is the lowest Q at 663 coincides with the PREDICTED PEAK.

14.7 RUN 6 Model Performance Evaluation

RUN 6 involved decreasing Juárez area source NO_x and VOC emissions by 50%. Figure 14.19 presents performance statistics for RUN 6, 8-hour ozone PEAK OBSERVED, and co-located daily PAIRED PREDICTED PEAK among all sites in the PdN region.

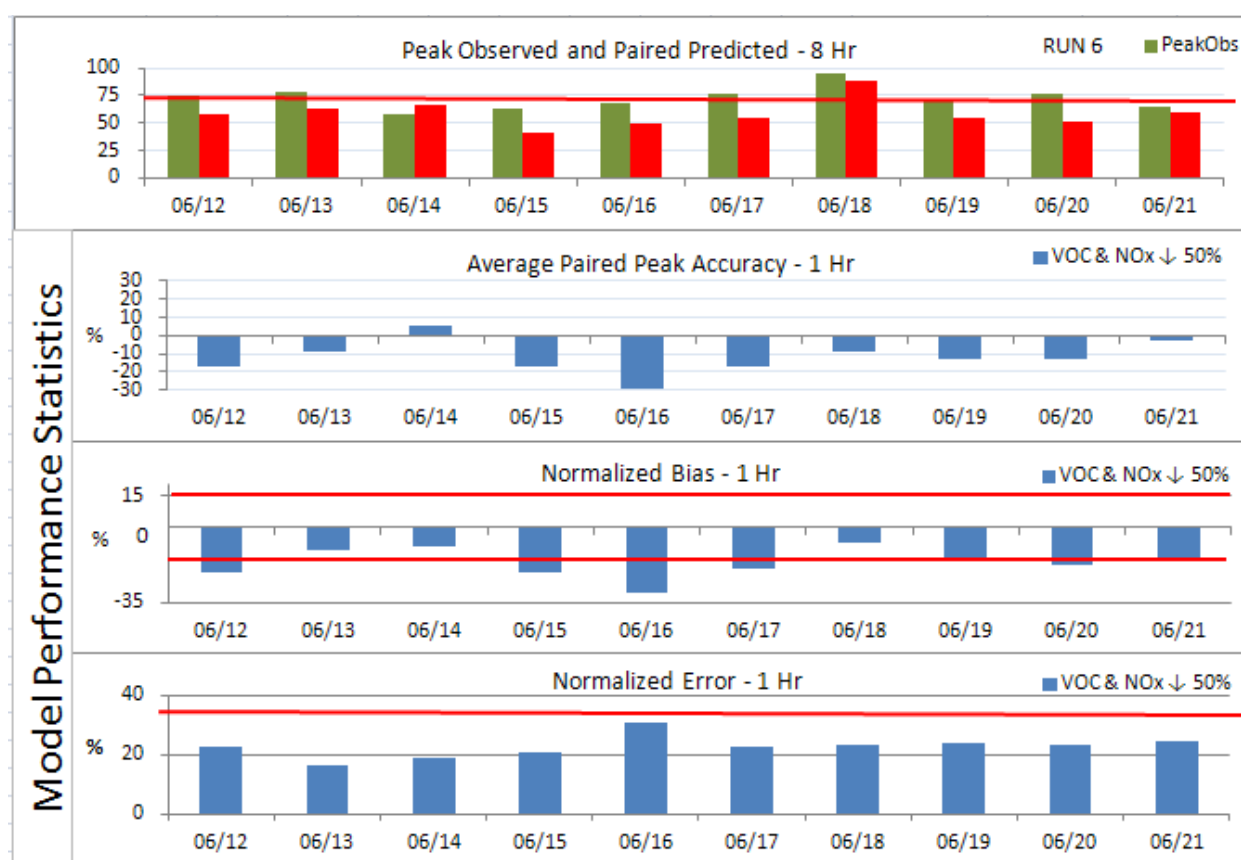


Figure 14.19 Model Performance Statistics - RUN 6

The simulation under-predicts 1-hour ozone on all 10 days as indicated by the negative NB for all simulated days. The simulation passed NB on 4 of 10 days. NB on 6/18 (-5.2%) indicated diminished performance over BASELINE. This simulation also

presented slightly diminished NE (26.2%) for 1-hour ozone. Both NB and NE operated within acceptable parameters.

Figure 14.20 presents diurnal PREDICTED and OBSERVED 1-hour ozone and H₂O₂:HNO₃ ratios for RUN 6. The PREDICTED PEAK on 6/18 for 1-hour ozone (92.7 ppb) is 10.6 ppb or ~13% less than BASELINE. The decrease indicates good model response to decreased VOC and NO_x emissions. The PAIRED PREDICTED PEAK (89.1 ppb) occurred at C663.

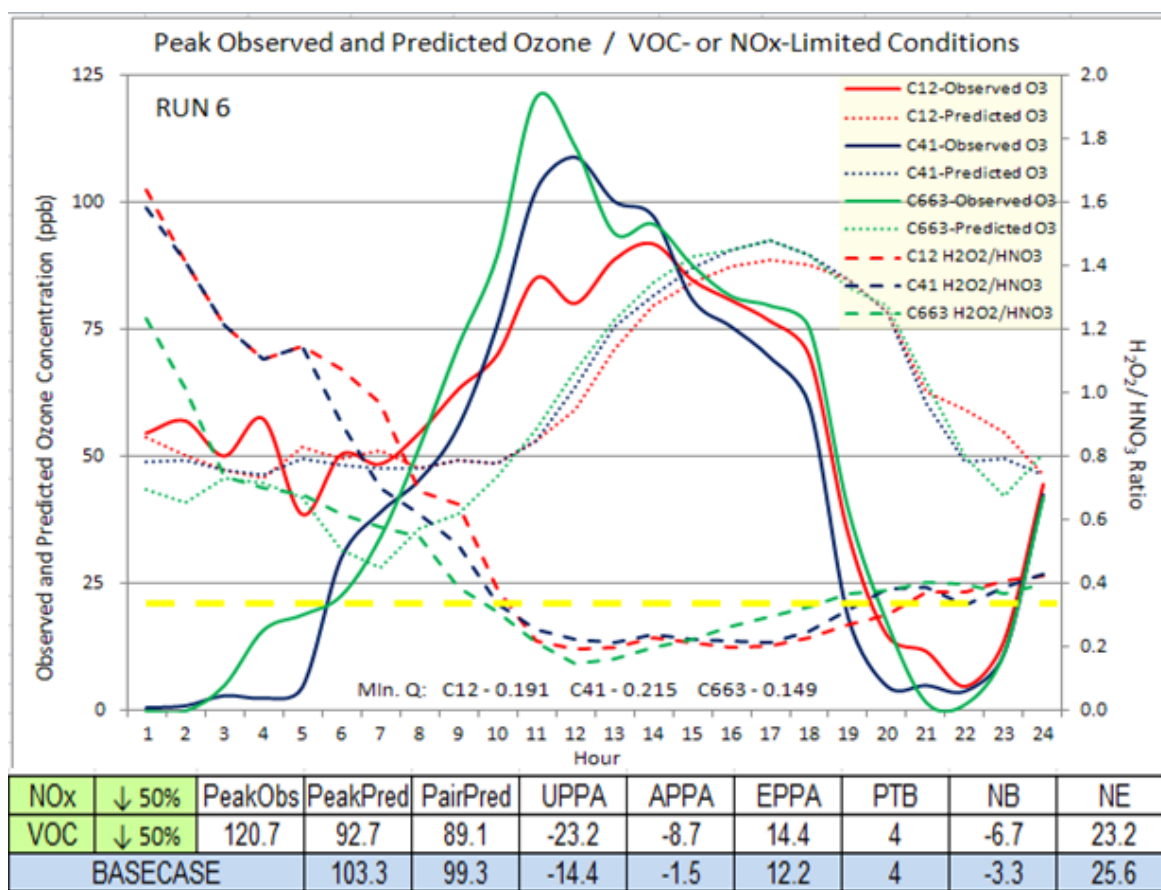


Figure 14.20 Diurnal Predicted and Observed 1-Hour Ozone (ppb) / H₂O₂:HNO₃ Ratios – RUN 6

The decrease of 10 ppb in the PAIRED PREDICTED PEAK compared to BASELINE is well below the 120 ppb OBSERVED PEAK. PTB remained unchanged (4 hours) compared to BASELINE. NE (23.2%) improved by 2.4 percentage points from BASELINE. The model performed within acceptable parameters for NB and NE. Figure 14.21 illustrates diurnal variability of PREDICTED and OBSERVED 8-hour ozone and H₂O₂:HNO₃ ratios for RUN 6. The 50% decrease in Juárez area source VOC and NO_x emissions reduced the PREDICTED PEAK 8-hour ozone to 84.5 ppb or ~9.4%.

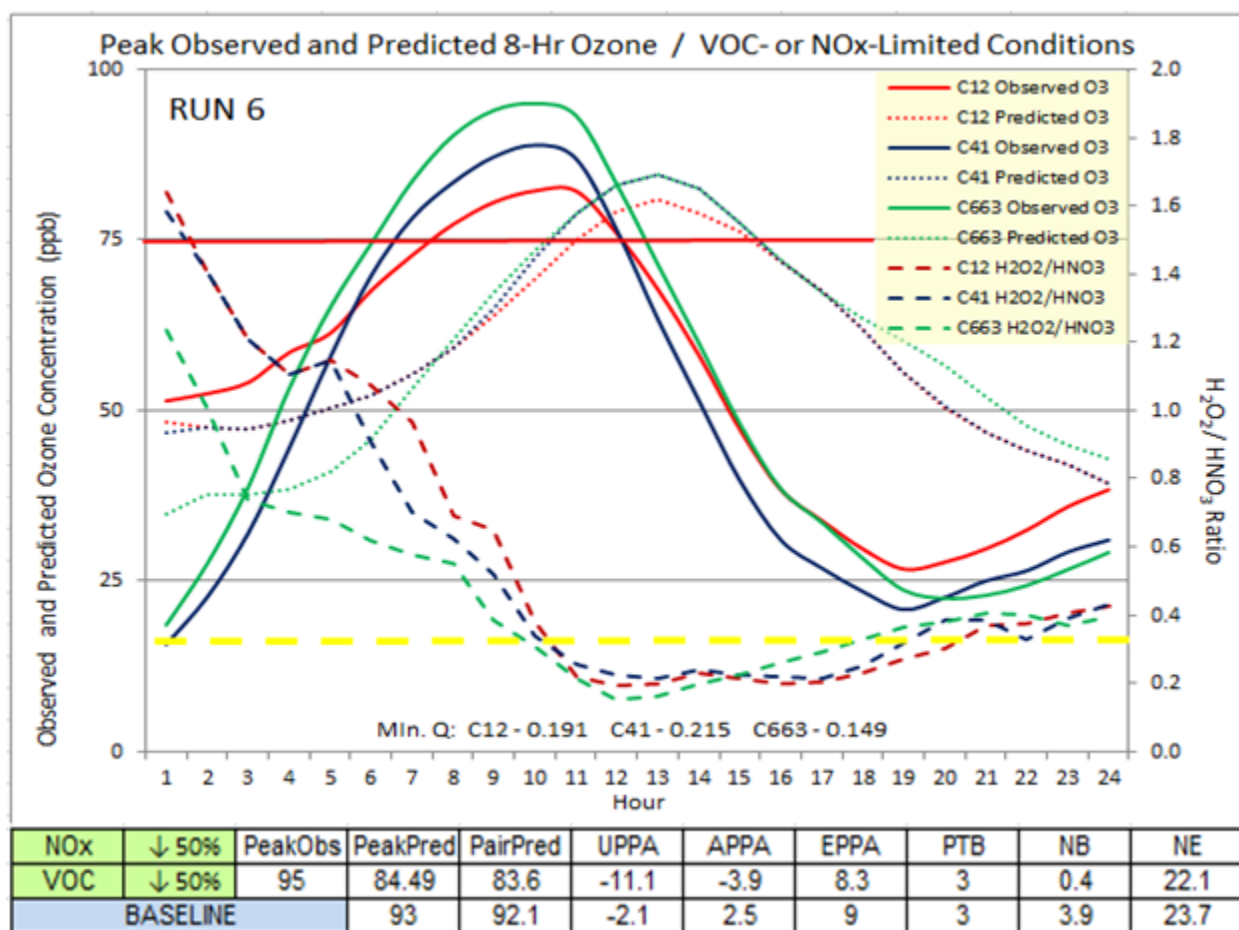


Figure 14.21 Diurnal Predicted and Observed 8-Hour Ozone (ppb) / H₂O₂:HNO₃ Ratios – RUN 6

PTB (3 hours) remained unchanged compared to BASELINE. NE (22.1%) slightly improved compared to BASELINE. The model performed within acceptable NB and NE parameters for the 8-hour ozone simulation. $\text{H}_2\text{O}_2\text{:HNO}_3$ ratios indicate a NO_x -limited condition exists during the early morning hours and shifts to VOC-limited at 10 AM due potentially to the decreased emissions applied to this simulation.

14.8 RUN 7 Model Performance Evaluation

RUN 7 involved increasing Juárez area source NO_x emissions by 75%. Figure 14.22 presents model performance statistics for RUN 7, 8-hour ozone PEAK OBSERVED, and co-located daily PAIRED PREDICTED PEAK among all sites in the PdN region.

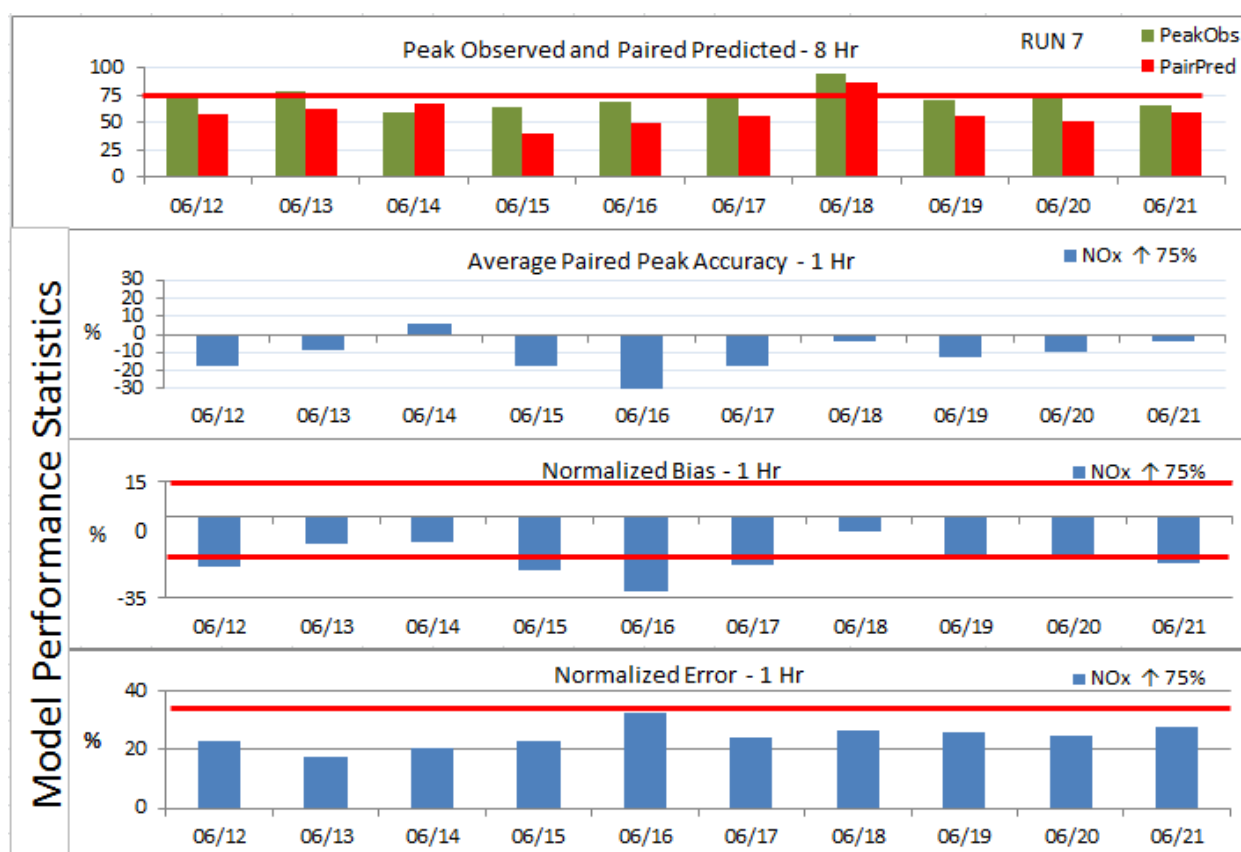


Figure 14.22 Model Performance and Statistics – RUN 7

The simulation under-predicts 1-hour ozone on all 10 days. The simulation passed NB on 3 of 10 days (6/13, 6/14, and 6/18). NB on 6/18 (-6.3%) indicates the simulation operating within acceptable parameters on the ozone event day. Under-

prediction accuracy is indicated for 1-hour APPA during 9 of the 10 simulation days. NE (26.3%) also operated within acceptable parameters on 6/18.

Figure 14.23 presents diurnal PREDICTED and OBSERVED 1-hour ozone and H₂O₂:HNO₃ ratios for RUN 7.

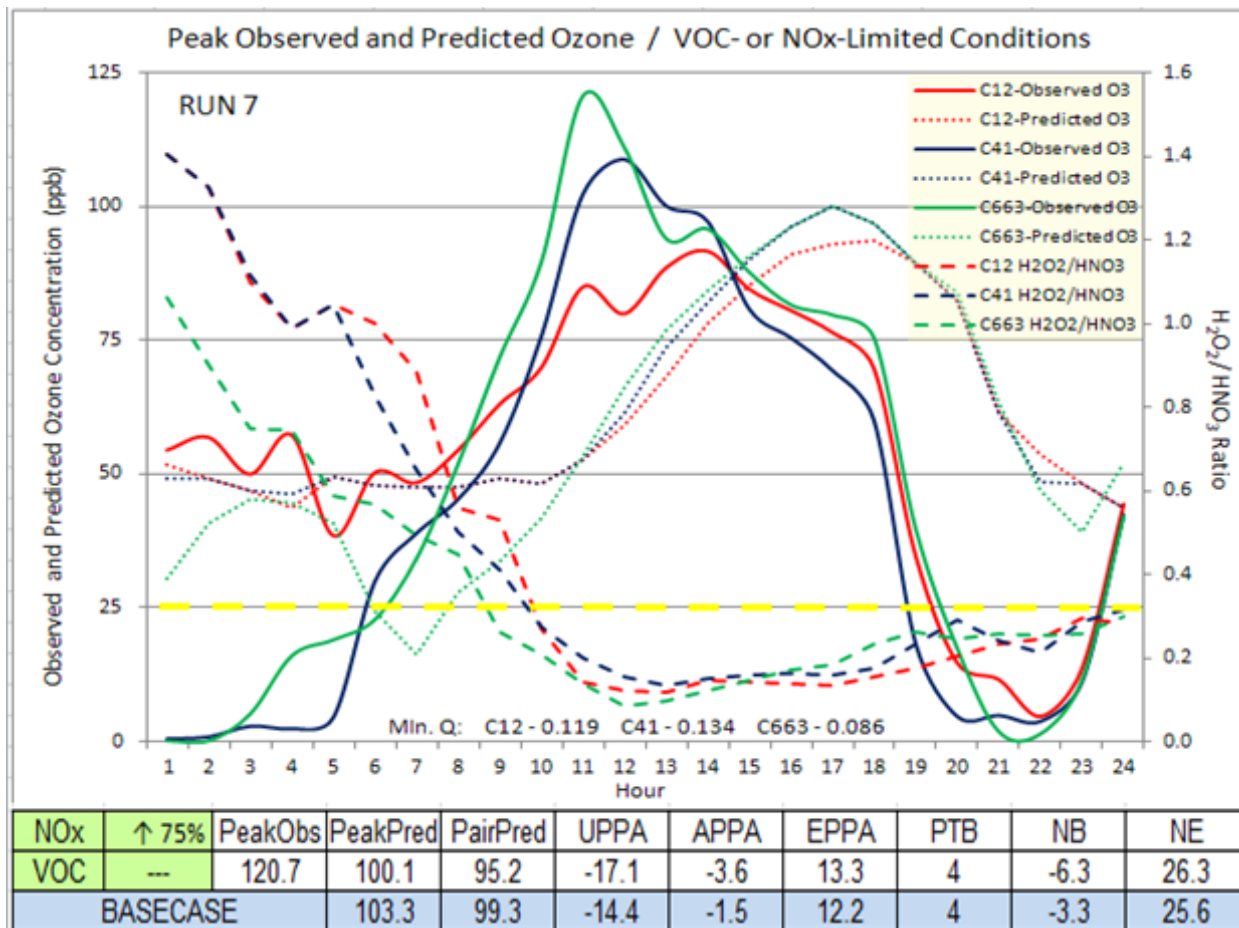


Figure 14.23 Diurnal Predicted and Observed 1-Hour Ozone (ppb) /
H₂O₂:HNO₃ Ratios – RUN 7

The 1-hour ozone PREDICTED PEAK on 6/18 (100.1ppb) was 3.2 ppb less than BASELINE. The model did not strongly respond to the 75% increase in NO_x emissions further indicating VOC-limited conditions. The PAIRED PREDICTED PEAK which

occurred at C663 (95.3 ppb) was 4.1 ppb less than BASELINE. The elevated NO_x emissions continue indicating the titrating effect of excess NO_x emissions which tends to scavenge ambient ozone.

Figure 14.24 illustrates diurnal PREDICTED and OBSERVED 8-hour ozone and H₂O₂:HNO₃ ratios for RUN 7.

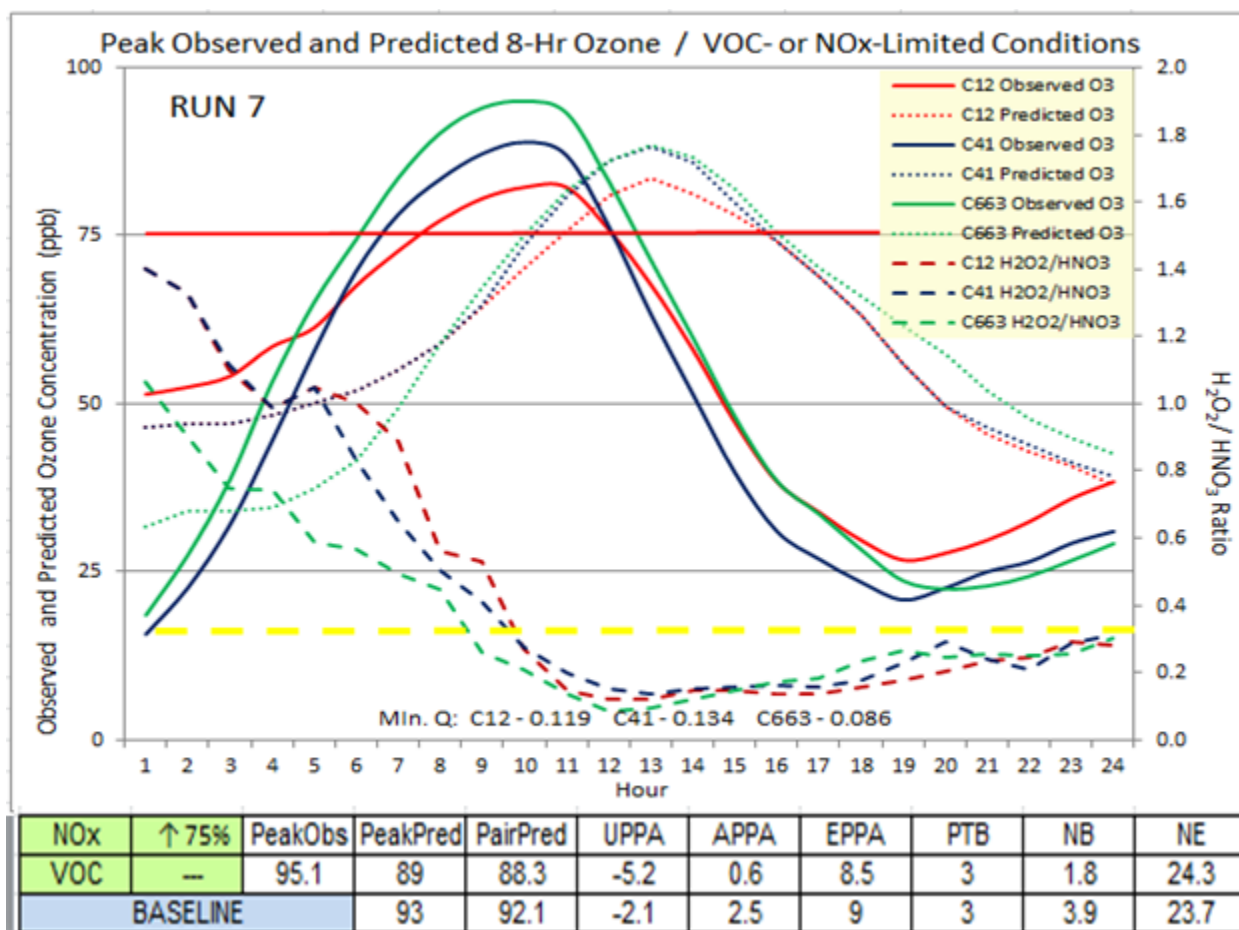


Figure 14.24 Diurnal Predicted and Observed 8-Hour Ozone (ppb) / H₂O₂:HNO₃ Ratios – RUN 7

The 75% increase in Juárez area source NO_x emissions reduced the 8-hour ozone PREDICTED PEAK to 89.1 ppb or 14.5%. PTB (3 hours) remained unchanged

compared to BASELINE. NE (24.3%) slightly diminishes compared to BASELINE (23.7%). The model performed within acceptable NB and NE parameters for the 8-hour ozone simulation.

$\text{H}_2\text{O}_2:\text{HNO}_3$ ratios indicate a NO_x -limited condition exists during the early morning hours and shifts to VOC-limited conditions at 9 AM due potentially to the increase in NO_x which will produce greater concentrations of HNO_3 but also slow the formation of ozone. The minimum Q observed (0.086) further confirms VOC-limited conditions control ozone formation.

14.9 RUN 8 Model Performance Evaluation

RUN 8 involved a 75% reduction in Juárez area source NO_x emissions. Figure 14.25 presents performance statistics for RUN 8, 8-hour ozone PEAK OBSERVED, and co-located daily PAIRED PREDICTED PEAK among all sites in the PdN region. The simulation under-predicts 1-hour ozone on all 10 days given negative NB for all days.

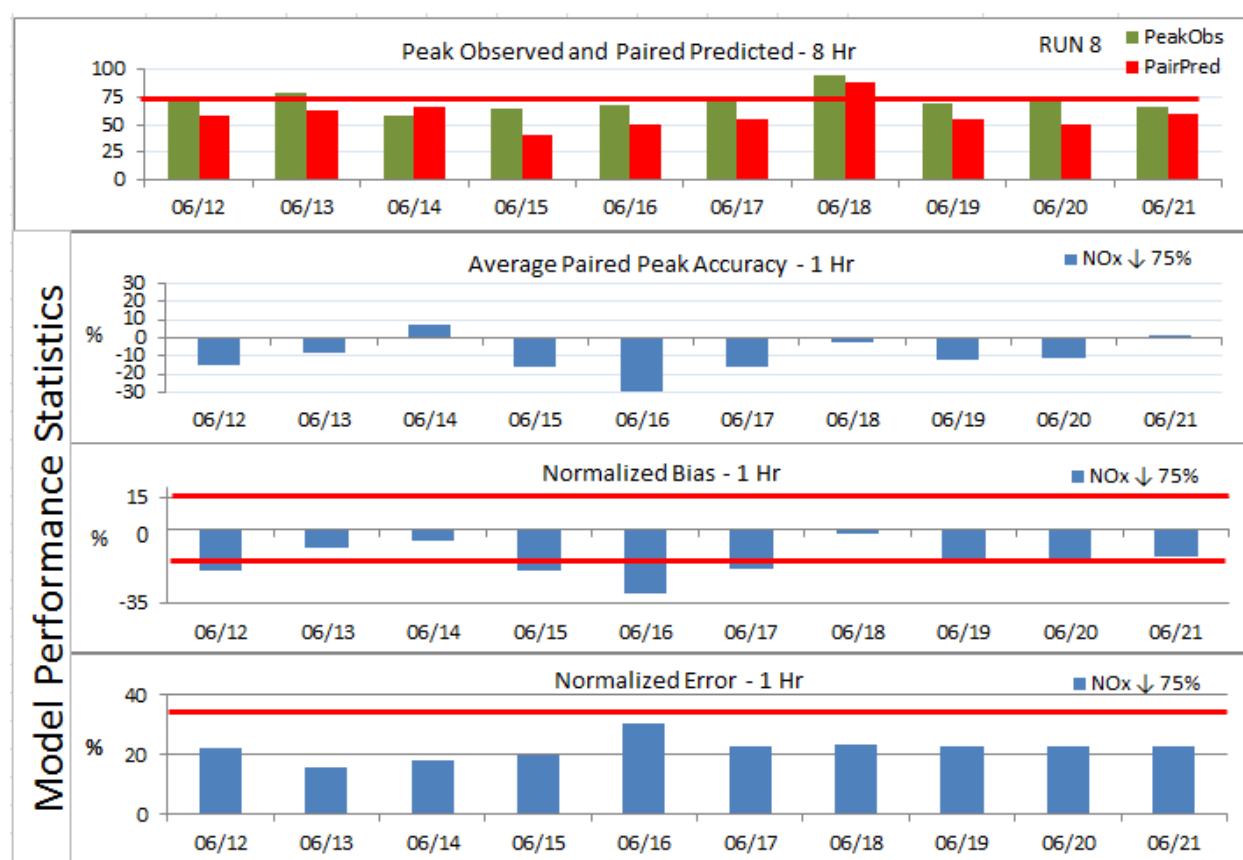


Figure 14.25 Model Performance Statistics – Run 8

The simulation passed NB on 3 of 10 days (6/13, 6/14, and 6/18). This simulation presented slightly improved NB (-1.8%) compared to BASELINE NB (-3.3%) on 6/18. The simulation also presented improved NE (23.3%) compared to BASELINE NE

(25.6%) for 1-hour ozone on 6/18. APPA indicates under-prediction accuracy of 1-hour ozone during 8 of the 10 simulation days.

Figure 14-26 presents diurnal PREDICTED and OBSERVED 1-hour ozone and H₂O₂:HNO₃ ratios for RUN 8. The PREDICTED PEAK on 6/18 for 1-hour ozone (102.3 ppb) was 1 ppb less than BASELINE (103.3 ppb). PAIRED PREDICTED PEAK (97.6 ppb) is slightly lower than BASELINE (99.3 ppb) yet much less than PEAK OBSERVED (120.7 ppb). The minimal difference in 1-hour ozone between BASELINE and NOx modifications in this simulation indicate VOC-limited conditions exist in the PdN region.

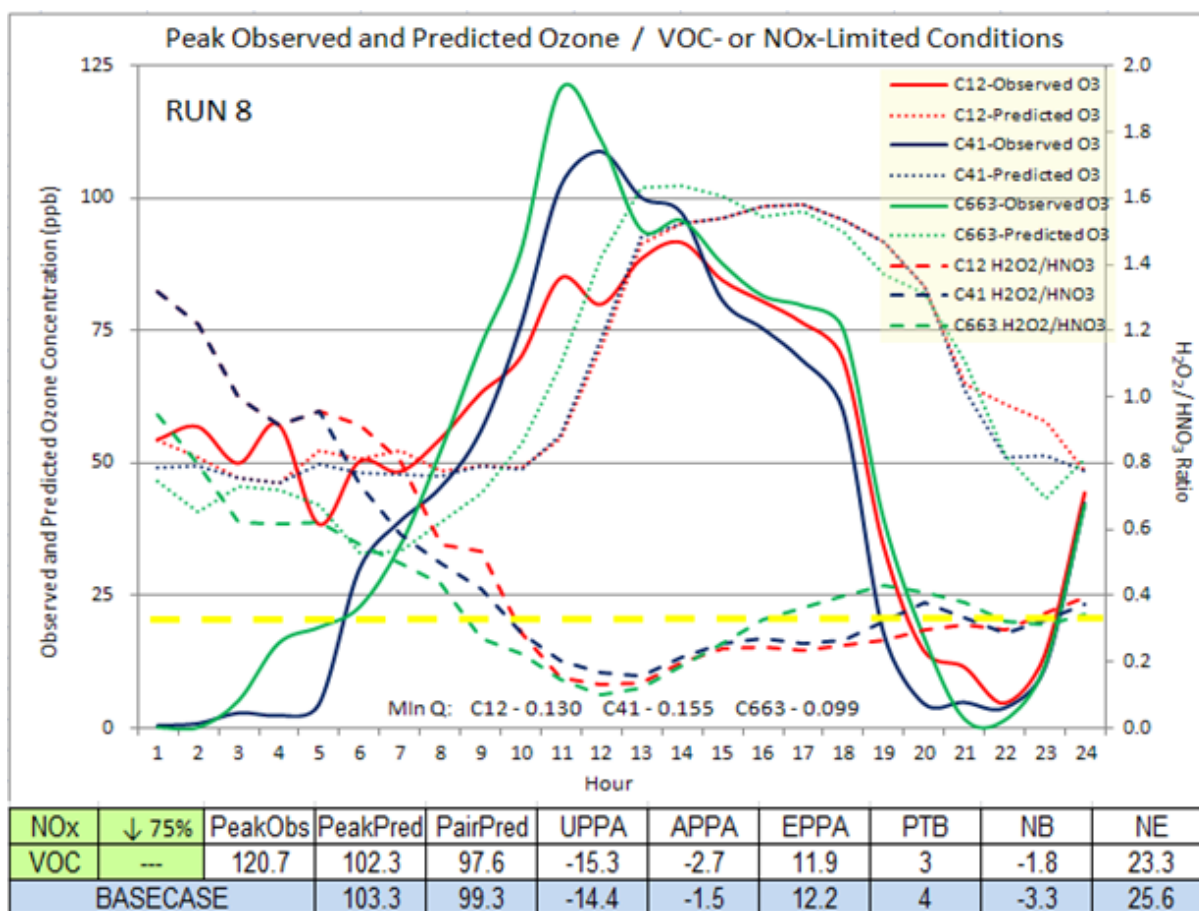


Figure 14.26 Diurnal Predicted and Observed 1-Hour Ozone (ppb) / H₂O₂:HNO₃ Ratios – RUN 8

Figure 14.27 illustrates diurnal PREDICTED and OBSERVED 8-hour ozone and $\text{H}_2\text{O}_2\text{:HNO}_3$ ratios for RUN 8. The 75% decrease in Juárez area source NO_x emissions slightly increased the PREDICTED PEAK 8-hour ozone to 93.28 ppb compared to BASELINE (93 ppb), which for all intents and purposes is an insignificant change in 8-hour ozone. PTB remained unchanged (3 hours) compared to BASELINE. NE (24.5%) slightly diminishes compared to BASELINE (23.7%). The model performed within acceptable NB and NE parameters for the 8-hour ozone simulation.

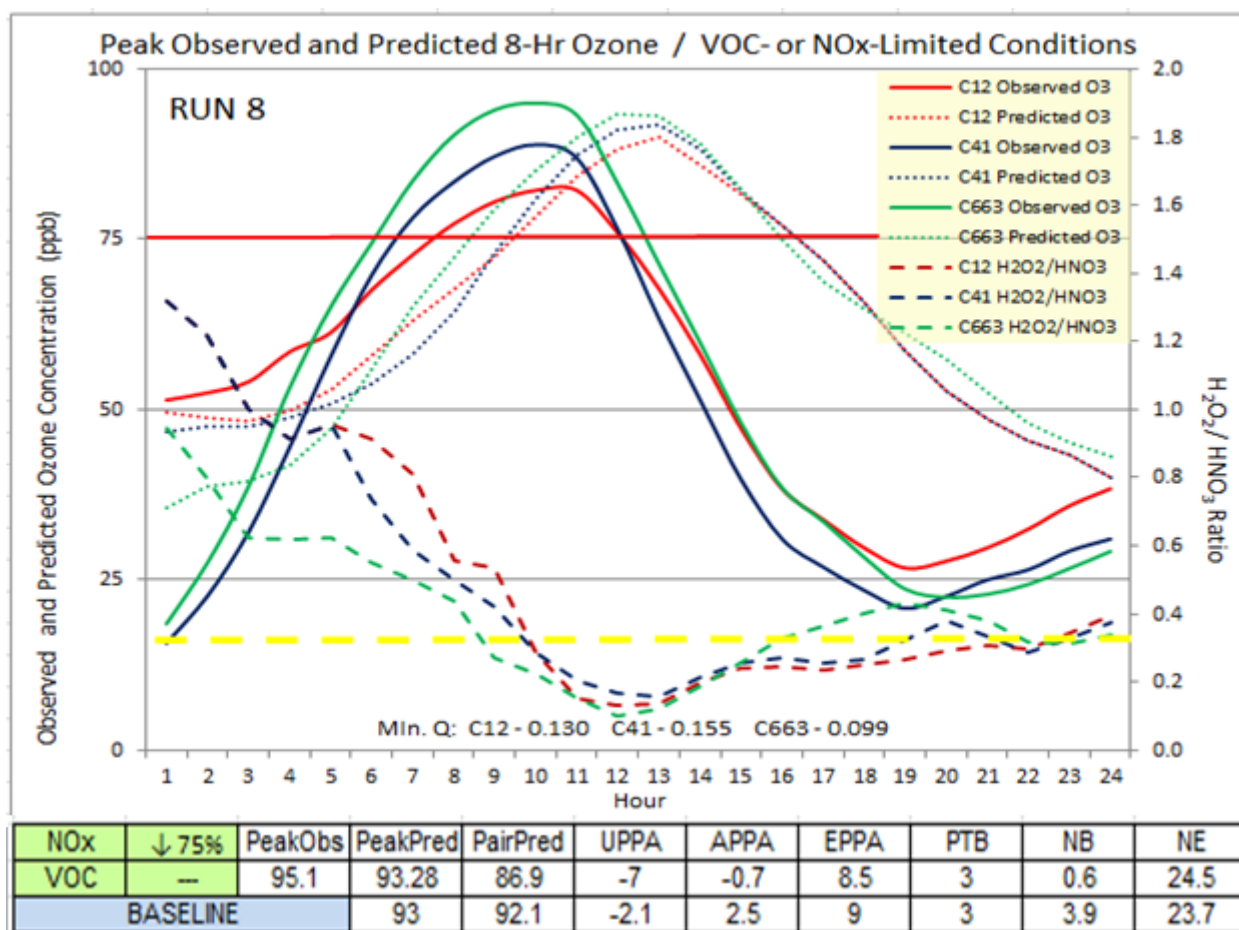


Figure 14.27 Diurnal Predicted and Observed 8-Hour Ozone (ppb) / $\text{H}_2\text{O}_2\text{:HNO}_3$ Ratios – RUN 8

$\text{H}_2\text{O}_2:\text{HNO}_3$ ratios indicate a NO_x -limited condition exists during the early morning hours and shifts to VOC-limited at 9 AM due potentially to sufficient NO_x which may titrate ambient ozone. The minimum Q observed (0.099) confirms a VOC-limited conditions control ozone formation during the period of peak ozone formation.

14.10 RUN 9 Model Performance Evaluation

RUN 9 involved a 75% increase in Juárez area source VOC emissions. Figure 14.28 presents performance statistics for RUN 9, 8-hour ozone PEAK OBSERVED, and co-located daily PAIRED PREDICTED PEAK among all sites in the PdN region.

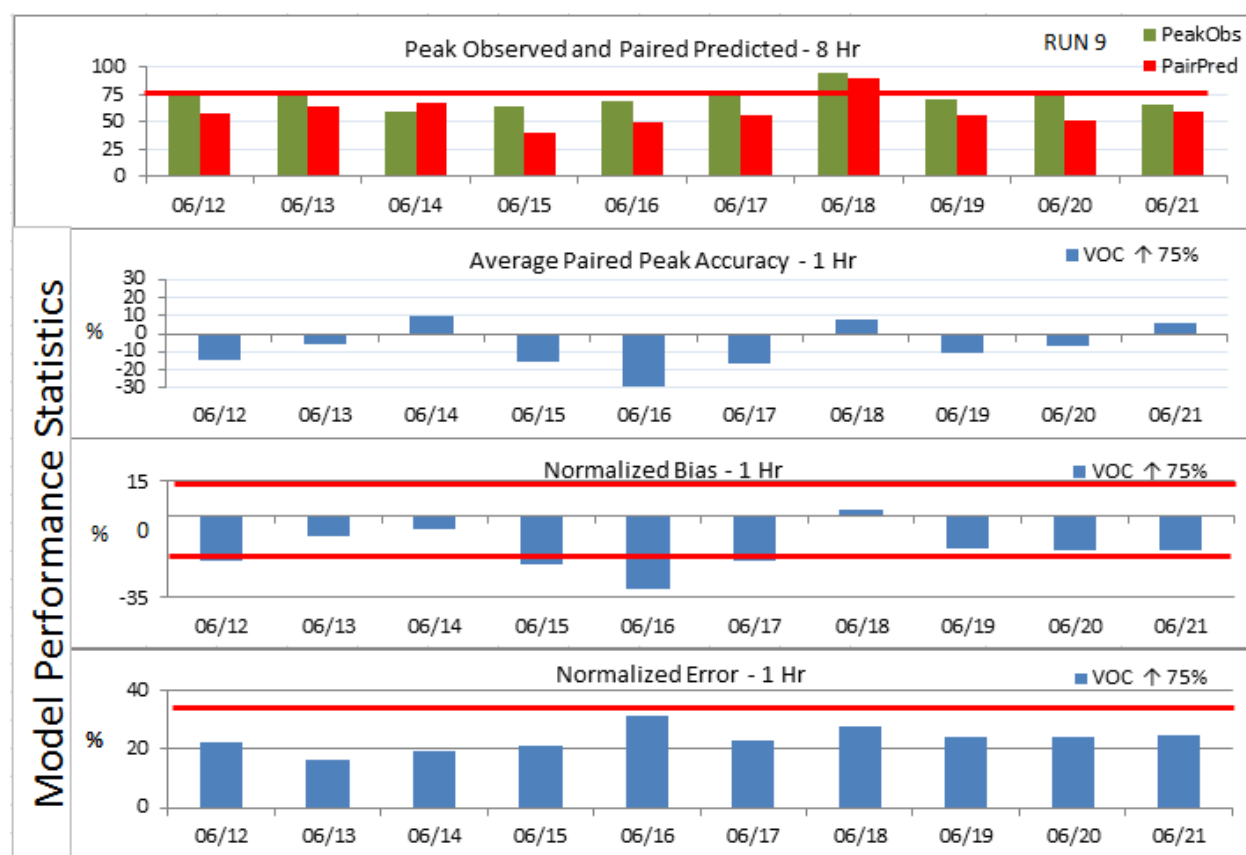


Figure 14.28 Model Performance Statistics – RUN 9

The simulation under-predicts 1-hour ozone on 9 of 10 simulation days given the negative NB on those days for which the under-prediction is indicated. The simulation passed NB on 6 of 10 days. This simulation slightly over-predicts NB (3.1%) compared to BASELINE NB (-3.3%) on 6/18. The simulation also presented slightly diminished NE

(27.8%) compared to BASELINE NE (25.6%) for 1-hour ozone on 6/18. APPA indicates negative 1-hour prediction accuracy during 7 of the 10 simulation days. APPA was positive on 6/14, 6/18, and 6/21. NE was within acceptable parameters during all 10 simulation days.

Figure 14.29 presents diurnal PREDICTED and OBSERVED 1-hour ozone and H₂O₂:HNO₃ ratios for RUN 9.

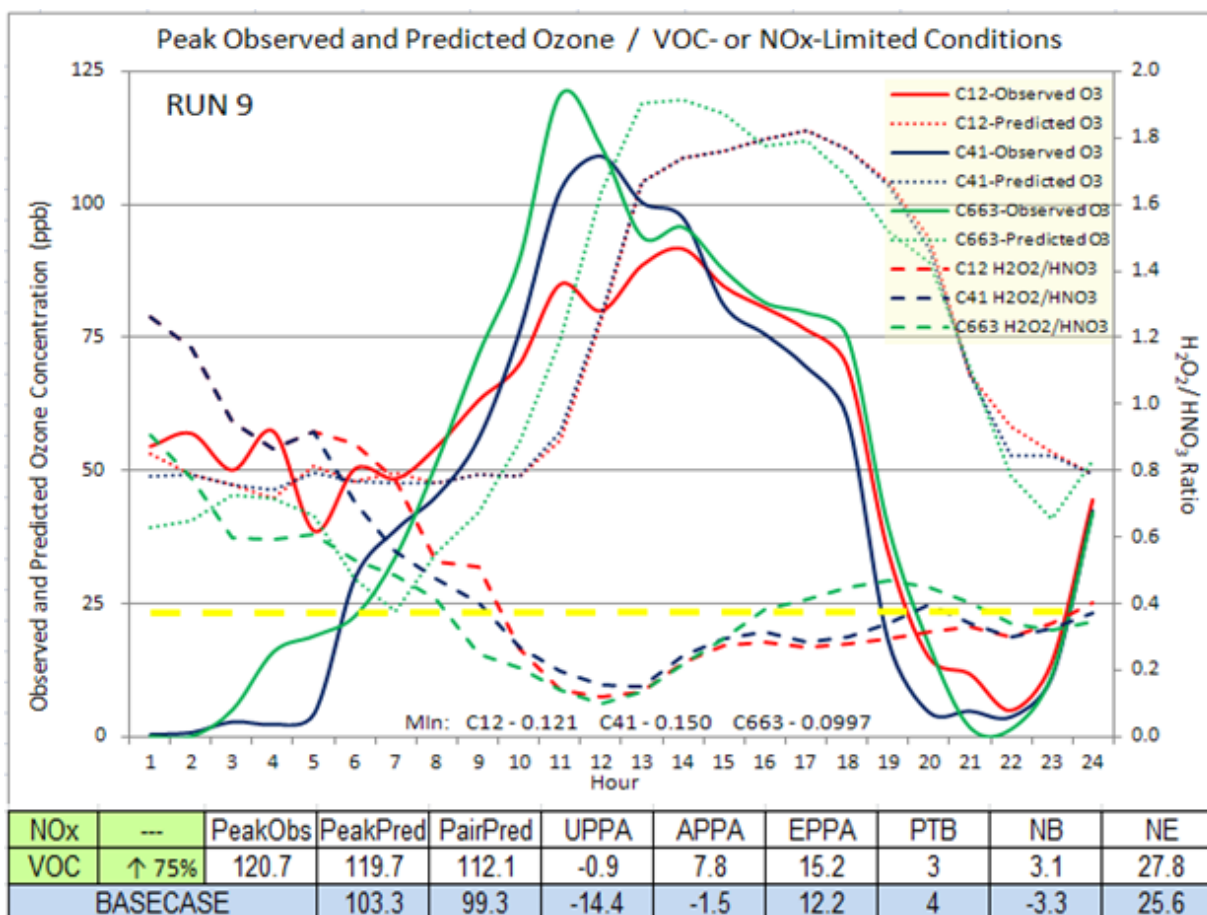


Figure 14.29 Diurnal Predicted and Observed 1-Hour Ozone (ppb) / H₂O₂:HNO₃ Ratios – RUN 9

1-hour PREDICTED PEAK on 6/18 (119.7 ppb) was ~16% greater than BASELINE (103.3 ppb) and only 1 ppb less than 1-hour PEAK OBSERVED ozone

(120.7 ppb) which occurred at C663. PAIRED PREDICTED PEAK (112.1 ppb) was ~13% greater than BASELINE (99.3 ppb). The elevated 1-hour ozone concentration indicates a strong response predicted by the model.

Figure 14.30 illustrates diurnal PREDICTED and OBSERVED 8-hour ozone and H₂O₂:HNO₃ ratios for RUN 8.

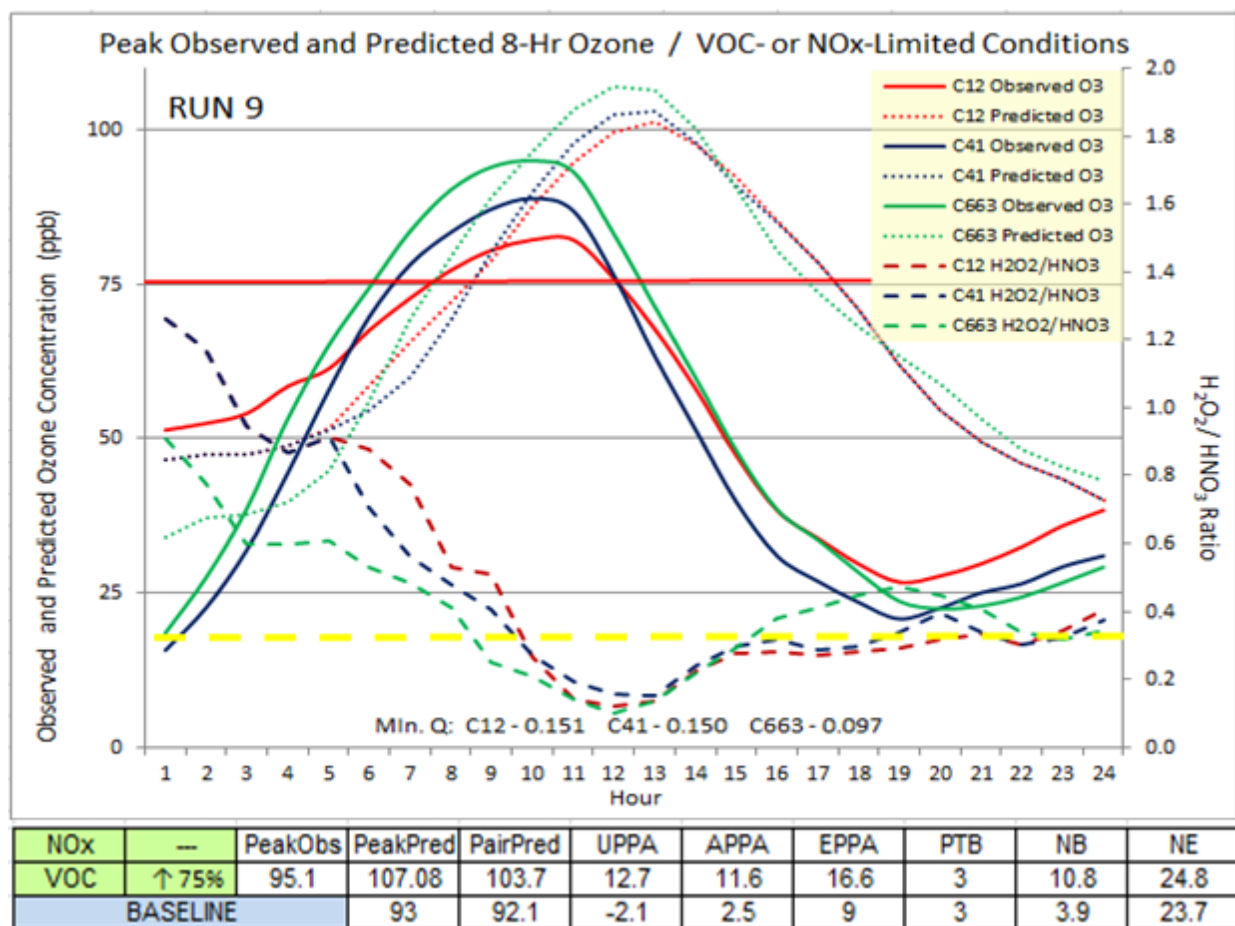


Figure 14.30 Diurnal Predicted and Observed 8-Hour Ozone (ppb) / H₂O₂:HNO₃ Ratios – RUN 9

The 75% increase in Juárez area source VOC emissions increased the 8-hour ozone PREDICTED PEAK to 107 ppb compared to BASELINE (93 ppb). This indicates

strong model response to increased VOC emissions. PTB (3 hours) remained unchanged compared to BASELINE. NE (24.8%) slightly diminishes compared to BASELINE (23.7%). The model performed within acceptable NB and NE parameters for the 8-hour ozone simulation.

$\text{H}_2\text{O}_2:\text{HNO}_3$ ratios indicate a NO_x -limited condition exists during the early morning hours and shifts to VOC-limited at 0800. The minimum Q observed (0.097) confirms VOC-limited conditions control ozone formation. This indicates the early morning VOC emissions quickly participated in ozone formation photochemistry.

Also, the simulation with a 75% increase in VOC emissions predicts ozone much closer to PEAK OBSERVED. This simulation may be considered a potential BASELINE if other parameters as yet undetermined can be modified to narrow the PTB and potentially allocate the 75% increase across a broader range of emissions sources.

14.11 RUN 10 Model Performance Evaluation

RUN 10 involved a 75% reduction on Juárez area source VOC emissions. Figure 14.31 presents performance statistics for RUN 10, 8-hour ozone PEAK OBSERVED, and co-located daily PAIRED PREDICTED PEAK among all sites in the PdN region.

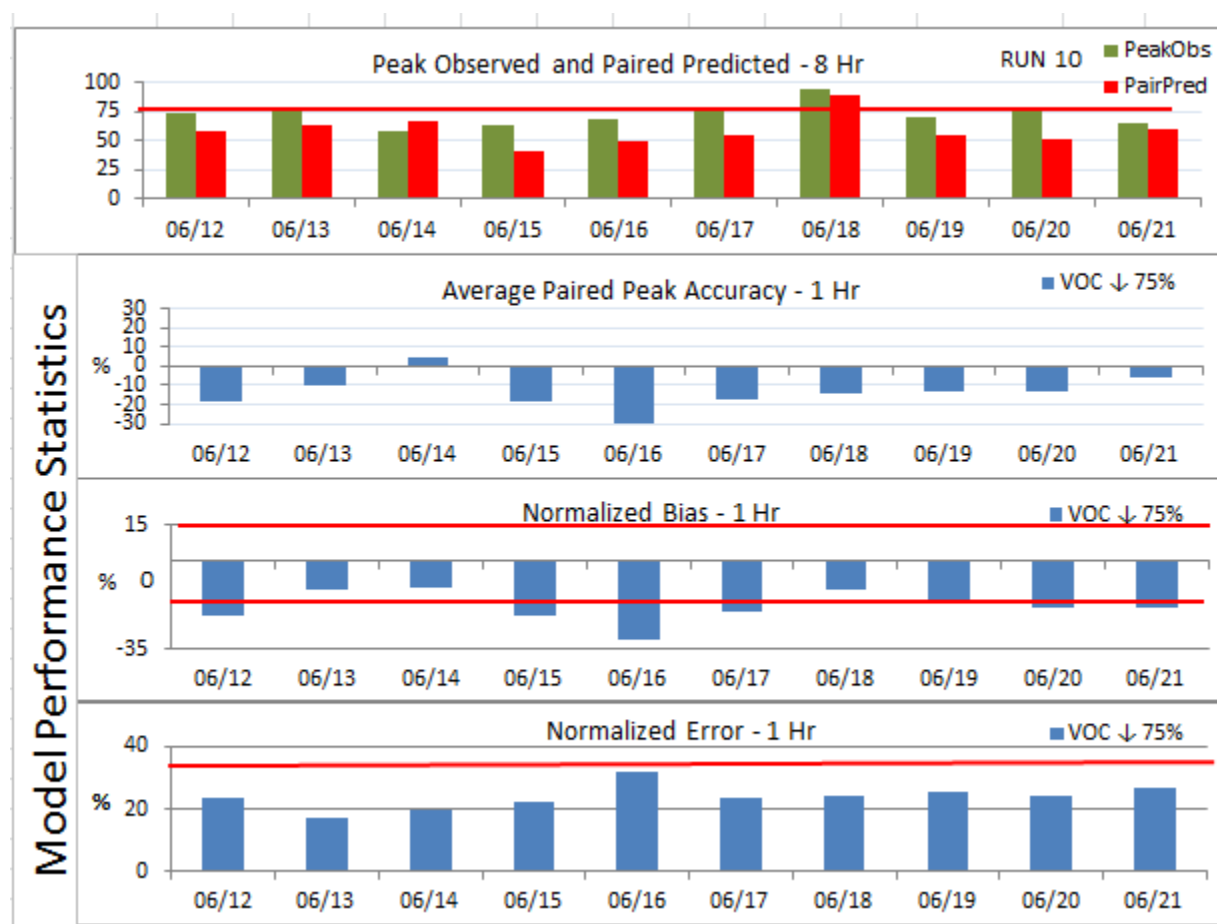
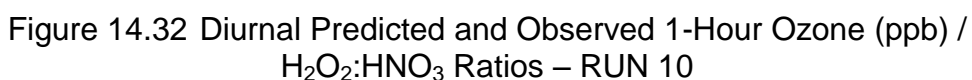


Figure 14.31 Model Performance Statistics - RUN 10

The simulation the simulation under-predicts 1-hour ozone on all 10 days given negative NB throughout the simulation period. NB was within acceptable parameters during 3 days (6/13, 6/14, and 6/18). This simulation predicts slightly diminished NB (-

Figure 14.32 presents diurnal predicted and observed 1-hour ozone and $\text{H}_2\text{O}_2:\text{HNO}_3$ ratios for RUN 10.



The PREDICTED PEAK on 6/18 for 1-hour ozone (86.6 ppb) was 16% less than BASELINE (103.3 ppb). PAIRED PREDICTED PEAK (80.1 ppb) is 33% less than PEAK OBSERVED (120.7 ppb). 1-hour PAIRED PREDICTED PEAK (80.1 ppb) is 19% less than BASELINE PAIRED PREDICTED PEAK (99.3 ppb). The model displays strong response to VOC as indicated by the substantial reduction in 1-hour and 8-hour ozone concentrations.

Figure 14.33 illustrates diurnal PREDICTED and OBSERVED 8-hour ozone and H₂O₂:HNO₃ ratios for RUN 10.

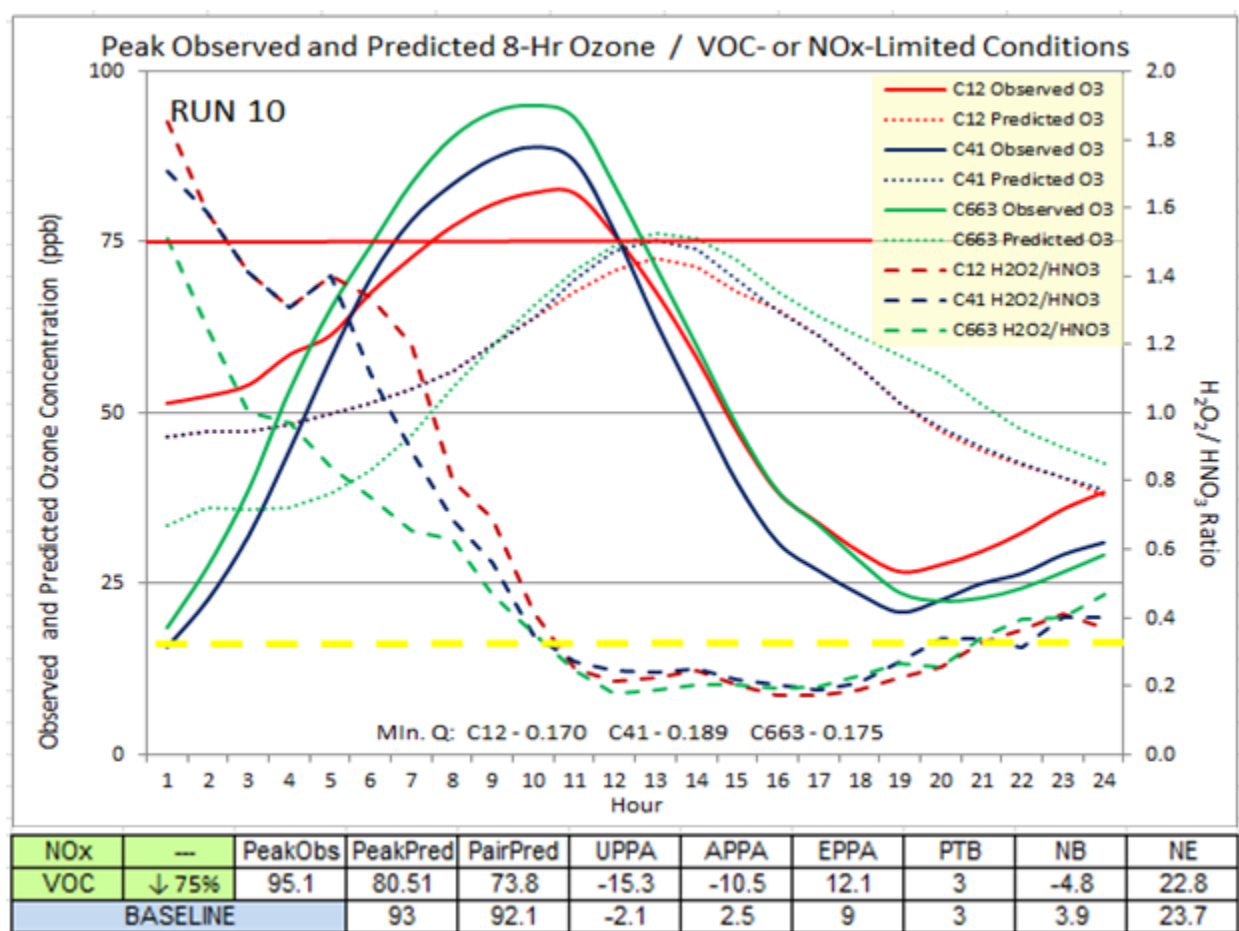


Figure 14.33 Diurnal Predicted and Observed 8-Hour Ozone (ppb) / H₂O₂:HNO₃ Ratios – RUN 10

The 75% decrease in Juárez area source VOC emissions strongly influenced predicted 8-hour ozone concentrations. PREDICTED PEAK 8-hour ozone (80.5 ppb) is 13% less than the BASELINE 8-hour ozone PREDICTED PEAK (93 ppb). PTB (3 hours) remained unchanged compared to BASELINE. NE (22.8%) slightly improves compared to BASELINE NE (23.7%).

The model performed within acceptable NB and NE parameters for the 8-hour ozone simulation. $\text{H}_2\text{O}_2:\text{HNO}_3$ ratios indicate a NO_x -limited condition exists during the early morning hours and shifts to VOC-limited at 10 AM. The reduction in VOC emissions potentially slowed the photochemical reaction delaying production of HNO_3 . The minimum Q observed (0.175) confirms a VOC-limited environment controls ozone formation.

14.12 RUN 11 Model Performance Evaluation

RUN 11 involved a 75% increase in Juárez area source NO_x and VOC emissions. Figure 10-34 presents performance statistics for RUN 11, PEAK OBSERVED 8-hour ozone, and co-located daily PAIRED PREDICTED PEAK ozone among all sites in the PdN region.

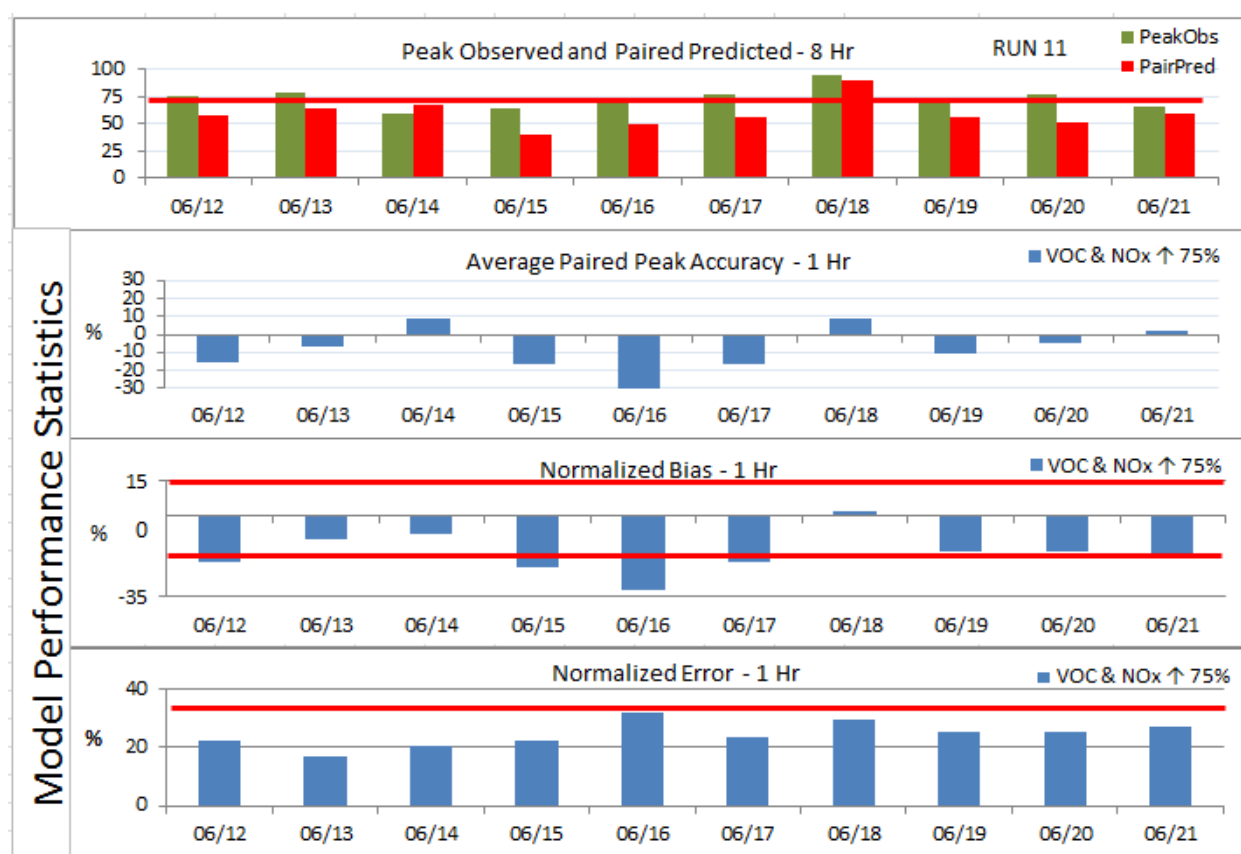


Figure 14.34 Model Performance Statistics - RUN 11

The simulation under-predicts 1-hour ozone on 9 of 10 days given negative NB the days indicated. The simulation was within acceptable parameters for NB on 3 of 10 days (6/13, 6/14, and 6/18). Positive APPA on 3 of 10 days indicates model over—

prediction accuracy for 1-hour ozone compared to co-located PAIRED PEAK ozone concentrations.

This simulation predicts improved NB (1.8%) compared to BASELINE NB (-3.3%) on 6/18 indicating a slight over-prediction bias during the exceedance day. Diminished 1-hour ozone NE (29.5%) was observed compared to BASELINE NE (25.6%) on 6/18. Both NB and NE operated within acceptable parameters.

Figure 14.35 presents diurnal PREDICTED and OBSERVED 1-hour ozone and H₂O₂:HNO₃ ratios for RUN 11.

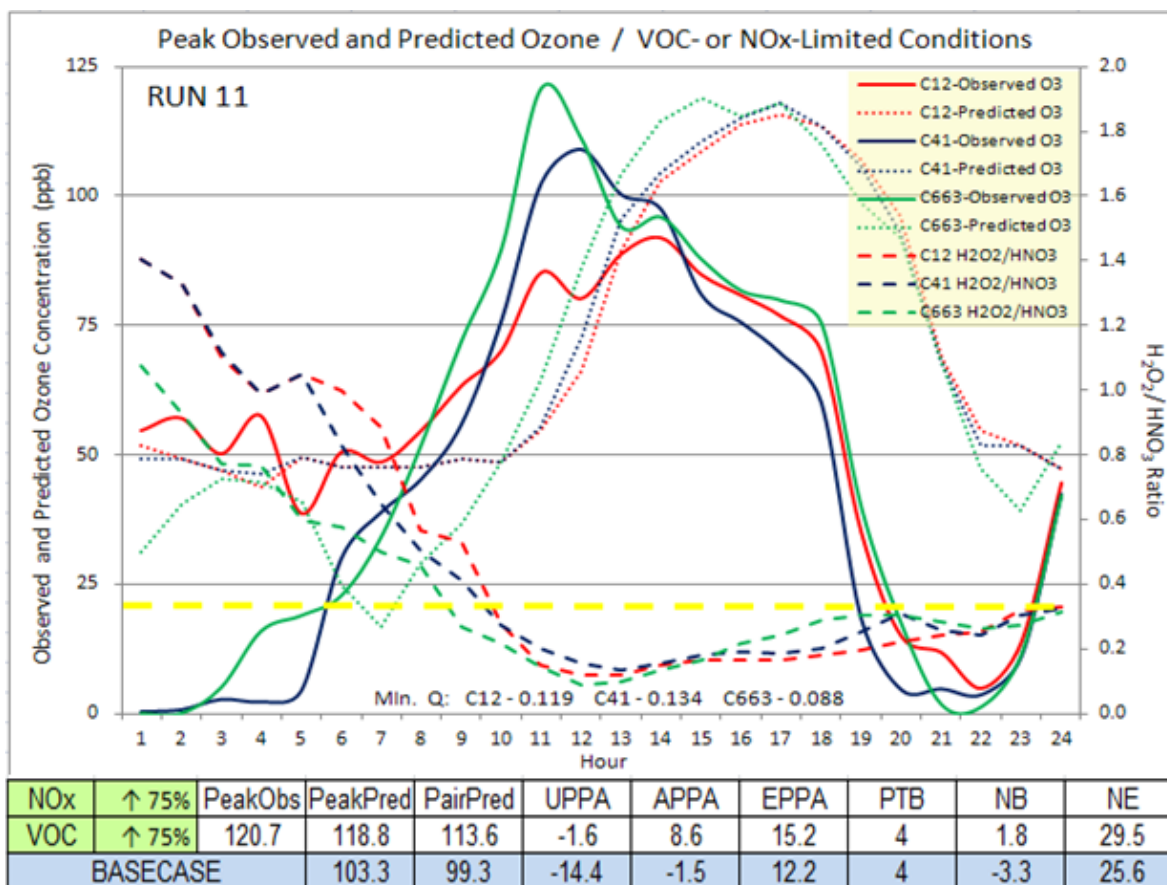


Figure 14.35 Diurnal Predicted and Observed 1-Hour Ozone (ppb) / H₂O₂:HNO₃ Ratios – Run 11

1-hour ozone PEAK PREDICTED (118.8 ppb) on 6/18 was ~14% greater than BASELINE PEAK PREDICTED (103.3 ppb). PAIRED PREDICTED PEAK (113.6 ppb) is 5% less than PEAK OBSERVED (120.7 ppb) and exceeds BASELINE (99.3 ppb) by 13%. The simulation produced a strong response to VOC emissions modifications and indicates VOC-limited conditions exist in the PdN region.

Figure 14.36 illustrates diurnal PREDICTED and OBSERVED 8-hour ozone and H₂O₂:HNO₃ ratios for RUN 11.

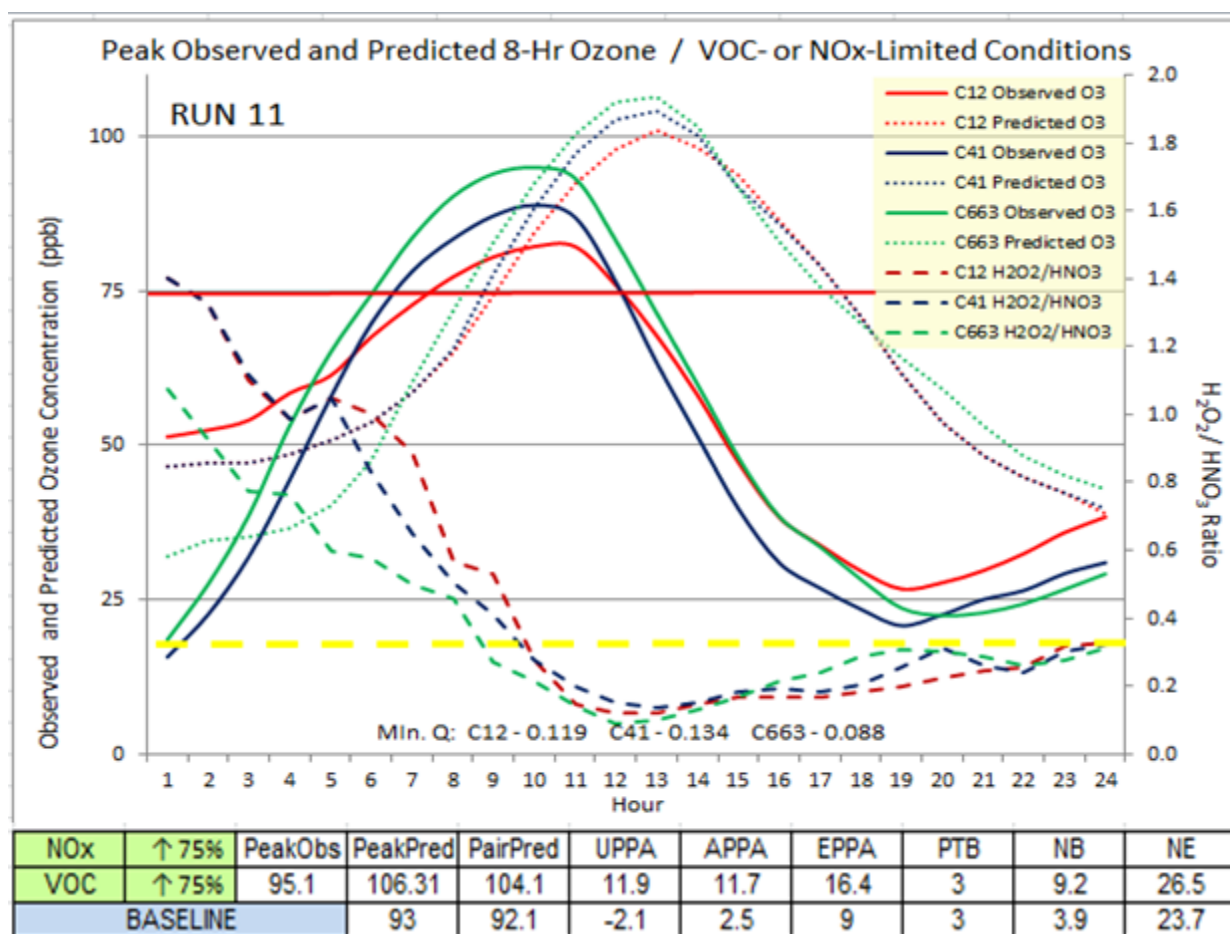


Figure 14.36 Diurnal Predicted and Observed 8-Hour Ozone (ppb) / H₂O₂:HNO₃ Ratios – Run 11

The 75% increase in Juárez area source VOC and NO_x emissions strongly influenced predicted 8-hour ozone concentrations. 8-hour ozone PREDICTED PEAK on 6/18 (106.3 ppb) is ~14% greater than BASELINE (93 ppb). PAIRED PREDICTED PEAK (104.1 ppb) exceeds PEAK OBSERVED at C663 (95.1 ppb) by ~9% and exceeds BASELINE (92.1 ppb) by 13%. PTB (3 hours) remained unchanged compared to BASELINE. NE (22.8%) slightly improved compared to BASELINE NE (23.7%).

H₂O₂:HNO₃ ratios indicate a NO_x-limited condition exists during the early morning hours and shifts to VOC-limited at 9 AM. Elevated VOC emissions potentially accelerate the photochemical reactions and promote early HNO₃ production. The minimum Q observed (0.088) confirming a VOC-limited conditions control ozone formation.

Given the modifications in emissions for this simulation involved both NO_x and VOC precursors and the difference in PEAK PREDICTED 1-hour and 8-hour ozone of only 1 ppb compared to RUN 9 with VOC-only emissions modifications, this simulation may also be considered a potential BASELINE RUN given the increased NO_x minimally impacted the predicted ozone results.

14.13 RUN 12 Model Performance Evaluation

RUN 12 involved a 75% reduction in Juárez area source NO_x and VOC emissions. Figure 14.37 presents performance statistics for RUN 12, 8-hour ozone PEAK OBSERVED, and co-located daily PAIRED PREDICTED PEAK among all sites in the PdN region.

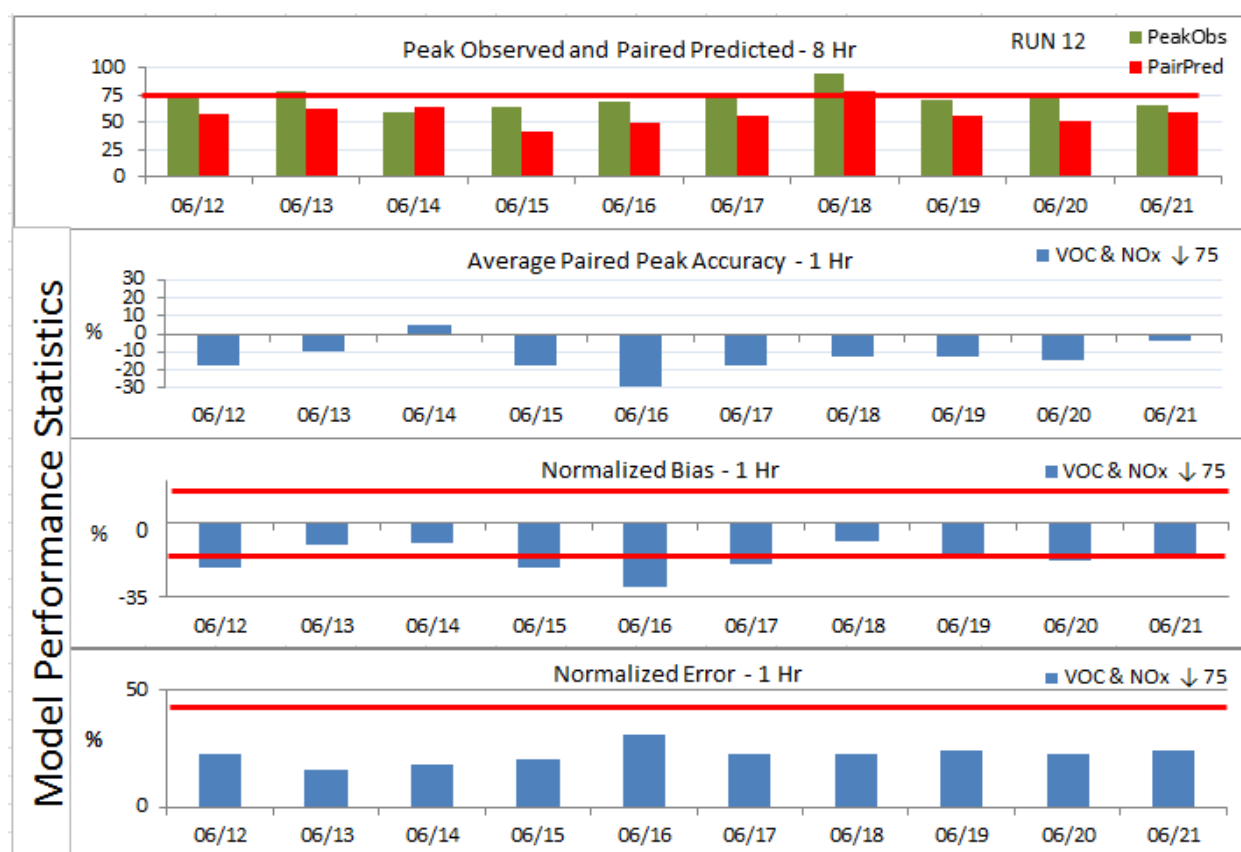


Figure 14.37 Model Performance Statistics – RUN 12

The simulation under-predicts 1-hour ozone on all 10 days as indicated by negative NB for all days in the simulation. 1-hour ozone was predicted within acceptable parameters for NB on 3 of 10 days (6/13, 6/14, and 6/18). This simulation predicts

slightly diminished NB (-8.7%) compared to BASELINE NB (-3.3%) on 6/18. Slightly improved NE (22.4%) was observed compared to BASELINE NE (25.6%) for 1-hour ozone on 6/18. NE is within allowable limits ($\leq 35\%$) for all 10 days in the simulation. APPA indicates under-prediction accuracy for 1-hour ozone during 9 of the 10 simulation days. Only 6/14 presented positive APPA.

Figure 14.38 presents diurnal PREDICTED and OBSERVED 1-hour ozone and $\text{H}_2\text{O}_2:\text{HNO}_3$ ratios for RUN 12.

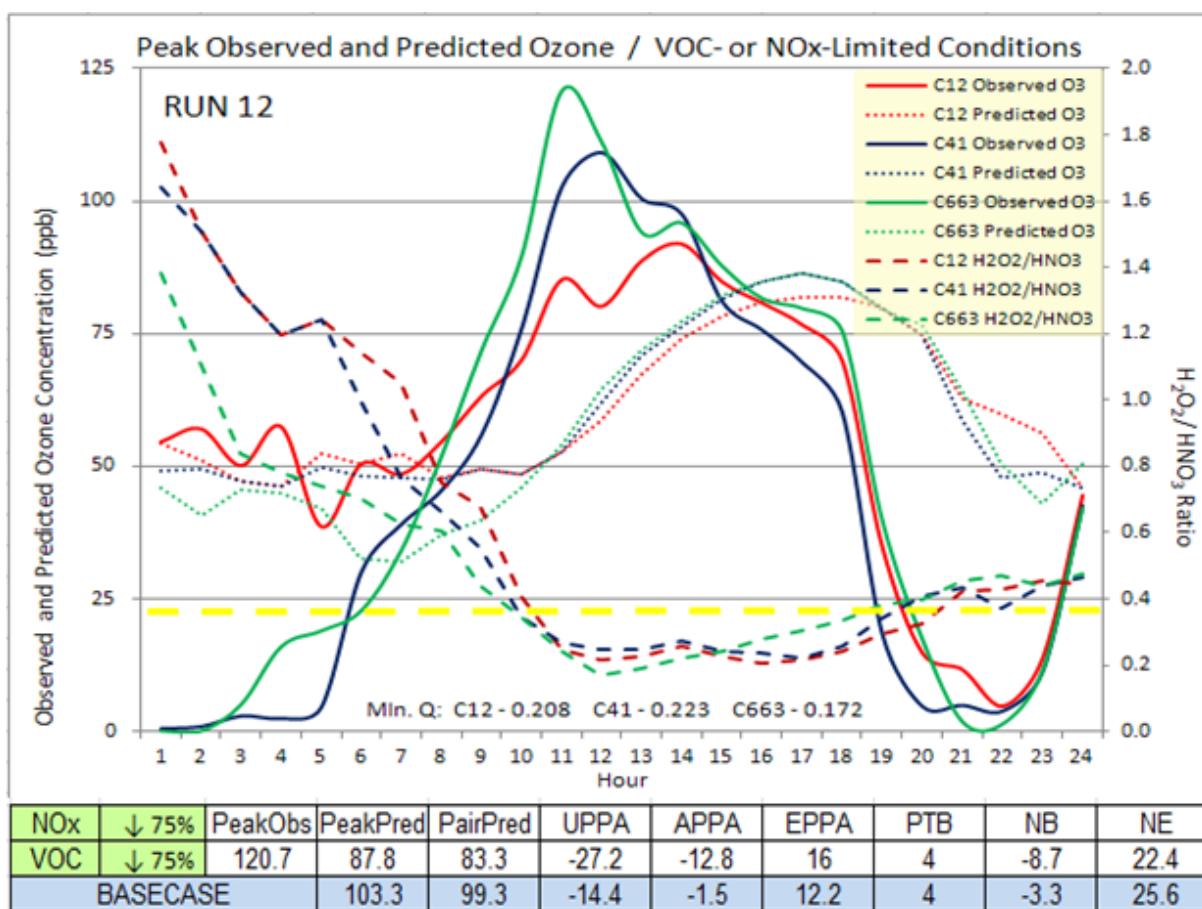


Figure 14.38 Diurnal Predicted and Observed 1-Hour Ozone (ppb) / $\text{H}_2\text{O}_2:\text{HNO}_3$ Ratios – Run 12

1-hour ozone PREDICTED PEAK on 6/18 (87.8 ppb) was 18% less than BASELINE PREDICTED PEAK (103.3 ppb). PAIRED PREDICTED PEAK (83.3 ppb) is 30% less than PEAK OBSERVED (120.7 ppb) and 16% less than the BASELINE PAIRED PREDICTED PEAK (99.3 ppb). The model displays strong response to VOC modifications and indicates VOC-limited conditions exist in the PdN region.

Figure 14.39 illustrates diurnal predicted and observed 8-hour ozone and H₂O₂:HNO₃ ratios for RUN 12.

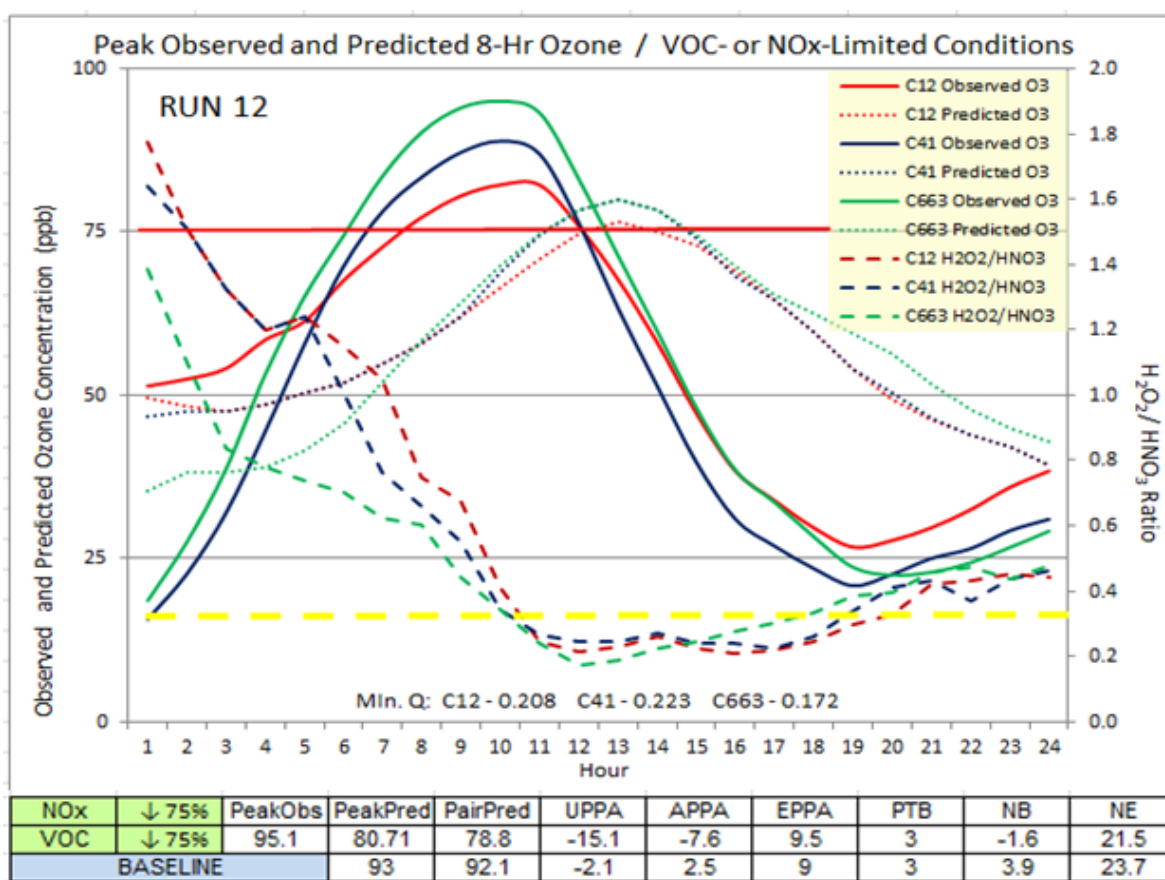


Figure 14.39 Diurnal Predicted and Observed 8-Hour Ozone (ppb) / H₂O₂:HNO₃ Ratios – Run 12

The 75% decrease in Juárez area source VOC and NO_x emissions strongly influenced predicted 8-hour ozone concentrations. PREDICTED PEAK 8-hour ozone on 6/18 (80.7 ppb) is ~13% less than 8-hour BASELINE PREDICTED PEAK (93 ppb). PAIRED PREDICTED PEAK (78.8 ppb) is 17% less than PEAK OBSERVED at C663 (95.1 ppb) and 13% less than BASELINE PAIRED PREDICTED PEAK (92.1 ppb). PTB (3 hours) remained unchanged compared to BASELINE. NE (21.5%) slightly improved compared to BASELINE NE (23.7%) for 8-hour ozone.

H₂O₂:HNO₃ ratios indicate a NO_x-limited condition exists during the early morning hours and shifts to VOC-limited conditions at 10 AM. Reduced VOC emissions may potentially slow the photochemical reactions and HNO₃ production. Such may have caused the H₂O₂:HNO₃ ratio to convert to VOC-limited conditions after 10 AM. The minimum Q observed is 0.172 confirming VOC-limited conditions control ozone formation.

14.14 Summary

CAMx simulations were conducted to evaluate model performance after modifications to VOC and NOx emissions. 12 modified emissions scenarios were developed representing an increase or decrease of either 50% or 75% of VOC and / or NOx emissions. All the simulations functioned within acceptable limits for NE and NB on 6/18 which was the date of an ozone event in the PdN region. NB was exceeded (failed) on several days of the modeling simulation on all scenarios including the BASELINE.

The point source modeled EI appears to support substantial improvement given the minimal NOx emissions reported in the source dataset. Notwithstanding the limitations in NOx emissions, emissions increases of this pollutant generate little change in 1-hour or 8-hour ozone.

15 Time-Series Plots

Time-series (TS) plots of OBERVED and PREDICTED 1-hour ozone are illustrated in this section. TS plots were prepared for the 3 CAMS discussed in the previous section: C12, C41, and C663. Of note are several days of missing observed 1-hour ozone data at both C41 and C663. The date is read mm/dd/y. June 12, 2006 is the 1st value in the x-axis. As indicated earlier in this report, the simulation initiates at 0600 Local Standard Time on June 12.

TS plots for 5 simulations (BASELINE, RUNs 9, 10, 11, and 12) are discussed in this section. The 5 simulations were selected for the following reasons:

- The BASELINE RUN provides initial data to observe model performance during the 10-day simulation. One views how well or poorly the PREDICTED and OBSERVED 1-hour ozone concentrations track each other;
- RUNs 9 and 10 increased and decreased only VOC emissions by 75%;
- RUNs 11 and 12 increase and decrease both VOC and NO_x emissions by 75%; and
- These RUNs represented the greatest fluctuations in PREDICTED ozone concentrations on 6/18 and provide an initial screen to evaluate the performance of the photochemical modeling system.

15.1 Time-Series and Pairwise Scatterplots - BASELINE

Figure 15.1 illustrates the TS plot for the BASELINE simulations for C12, C41, and C663. Missing data for 6/15 – 6/18 is noticeable. Any flagged data is labeled -999 and skipped from statistical analysis. The -999 value is deleted to not add artifact data into the time-series plot.

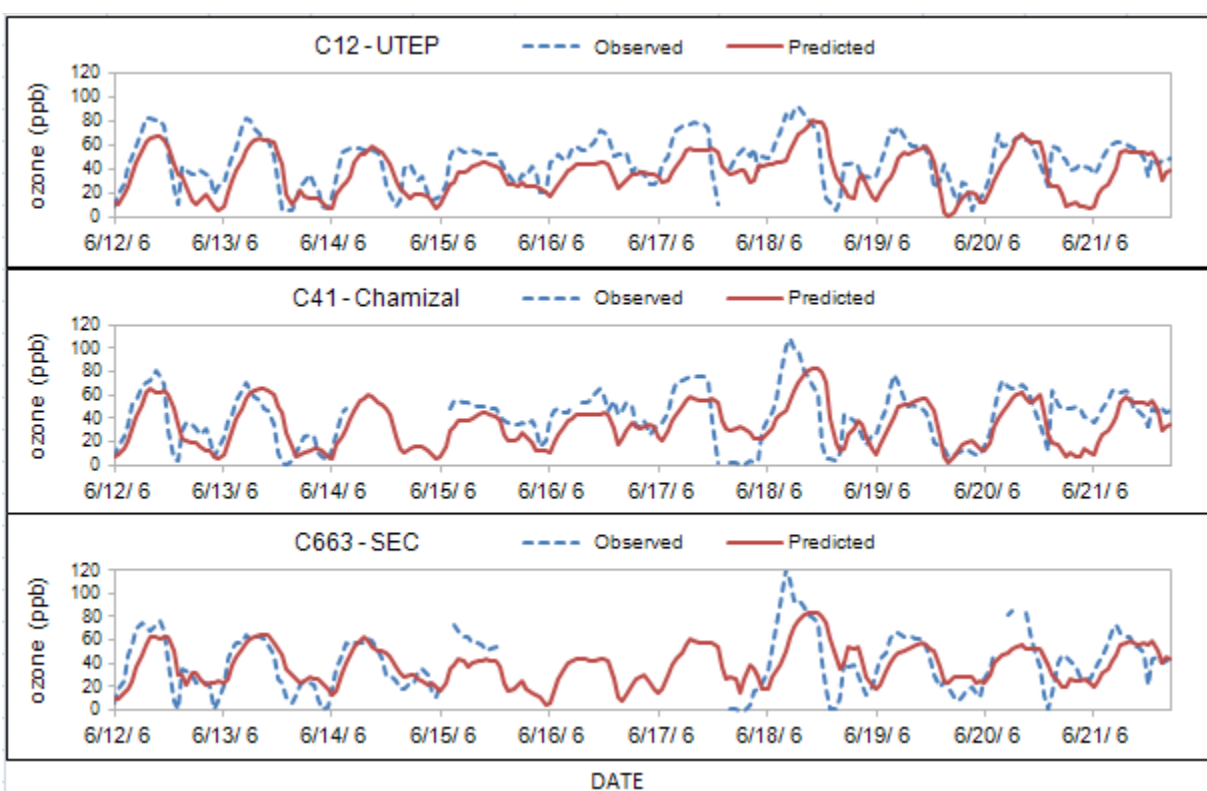


Figure 15.1 Time-Series Plots for BASELINE Simulation

Figure 15.2 depicts a pairwise scatterplot for the BASELINE simulation. The scatterplots represent the 10 day simulation period at 3 CAMS in the PdN region. A moderate correlation ($R^2 = 0.4138$, 0.3408 , and 0.3749 for C12, C41, and C663 respectively) exists between the paired data.

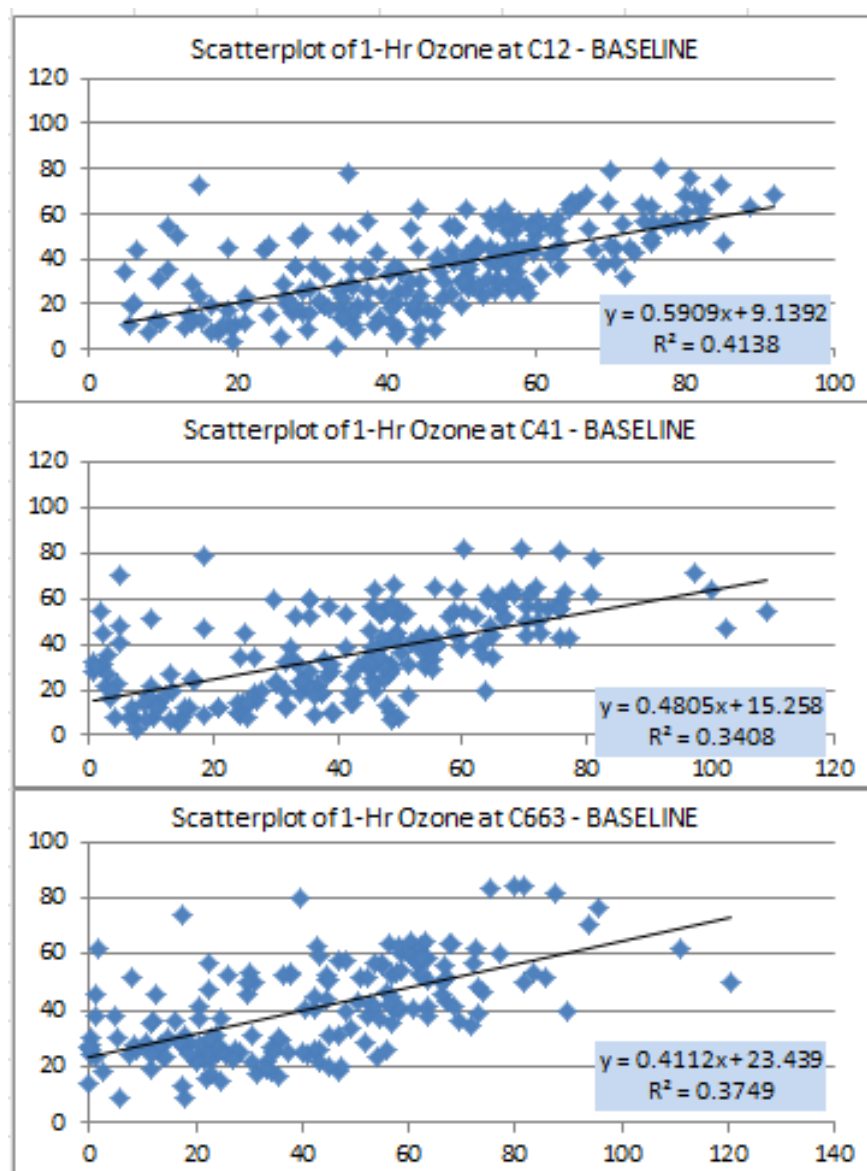


Figure 15.2 Pairwise Scatterplots - BASELINE Simulation

15.2 Time-Series and Pairwise Scatterplots - RUN 9

Figure 15.3 illustrates the TS plot for RUN 9 which increased VOC emissions by 75%. This simulation produced significantly higher 1-hour ozone on 6/18. It appears from comparing RUN 9 TS plots to BASELINE that the most visible increase in 1-hour ozone occurred on 6/18. On this simulation the VOC emissions were sufficient to generate results which more closely matched the OBSERVED ozone concentrations. One may assume the BASELINE model underestimated actual VOC emissions.

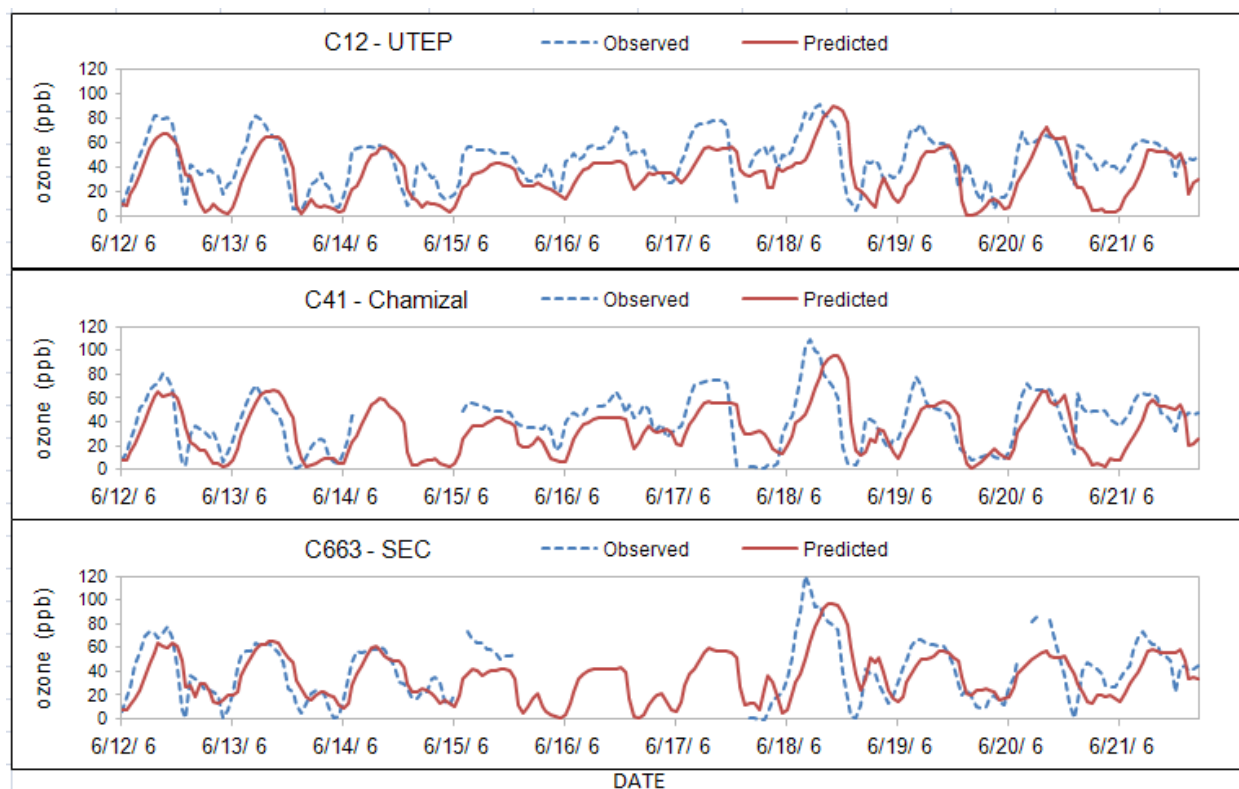


Figure 15.3 Time-Series Plots - RUN 9

Figure 15.4 depicts pairwise scatterplots for RUN 9 for C12, C41, and C663. The correlation coefficient ($R^2 = 0.4327, 0.3393, \text{ and } 0.4048$ for C12, C41, and C663

respectively) improves slightly compared to the BASELINE R^2 . This may be due to a change in Peak Time Bias on RUN 9 which improved to 3 hours from 4 hours. The 4-hour lag in the BASELINE peak compared to the 3-hour lag in the RUN 9 peak moves the data up one hour providing closer tracking of the data.

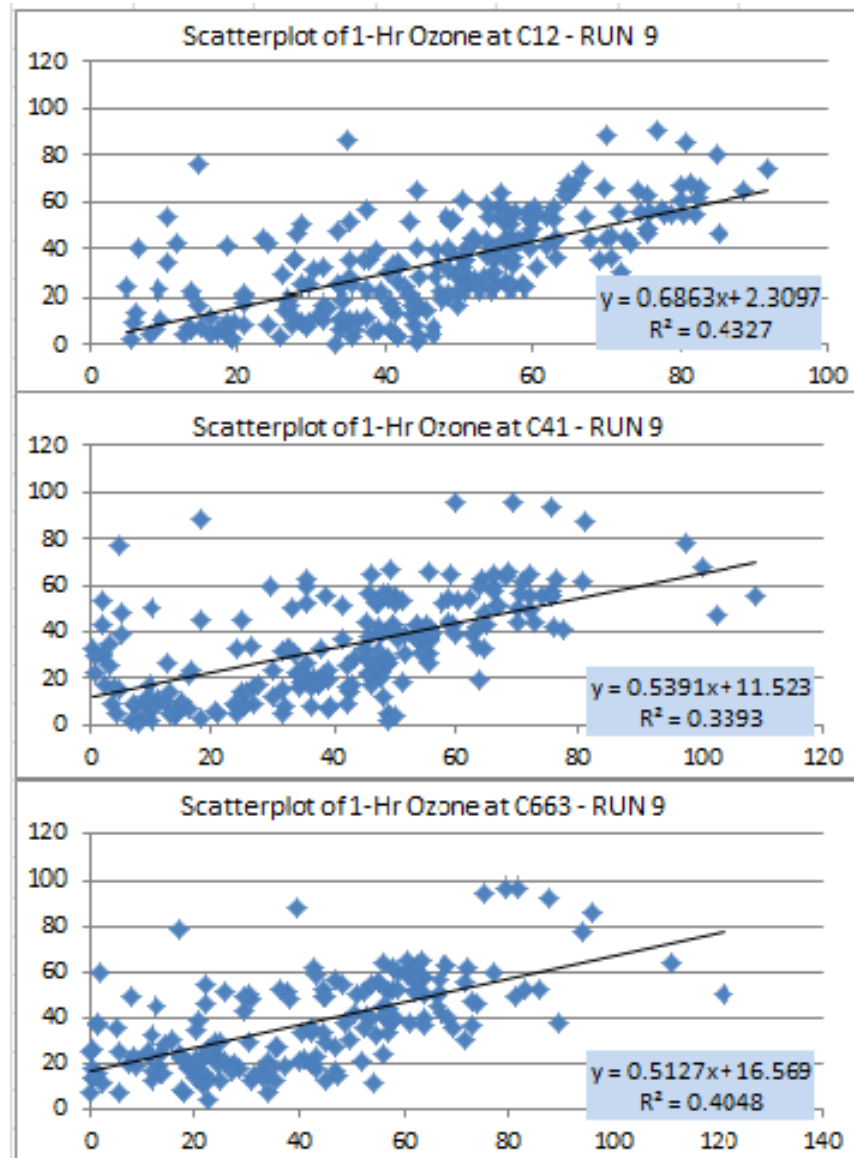


Figure 15.4 Pairwise Scatterplots - RUN 9

15.3 Time-Series and Pairwise Scatterplots – RUN 10

Figure 15.5 illustrates the TS plot for RUN 10 which reduced VOC emissions by 75%. A significant reduction in 1-hour ozone is observed on 6/18 compared to BASELINE. The reduction in ozone concentration is due to reduced emissions entering the modeling domain thus lowering the amount of VOCs available to participate in the photochemical reaction.

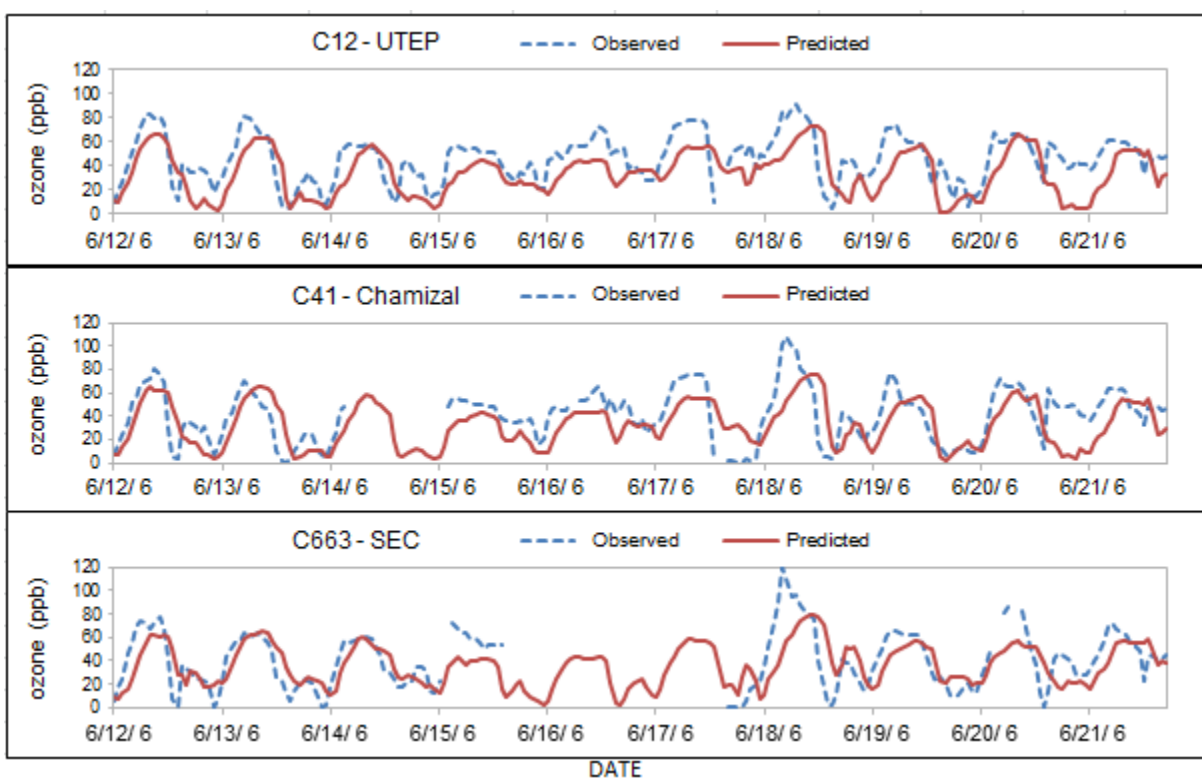


Figure 15.5 Time-Series Plot - RUN 10

Figure 15.6 depicts pairwise scatter plots for RUN 10. The scatterplots represent the 10 day simulation period at the 3 CAMS in the PdN region. The correlation coefficient ($R^2 = 0.43, 0.3425, \text{ and } 0.3832$ for C12, C41, and C663 respectively) does

not differ significantly compared to the BASELINE R^2 . This may be due to the unchanged PTB which essentially maintains the 4-hour PTB between the Peak Time observed by both simulations.

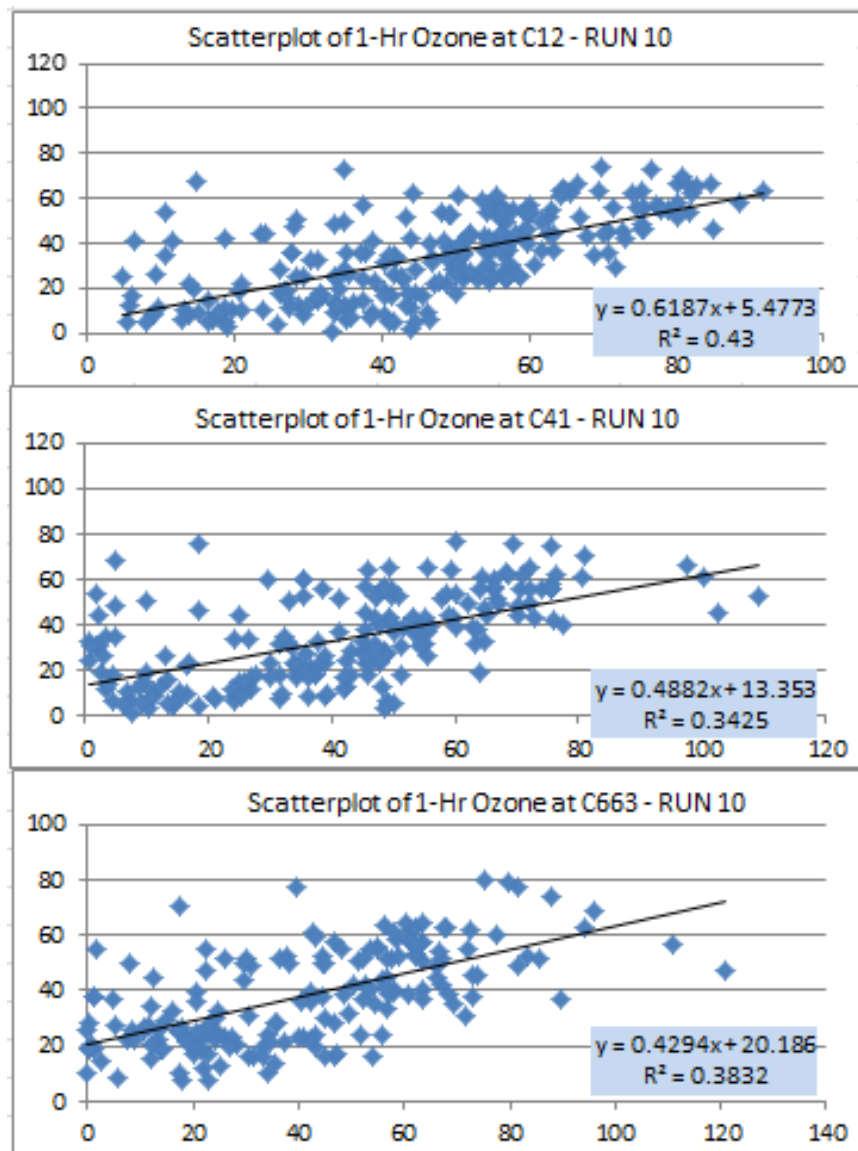


Figure 15.6 Pairwise Scatterplots - RUN 10

15.4 Time-Series and Pairwise Scatterplots – RUN 11

Figure 15.7 illustrates the TS plot for RUN 11 which increased both NO_x and VOC emissions by 75%. The obvious distinction between this TS plot and BASELINE is the elevated 1-hour concentrations on 6/18 at C12 and C663. This simulation appears to over-predict 1-hour ozone concentrations at C12 on 6/18. The over-prediction is potentially due to additional VOC and NO_x emissions entering the modeled domain. This is also a simulation where additional NO_x emissions did not necessarily reduce 1-hour ozone concentrations on the day of the 8-hour ozone event.

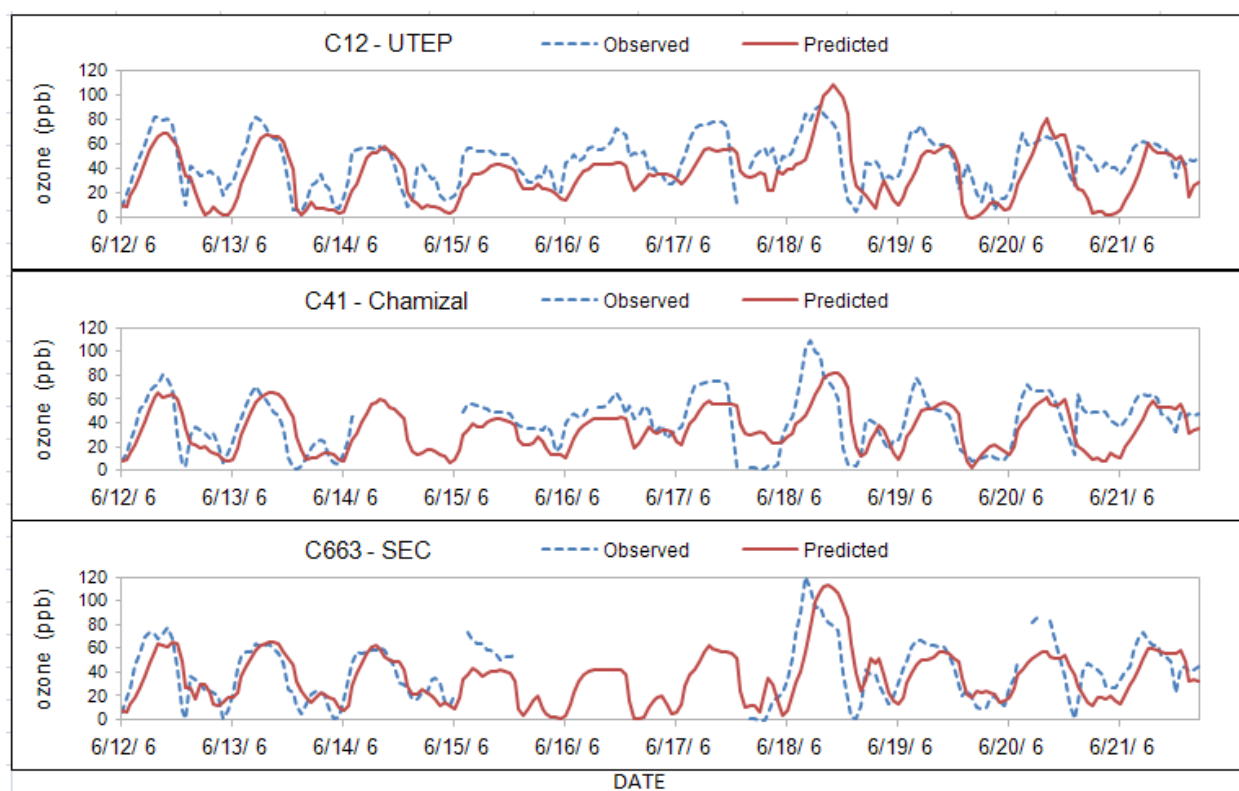


Figure 15.7 Time-Series Plots - RUN 11

Figure 15.8 depicts pairwise scatterplots for RUN 11 representing the 10 day simulation period at 3 CAMS in the PdN region. The correlation coefficients ($R^2 = 0.4297$, 0.336 , and 0.4209 for C12, C41, and C663 respectively) present a slight improvement compared to the BASELINE R^2 . The significant (11%) improvement is indicated for C663 ($R^2 = 0.4209$ vs $R^2 = 0.3749$ for BASELINE). While the PTB remains unchanged the 2 sets of data more closely track each other as PREDICTED closely tracks OBSERVED data.

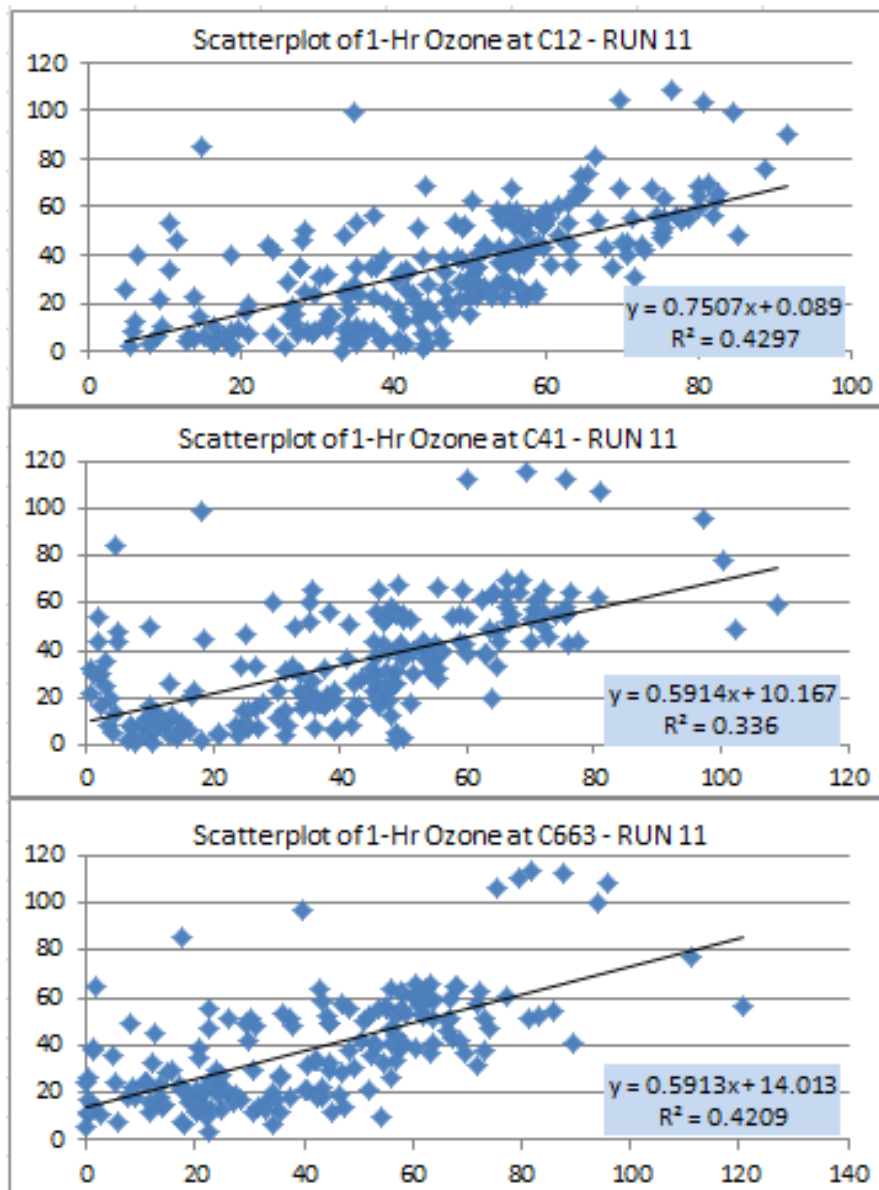


Figure 15.8 Pairwise Scatterplots - RUN 11

15.5 Time-Series and Pairwise Scatterplots – RUN 12

Figure 15.9 illustrates the TS plot for RUN 12 which decreased both NO_x and VOC emissions by 75%. The 4-hour lag in Peak Time is similar to BASELINE on 6/18 for the 3 CAMS. The 1-hour reduction in ozone is also noticeable compared to BASELINE.

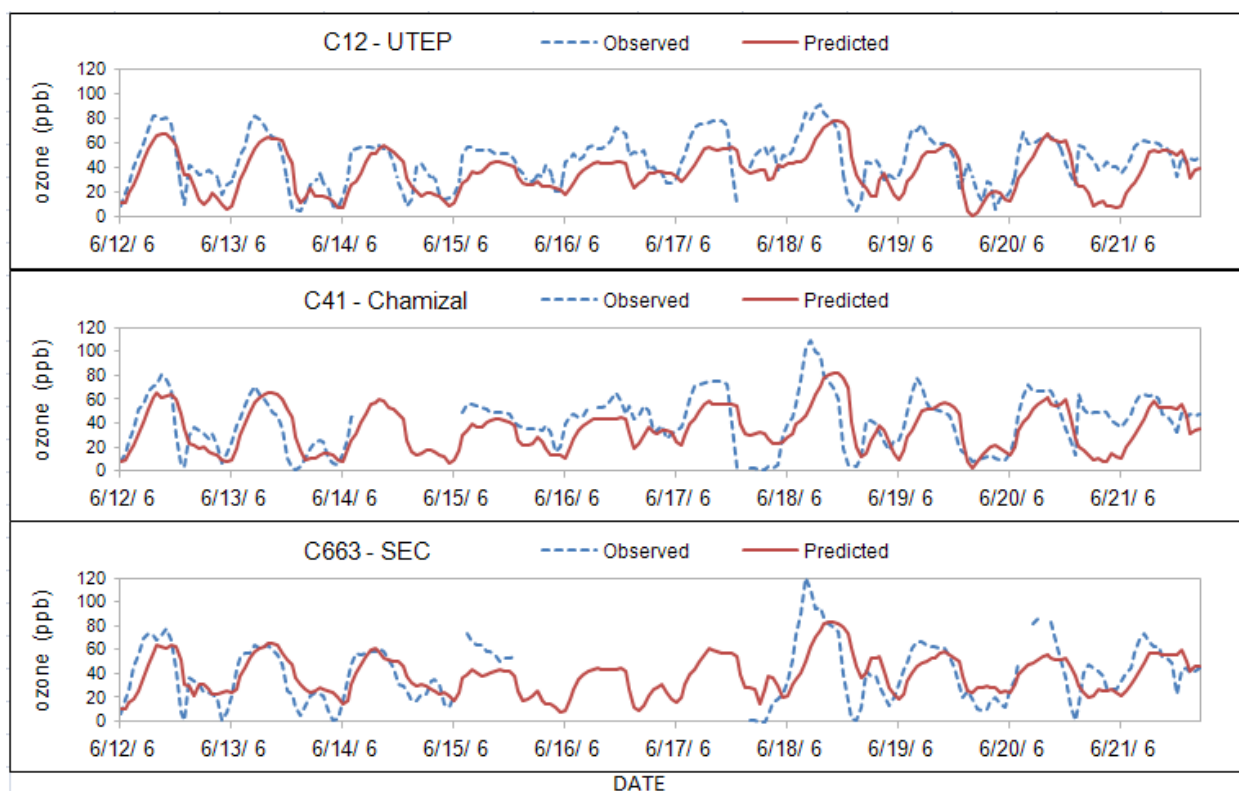


Figure 15.9 Time-Series Plots - RUN 12

Figure 15.9 depicts pairwise scatterplots for RUN 12 representing the 10 day simulation period at 3 CAMS in the PdN region. The correlation coefficients ($R^2 = 0.4182$, 0.3426 , and 0.376 for C12, C41, and C663 respectively) do not indicate a significant improvement nor are diminished compared to the BASELINE R^2 . PTB between RUN 12 and BASELINE are unchanged.

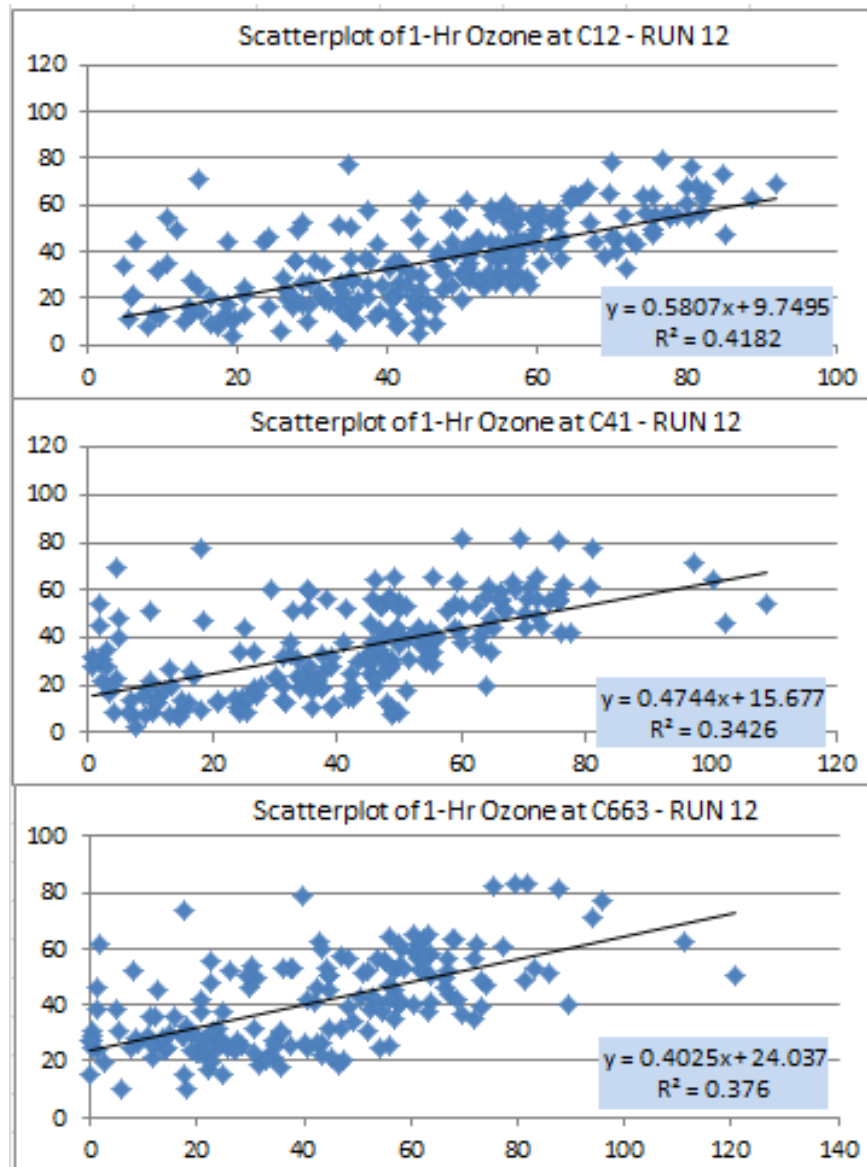


Figure 15.10 Pairwise Scatterplots - RUN 12

16 Discussion

Air quality in the PdN region continues improving year over year. As a result, El Paso currently attains the 75 ppb ozone NAAQS. However, elevated ozone may cause El Paso to be designated nonattainment of the 8-hour ozone NAAQS should a more stringent standard be enacted. Since most emissions on the US side of the US-Mexico border are extensively controlled through compliance with State Implementation Plans (SIPs), it is possible that emission reductions may be achieved across the border in Cd. Juárez.

Photochemical modeling is conducted in order to assess whether potential air quality control strategies (PAQCS) are effective at reducing ozone to a specified target prior to implementing a SIP. This was part of the process undertaken when the 15% VOC reduction SIPs were implemented by EPA and enforced by the States with areas in nonattainment of the NAAQS.

16.1 Purpose of the Dissertation

This dissertation evaluated the sensitivity of CAMx by focusing on area source VOC and NO_x emissions generated in Cd. Juárez. The CAMx photochemical model was applied to conduct sensitivity analysis on 12 distinct simulations where VOC and / or NO_x emissions were increased or decreased by either 50% or 75% for each modeling simulation. It is possible that the sensitivity analysis may be applied for development of PAQCS based on results generated during the simulation. However, further modeling simulations should be conducted focusing on specific source categories, meteorology, and emissions inventories.

Meteorology and emissions are potentially the most important parameters which establish the foundation of photochemical modeling simulations. An accurate meteorological platform is the initial step in building better photochemical modeling scenarios. Accurate EIs are also an overarching goal given this data is fundamental to recommending effective PAQCS. ENVIRON (2011) reports that the model may generate output which is within acceptable limits for bias and error, yet such output may be erroneous. Therefore quality assurance procedures should be developed to build confidence in both the meteorology and emissions integrated into the simulation.

Simulations conducted for this dissertation indicated much more effort should be applied to improving the EI. Merely achieving acceptable parameters of NE and NB is insufficient when better model performance was achieved by increasing VOC emissions.

16.2 Meteorological Inputs

UTEP's air quality team prepared a WRF meteorological platform. The TCEQ also developed a WRF platform as part of the Rider 8 photochemical modeling campaign conducted in nonattainment and near nonattainment regions across the State of Texas. Both WRF modeling domains were assessed to observe and compare parameters integrated into the respective meteorological models. Comparisons of distinct WRF platforms offered 2 opportunities to model the mesoscale and regional meteorology and apply it to photochemical modeling simulations. The importance of this is that at the time the meteorological inputs are as precise as possible, the same

meteorological platform is applied for all future photochemical modeling simulations including basecase and future case scenarios.

Assessment of the meteorological models indicated that the UTEP WRF domain had slightly improved photochemical modeling results by producing lower bias and error compared to the TCEQ domain (ENVIRON, 2012). An important consideration regarding the 2 WRF domains is the TCEQ modeling domain establishes the centerline in central Texas while the UTEP WRF domain establishes the PdN region as the center of the modeling domain.

Early concerns in preparing the WRF domain for the photochemical modeling simulation addressed the location of the PdN region in relation to the larger 12 km and 36 km modeling domains. The TCEQ domain established the PdN domain near the western boundary of the 12 km domain which could impact model boundary conditions.

The CAMx simulation applied during this evaluation of the photochemical model was run for a 4 km grid using meteorological data from UTEP's application of WRF. Boundary conditions for the 4 km grid were extracted from CAMx runs on the 36/12 km grid in a manner referred to as 1-way nesting. This was necessary to most appropriately accommodate the potentially different meteorology and different vertical grid structures between the 4 km (UTEP) and 12 km (TCEQ) meteorological data.

16.3 Emissions Inventories and Recommended Improvements

Accurate EIs are all-important factors in photochemical modeling and recommending potential air quality control strategies. The intent of developing PAQCS is to recommend emissions reductions that are not only meaningful, but also effective at

achieving the intended result of reducing ozone concentrations. Recommendations with inaccurate data will likely lead to ineffective PAQCS which may fail to achieve their objective.

Previous photochemical modeling studies undertaken for the PdN region report inaccuracy in the EI. The modeled EI data prepared for this dissertation is based on minor inaccuracies in the Juárez EI and missing data which at this time are not reported in any EI. It should be noted that the EI developed for regulatory air quality planning purposes and the modeling EI are both provided by TCEQ. ENVIRON, in turn, applied the TCEQ apportioned EI modeling data to run the BASELINE simulation. It should also be noted that the AFS point source EI file for Mexico was prepared for EPA by a Eastern Research Group which worked within data access constraints and the laws of Mexico to obtain the point source EI data applied for this research. It should also be noted that the author recently obtained a 2008 point source EI for Juárez with over 200 data records (facilities) which will be utilized to improve the current point source AFS dataset in a timely manner.

NO_x and VOC emissions modeled by CAMx were compiled in tons per day (TPD). 542 TPD of VOC and 154 TPD of NO_x comprise the BASELINE modeled EI for the 2 pollutants. Of note in the datasets are the low point source NO_x and VOC emissions from Juárez.

An additional dataset not included in this dissertation are emissions from the international ports of entry located along the mid-line of the PdN community. 4 POEs at the US-Mexico border contribute mobile source emissions consisting of NO_x and VOCs among other motor vehicle emissions. Including mobile source emissions from the

POEs in the simulations would likely contribute to an improved EI for the PdN region and may have improved the sensitivity results for the modeling simulations.

As indicated by RUNs 9 and 11, the increase of 75% of VOC in RUN 9 or 75% of both NO_x and VOC in RUN 11 produced output closely associated with observed ozone. However, if a majority of POE emissions are NO_x, then the potential exists to minimally impact ozone concentrations. Excess NO_x may also reduce predicted as well as observed ambient ozone concentrations. It is possible that reducing current bridge wait times or vehicle traffic on the POEs may increase ozone since the simulations indicated that increasing NO_x tends to reduce ozone and decreasing NO_x tends to increase ozone.

Area source emissions inventories are updated on 3-year cycles. Occasionally a revised emissions factor, modified activity data, or questionnaire response may cause specific source category emissions to dramatically increase or decrease. Notwithstanding any dramatic increase or decrease in emissions the photochemical model output does not significantly change predicted ozone levels if the emissions from a specific source category account for a very low percentage of total modeled emissions.

However, EIs which significantly lack accurate or complete information will extensively impact model simulation results. The AIRS Facility Subsystem (AFS) point source EI lists a very small number of Juárez point sources. For example, the modeled point source emissions inventory for Juárez indicates <0.9 TPD of NO_x and <8 TPD of VOC point source emissions. The primary VOC source is a PEMEX gasoline terminal in south Juárez. The Juárez point source EI does not consider 3 electric generating

facilities and almost 200 maquiladora facilities most of which do not control VOC emissions due to Mexico's lack of regulations regarding the control of this pollutant. El Paso point source data appears accurate.

16.3.1 VOC Emissions

The modeled EI consists of 542 TPD of total VOC emissions. Area sources comprise 242.5 TPD (45%) of regional VOC emissions. The remaining VOC emissions are allocated among the various point, onroad and nonroad mobile sources.

Cd. Juárez area sources contribute 132.4 TPD (47.5%) of modeled VOC emissions. The modeled Juárez EI indicates point source VOC emissions of 7.8 TPD (2.8%) where the PEMEX terminal is the primary contributor. Onroad and nonroad mobile sources contribute VOC emissions of ~23.9 TPD (8.6%).

The 2008 area source EI reported in Section 10 indicates VOC emissions of 28,433 TPY. This equates to ~77 TPD if the year is divided into 365 days and 108 TPD if weekend emissions are cut completely. Notwithstanding, the modeled simulation includes slightly reduced Weekend emissions therefore there is a discrepancy in reported vs. modeled emissions.

US jurisdictions contribute 252 TPD of VOC emissions in the BASELINE Weekday simulation. Area source VOC emissions in El Paso account for ~110 TPD (43.6%). Mobile sources account for 24.6 TPD (~9.7%), and point sources contribute ~4 TPD (1.5%) of VOC emissions on the US side. The latter value is consistent with the point source EI reported for El Paso. However, the area source modeled VOC EI is inconsistent with the EI data reported in Section 10. In 2005, the TCEQ reports ~23 TPD of area source VOC emission for El Paso while the model indicates 110 TPD of

area source emissions. The difference between the modeled and the air quality planning area source EI is approximately 5-fold.

Biogenics comprise 226.9 TPD (42%) of regional VOC emissions. The Model of Emissions of Gases and Aerosols from Nature (MEGAN) was applied to estimate this variable. PdN biogenic VOC emissions consist primarily of monoterpenes which have minimal participation in ozone formation photochemistry. Biogenics were split between the 2 jurisdictions for the purposes of allocating emissions across both jurisdictions (US and Mexico), but CAMx allocated the emissions as a single source classification across the 4 km modeling domain. Considering the very low reactivity of biogenic emissions, one may stipulate that area sources comprise almost 90% of all VOC emissions if just the VOC emissions from anthropogenic sources were considered in the simulation.

16.3.2 NO_x Emissions

The daily modeled NO_x EI (154 TPD) for the BASELINE modeling simulation consists of 23.4 TPD (15.2%) for area sources. Mobile sources constitute 125.8 TPD (~82%) and point sources account for 1.9 TPD (1.2%) of regional NO_x emissions. Biogenic NO_x is generated by soil nitrification which occurs below the soil surface and is emitted into the atmosphere.

ENVIRON (2012) reports 43.7 TPD for Weekday point source NO_x emissions. However, reviewing the BASELINE MRGUAM file, only 1.9 TPD of NO_x is reported as point source emissions for the entire PdN region as just indicated. This is likely inaccurate for a community of 2.6 million inhabitants, with several electric generation facilities, a refinery, a variety of major point sources, and several hundred maquiladora twin-plant manufacturing facilities generating emissions on a daily basis. The

discrepancy, while unexplained, is cause for concern when developing modeling scenarios for the purpose of recommending PAQCS. However, for purposes of this dissertation, the discrepancy was less of a priority given the sensitivity of the model to emissions modifications was examined based on the existing BASELINE modeled EI established by a contractor for a TCEQ-funded project.

The daily modeled CAMx BASELINE simulation indicates Juárez produces 61 TPD of total NO_x emissions. The Weekday modeled NO_x EI applied to the BASELINE simulation indicates area sources account for 20.1 TPD (33%), onroad and nonroad mobile sources account for 38.7 TPD (63%), point sources comprise 0.9 TPD (1.4%), and biogenics account for 1.4 TPD (2.3%).

EI Paso BASELINE NO_x emissions for a Weekday simulation indicate 85 TPD allocated as follows: area sources 3.3 TPD (3.8%), onroad and nonroad mobile sources 79.3 TPD (93.2%), point sources 0.94 TPD (1.1%) and biogenics 1.4 TPD (1.6%).

The EI developed for EI Paso by TCEQ for regulatory air quality planning purposes suggests a different perspective in the NO_x EI. As indicated in Section 10, 2008 point source NO_x emissions 4,687 TPY (12.8 TPD if allocated evenly throughout the year) exceed the modeled daily EI by almost 11 TPD. If applying 2005 point source NO_x, 3,397 TPY (9.3 TPD if allocated evenly throughout the year) the difference is 8.3 TPD when compared to the modeled EI.

16.3.3 Emissions Inventory Summary

It must be reiterated that the simulated BASELINE EI for both jurisdictions likely underreports both VOC and NO_x emissions therefore it is recommended that the

modeled EI be reevaluated and prepared to represent emissions more in line with actual emissions reported in the regulatory EI.

The AIRS Facility Subsystem (AFS) dataset was missing substantial emissions data from Mexico-based point sources. A limited number of data records are listed in the AFS file where each record represents specific pollutant emissions. A dataset which contains point source emissions for Juárez was recently obtained listing over 200 facilities representing the 2008 point source EI. A revised AFS point source dataset could improve the Juárez EI and potentially improve model performance.

16.4 Model Performance Evaluation

CAMx simulations were conducted for 12 distinct modeling scenarios. Each modeling simulation was conducted for a 10-day period identified as an ozone episode. Dates of the episode were June 12 – 21, 2006. The “ozone event” occurred June 18, the day the exceedance was observed. This is the day that is reviewed in the following 2 tables.

Tables 16.1 and 16.2 present 1-hour and 8-hour ozone simulation results respectively for BASELINE and 12 modified Cd. Juárez area source VOC and NOx emissions scenarios. The section identified as Model Output and Statistics indicates the following:

- Cell – identifies the grid cell observing the peak 1-hour (Table 16.1) or 8-hour (Table 16.2) ozone concentration;
- PredPeak identifies the PEAK ozone concentration for the simulation regardless of the location of the regional CAMS;

- PeakObs identifies the peak 1-hour or 8-hour average ozone concentration OBSERVED at one (or more in the event that 2 CAMS observed an identical PEAK ozone concentration) regional CAMS; and
- PairPred indicates the PAIRED PREDICTED PEAK ozone concentration which is paired to a CAMS OBSERVED hourly average concentration;

The following statistics have been previously discussed.

- Unpaired peak prediction accuracy (UPPA);
- Bias in paired peak accuracy among all valid sites (APPA);
- Error in paired peak accuracy among all valid sites (EPPA);
- Bias in peak timing (PTB);
- Overall normalized bias (NB); and
- Overall normalized error (NE).

Data reported in the bottom portion of both tables compares the following:

- PREDICTED PEAK (PredPeak) results generated by modified emissions and the BASELINE PREDICTED PEAK (BL-PredPeak);
- PAIRED PREDICTED PEAK (PairPred) for the simulation modification and the BASELINE PAIRED PREDICTED PEAK (BL-PairPred); and
- PREDICTED PEAK for the modified simulation versus the PEAK OBSERVED highest monitored value in the PdN regional monitoring network.

Table 16.1 Simulation Results for 1-Hour Ozone

Date ID		BASELINE	1201-0000	1201-0900	1201-1100	1201-1300	1201-2100	1201-2300	1202-1000	1202-1300	1202-1500	1202-1800	1202-2330	1203-0200
RUN ID			1	2	3	4	5	6	7	8	9	10	11	12
Model Output and Statistics	Cell	13,18	13,18	13,17	11,26	13,17	13,18	13,18	13,18	13,17	13,17	11,26	13,17	11,26
	PredPeak	103.3	102.1	102.4	91.7	113.9	113.0	92.7	100.1	102.3	119.7	86.8	118.8	87.8
	PeakObs	120.7	120.7	120.7	120.7	120.7	120.7	120.7	120.7	120.7	120.7	120.7	120.7	120.7
	PairPred	99.3	89.1	98.4	86.7	107.8	108.7	89.1	95.2	97.6	112.1	80.1	113.6	83.3
	UPPA	-14.4	-23.2	-15.1	-24	-5.6	-6.4	-23.2	-17.1	-15.3	-0.9	-28.1	-1.6	-27.2
	APPA	-1.5	-8.7	-2.1	-10	4.8	5.2	-8.7	-3.6	-2.7	7.8	-14.6	8.6	-12.8
	EPPA	12.2	14.4	11.9	15.3	13.1	13.2	14.4	13.3	11.9	15.2	17.2	15.2	16
	PTB	4	4	3	4	3	4	4	4	3	3	4	4	4
	NB	-3.3	-6.7	-2.1	-8.7	1.2	0.1	-6.7	-6.3	-1.8	3.1	-11.5	1.8	-8.7
	NE	25.6	23.2	24.2	24.2	27.1	28.1	23.2	26.3	23.3	27.8	23.9	29.5	22.4
	NOX		↑ 50%	↓ 50%			↑ 50%	↓ 50%	↑ 75%	↓ 75%			↑ 75%	↓ 75%
	VOC				↓ 50%	↑ 50%	↑ 50%	↓ 50%			↑ 75%	↓ 75%	↑ 75%	↓ 75%
Difference between Peaks (%)	PredPeak BL-PredPeak		-1.1	-0.8	-11.2	10.3	9.4	-10.3	-3.1	-1.0	15.8	-16.0	15.0	-15.0
	PairPred BL-PairPred		-10.3	-0.9	-12.7	8.6	9.5	-10.3	-4.1	-1.7	12.9	-19.3	14.4	-16.1
	PredPeak Peak Obs		-15.4	-15.1	-24.0	-5.6	-6.4	-23.2	-17.1	-15.3	-0.9	-28.1	-1.6	-27.2
Difference between Peaks(ppb)	PredPeak BL-PredPeak		-1.2	-0.9	-11.6	10.6	9.7	-10.6	-3.2	-1.0	16.4	-16.5	15.5	-15.5
	PairPred BL-PairPred		-10.2	-0.9	-12.6	8.5	9.4	-10.2	-4.1	-1.7	12.8	-19.2	14.3	-16.0
	PredPeak Peak Obs		-18.6	-18.3	-29.0	-6.8	-7.7	-28.0	-20.6	-18.4	-1.0	-34.0	-1.9	-32.9

Table 16.2 Simulation Results for 8-Hour Ozone

Date ID		BASELINE	1201-0000	1201-0900	1201-1100	1201-1300	1201-2100	1201-2300	1202-1000	1202-1300	1202-1500	1202-1800	1202-2330	1203-0200
RUN ID			1	2	3	4	5	6	7	8	9	10	11	12
Model Output and Statistics	Cell	13,18	13,18	13,17	11,27	13,17	13,18	13,18	14,17	13,17	13,17	11,27	13,17	11,27
	PeakObs	95.1	95.1	95.1	95.1	95.1	95.1	95	95.1	95.1	95.1	95.1	95.1	95.1
	PredPeak	93	90.11	94.05	83.22	102.9	101.8	84.49	89	93.28	107.1	80.51	106.3	80.71
	PairPred	92.1	83.6	92.6	80.3	100.5	100	83.6	88.3	86.9	103.7	73.8	104.1	78.8
	UPPA	-2.1	-11.1	-1	-12.4	8.3	7.1	-11.1	-5.2	-7	12.7	-15.3	11.9	-15.1
	APPA	2.5	-3.9	3	-5.9	9	8.5	-3.9	0.6	-0.7	11.6	-10.5	11.7	-7.6
	EPPA	9	8.3	9.5	8.9	14.3	13.7	8.3	8.5	8.5	16.6	12.1	16.4	9.5
	PTB	3	3	3	3	3	3	3	3	3	3	3	3	3
	NB	3.9	0.4	5.4	-1.8	8.8	7.4	0.4	1.8	0.6	10.8	-4.8	9.2	-1.6
	NE	23.7	22.1	22.4	23	24.4	25.4	22.1	24.3	24.5	24.8	22.8	26.5	21.5
	NOX		↑ 50%	↓ 50%			↑ 50%	↓ 50%	↑ 75%	↓ 75%			↑ 75%	↓ 75%
	VOC				↓ 50%	↑ 50%	↑ 50%	↓ 50%			↑ 75%	↓ 75%	↑ 75%	↓ 75%
Difference between Peaks (%)	PredPeak BL-PredPeak		-3.1	1.1	-10.5	10.6	9.4	-9.2	-4.3	0.3	15.1	-13.4	14.3	-13.2
	PairPred BL-PairPred		-9.2	0.5	-12.8	9.1	8.6	-9.2	-4.1	-5.6	12.6	-19.9	13.0	-14.4
	PredPeak Peak Obs		-5.2	-1.1	-12.5	8.1	7.0	-11.1	-6.4	-1.9	12.6	-15.3	11.8	-15.1
Difference between Peaks(ppb)	PredPeak BL-PredPeak		-2.9	1.1	-9.8	9.8	8.8	-8.5	-4.0	0.3	14.1	-12.5	13.3	-12.3
	PairPred BL-PairPred		-8.5	0.5	-11.8	8.4	7.9	-8.5	-3.8	-5.2	11.6	-18.3	12.0	-13.3
	PredPeak Peak Obs		-5.0	-1.1	-11.9	7.8	6.7	-10.5	-6.1	-1.8	12.0	-14.6	11.2	-14.4

16.4.1 Predicted Peak to Baseline Predicted Peak Comparison

Comparison of the simulation PREDICTED PEAK (PredPeak) results and emissions modifications to BASELINE PredPeak resulted in the following 1-hour and 8-hour ozone observations on 6/18:

- Increasing NO_x emissions 50%:
 - Reduces peak 1-hour ozone (-1.2 ppb / -1.1%)
 - Reduces peak 8-hour ozone (-2.9 ppb / -3.1%)
 - Additional NO_x titrates ozone thus lowering these concentrations.
- Decreasing NO_x emissions 50%
 - Reduces peak 1-hour ozone (-0.9 ppb / -0.8%)
 - Increases peak 8-hour ozone increases (+1.1 ppb / +1.1%)
 - Reduced NO_x limits titration of ozone allowing concentrations to increase regarding the 8-hour average; the 50% reduction in NO_x does very little to impact the hourly PredPeak.
- Increasing NO_x emissions 75%
 - Reduces peak 1-hour ozone (-3.2 ppb / -3.1%)
 - Reduces peak 8-hour ozone (-4.0 ppb / -4.3%)
 - Elevated NO_x titrates ozone more effectively than the 50% NO_x increase.
- Decreasing NO_x emissions 75%
 - Reduces peak 1-hour ozone (-1.0 ppb / -1.0%)
 - Increases peak 8-hour ozone (+0.3 ppb / +0.3 %)
 - Reduced NO_x limits titration of ozone and minimally changes ozone concentrations.

- Increasing VOC emissions 50%
 - Increases peak 1-hour ozone (+10.6 ppb / +10.3%)
 - Increases peak 8-hour ozone (+9.8 ppb / +10.6%)
 - Photochemistry improves as PTB is reduced to 3 hours from 4 hours and elevated VOC contributes to photochemical ozone formation.
- Decreasing VOC emissions 50%
 - Decreases peak 1-hour ozone (-11.6 ppb / -11.2%)
 - Decreases peak 8-hour ozone (-9.8 ppb / -10.5%)
 - Limited reactive VOC reduces ozone concentrations.
- Increasing VOC emissions 75%
 - Increases peak 1-hour ozone (+16.4 ppb / +15.8%)
 - Increases peak 8-hour ozone (+14.1 ppb / +15.1%)
 - Increased photochemistry increases ozone concentrations and reduces PTB to 3 hours from 4 hours allowing more daylight hours to form ozone.
- Decreasing VOC emissions 75%
 - Decreases peak 1-hour ozone (-16.5 ppb / -16.0%)
 - Decreases peak 8-hour ozone (-12.5 ppb / -13.4%)
 - Limited reactive ambient VOC emissions substantially reduce ozone concentrations.
- Increasing both VOC and NO_x emissions 50%
 - Increases peak 1-hour ozone (+9.7 ppb / +9.4%)
 - Increases peak 8-hour ozone (+8.8 ppb / +9.4%)

- While ozone concentrations increase, the increase is limited by NOx emissions compared to VOC-only emissions increases.
- Decreasing both VOC and NOx emissions 50%
 - Decreases peak 1-hour ozone (-10.6 ppb / -10.3%)
 - Decreases peak 8-hour ozone (-8.5 ppb / -9.2%)
 - Ozone concentrations decrease, but the decrease is limited by NOx emissions compared to VOC-only decreases. In essence, NOx prevents ozone reductions.
- Increasing both VOC and NOx emissions 75%
 - Increases peak 1-hour ozone (+15.5ppb / +15%)
 - Increases peak 8-hour ozone (+13.3 ppb / +14.3%)
 - While ozone concentrations increase, the increase is limited by NOx emissions compared to VOC-only emissions increases.
- Decreasing both VOC and NOC emissions 75%
 - Decreases peak 1-hour ozone (-15.5 ppb / -15.0%)
 - Decreases peak 8-hour ozone (-12.3 ppb / -13.2%)
 - Ozone concentrations decrease, but the decrease is limited by NOx emissions compared to VOC-only decreases.

Modifications to VOC-only emissions resulted in the greatest variability in PREDICTED PEAK 1-hour and 8-hour ozone. Combining emissions modifications did not produce significant variation compared to VOC-only emissions modifications. Combined increases in VOC and NOx generated a slight 1ppb reduction in 1-hour and 8-hour ozone compared to VOC-only emissions modifications. This may be due to the

limits on ozone formation potential caused by excess NO_x. Combined decreases in VOC and NO_x generated a slight increase in both 1-hour and 8-hour ozone compared to the VOC-only emissions modification. The determination may be made that ozone formation is VOC-limited. Changes in NO_x emissions minimally impact ozone while modifications to VOC emissions produce the greatest variability in 1-hour and 8-hour ozone in either a positive or negative direction.

16.4.2 Paired Predicted Peak Comparison

Comparisons of the PAIRED PREDICTED (PairPred) PEAK consider the maximum 1-hour or 8-hour ozone PAIRED PREDICTED PEAK results in simulations with modified emissions to the BASELINE PAIRED PREDICTED PEAK (BL-PairPred) 1-hour or 8-hour ozone concentration. The PairPred PEAK concentration considers the CAMx predicted ozone value and the 'Paired' value observed at the CAMS. CAMx produces an ozone value for the center of the grid cell, and if a CAMS is located within the cell, CAMx interpolates the value at the coordinate point of the CAMS taking into consideration the PREDICTED PEAK value at the center of adjacent grid cells to calculate the interpolated value.

For all intents and purposes, this comparison considers the BASELINE PAIRED PREDICTED PEAK as a starting point from which to interpret the results of simulations with modified emissions and focuses on the CAMS data since this may be applied in an attainment demonstration. The PREDICTED PEAK may occur anywhere in the modeled domain, but there must be an ozone concentration measured at the CAMS for the value to be considered valid from a regulatory perspective.

Sensitivity analysis associated with reviewing the PAIRED PREDICTED PEAK parameter considers the results from emissions modifications for each RUN compared to the initial BASELINE PairPred 1-hour and 8-hour ozone concentration as indicated in the following:

- Increasing NO_x emissions 50%:
 - Reduces peak 1-hour ozone (-10.2 ppb / -10.3%)
 - Reduces peak 8-hour ozone (-8.5 ppb / -9.2%)
 - Increasing NO_x succeeded in reducing ozone concentrations indicating this pollutant's potential for scavenging ozone.

Decreasing NO_x emissions 50%

- Reduces peak 1-hour ozone (-0.9 ppb / -0.9%)
 - Increases peak 8-hour ozone (+0.5 ppb / +0.5%)
 - The reduction in NO_x emissions did little to modify 1-hour ozone concentrations and minimally increased 8-hour ozone.
- Increasing NO_x emissions 75%
 - Reduces peak 1-hour ozone (-4.1 ppb / -4.1%)
 - Reduces peak 8-hour ozone (-3.8 ppb / -4.1%)
 - Increasing NO_x emissions 75% appears to reduce 1-hour and 8-hour ozone although not to the extent of the 50% NO_x emissions.
 - Decreasing NO_x emissions 75%
 - Reduces peak 1-hour ozone (-1.7 ppb / -1.7%)
 - Reduces peak 8-hour ozone (-5.2 ppb / -5.6%)

- Decreasing NO_x by 75% minimally impacts 1-hour ozone yet substantially reduces 8-hour ozone in the event an 8-hour ozone attainment demonstration must be developed.
- Increasing VOC emissions 50%
 - Increases peak 1-hour ozone (+8.5 ppb / +8.6%)
 - Increases peak 8-hour ozone (+8.4 ppb / +9.1%)
 - Elevated 1-hour and 8-hour ozone concentrations due to the 50% increase in VOC emissions indicates the model is sensitive to VOC emissions modifications.
- Decreasing VOC emissions 50%
 - Reduces peak 1-hour ozone (-12.6 ppb / -12.7%)
 - Reduces peak 8-hour ozone (-11.8 ppb / -12.8%)
 - Simulation results indicate the sensitivity to modifications in VOC emissions.
- Increasing VOC emissions 75%
 - Reduces peak 1-hour ozone (+12.8 ppb / +12.9%)
 - Increases peak 8-hour ozone (+11.6 ppb / +12.6%)
 - Elevation in both 1-hour and 8-hour ozone as a result of a 75% increase in VOC emissions indicates good model response to the emissions modification.
- Decreasing VOC emissions 75%
 - Reduces peak 1-hour ozone (-19.2 ppb / -19.3%)
 - Reduces peak 8-hour ozone (-18.3 ppb / -19.9%)

- The 75% decrease in VOC emissions produces a significant reduction in 1-hour and 8-hour ozone indicating excellent model response to the emissions modification. Ozone concentrations are also significantly lower compared to the 50% VOC emissions reduction.
- Increasing both VOC and NOx emissions 50%
 - Increases peak 1-hour ozone (+9.4 ppb / +9.5%)
 - Increases peak 8-hour ozone (+7.9 ppb / +8.6%)
 - Increasing both VOC and NOx by 50% generated slightly higher 1-hour and 8-hour ozone than the 50% increase in VOC emissions alone. Additional NOx may have contributed to the slight increase, but a 1 ppb increase is likely not significant further indicating that the VOC emissions were the driving force in elevated 1-hour and 8-hour ozone.
- Decreasing both VOC and NOx emissions 50%
 - Reduces peak 1-hour ozone (-10.2 ppb / -10.3%)
 - Reduces peak 8-hour ozone (-8.5 ppb / -9.2%)
 - The 50% reduction in both VOC and NOx emissions significantly reduces 1-hour and 8-hour ozone. However, the reduction is less than the 50% reduction in VOC emissions alone. It is possible that the coinciding NOx reduction may have prevented a deeper reduction in ozone.
- Increasing both VOC and NOx emissions 75%
 - Increases peak 1-hour ozone (+14.3 ppb / +14.4%)
 - Increases peak 8-hour ozone (+12.0 ppb / +13.0%)

- The 75% increase in both VOC and NO_x emissions significantly increases PairPred 1-hour and 8-hour ozone indicating good model response. The amount is also slightly higher ozone concentrations that was produced by VOC-only modifications.
- Decreasing both VOC and NOC emissions 75%
 - Reduces peak 1-hour ozone (-16.0 ppb / -16.1%)
 - Reduces peak 8-hour ozone (-13.3 ppb / -14.4%)
 - The 75% reduction in both VOC and NO_x emissions significantly reduces 1-hour and 8-hour Paired PredPeak ozone. However, the reduction is less than the 75% reduction in VOC emissions alone. It is possible that the coinciding NO_x reduction may have prevented a deeper reduction in ozone.

Ozone is impacted by modifications to VOC emissions and minimally influenced by NO_x emissions in the current simulations. Reduced NO_x emissions in combination with VOC emissions reductions produce higher ozone concentrations compared to equivalent VOC-only emissions reductions.

16.4.3 Predicted Peak to Observed Peak Comparison

Comparison of PREDICTED PEAK (PredPeak) to the PEAK OBSERVED (PeakObs) is applied to assess whether the model is generating results that are closer to or further from the PEAK OBSERVED values rather than other predicted values such as the BASELINE PREDICTED PEAK or the PAIRED PREDICTED PEAK. This procedure assesses whether the modeled emissions inventory is adequate for predicting a peak ozone concentration which is fairly close to the PEAK OBSERVED.

As indicated in Table 16.1, NB improves and slightly over-predicts 1-hour ozone compared to BASELINE NB. The PREDICTED PEAK vastly improves with a 75% increase in VOC-only or combined VOC-NOx emissions.

The improved PredPeak and reduced NB coupled with a narrowed difference between PredPeak and PeakObs provides a foundation from which to build a more accurate emissions inventory. The following describes results of PredPeak vs PredObs:

- BASELINE MODEL
 - Peak 1-hour ozone is under-predicted (-17.4 ppb / -14.4%)
 - Peak 8-hour ozone is under-predicted (-2.1 ppb / -2.2%)
 - The BASELINE model, from which all subsequent simulations were compared, generated a PredPeak 17.4 ppb (14.4%) less than the PeakObs for 1-hour ozone and 2.1 ppb (-2.2%) less than PeakObs 8-hour ozone. The minimal difference in 8-hour ozone is a point of concern given the difference in Modeled EI vs. the regulatory EI developed by TCEQ.
- Increasing NOx emissions 50%:
 - Peak 1-hour ozone is under-predicted (-18.6 ppb / -15.4%)
 - Peak 8-hour ozone is under-predicted (-5.0 ppb / -5.2%)
 - The slight decrease in 1-hour ozone of 18.6 ppb (-15.4%) appears to indicate minimal 1-hour ozone reduction compared to BASELINE given the 50% increase in NOx emissions. The gap also expands almost 3 ppb comparing 8-hour ozone of the BASELINE simulation. This is a very good example of the scavenging effect of excess NOx.
- Decreasing NOx emissions 50%

- Peak 1-hour ozone is under-predicted (-18.3 ppb / -15.1%)
- Peak 8-hour ozone is minimally under-predicted (-1.1 ppb / -1.1%)
- The 50% reduction in NO_x appears almost similar to the 50% increase in NO_x when observing 1-hour ozone. Decreasing NO_x also appears to narrow the gap between 8-hour ozone comparing to the BASELINE simulation.
- Increasing NO_x emissions 75%
 - Peak 1-hour ozone is under-predicted (-20.6 ppb / -17.1%)
 - Peak 8-hour ozone is under-predicted (-6.1 ppb / -6.4%)
 - The 75% increase in NO_x emissions significantly reduces 1-hour and 8-hour ozone. This is a good example of the scavenging effect of excess NO_x on ozone concentrations.
- Decreasing NO_x emissions 75%
 - Peak 1-hour ozone is under-predicted (-18.4 ppb / -15.3%)
 - Peak 8-hour ozone is under-predicted (-1.8 ppb / -1.9%)
 - The 75% decrease in NO_x does not significantly change 1-hour and 8-hour ozone level compared to BASELINE.
- Increasing VOC emissions 50%
 - Peak 1-hour ozone is under-predicted (-6.8 ppb / -5.6%)
 - Peak 8-hour ozone is over-predicted (+7.8 ppb / +8.1%)
 - The 50% increase in VOC emissions narrows by 10.6 ppb the difference in PredPeak versus PeakObs when compared to the BASELINE simulation for 1-hour ozone. This indicates the model responds to

modifications in VOC emissions compared to the lack of change when NO_x emissions were modified. The over-prediction in 8-hour ozone indicates VOC emissions may enhance photochemistry resulting in elevated ozone concentrations. A question that arises is if the 50% increase in VOC emissions is in an acceptable range given the major difference between the regulatory EI and the simulated EI.

- Decreasing VOC emissions 50%
 - Peak 1-hour ozone is under-predicted (-29.0 ppb / -24.0%)
 - Peak 8-hour ozone is under-predicted (-11.9 ppb / -12.5%)
 - The 50% reduction in VOC emissions decreases predicted 1-hour ozone concentrations by 11.6 ppb less than the PredPeak for the BASELINE simulation indicating good model response to the reduced VOC emissions. 8-hour ozone also shows a significant reduction of 9.8 ppb less than the BASELINE simulation. The large under-prediction of 8-hour ozone indicates VOC reduction strategies may be effective PAQCS in the event EI Paso is designated nonattainment and an attainment demonstration is required.
- Increasing VOC emissions 75%
 - Peak 1-hour ozone is under-predicted (-1.0 ppb / -0.9%)
 - Peak 8-hour ozone is over-predicted (+12.0 ppb / +12.6%)
 - The 75% increase in VOC emissions narrows the difference between simulated PredPeak and monitored PeakObs the most of all 12 simulations. This indicates the model responds to modifications in VOC.

The over-prediction in 8-hour ozone indicates VOC emissions may enhance photochemistry resulting in elevated ozone concentrations. A question that arises is if the 75% increase in VOC emissions is in an acceptable range given the wide difference between the regulatory EI and the simulated EI. While the purpose of this dissertation is to evaluate the performance of CAMx to modifications in simulated emissions, the logical next step is to recommend emissions reduction PAQCS.

- Decreasing VOC emissions 75%
 - Peak 1-hour ozone is under-predicted (-34.0 ppb / -28.1%)
 - Peak 8-hour ozone is under-predicted (-14.6 ppb / -15.3%)
 - The 75% reduction in VOC emissions predicts 1-hour ozone concentrations that are 16.6 ppb less than the PredPeak for the BASELINE simulation indicating good model response to the reduced VOC emissions. 8-hour ozone also shows a significant reduction of 13.2 ppb less than the BASELINE simulation PredPeak. The large under-prediction of 8-hour ozone indicates VOC reduction strategies may be effective PAQCS in the event El Paso is designated nonattainment and an attainment demonstration is required.
- Increasing both VOC and NO_x emissions 50%
 - Peak 1-hour ozone is under-predicted (-7.7 ppb / -6.4%)
 - Peak 8-hour ozone is over-predicted (+6.7 ppb / +7.0%)
 - The 50% increase in both VOC and NO_x generated simulated results which are comparable to increases in VOC-only emissions. NO_x continues

to play little role in the predicted ozone results, However, the additional NO_x does produce an additional reduction of 0.9 ppb in 1-hour ozone and 1.1 ppb in 8-hour ozone indicating the potential of NO_x to reduce ozone concentrations.

- Decreasing both VOC and NO_x emissions 50%
 - Peak 1-hour ozone is under-predicted (-28.0 ppb / -23.2%)
 - Peak 8-hour ozone is under-predicted (-10.5 ppb / -11.1%)
 - The 50% reduction in both NO_x and VOC emissions decreases predicted 1-hour ozone concentrations by 11.4 ppb less than the PredPeak for the BASELINE simulation indicating good model response to the reduced VOC emissions. 8-hour ozone also shows a significant reduction of 13.2 ppb less than the BASELINE simulation PredPeak. The large under-prediction of 8-hour ozone indicates VOC reduction strategies may be effective PAQCS in the event El Paso is designated nonattainment and an attainment demonstration is required.
- Increasing both VOC and NO_x emissions 75%
 - Peak 1-hour ozone is under-predicted (-1.9 ppb / -1.6%)
 - Peak 8-hour ozone is over-predicted (+11.2 ppb / +11.8%)
 - The 75% increase in both VOC emissions narrows the difference between simulated PredPeak and monitored PeakObs with a difference on only 0.9 ppb to the VOC-only emissions increase. This indicates the model responds to modifications in VOC and emissions are slightly limited by the additional NO_x emissions.

- Decreasing both VOC and NOC emissions 75%
 - Peak 1-hour ozone is under-predicted (-32.9 ppb / -27.2%)
 - Peak 8-hour ozone is under-predicted (-14.4 ppb / -15.1%)
 - The 75% reduction in both NOx and VOC emissions predicts 1-hour ozone which is comparable to VOC-only emissions reductions yet only 1 ppb higher for 1-hour and 0.2 ppb higher for 8-hour ozone

CAMx under-predicts ozone concentrations compared to the PeakObs in almost all the simulations. The difference between PredPeak and PeakObs substantially narrows when VOC alone or VOC and NOx emissions are increased by 50% or 75%. NOx alone plays no major role in substantially increasing or decreasing 1-hour or 8-hour ozone. However, the 8-hour average over-predicts PeakObs 8-hour ozone for both elevated VOC and VOC-NOx emissions. Yet, while there is an over-prediction of 8-hour ozone there is an opportunity to improve the EI to this level of emissions, and from this level, begin recommending PAQCS which are meaningful and effective from an air quality planning perspective.

16.5 Individual Simulation Results

Results obtained by each simulation for BASELINE and modified emissions RUNs indicate VOC-only and combinations of VOC and NOx emissions modifications generated the highest variability in predicted 1-hour and 8-hour ozone concentrations. NOx-only emissions modifications produced low variability in either 1-hour or 8-hour ozone concentrations.

Model simulation output data was observed for 3 CAMs. The purpose of the 3 CAMS (C663, C12, and C41) is C663 observes the highest daily maximum 1-hour ozone across the PdN region, C12 at UTEP is the site in El Paso observing the most exceedances on the US side of the border, and an Auto-GC deployed at C41 provided the opportunity to observe hourly TNMHC concentrations. The model predicted the grid cell in which C663 is located presented the highest ozone concentrations which concords with observed ozone concentrations.

16.6 Limiting Factors in Regional Ozone Formation

Ozone formation conditions in the PdN region appear VOC-limited. 2 sections in this dissertation discussed conditions which limit ozone formation. One method observed the TNMHC-NO_x ratios. The other method observed model output data and the HNO₃-H₂O₂ ratios. The date of interest throughout this report, 6/18, is the day of the ozone event. This day would be the focus of further investigation by regulatory entities due to the need to model an attainment demonstration in the event El Paso is designated nonattainment of the ozone NAAQS.

Understanding the ozone formation limiting conditions is key to developing control strategies to effectively reduce 8-hour ozone due to the high monetary cost of achieving attainment of the air quality standards. Under all the modeling simulations the region tends to be VOC-limited during early morning hours when ozone limiting determinations are made.

CAMx output includes H₂O₂ and HNO₃ data which help to develop a similar conclusion. In this particular case, CAMx generates output of chemical species which is

the product involved in the formation and destruction of ozone. Results from the CAMx simulation indicate VOC-limited conditions control the formation of ozone. The $\text{H}_2\text{O}_2:\text{HNO}_3$ ratios during morning hours and the height of the ozone event were consistently $\leq 35\%$. Effectively 2 distinct methods of developing a conclusion as to the ozone limiting conditions in the PdN region confirm this factor which will assist in developing emissions control strategies.

16.7 Attainment Demonstrations

Attainment demonstrations addressed 15% VOC reductions as indicated in the SIPs for El Paso and across the state of Texas. Ozone reduction strategies at the time depended on EKMA diagrams to assess NO_x - or VOC-limited conditions. Broad brush control strategies such as these resulted in significant reductions in the ozone design value over the past decades.

However, as the 8-hour ozone standard becomes more stringent and sensitivity of photochemical modeling improves, it is possible to develop control strategies which can allocate VOC emissions reductions across several specific source categories and conduct more focused sensitivity analysis to determine which sources to control at lower costs and maximum effect.

As indicated by results of the sensitivity analysis conducted for this dissertation, a broad brush approach was applied to primarily evaluate CAMx response to emissions modifications. Simulation results indicate that ozone in the PdN region responds primarily to VOC emissions modifications due to the VOC-limited conditions which exist in the PdN. Reducing VOC either alone or in combination with NO_x emissions

reductions effectively reduced 1-hour and 8-hour ozone. Reducing NO_x alone had minimal effect on ozone. However, through the broad brush approach in reducing Juárez area source VOC emissions, a recommendation may be made to further assess source-specific VOC emissions control strategies to achieve attainment at some future date should an attainment demonstration be required for El Paso.

Data discussed in Section 4 addressed reviewing ambient TNMHC and NO_x concentrations between 6 AM – 9 AM. Insufficient photochemistry occurs during this time of day to effectively oxidize ambient TNMHC and NO_x into different chemical species such as H₂O₂ or HNO₃. The TNMHC:NO_x ratio provides a point of departure to develop control strategies. As indicated in Section 4 the ambient concentrations of TNMHC and NO_x suggest VOC-limited conditions prevailed on 6/18. If this is the case, then controls on VOC emissions could effectively reduce ozone concentrations to potentially prevent an exceedance as long as meteorological conditions favorable to ozone formation are similar during future ozone episodes and events.

17 Conclusions

This research evaluated the CAMx photochemical modeling system to assess the sensitivity of the model for 12 unique air pollution emission scenarios. Cd. Juárez area source emissions were modified by increasing or decreasing by 50% and 75% the quantity of VOC and / or NOx pollutants for each simulation scenario.

The modeled emissions inventory and the regulatory emissions inventory developed by TCEQ appear to vary substantially insofar as emissions from Mexican sources are concerned. Emissions modeled in the simulations are not complete and appear to not represent total emissions generated in the PdN region. Further review and modifications of the Juárez EI is recommended in order to more accurately reflect the actual conditions which lead to the formation of ozone across the PdN community.

The modeled point source EI under-reports all emissions compared to the actual point source EI for all 3 jurisdictions. The international ports of entry, a major source of motor vehicle exhaust emissions, are not identified in the modeled simulation nor in the EI reported by either the TCEQ or Mexico's Environmental agencies. The biogenics VOC emissions inventory also requires further review to confirm the types of VOC emissions generated in the PdN. One should confirm the reactivity of biogenic VOC emissions and determine if biogenic VOCs play a role in PdN regional ozone formation.

The photochemical modeling system responded well and within acceptable parameters for NB and NE to modifications in Juárez area source emissions. However, 1-hour and 8-hour PREDICTED PEAK ozone was consistently under-predicted perhaps due to the incomplete emissions database provided in the modeled EI. RUN 9 and RUN 11, which increased VOC and NOx emissions by 75% produced simulated ozone

concentrations which were closer to observed ozone levels. In essence, VOC alone or a combination of VOC and NO_x emissions developed into a modeled emissions inventory may need to be increased by 75% in order to develop a BASELINE model which can then be modified to provide an ozone attainment demonstration.

Given the issues just raised with the modeled emissions inventory it is recommended that daily modeled emissions be modified to attempt to generate model results which narrow NB and reduce NE and achieve results closer to observed. Perhaps a first step to improving modeled results includes updating the point source emissions inventories for all 3 jurisdictions and adding emissions sources not included in simulations conducted for this dissertation.

In summary, the CAMx photochemical model performs adequately in assessing the impact of emissions which contribute to ozone formation in the PdN region. Modifications to VOC and / or NO_x emissions generate output which appears logical. The model responds well to additions of excess NO_x emissions by decreasing ambient ozone due to the titrating effect of this pollutant. CAMx also responds well to increased and decreased VOC emissions further confirming the VOC-limited nature of ambient air pollutants which control the formation of ambient ozone.

18 References

- Ambient Monitoring and Assessment Committee of the Northeast States for Coordinated Air Use Management (NESCAUM). Preview of 1994 Ozone Precursor Concentrations in the Northeastern U.S, 1994.
- Atkinson, Roger and Janet Arey. Studies of the Atmospheric Chemistry of Volatile Organic Compounds and of their Atmospheric Reaction Products. Final Report to the California Air Resources Board Contract No. 99-330. January 2004.
- Baker, Rick. Update of Diesel Construction Equipment Emission Estimates for the State of Texas – Phase I and II. Final Report. Eastern Research Group, July 31, 2009.
- Berg, N. J., Eastern Research Group. 1997. Photochemical Assessment Monitoring Stations (PAMS) Performance Evaluation Program Final Report Contract No. 68-D3-0095.
- Berkowitz, Carl and YuLong Xie. Source Attribution and Emission Adjustment Study Task 1: Back-Trajectory Climatology and Identification of Key Source Regions - Final report. January 10, 2005.
- Carter, William P. L. Development of Ozone Reactivity Scales for Volatile Organic Compounds. J. of the Air and Waste Management Association, Vol 44, pages 881-899, January 20, 1994.
- Carter, William P. L. and Irina Malkina. Development and Application of Improved Methods for Measurement of Ozone Formation Potentials of Volatile Organic Compounds. Final Report to the California Air Resources Board, Contract No. 97-314. May 22, 2002.
- Carter, William P.L. and John H. Seinfeld. Winter Ozone Formation and VOC Incremental Reactivities in the Upper Green River Basin of Wyoming. Atmospheric Environment 50, 255-266, 2012.
- Carter, William P. L. and John A. Pierce, Dongmin Luo, and Irina L. Malkina. Environmental Chamber Study of Maximum Incremental Reactivities of Volatile Organic Compounds. Atmos. ENVIRON, Vol 29, pages 2499-2511, 1995.
- Chinkin, Lyle R., et.al. . March 15, 2006. Final Validation of Central California Ozone Study (CCOS); Field Data, Final Report, STI-905003.07-2851-FR2.
- Doty, K. July, 2002. Meteorological Modeling for the Southern Appalachian Mountains Initiative (SAMI). Final Report. Tennessee Valley Authority, Energy Research and Technology Applications.

- Dunker A.M., G. Yarwood, J.P. Ortmann, G.M. Wilson. 2002a. The Decoupled Direct Method for Sensitivity Analysis in a Three-dimensional Air Quality Model – Implementation, Accuracy and Efficiency. *Environmental Science and Technology*, 36:2965-2976.
- Dunker A.M., G. Yarwood, J.P. Ortmann, G.M. Wilson, 2002b. Comparison of Source Apportionment and Source Sensitivity of Ozone in a Three-Dimensional Air Quality Model, *Environmental Science and Technology*, 36:2953-2964.
- Eastern Research Group. August 31, 2008. Auto Refinishing Coatings: VOC Emission Inventory: FINAL REPORT.
- Eastern Research Group. July 15, 2009. Minor Point Source Emissions - Phase 2.
- Eastern Research Group, Inc. August 31, 2005. Data Collection, Sampling, and Emissions Inventory Preparation Plan for Selected Commercial and Industrial Equipment: Phase II - Final Report.
- Emissions Inventory Improvement Program. 1996. Consumer and Commercial Solvent Use. Volume III, Chapter 5. Emission Inventory Improvement Program. August.
- Emissions Inventory Improvement Program. 1997. Solvent Cleaning. Volume III, Chapter 6. Emission Inventory Improvement Program. August.
- Emissions Inventory Improvement Program. 2000. Area Sources Category Method Abstract – Structural Fires. Emission inventory Improvement Program. May.
- Emissions Inventory Improvement Program. 2001a. Asphalt Paving. Volume III, Chapter 17. Emission Inventory Improvement Program. January.
- Emissions Inventory Improvement Program. 2001b. Pesticides – Agricultural and Nonagricultural. Volume III, Chapter 9. Emission Inventory Improvement Program. June.
- Emissions Inventory Improvement Program. 2001c. Structure Fires. Volume III, Chapter 18. Emission Inventory Improvement Program. January.
- Emissions Inventory Improvement Program, 2001d. Landfills. Volume III, Chapter 15. Emission Inventory Improvement Program. January.
- Emery, C.A, and J. Johnson. 2009. “June 2006 Texas MM5 Modeling. Task 1: MRF PBL.” Presentation to the Texas Commission on Environmental Quality, Alamo Area Council of Governments, and Capitol Area Council of Governments.

- Emery, C.A., J. Johnson, P. Piyachaturawat. 2009. "Application of MM5 for the Austin / San Antonio Joint Meteorological Model Refinement Project." Prepared for the Alamo Area Council of Governments, San Antonio, TX and the Capitol Area Association of Governments, Austin, TX. Prepared by ENVIRON International Corporation, Novato, CA.
- ENVIRON International Corporation, 31 August 2001. Area and Mobile Source Emissions Inventory Technical Support Project: 1990-2010 Emission Inventory Trends and Projections.
- ENVIRON International Corporation, 31 August 31, 2012. Final Report: CAMx 4-km Modeling of EL Paso / Juárez.
- ENVIRON International Corporation. August, 2009. "User's Guide: Environmental Processor System, Version 3" ENVIRON International Corporation, Novato, CA.
- ENVIRON International Corporation. 2008. "User's Guide: Comprehensive Air quality Model with extensions (CAMx), version 4.50." Prepared by ENVIRON International Corporation, Novato, CA.
- ENVIRON International Corporation. 2011. "User's Guide: Comprehensive Air quality Model with extensions (CAMx), version 5.40." Prepared by ENVIRON International Corporation, Novato, CA.
- ENVIRON International Corporation. 2009. "Supplemental User's Guide: Comprehensive Air Quality Model with Extensions (CAMx), version 4.53." Prepared by ENVIRON International Corporation, Novato, CA.
- ENVIRON International Corporation, 31 August 2001. Final Report: Area and Mobile Source Emissions Inventory – Technical Support Project: 1990-2010 Emissions Inventory Trends and Projections.
- ENVIRON International Corporation and Pacific Environmental Services, Inc. Development of Source Speciation Profiles from the TNRCC Point Source Database, Final Report. August 31, 2001.
- ENVIRON International Corporation, 2009. Application of CAMx for the Austin / San Antonio Joint Meteorological Model Refinement Project.
- Environmental Protection Agency, 2008. 40 CFR Part 52. Final Rule to Implement the 8-Hour Ozone National Ambient Air Quality Standard.
- Environmental Protection Agency, 1994. Preview of 1994 Ozone Precursor Concentrations in the Northeastern U.S.

- US Environmental Protection Agency, Emission Inventory Branch Technical Support Division and Radian Corporation, 1991. Emissions Inventory Requirements for Ozone State Implementation Plans, Research Triangle Park, NC, EPA-450/4-91-010.
- Environmental Protection Agency, 1992. Procedures for the Preparation of Emissions Inventories for Carbon Monoxide and Precursors of Ozone. Volume II, Emissions Inventory Requirements for Photochemical Air Quality Simulation Models. EPA 454/R-92-026. Research Triangle Park, NC.
- Environmental Protection Agency, 1997. Introduction to the Emission Inventory Improvement Program, EPA 454/R-97-004. Research Triangle Park, NC.
- Environmental Protection Agency, 1996. PAMS Data Analysis Results Report. EPA-454/R-96-006. Research Triangle Park, NC.
- Environmental Protection Agency, 1996. Air quality criteria for particulate matter, EPA/600/P-95/001aF-cF.3v. Research Triangle Park, NC.
- Environmental Protection Agency, 2003. Air quality criteria for particulate matter. Draft Report EPA/600/P-99/002aB. Research Triangle Park, NC.
- Environmental Protection Agency. April 2007. "Guidance on the Use of Models and Other Analyses for Demonstrating Attainment of Air Quality Goals for Ozone, PM_{2.5}, and Regional Haze". EPA -454/B-07-002. Research Triangle Park, NC.
- Environmental Protection Agency, NAAQS. Accessed 2010. <http://www.EPA.gov/air/criteria.html>
- Federal Aviation Administration (FAA), 2001. *Emissions and Dispersion Modeling System (EDMS) Reference Manual*. Office of Environment and Energy. FAA-AEE-01-01. May 2001.
- Federal Register, 2010. Vol. 75, No. 11. January 19, 2010.
- Finlayson-Pitts, B. J., and J. J. N. Pitts, Chemistry of the Upper and Lower Atmosphere, 969 pp., Academic, San Diego, Calif., 2000.
- Fujita, Eric, et.al. Central California Ozone Study (CCOS) Volume I. Conceptual Program Plan Version 2.1. September 7, 1999.
- Funk, Tami H., Patricia S. Stiefer, and Lyle R. Chinkin. Development of Gridded Spatial Allocation Factors for the State of Texas. Final Report 3.

- Gillani, Noor V., and Kevin Doty, August 31, 2008. Top-down Emissions Verification (TDEV) of Industrial Emissions in Houston Based on TexAQS II Data. Final Report.
- Grell, G. A., J. Dudhia, and D. R. Stauffer. 1994. "A Description of the Fifth Generation Penn State/NCAR Mesoscale Model (MM5)." NCAR Technical Note (NCAR TN-398-STR).
- Guenther, A. B., Jiang, X., Heald, C. L., Sakulyanontvittaya, T., Duhl, T., Emmons, L. K., and Wang, X. 2012. The Model of Emissions of Gases and Aerosols from Nature version 2.1 (MEGAN2.1): an extended and updated framework for modeling biogenic emissions, *Geosci. Model Dev. Discuss.*, 5, 1503-1560.
- Harbour RL, 1972. Franklin Mountains, Texas and New Mexico. USGS Bulletin 1298. U.S. Government Printing Office, Washington, D.C.
- Jolly, J.R., F. Mercado, D. W. Sullivan. 2004. A Comparison of Ambient and Emissions VOC to NO_x Ratios at Two Monitors in Houston, Texas.
- Kim, Y. et. al., 31 August 2010. Formation of Secondary Aerosols: Impact of the Gas-Phase Chemical Mechanism. CEREIA, Joint Laboratory E´cole des Ponts ParisTech / EDF R&D, Universit´e Paris-Est.
- Li WW, Sarnat JA, Raysoni AU, Sarnat SE, Stock TH, Holguin F, Greenwald R, Olvera HA, Johnson BA, 2011. Characterization of traffic related air pollution in elementary schools and its impact on asthmatic children in El Paso, Texas. 2010. Mickey Leland National Urban Air Toxic Research Center, NUATRC Report Number 20, Houston, Texas. June 2011.
- Oltmans, S., Arlyn Andrews, and Laura Patrick. Influence of Transport by the Nocturnal Jet on Ozone Levels in Central Texas. 2009 Year-end Report. March 12, 2010.
- Paso del Norte Group, 2009. The Paso del Norte Region, US-Mexico: Self-Evaluation Report, OECD Reviews of Higher Education in Regional and City Development, IMHE, Regional Stakeholders Committee.
<http://www.oecd.org/dataoecd/48/2/44210876.pdf> (accessed March, 2012).
- Paulson, S. (1999) "Total Non-Methane Organic Carbon Development and Validation of a New Instrument and Measurements of Total Non-Methane Organic Carbon and C₂-C₁₀ Hydrocarbons in the South Coast Air Basin", ARB Contract No. 95-335.
- Seinfeld, J. H., and S. N. Pandis, *Atmospheric Chemistry and Physics: From Air Pollution to Climate Change*, 1326 pp., John Wiley, New York, 1998.
- Skamarock WC, Klemp JB, Dudhia J, 2001. Prototypes for the WRF (Weather Research and Forecasting) model. Reprints, Ninth Conf. on Meso-scale Processes, Fort Lauderdale, FL, Amer. Meteor. Soc., J11-J15.

Sonoma Technology, Inc. Evaluating Ozone Precursor Emission Inventories, 2000.

Manahan, Stanley E. Environmental Chemistry, 8th Ed. CRC Press, Boca Raton, Florida, 2005.

Tanaka, P. L., D. T. Allen, E. C. McDonald-Buller, S. Chang, Y. Kimura, C. B. Mullins, G. Yarwood, and J. D. Neece. 2003. Development of a chlorine mechanism for use in the carbon bond IV chemistry model.

Texas Air Control Board. Post-1982 Ozone Control Strategies, Dallas, El Paso, and Tarrant County; Texas State Implementation Plan, August, 1985.

Texas Air Control Board. Revision to the State Implementation Plan for the Inspection and Maintenance Program, July, 1992.

Texas Air Control Board, Texas State Implementation Plan: Control Strategies, December, 1977.

Texas Commission on Environmental Quality, 2005r. Highly-reactive Volatile Organic Compound Allowable Limits for Sites Located in the Houston/Galveston/Brazoria Nonattainment Area. Interoffice Memorandum, April 7, 2005.

Texas Commission on Environmental Quality, 2006. Dallas–Fort Worth Nonattainment Area Ozone Conceptual Model, TCEQ DataAnalysis Team, October 17, 2006

Texas Commission on Environmental Quality. 2006a. Revisions to the State Implementation Plan (SIP) for the Control of Ozone Air Pollution: El Paso County 8-Hour Ozone Maintenance Plan. January, 2006.

Texas Commission on Environmental Quality. 2006. TEXAQS/GoMACCS Comprehensive Chemical Analysis of TexAQS II data.

Texas Commission on Environmental Quality, 2007. Appendix D. Appendix D: Sub-domain modeling Case Studies.

Texas Commission on Environmental Quality. 2008. Emissions Modeling of Specific Highly Reactive Volatile Organic Compounds (HRVOC) in the Houston-Galveston-Brazoria Ozone Nonattainment Area.

Texas Commission on Environmental Quality, January 30, 2008. SIP Revision: El Paso, Carbon Monoxide Maintenance Plan.

Texas Commission on Environmental Quality, 2012. Emission Inventory Guidelines. RG-360A/11. Revised February 2012

- Thomas, R. 2008. Emissions Modeling of Specific Highly Reactive Volatile Organic Compounds (HRVOC) in the Houston-Galveston-Brazoria Ozone Nonattainment Area.
- Thomas, R. 2004. Preparing Point Source Emissions Inventories for Ozone SIP Modeling: Base Case and Future Case.
- Yarwood, G., S. Rao, M. Yocke, and G.Z. Whitten. 2005. Updates to the Carbon Bond chemical mechanism: CB05. Final Report prepared for EPA, Research Triangle Park, NC. Available at http://www.CAMx.com/publ/pdfs/CB05_Final_Report_120805.pdf.
- Yarwood, G., G. Wilson, S. Shepard, A. Guenther. 2007. User's Guide to the Global Biosphere Emissions and Interactions System (GloBEIS3); Version 3.2. Prepared by ENVIRON International Corporation, Novato, CA and the National Center for Atmospheric Research, Boulder, CO.

19 Appendices

Appendix 1: Acronyms and Abbreviations

ACT	Alternative Control Techniques
AFS	AIRS Facility Subsystem
AIRS	Aerometric Information Retrieval System
AMS	AIRS Area and Mobile Subsystem
AQAC	Air Quality Advisory Committee
AQCR	Air quality control region
AQMP	Air Quality Modeling Procedures / or Management Plan
AQP&A	Air Quality Planning and Assessment
ARB	Air Resources Board
ASEI	Area source emissions inventory
ASTM	American Society for Testing and Materials
ATSDR	Agency for Toxic Substances and Disease Registry
AWMA	Air and Waste Management Association
BACM	Best available control measures
BACT	Best available control technology
BART	Best available retrofit technology
BCI	Base case inventory
BEA	Bureau of Economic Analysis
BECC	Border Environment Cooperation Commission
BID	Background information document
BLI	Baseline inventory
BMPs	Best management practices
BPA	Beaumont-Port Arthur (Metroplex)
BTEX	benzene, toluene, ethyl benzene, and xylene
C	centigrade or carbon
CAAA-1990	Clean Air Act Amendments of 1990
CAFO	Concentrated animal feeding operation
Cal-EPA	California Environmental Protection Agency
CAMS	Continuous air monitoring station
CAIR	Clean Air Interstate Rule
CAMx	Comprehensive Air Quality Model with Extensions
CARB	California Air Resources Board
CARE	Clean Air Responsibility Enterprise Committee
CASAC	Clean Air Scientific Advisory Committee
CAS	Chemical Abstract Services
CB4	Carbon bond 4
CB5	Carbon bond 5
CB6	Carbon bond 6
CCOS	Central California Ozone Study
CE	Control Efficiency
CEIS	Computerized Emissions Inventory System
CEMS	Continuous Emission Monitoring System
CERCLA	Comprehensive Environmental Responsibility, Compensation and Liability Act

CFC	Chlorofluorocarbon
CFM	Cubic feet per minute
CFR	Code of Federal Regulations
CH ₄	Methane
C ₂ H ₆	Ethane
CH ₂ O	Formaldehyde
CHIEF	Clearinghouse for inventories and emission factors
CM	Conceptual model
CMAQ	Congestion Mitigation Air Quality
CMC	Chemical mechanism compiler
CMSA	Consolidated metropolitan statistical area
CO	Carbon monoxide
CO ₂	Carbon dioxide
COG	Council of Governments
COH	Coefficient of haze
CORE	Control operations review and evaluation
CSI	Common sense initiative
CTC	Control technology center
CTG	Control techniques guidelines
DQOs	Data quality objectives
DERC	Discrete emission reduction credit
DFW	Dallas-Fort Worth (Metroplex)
DM&A	Data Management & Analysis
DV	Design value
EF	Emission factor
EFIG	Emission factor and inventory group
EGAS	Economic Growth Analysis System
EGF	Electric generating facility
EI	Emissions inventory
EIA	Energy Information Administration
EIIP	Emission inventory improvement program
EIQA	Emission inventory quality assurance
EPA	U.S. Environmental Protection Agency
EPS3	Emissions Processor System, Version 3
ER	Effective Reactivity
ERG	Eastern Research Group, Inc
ESL	Effects screening level
ETBE	Ethyl tertiary-butyl ether
FCAA	Federal Clean Air Act
FCAAA	Federal Clean Air Act Amendments
FIPS	Federal information processing standards
FIRE	Factor information retrieval system
FMVCP	Federal Motor Vehicle Control Program
FR	Federal Register
GACT	Generally available control technology
GAQM	Guideline on Air Quality Models

GC	Gas Chromatograph or Gas Chromatography
GC/MS	Gas Chromatography / Mass Spectrometry
GIS	Geographic Information System
GLC	Ground-level Concentration
GLOBEIS	Global Biosphere Emissions and Interactions System
GPT	Gas-phase titration
HAN	Heavy aromatic naphtha
HAPs	Hazardous Air Pollutant
HC	Hydrocarbon
HCFC	Hydrochlorofluorocarbon
HGB	Houston-Galveston-Brazoria
HON	Hazardous Organic NESHAP
HOV	High-Occupancy Vehicle
HRVOC	Highly Reactive Volatile Organic Carbon
HVLP	High-volume, low-pressure
ID	Identification
ILEV	Inherently low-emission vehicle
IRON-PIG	Incremental Reactions for Organics and NO _x Plume in Grid
ISC	Industrial source complex
ISCST	Industrial source complex short-term
ISCLT	Industrial source complex long-term
ISO	International Standards Organization
IUPAC	International Union of Pure and Applied Chemistry
JAC	Joint Advisory Committee for the Improvement of Air Quality
Kg	Kilogram
L	Liter
LAB	Laboratory
LAEEM	Landfill Air Emissions Estimation Model
LAER	Lowest achievable emission rate
Lb	Pound
LEADS	Leading Environmental Analysis and Display System
LEV	Low-emission vehicle
LPST	Leaking petroleum storage tanks
LTTO	Landing, taxi, and takeoff
LUST	Leaking underground storage tanks
MACT	Maximum available control technology
MAERT	Maximum Allowable Emission Rate Table
MDERC	Mobile discrete emission reduction credit
MERC	Mobile emission reduction credit
MIR	(Carter) maximum incremental reactivity (conversion factor)
MH	Mixing height
mL	millilambert
ml	Milliliter
MM5	Mesoscale Model version 5
MMBtu	Million British thermal units
MPO	Metropolitan Planning Organization

MRF	Medium range forecast
MS	Mobile Source
MSA	Metropolitan statistical area
MSDS	Material Safety Data Sheet
MSS	Maintenance, startup, and shutdown
MTBE	methyl tertiary-butyl ether
MW	megawatt
NAPAP	National Acid Precipitation and Assessment Program
NAA	Nonattainment area
NAAQS	National Ambient Air Quality Standards
NAAS	National Air Audit System
NADP	National Atmospheric Deposition Program
NAMS	National air monitoring station
NAQTS	National air quality trend station
NAR	Nonattainment review
NASN	National Air Surveillance Network
NCAMS	Noncontinuous air monitoring station
NCAR	National Center for Atmospheric Research
NCP	National contingency plan or noncriteria pollutant
NEI	National Emissions Inventory
NEDS	National Emissions Data System
NEIIF	National Emissions Inventory Input Format
NEPA	National Environmental Policy Act
NESCAUM	Northeast States for Coordinated Air Use Management
NESHAPS	National Emission Standards for Hazardous Air Pollutants
NMIM	National Mobile Inventory Model
NIST	National Institute of Standards and Technology
NMOC	nonmethane organic carbon
NMVOC	Nonmethane VOC
NO _x	Nitrogen oxides
NOAA	National Oceanic and Atmospheric Administration
NPS	nonpoint source
NSPS	New Source Performance Standards
NSR	New Source Review
NO _x	Nitrogen Oxides
NSPS	New Source Performance Standard
OAQPS	Office of Air Quality Planning and Standards
ORD	Office of Research and Development
O ₃	Ozone
OBD	On-board diagnostic
PAH	Polycyclic aromatic hydrocarbon
PAMS	Photochemical air monitoring stations
PAN	Peroxyacetyl nitrate
PAQCS	Potential air quality control strategy
Pb	Lead
PBR	Permit by rule (formerly “standard exemption”)

PBL	Planetary boundary layer
PdN	Paso del Norte
PIG	Plume in grid
PM	Particulate matter
PM ₁₀	PM with an aerodynamic diameter of 10 micrometers or less
PM _{2.5}	PM with an aerodynamic diameter of 2.5 micrometers or less
PMI	Preventive maintenance instructions
PMR	Pollutant mass rate
PMSA	Primary Metropolitan Statistical Area
POHC	Principal organic hazardous constituent
PPB	Parts per billion
PPMv	Parts per million - volume
PPM	Parts per million
PPMv	Parts per million - volume
PSD	Prevention of significant deterioration
PSDB	Point source database
PSI	Pollutant Standard Index
PSEI	Point Source Emissions Inventory
PVC	Polyvinyl chloride
QA	Quality assurance
QAPP	Quality assurance project plan
QC	Quality control
QMP	Quality management plan
RACM	Reasonably Available Control Measures
RACT	Reasonably Available Control Technology
RE	Rule effectiveness
RHC	Reactive hydrocarbons
ROP	Rate of progress
ROG	Reactive organic gas
RP	Rule penetration
RRF	Relative reduction factor
RRTM	Rapid radiative transfer model
RSD	Resultant standard deviation
RVP	Reid vapor pressure
RXN	Reaction
SA	San Antonio
SAF	Seasonal activity factor
SAMS	SIP air pollutant inventory management system
SAP	Secondary air pollutant
SAPRC	Statewide Air Pollution Research Center
SARA	Superfund Amendments and Reauthorization Act
SAROAD	Storage and retrieval of aerometric data
SCAQMD	South Coast Air Quality Management District (in California)
SCC	Source category code or source classification code
SCCM	Standard cubic centimeters per minute
SCFM	Standard cubic feet per minute

SD	Standard deviation
SE	Standard error
SEMARNAT	Secretaría de Medio Ambiente y Recursos Naturales (in Mexico)
SVOC	Semi-volatile organic carbon
SIC	Source Identification Code or Standard Industrial Classification
SIMS	Surface Impoundment Modeling System
SIP	State Implementation Plan
SLAMS	State and local air monitoring station
SLPM	Standard liters per minute
SMSA	Standard metropolitan statistical area
SOCMI	Synthetic Organic Chemical Manufacturing Industry
SODAR	Sonic detection and ranging
SO ₂	Sulfur dioxide
SPM	Special-purpose monitoring
SPNSS	Standards of performance for new stationary sources
SRM	Standard reference material
SRU	Sulfur recovery unit
STARS	State of Texas Air Reporting System
STEERS	State of Texas Environmental Electronic Reporting System
TAC	Texas Administrative Code
TASN	Texas Air Sampling Network
TBA	Tertiary-butyl alcohol
TCEQ	Texas Commission on Environmental Quality
TDF	Tire derived fuel
TERP	Texas Emissions Reduction Program
THC	Total hydrocarbons
TIGER	Topologically Integrated Geographic Encoding and Referencing
TIP	Transportation Improvement Program
TLV	(Health) threshold limit value
TNRIS	Texas Natural Resources Information System
TOC	Total organic carbon
TPY	Tons per year
TRB	Transportation Research Board
TRI	Toxics Release Inventory
TRIS	Toxics release information system
TxLED	Texas low emission diesel
TSD	Technical support documents
TSCA	Toxic Substances Control Act
TSDF	Treatment, storage, and disposal facility
TTI	Texas Transportation Institute
U/M	Upset and Maintenance
UAM	Urban Airshed Model
ULEV	Ultralow Emission Vehicle
UMTA	Urban Mass Transit Administration
U.S.	United States

USDA	U.S. Department of Agriculture
USDOT	U.S. Department of Transportation
USGS	U.S. Geological Survey
USOMB	U.S. Office of Management and Budget
USSCS	U. S. Soil Conservation Service
UST	Underground storage tank
UTM	Universal Transverse Mercator
VAC	Volts alternating current
VDC	Volts direct current
VIN	Vehicle or Vendor Identification Number
VKT	Vehicle Kilometers Traveled
VMT	Vehicle Miles Traveled
VOC	Volatile organic compound
VRS	Vapor recovery system
VTCS	Vernon's Texas Civil Statutes
WD	Wind direction
WGA	Western Governors Association
WS	Wind speed
WDR	Wind direction resultant
WSR	Wind speed resultant
XATEF	Crosswalk/Air Toxic Emission Factor Database
ZEV	Zero emission vehicle

Appendix 2: Chemical Species Assessed by CAMx

Species Name	Description	Molecular Weight	HRVOC	EI	CAMx Output
O3	Ozone	48			yes
CO	Carbon monoxide	28		yes	yes
SO2	Sulfur dioxide	64		yes	yes
NO	Nitric oxide	30		yes	yes
NO2	Nitrogen dioxide	46		yes	yes
NO3	Nitrate radical	62			yes
N2O5	Dinitrogen pentoxide	108			yes
HNO3	Nitric acid				yes
HONO	Nitrous acid				yes
PAN	Peroxyacetyl Nitrate	32			yes
PNA	Peroxynitric acid				
NTR	Organic nitrates	16			
NOx	NO + NO2				
NOy	NO + NO2 + HNO3 + HONO + PNA + PAN + NO3 + 2*N2O5 + NTR				
NOz	HNO3 + HONO + PNA + PAN + NXOY + NTR				
Ox	O3 + NO2				
AACD	Acetic acid	32			
ACET		58		yes	
ALD2	Acetaldehyde	44		yes	yes
ALDX	Propionaldehyde and higher aldehydes	44		yes	yes
BENZ	Benzene	78		yes	yes
BZO2	Peroxy radical from OH addition to benzene	96			
C2O3	Acetylperoxy radical	32			
CAO2	Peroxy radical from aromatic degradation products				
CAT1	Methyl-catechols	112	√		yes
CH4	Methane	16		yes	
CRES	Cresols	128			yes
ETH	Ethene	28		yes	yes
ETHA	Ethane	30		yes	yes
ETHY	Ethyne (Acetylene)	26		yes	yes
ETOH	Ethanol	46		yes	yes
FORM	Formaldehyde (HCHO)	30	√	yes	yes
H2O2	Hydrogen peroxide	34			yes

Species Name	Description	Molecular Weight	HRVOC	EI	CAMx Output
IOLE	Internal olefin carbon bond (R-C=C-R)	56		yes	yes
ISO2	Peroxy radical from OH addition to isoprene				
ISOP	Isoprene	68	√	yes	yes
KET	Ketone carbon bond (C=O)	28		yes	yes
MEO2	Methylperoxy radical	16			
MEOH	Methanol	32		yes	yes
MEPX	Methylhydroperoxide	16			
MGLY	Methylglyoxal	48			yes
O	Oxygen atom in the O3(P) electronic state				
O1D	Oxygen atom in the O1(D) electronic state				
O2	Oxygen				
OH	Hydroxyl radical				
OLE	Terminal olefin carbon bond (R-C=C)	28		yes	yes
OPAN	Peroxyacyl nitrate (PAN compound) from OPO3				
OPEN	Aromatic ring opening product (unsaturated dicarbonyl)	64			yes
OPO3	Peroxyacyl radical from OPEN				
PACD	Peroxyacetic and higher peroxydicarboxylic acids	32			
PANX	C3 and higher peroxyacyl nitrate	32			yes
PAR	Paraffin carbon bond (C-C)	14.5		yes	yes
PRPA	Propane	44		yes	yes
RO2	Operator to approximate total peroxy radical concentration				
ROOH	Higher organic peroxide				
ROR	Secondary alkoxy radical				
SULF	Sulfuric acid (gaseous)				
TERP	Monoterpenes	136		yes	yes
TO2	Peroxy radical from OH addition to TOL	92			
TOL	Toluene and other monoalkyl aromatics	92	√	yes	yes
XLO2	Peroxy radical from OH addition to XYL				
XO2	NO to NO2 conversion from alkylperoxy (RO2) radical				
XO2H	NO to NO2 conversion (XO2) accompanied by HO2 production				

Species Name	Description	Molecular Weight	HRVOC	EI	CAMx Output
XO2N	NO to organic nitrate conversion from alkylperoxy (RO2) radical				
XYL	Xylene and other polyalkyl aromatics	106	v	yes	yes
NR	Nonreactive organic product	16		yes	
NASN	Not assigned organic product	1		yes	

Appendix 3: List of Auto GC Volatile Organic Compounds

Compound Name	CAN	CARB	AGC	Compound Name	CAN	CARB	AGC
1,1,2,2-Tetrachloroethane (ppbv) <43818>				Dichlorodifluoromethane (ppbv) <43823>			
1,2-Trichloroethane (ppbv) <43820>				Dichloromethane (ppbv) <43802>			
1,1-Dichloroethane (ppbv) <43813>				Ethane (ppbv) <43202>			
1,1-Dichloroethylene (ppbv) <43826>				Ethyl Acetate (ppbv) <43209>			
1,2,3-Trimethylbenzene (ppbv) <45225>	✓		✓	Ethylbenzene (ppbv) <45203>			
1,2,4-Trimethylbenzene (ppbv) <45208>	✓		✓	Ethylene (ppbv) <43203>	✓		✓
1,2-Dichloropropane (ppbv) <43829>				Ethylene Dibromide (ppbv) <43843>			
1,3,5-Trimethylbenzene (ppbv) <45207>				Ethylene Dichloride (ppbv) <43815>			
1,3-Butadiene (ppbv) <43218>	✓		✓	Formaldehyde		✓	
1-Butene (ppbv) <43280>	✓		✓	Isobutane (ppbv) <43214>			
1-Heptene (ppbv) <43328>				Isobutyraldehyde (ppbv) <43512>		✓	
1-Hexene & 2-Methyl-1-Pentene (ppbv) <43173>	✓		✓	Isopentane (ppbv) <43221>			
1-Pentene (ppbv) <43224>	✓		✓	Isoprene (ppbv) <43243>	✓		✓
2,2,4-Trimethylpentane (ppbv) <43250>				Isopropylbenzene (ppbv) <45210>			
2,2-Dimethylbutane (ppbv) <43244>				M-Diethylbenzene (ppbv) <45218>			
2,3,4-Trimethylpentane (ppbv) <43252>				M-Ethyltoluene (ppbv) <45212>			
2,3-Dimethylbutane (ppbv) <43284>				M/P Xylene (ppbv) <45109>	✓		✓
2,3-Dimethylpentane (ppbv) <43291>				Methyl Butyl Ketone (ppbv) <43559>			
2,4-Dimethylpentane (ppbv) <43247>				Methyl Chloroform (ppbv) <43814>			
2-Chloropentane (ppbv) <43331>				Methyl Ethyl Ketone (ppbv) <43552>			
2-Methyl-1-Pentene (ppbv) <43246>				Methyl Isoamyl Ketone (ppbv) <16521>			
2-Methyl-2-Butene (ppbv) <43228>	✓		✓	Methyl Isobutyl Ketone (ppbv) <43560>			
2-Methyl-3-Hexanone (ppbv) <43564>				Methyl Tert-Butyl Ether (ppbv) <43372>			
2-Methylheptane (ppbv) <43960>				Methylcyclohexane (ppbv) <43261>			
2-Methylhexane (ppbv) <43263>				Methylcyclopentane (ppbv) <43262>			
2-Methylpentane (ppbv) <43285>				N-Butane (ppbv) <43212>			
3-Heptanone (ppbv) <43563>				N-Decane (ppbv) <43238>			
3-Hexanone (ppbv) <43557>				N-Heptane (ppbv) <43232>			
3-Methyl-1-Butene (ppbv) <43282>	✓			N-Hexane (ppbv) <43231>			
3-Methylheptane (ppbv) <43253>				N-Nonane (ppbv) <43235>			
3-Methylhexane (ppbv) <43249>							

Compound Name	CAN	CARB	AGC	Compound Name	CAN	CARB	AGC
3-Methylpentane (ppbv) <43230>				N-Octane (ppbv) <43233>			
3-Pentanone (ppbv) <43553>				N-Pentane (ppbv) <43220>			
4-Methyl-1-Pentene (ppbv) <43234>				N-Propyl Acetate (ppbv) <43434>			
Acetylene (ppbv) <43206>	✓		✓	N-Propylbenzene (ppbv) <45209>			
Acrolein - Unverified (ppbv) <43505>		✓		N-Undecane (ppbv) <43954>			
Alpha.-Pinene (ppbv) <43256>	NO DATA						
Benzene (ppbv) <45201>				O-Xylene (ppbv) <45204>	✓		✓
Beta.-Pinene (ppbv) <43257>	NO DATA						
Bromomethane (ppbv) <43819>				P-Ethyltoluene (ppbv) <45213>			
Butyl Acetate (ppbv) <43514>				Propane (ppbv) <43204>			
Butyraldehyde (ppbv) <43510>	✓	✓		Propylene (ppbv) <43205>	✓		✓
Carbon Disulfide (ppbv) <42153>				Styrene (ppbv) <45220>			
Carbon Tetrachloride (ppbv) <43804>				Sum Of Pams Target Compounds (ppb C) <43000>			
Chlorobenzene (ppbv) <45801>				Tetrachloroethylene (ppbv) <43817>			
Chloroform (ppbv) <43803>				Toluene (ppbv) <45202>	✓		✓
Chloromethane (ppbv) <43801>				Total Nmoc (ppb C) <43102>			
Chloroprene (ppbv) <43835>				Trans-1,3-Dichloropropene (ppbv) <43830>			
Cis-1,3-Dichloropropene (ppbv) <43831>				Trans-2-Butene (ppbv) <43216>	✓		✓
Cis-2-Butene (ppbv) <43217>	✓		✓	Trans-2-Hexene (ppbv) <43289>			
Cis-2-Hexene (ppbv) <43290>				Trans-2-Pentene (ppbv) <43226>	✓		✓
Cis-2-Pentene (ppbv) <43227>	✓		✓	Trichloroethylene (ppbv) <43824>			
Cyclohexane (ppbv) <43248>				Trichlorofluoromethane (ppbv) <43811>			
Cyclopentane (ppbv) <43242>				Vinyl Chloride (ppbv) <43860>			

Chemical specie which are shaded in green represent highly reactive volatile organic compounds (HRVOC) which contribute to rapid ozone formation. VOCs sampled and monitored at the various EL Paso CAMS and nonconituous air monitoring stations (NCAMS) are collected through the following three methods: auto gas-chromatograph (AGC), carbonyl cartridge (CARB) and summa canister (CAN)

Appendix 4: 7-Digit Source Classification Code Table

SCC7	SCC7 Description
2102004	INDUSTRIAL FUEL COMBUSTION: DISTILLATE OIL: BOILERS/IC ENG.
2102005	INDUSTRIAL FUEL COMBUSTION: RESIDUAL OIL
2102006	INDUSTRIAL FUEL COMBUSTION: NATURAL GAS: BOILERS/IC ENG.
2102007	INDUSTRIAL FUEL COMBUSTION: LIQUIFIED PETROLEUM GAS (LPG)
2102011	INDUSTRIAL FUEL COMBUSTION: KEROSENE
2103006	COMMERCIAL/INSTITUTIONAL FUEL COMBUSTION: NATURAL GAS
2103007	COMMERCIAL/INSTITUTIONAL FUEL COMBUSTION: LPG
2103011	COMMERCIAL/INSTITUTIONAL FUEL COMBUSTION: KEROSENE COMBUSTORS
2104006	RESIDENTIAL FUEL COMBUSTION: NATURAL GAS ALL COMBUSTORS
2104007	RESIDENTIAL FUEL COMBUSTION: LIQUIFIED PETROLEUM GAS (LPG)
2104008	RESIDENTIAL WOOD COMBUSTION: FIREPLACES
2294000	PAVED ROADS: ALL PAVED ROADS: TOTAL: FUGITIVES
2311010	GENERAL BUILDING CONSTRUCTION: TOTAL
2311020	HEAVY CONSTRUCTION: TOTAL
2311030	ROAD CONSTRUCTION: TOTAL
2325000	MINING & QUARRYING: ALL PROCESSES
2401001	ARCHITECTURAL COATINGS: TOTAL: ALL SOLVENT TYPES
2401025	METAL FURNITURE: TOTAL: ALL SOLVENT TYPES
2401060	LARGE APPLIANCES: TOTAL: ALL SOLVENT TYPES
2401200	SPECIAL PURPOSE: TOTAL: ALL SOLVENT TYPES
2440020	MISC. INDUSTRIAL: TOTAL: ALL SOLVENT TYPES
2460100	CONSUMER/COMMERCIAL: ALL PERSONAL CARE PRODUCTS
2501060	PETROLEUM PRODUCTS: GASOLINE SVC STATIONS: STAGE 1, 2 & Filling
2610000	OPEN BURNING: ALL CATEGORIES: LAND CLEARING
2610030	WASTE DISPOSAL TREATMENT & LANDFILLS: MUNICIPAL
2630020	WASTEWATER TREATMENT: TOTAL PROCESSED: PUBLIC OWNED
2801000	AGRICULTURE: CROPS: TOTAL
2801700	AGRICULTURE: FERTILIZER APPLICATION: ANHYDROUS AMMONIA
2805001	AGRICULTURE: BEEF CATTLE FEEDLOTS: CONFINEMENT
2805003	AGRICULTURE: BEEF CATTLE PASTURE/RANGE: CONFINEMENT
2805018	AGRICULTURE: DAIRY CATTLE: COMPOSITE:NEC
2805019	AGRICULTURE: DAIRY CATTLE: FLUSH DAIRY: CONFINEMENT
2805021	AGRICULTURE: DAIRY CATTLE: SCRAPE DAIRY: CONFINEMENT
2805023	AGRICULTURE: DAIRY CATTLE: DRYLOT/PASTURE DAIRY: CONFINEMENT
2806010	DOMESTIC ANIMALS: WASTE EMISSIONS: CATS: TOTAL
2806015	DOMESTIC ANIMALS: WASTE EMISSIONS: DOGS: TOTAL
2810020	OTHER COMBUSTION: PERSCRIBED BURNING OF RANGELAND

Appendix 5: WRF Meteorology Applied to CAMx Modeling

WRF 4 km Meteorology

WRF 4 km outputs covering the PdN region were prepared for the dates 12 June, 2006 at 1200 hrs UTC to 22 June, 2006 at 1200 UTC. The WRF domain covered 97x97 grid cells with 34 vertical layers in an LCC projection centered at 31.7°N, -106.4°W and true latitudes at 33°N and 45°N. Time-shifting was applied to output hourly data from 0600 hrs CST on 13 June, 2006 to 0000 hrs CST on 22 June, 2006. Figure A5.1 illustrates the WRF domain developed for the PdN region. The mesoscale meteorology developed for this report extends from eastern California to east Texas and from Durango and the southernmost point of Baja California, Mexico to the northern boundaries of Colorado and Kansas.

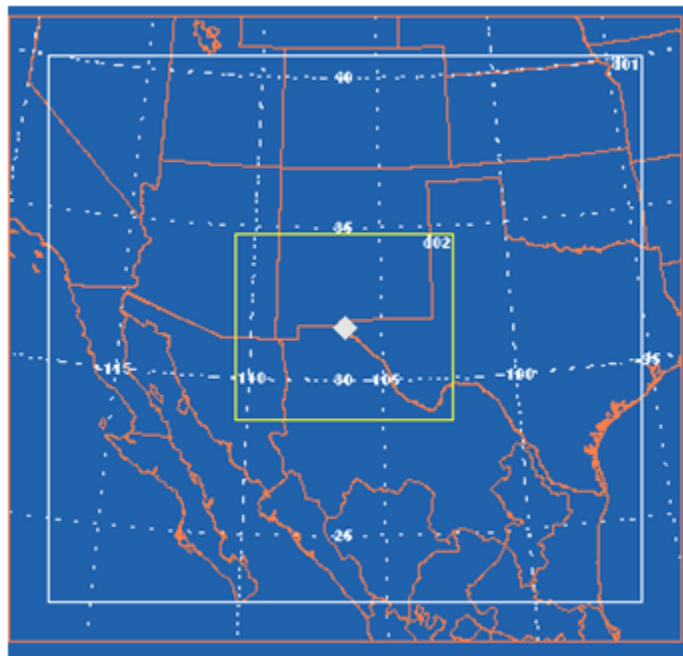


Figure A5.1 UTEP-WRF Domain Centered over the PdN Region

The UTEP WRF domain established the center in PdN region while the TCEQ 36-12-4 domain sets El Paso very near to the western boundary of the 12 km domain as indicated in Figure A5.2.

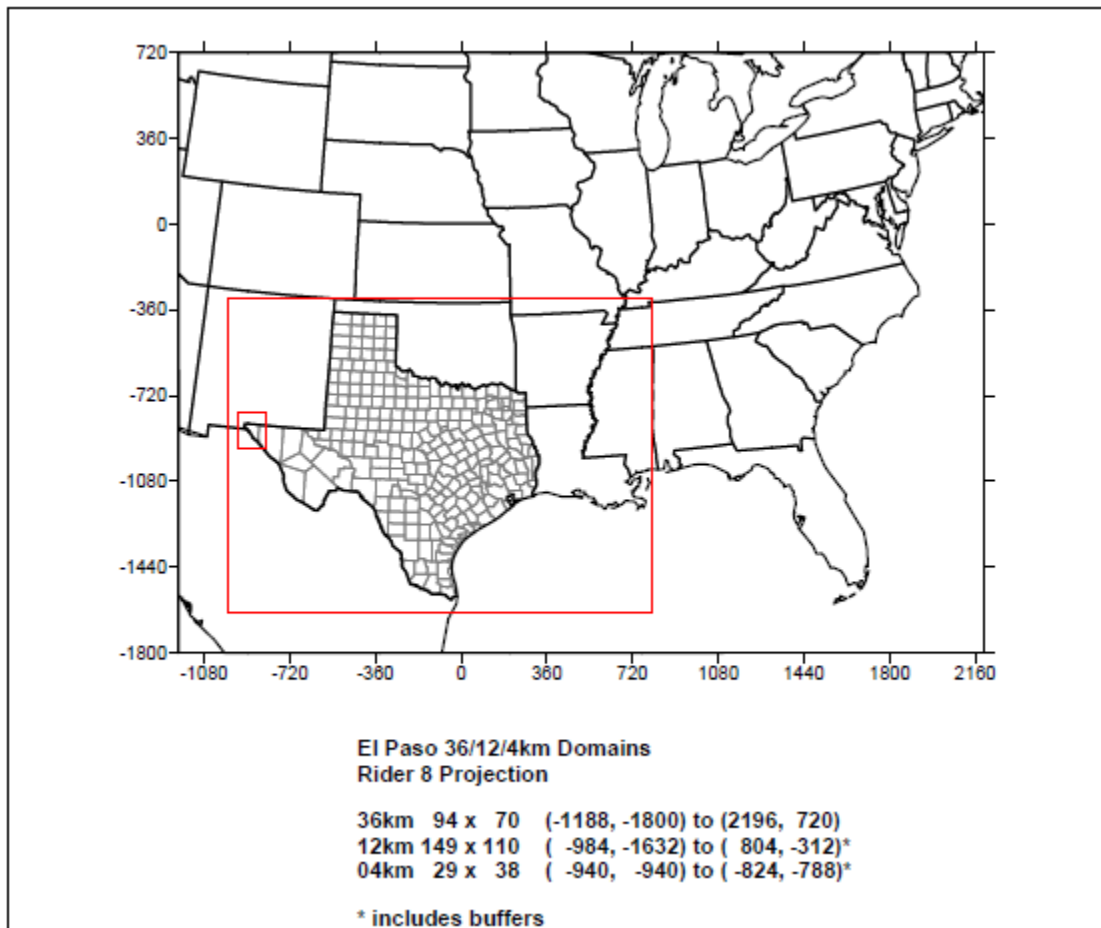


Figure A5.2 TCEQ - WRF Domain Centered over the East Texas

The data incorporated into the WRF model as initial and lateral boundary conditions are obtained from a NCEP Final Analysis (FNL) dataset with a 6 hour interval. This is the global dataset in the format of the grid with the resolution of $1 \times 1^\circ$. WRF Physics Options that were selected are:

- Microphysics option: WSM 3-class simple ice scheme;
- Surface-layer option: Monin-Obukhov.
- Land-surface option: thermal diffusion scheme;
- PBL: YSU scheme;
- Cumulus option: Grell-Devenyi ensemble scheme; and
- Four Dimensional Data Assimilation (FDDA) is grid (or analysis) nudging.

A WRF simulation was established for the period June 12-21, 2006. This episode showed high pressure aloft with subsidence causing warming and drying with maximum solar irradiance which is favorable for ozone formation. The strong inversion trapped the pollutants with light, stagnant conditions observed during the middle of a string of 8 consecutive days. Stagnant conditions were most pronounced on 18 June when daytime temperatures were over 100°F and peaked at 103°F.

The synoptic weather events were typical for elevated surface ozone concentrations produced in the heavily suppressed stagnant air. The movement of the subtropical high pressure system determined the direction and intensity of the annual monsoon season in the Borderland (June 15 - September 30). Figure A5.3 shows the H5 subtropical high immediately to the south of the PdN region causing considerable subsidence (downward vertical velocity) which with clear skies, high maximum temperatures, and light low level winds creases and traps high levels of ozone on 18 June.

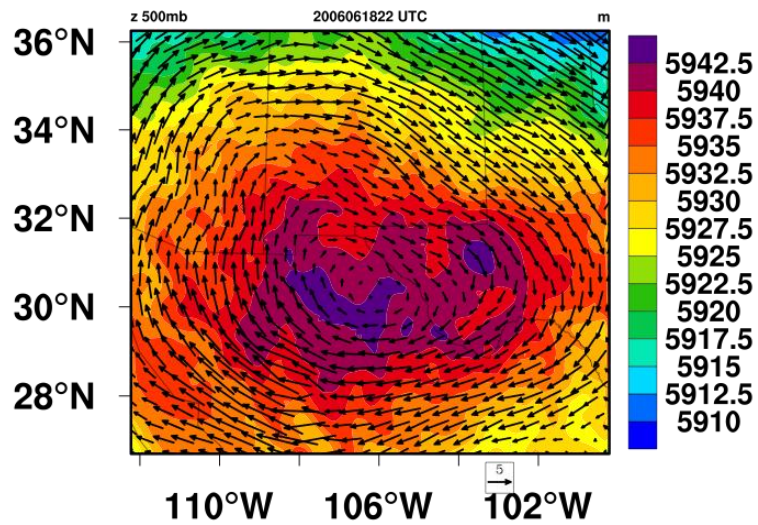


Figure A5.3 Geopotential Height at 500 mb

Figure A5.4 depicts pressure gradients at 850 mb, on 18 June. The white regions observed in Figure A5.4 correspond to mountainous areas.

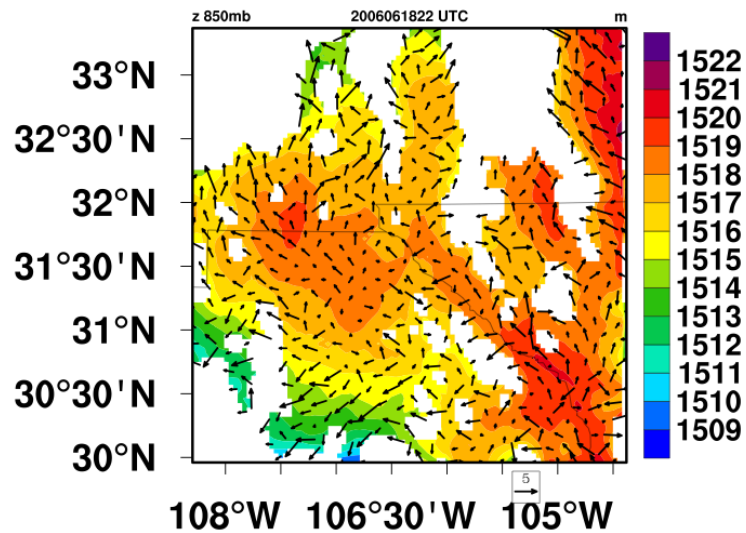


Figure A5.4 Z_850mb at 22UTC, June 18, 2006, 4 km resolution

High temperatures observed across the 36 km domain for 18 June are presented in Figure A5.5, the highest ozone day during the 10-day episode. Elevated temperatures over the PdN region are apparent.

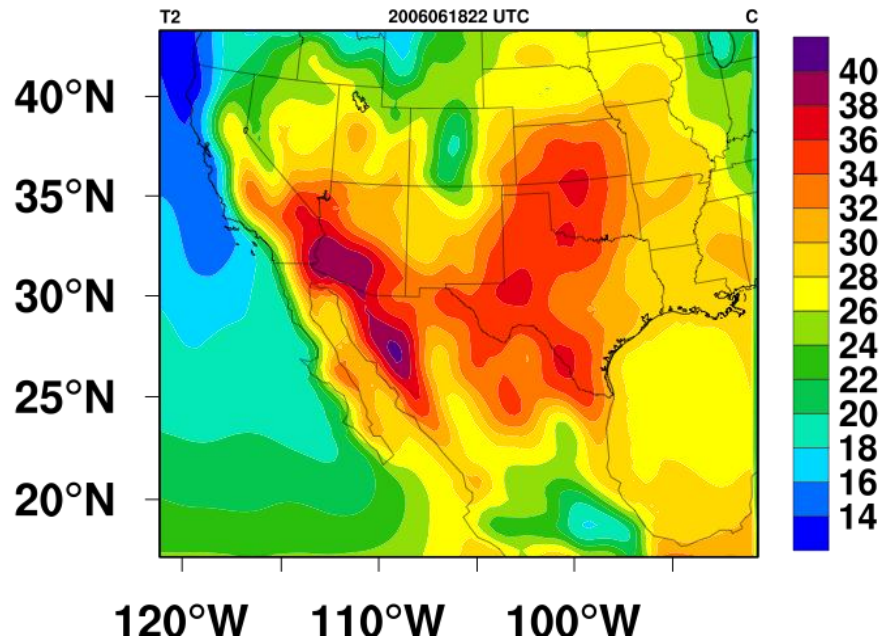


Figure A5.5 Temperature at 2m height above surface at 22 UTC, June 18, 2006, 36 km resolution

Weak surface pressure gradients are observed on Figure A5.6 for the sea level pressure graph in the 4 km PdN domain.

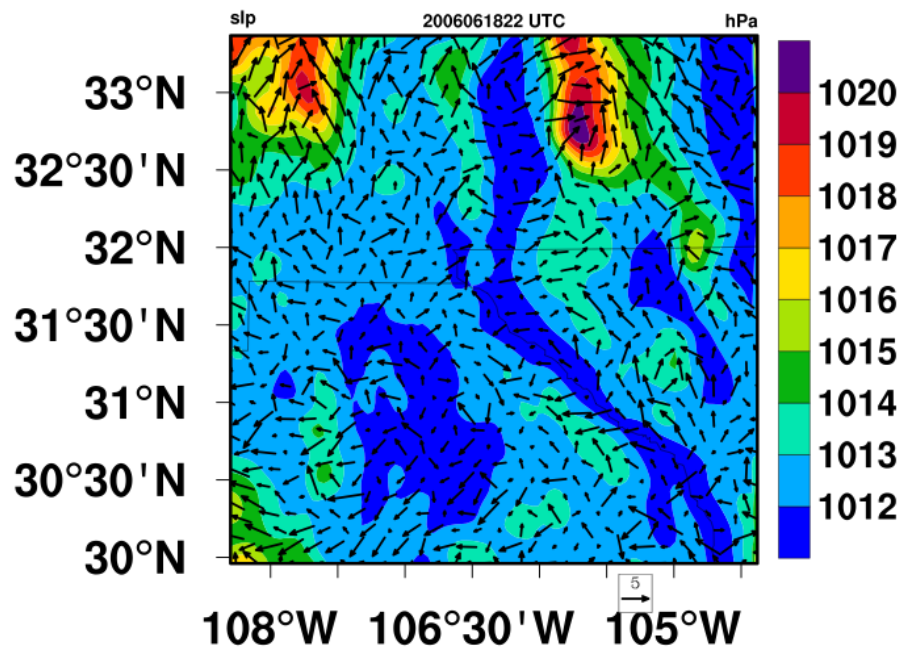


Figure A5.6 Sea level Pressure at 22 UTC, June 18, 2006

Figure A5.7 depicts the low relative humidity pocket coinciding with the center of the high pressure ridge over the PdN region. This corresponds to subsiding air which warms dry air adiabatically at 5.5°F / 1000ft and the dew point decreases at 4°F / 1000ft. Conditions such as these create pockets of minimal relative humidity. RH in Figure 11.9 is plotted over the 12 km domain at 2200 UTC on 18 June.

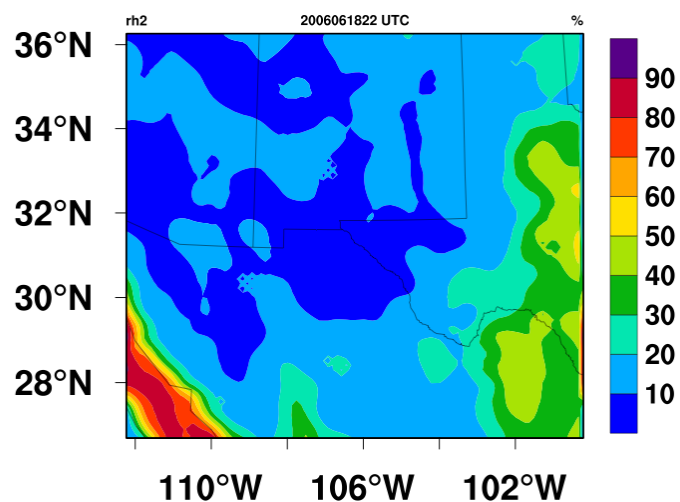


Figure A5.7 Relative Humidity at 2 M Height

Figure A5.8 illustrates the Planetary Boundary Layer (PBL) Height to be lower for the PdN region on 18 June. A low PBL is another major contributing factor to the high ozone values observed on that day.

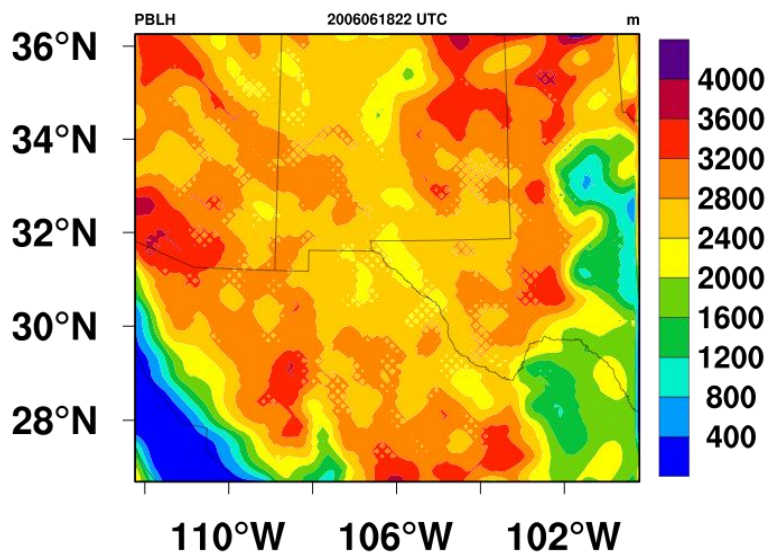


Figure A5.8 PBL Height at 22 UTC on June 18, 12 km resolution

PBL height for 16 June and 18 June are plotted in Figures A5.9a and A5.9b. Ozone concentrations on 16 June were much lower than 18 June. The observed rise of the PBL on the time series graph corresponds with the solar elevation angle and the corresponding rise of temperature. PBL Height on 18 June was much lower indicating a compact inversion layer which lasted during most of the morning hours.

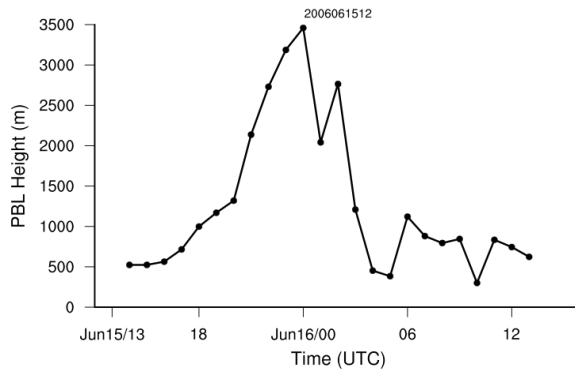


Figure A5.9a PBL on 16 June

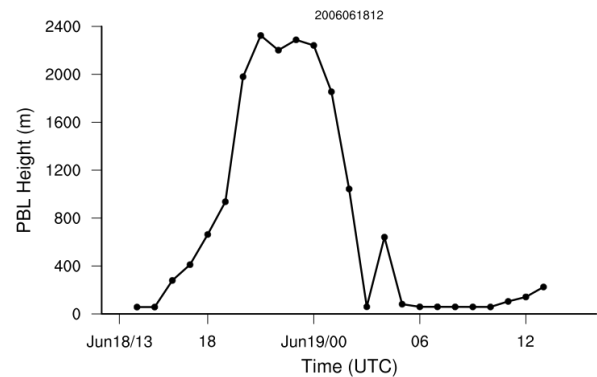


Figure A5.9b PBL on 18 June

Figure A5.9 PBL Height on June 16 and June 18 at C12

WRF performance was evaluated by comparing predicted and observed meteorological parameters obtained at local CAMS. Figure A5.10 depicts WRF predicted wind speed (WS) vs. WS observed at C41 for the period of June 12-21, 2006. WS predicted by WRF appears to track the time-series observed WS fairly well. A pairwise scatterplot comparing WRF WS and C41 WS indicates moderate correlation ($R = 0.34$) as indicated in Figure 11.13.

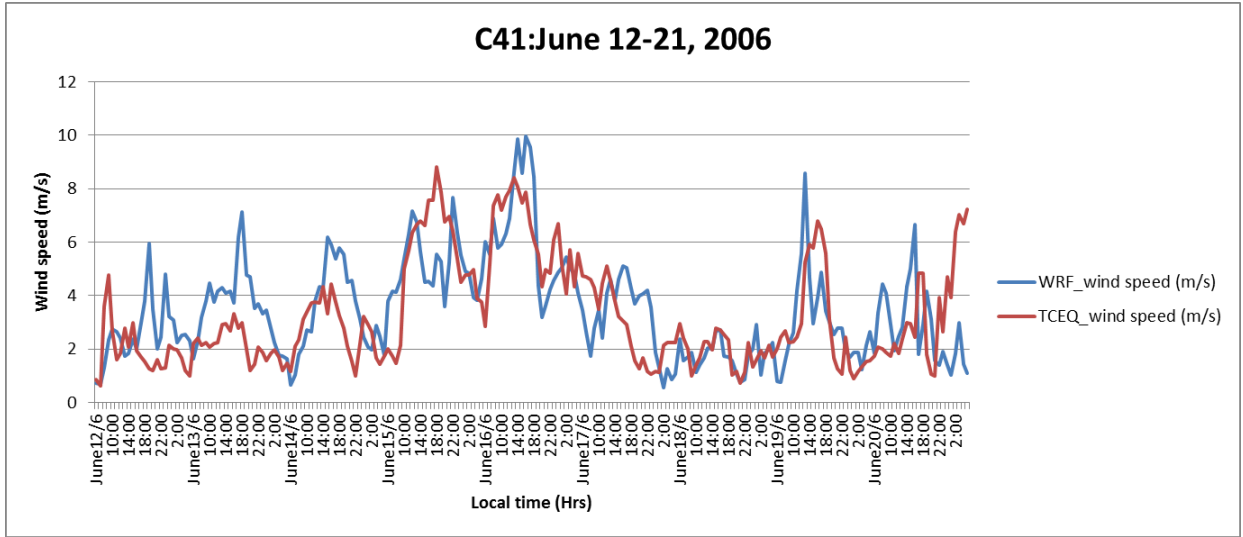


Figure A5.10 WRF Predicted vs. Observed WS at C41(m/s)

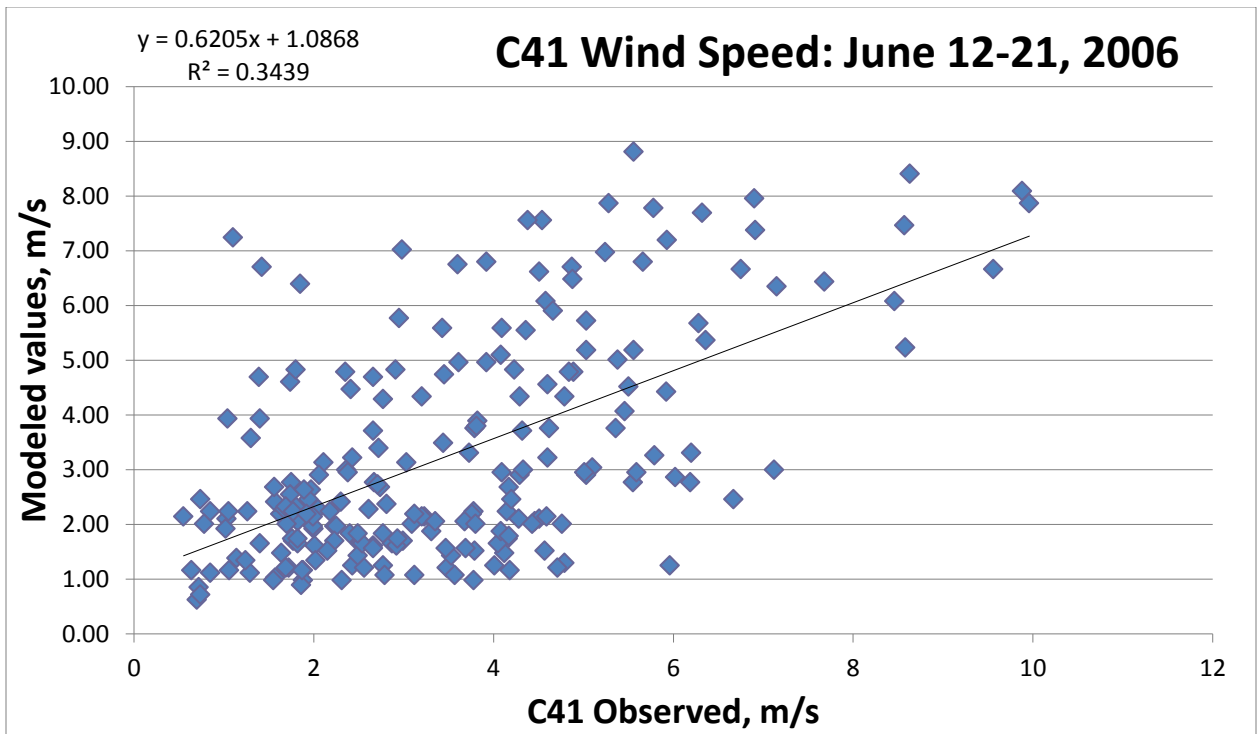


Figure A5.11 Pairwise Scatterplot of WRF predicted and C41 Observed Wind Speed (m/s)

Figure A5.12 shows a time-series plot of WRF predicted and C41 observed temperature data. The plots appear to track very well.

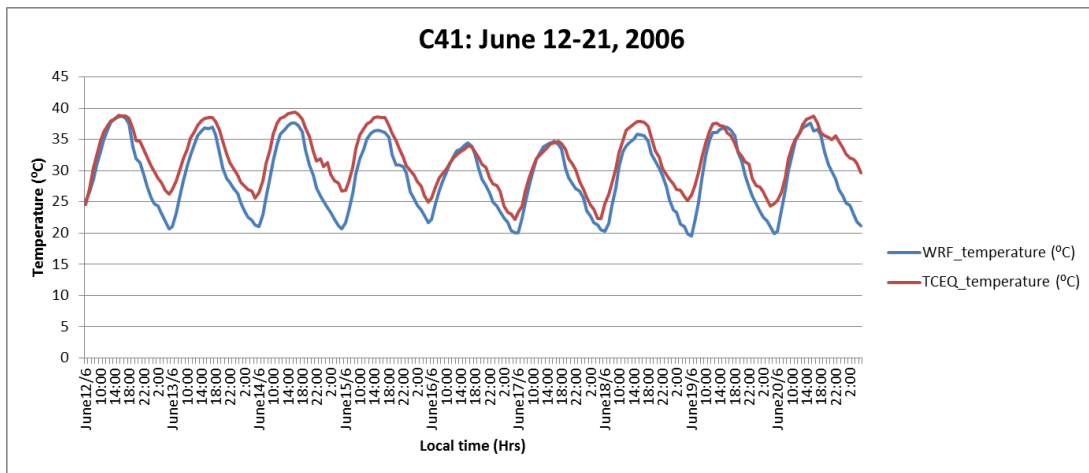


Figure A5.12 Time-series Plot of WRF Wind Speed vs. C41 Temperature (°C)

Figure A5.13 presents a pairwise scatterplot of WRF and C41 temperature data. The observed and predicted temperature variable correlates very well ($R^2=0.88$). An examination of the synoptic and local meteorology for the June 12-21, 2006 ozone episode was conducted to assess the manner in which meteorological parameters influence the formation, transport and dispersion of ozone in the PdN region. The predominant synoptic feature of the day which observed an ozone event was the expansion, intensification, and slow progression of an upper-level high pressure ridge. This meteorological event consisting of highly stable atmospheres, strong temperature inversions with low mixing heights and therefore low mixing volumes is known to be associated high ozone events.

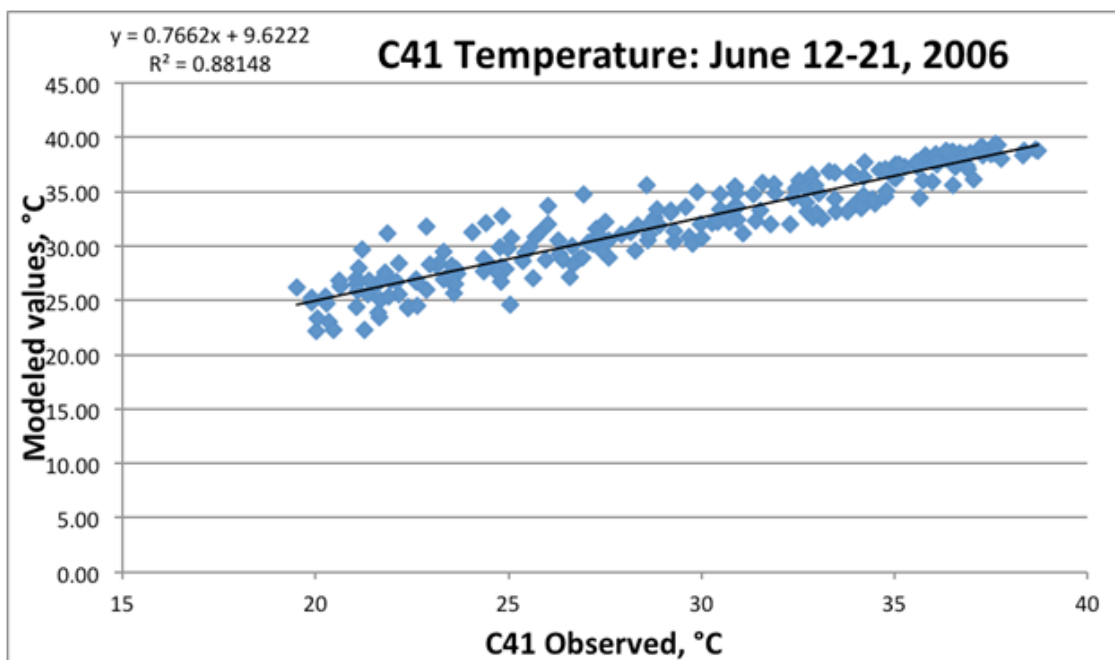


Figure A5.13 Pairwise Scatterplot of WRF Predicted vs C41Observed Temperature (°C)

This type of synoptic event can best be illustrated by reviewing the characteristics of the 500 mb constant pressure pattern over the western USA and other associated sub-synoptic patterns is indicated in Figure A5.3. There is an evident anticyclone observed near the PdN region which introduced aloft warming and increased atmospheric stability over the region. At the lower level, weak surface pressure gradients were also found to be associated with these synoptic high pressure conditions as indicated in Figure A5.6. Highly stable atmospheric conditions combined to favor the formation of elevated ozone concentrations on 18 June. Fair weather with weak surface winds was observed and therefore, horizontal dispersion and dilution were relatively weak. Maximum surface temperatures across the PdN region were near 33°C as indicated in Figure A5.5

Figure A5.7 shows surface relative humidity distribution from the 12 km domain. A dry area was found around the study region especially the southern El Paso-Juárez area. Lower relative humidity near the surface can be partly attributed to adiabatic heating due to small scale local downdrafts, which will lead to stronger temperature inversions. The resulting increase in atmospheric stability will suppress the vertical mixing process and cause lower level pollutants to be trapped near the ground. Historically, maximum daytime mixing heights have often been considered to be proportional to the mixing volume. Figure 11.11 illustrates the time series of PBL height on 18 June, 2006, a high ozone day, and 16 June, 2006, a low ozone day. The model provides very good simulations for diurnal variations of PBL height on both days. WRF simulation findings are that low mixing heights play an important role in the high ozone concentrations observed in the PdN region. When the PBL mixing height is shallow, ozone and its precursors are confined to a smaller volume than with a deeper mixed layer. The reduced mixing volume tends to keep precursor emissions concentrated near the ground.

WRFCAMx Preprocessing

The WRF model established 34 vertical layers identified as UTEP WRF Layers. CAMx data pre-processing involves applying WRFCAMx which converts WRF data into CAMx-ready meteorological input files. The 34 UTEP WRF layers are aggregated by WRFCAMx into 22 CAMx vertical layers over the 4 km domain using a density weighting method. Table A5.1 identifies the UTEP WRF and CAMx-ready vertical structure. This WRF domain was prepared by UTEP in order to address issues inherent in the TCEQ 36-12-4 domain.

Table A5.1 UTEP WRF CAMx Vertical Layer Structure

UTEP WRF Layer	Layer Top (m AGL)	CAMx Layer	Thickness (m)
34	19052		
33	17960		
32	17014		
31	16152		
30	15386	22	3605
29	14641		
28	13918		
27	13213	21	2841
26	12495		
25	11781		
24	11072		
23	10372	20	2121
22	9670		
21	8959		
20	8251	19	1432
19	7539		
18	6819	18	721
17	6098	17	725
16	5373	16	690
15	4683	15	638
14	4045	14	595
13	3450	13	542
12	2908	12	498
11	2410	11	450
10	1960	10	395
9	1565	9	349
8	1216	8	297
7	919	7	244
6	675	6	199
5	476	5	157
4	319	4	123
3	196	3	97
2	99	2	70
1	29	1	29

A vertical layer mapping structure was prepared by TCEQ for the 36-12-4 km continent-wide modeling domain, but it was not applied to the simulations conducted

for this report since simulation runtime extends for several days. Table A5.2 identifies the CAMx vertical structure developed by TCEQ.

Table A5.2 TCEQ CAMx Vertical Layer Structure

Corresponding WRF Layer	Layer Top (m AGL)	CAMx Layer	Thickness (m)
38	15179.1	28	3082.5
36	12096.6	27	2930
32	9166.6	26	2205.7
29	6960.9	25	1125
27	5835.9	24	937.9
25	4898	23	791.6
23	4106.4	22	733
21	3373.5	21	347.2
20	3026.3	20	335.9
19	2690.4	19	324.3
18	2366.1	18	262.8
17	2103.3	17	256.2
16	1847.2	16	249.9
15	1597.3	15	243.9
14	1353.4	14	143.6
13	1209.8	13	141.6
12	1068.2	12	139.7
11	928.5	11	137.8
10	790.6	10	90.9
9	699.7	9	90.1
8	609.7	8	89.3
7	520.3	7	88.5
6	431.8	6	87.8
5	344	5	87.1
4	256.9	4	86.3
3	170.6	3	85.6
2	85	2	51
1	33.9	1	33.9

An effort was made to map the UTEP WRF vertical layers in Table A5.1 to the TCEQ 36-12-4 vertical layers in Table A5.2. The difference between the UTEP WRF

and TCEQ WRF vertical structures was excessive therefore only the UTEP WRF vertical layers were applied for this report. UTEP WRF vertical layer thickness is much larger beginning at layer 3 and increases substantially as altitude above ground increases. TCEQ WRF vertical layer thickness is fairly consistent from layer 3 up to layer 10 and between layers 11 and 14. It may be beneficial to develop a new WRF vertical layer structure for the PdN region that is consistent with the TCEQ WRF vertical structures.

WRFCAMx output includes 6 meteorological variables:

- Height / pressure;
- Wind;
- Temperature;
- Vertical diffusivity;
- Moisture; and
- Cloud / rain.

GIS-based landuse files were applied to specify fractional land cover for each landuse category within each grid cell. WRFCAMx has several options for applying vertical diffusivity (K_v) computation. The UTEP WRF meteorology was configured with the Mellor Yamada Janjic (MYJ) turbulent kinetic energy (TKE) boundary layer option; the K_v method applied in WRFCAMx was MYJ with a minimum K_v set to $0.1 \text{ m}^2\text{s}^{-1}$. K_v addresses stable boundary layer (SBL) kinetic energy particularly during nighttime. An additional program developed by ENVIRON (KVPATCH) was applied to enhance low-level mixing. No precipitation events occurred during the simulation period therefore cloud / rain variables were inconsequential.

Victor Hugo Valenzuela was born in El Paso, Texas on January 10, 1960. After attending Austin High School, Victor attended the University of Texas at Austin and studied Engineering, Science, Architecture, and Computer Science before obtaining a Bachelors of Arts Degree in Government after 3 years at the UT. During that time Victor took a strong interest in the solar energy industry, and he opened a part-time business repairing, installing, and occasionally removing solar water heating systems. After college Victor expanded his solar business to include photovoltaics during which time he also worked as a laborer on a construction team which installed a 300 KW photovoltaic system in Austin, Texas.

Victor returned to El Paso in 1987 to a new job with the State of Texas and in 1996 entered the fledgling Environmental Science and Engineering program. After completing the core coursework requirements Victor contracted with the Pan American Health Organization to prepare Geographic Information Systems maps for PAHO's Binational Mosquito Surveillance Program.

Shortly thereafter, Victor's concern for rising fuel prices prompted him to learn to manufacture biodiesel in a laboratory at UTEP working under the direction of Prof. Russell Chianelli. During this endeavor Victor became interested in production of biofuel crops such as *Jatropha curcas* which may be cultivated to produce oilseed crops useful for the manufacture of the feedstock for production of biodiesel. During this time, Victor met and worked with Prof. Seiichi Miyamoto from Texas A&M Agri-Life Agricultural Extension Program. Part of the process of learning about cultivating

biofuel crops involved having a grasp of the fundamentals of soils science, drought resistance, and tolerance of this plant to soil salinity due to the growing problem of soil salinity in arable lands across the world. Victor continues growing jatropha plants in the hope the plants survive the climatic conditions of the desert southwest and eventually produce a seed crop.

In 2010, Victor found an opportunity to learn with earnest a topic which had interested him since his early days with the Texas Commission on Environmental Quality. Photochemical modeling is a fascinating subject which culminates at the moment with this dissertation and perhaps an opportunity to pursue a career opportunity in this area during the coming years.

Respectfully submitted:

Victor Hugo Valenzuela

Permanent Address: 3120 Taylor
 El Paso, Texas 79930

This dissertation was typed by the author.